Effect of Intra-abdominal Fat on the Accuracy of DXA Lumbar Spine Bone Mineral Density Measurement using DXA Body Composition Measurements

By

Sarah Elizabeth Darlington

Cardiff University

PhD Thesis
2012

DECLARATION

This work has not previously been accepted in substance for any degree and is not concurrently submitted in candidature for any degree.

Signed …… (candidate) Date……..

STATEMENT 1

This thesis is being submitted in partial fulfilment of the requirements for the degree of PhD.

Signed …… (candidate) Date……..

STATEMENT 2

This thesis is the result of my own independent work/investigation, except where otherwise stated.

Signed …… (candidate) Date……..

STATEMENT 3

I hereby give consent for my thesis, if accepted, to be available for photocopying and for inter-library loan, and for the title and summary to be made available to outside organisations.

Signed …… (candidate) Date……..

Abstract

In the diagnosis of osteoporosis, dual-energy X-ray absorptiometry (DXA) is the accepted method for measuring bone mineral density (BMD) due to its good precision. However, accuracy is compromised by two assumptions: (1) the body is composed of only soft tissue and bone mineral and (2) the composition of tissue overlying bone is equal to that adjacent to bone. To diagnosis osteoporosis, BMD is compared to that of a young healthy population to calculate a T-score. BMD is normal if T-score>-1 and osteoporotic if < -2.5.

The aim of this study was to use DXA whole body (WB) scans to quantify variation in abdominal fat thickness and to explore whether this information could be used to improve the accuracy of lumbar spine (LS) BMD measurement. Relevant data were extracted from archived DXA images for groups of patients who had received both LS and WB scans.

LS BMD increased with the width of the associated soft tissue baseline and BMD was correlated with fat thickness within the baseline.

For individuals, the bone mineral equivalence of the difference in fat thickness between a standard width baseline and a region over the spine corresponded to a maximum T-score difference of 0.6. However, the average for the groups gave a T-score difference of 0.2.

The predicted inaccuracy in LS BMD measurement resulting from a non-uniform fat distribution was within 0.013 g/cm^2 for groups and 0.017 g/cm^2 for individuals. From these measurements, errors in BMD of up to 6% and 3% for a standard width baseline were observed for individuals and groups respectively.

In the majority of patients, errors introduced by a non-uniform distribution of fat are unlikely to cause a mis-diagnosis. However, significant errors may occur in certain individuals. The clinical application of the proposed method to quantify errors in BMD requires further investigation.

Acknowledgements

I am indebted to Professor Wil Evans for his endless patience and guidance he gave as my supervisor and Professor Peter Wells for helpful comments on my thesis. I am grateful to the Department of Medical Physics at The University Hospital of Wales for giving me the opportunity to carry out this project. I thank my colleagues for their support throughout my period of study, especially Rebecca Pettit, Helen Blundell, Matthew Talboys and Kate Wells. I also thank Professor John Woodcock for his guidance throughout my career so far.

I received a great deal of encouragement from my grandmother (Katie) and grandfather (Cecil) who have both sadly passed away during the time I have been carrying out this research.

Finally to my mum and dad; thank you for your patience, support, understanding and especially encouragement during difficult times.

Sarah Elizabeth Darlington
August 2012

Contents

Abbreviations and Symbols

The following are abbreviations and symbols used in this thesis:

A	Cross sectional area (cm^2)
AP	Anterior-posterior
b	Subscript to denote bone
BA	Bone area (cm^2)
BC	Body composition
BCA	Body composition analysis
BEF	Bone equivalence factor (g/cm^2 per cm fat)
BE(F:L)F	Bone equivalence factor derived from the ratio of the area density of fat and lean tissue (g/cm^2 per F:L unit)
BMC	Bone mineral content (g)
BMD	Bone mineral density (g/cm^2)
BME	Bone mineral equivalence (g/cm^2)
BME(F:L)	Bone mineral equivalence derived from the ratio of the area density of fat and lean tissue (g/cm^2)
BMI	Body mass index (kg/m^2)
BUA	Broadband attenuation
CA	Central axis of spine
cb	Subscript to denote a quantity measured with the bone sector of the Hologic calibration wheel
cs	Subscript to denote a quantity measured with the soft tissue sector of the Hologic calibration wheel
CB	Central box i.e. analysis region placed over spine
CD	Crohn's Disease
CI	Confidence interval
CT	Computed tomography
CV%	Coefficient of variation (%)
DPA	Dual-photon absorptiometry
DXA	Dual-energy X-ray absorptiometry
DXR	Digital X-ray radiogrammetry

F:L	Fat to lean area density ratio which is numerically equivalent to the ratio of the fat and lean mass
FLS	Fracture liaison service
FM	Fat mass (g)
FRTx	Female renal transplant study group
g	Fraction of yellow to red bone marrow = YM/(YM+RM)
H	Height of analysis regions used for WB analysis
HRT	Hormone replacement therapy
I	Intensity of X-ray beam after passing through a material
I_0	Incident intensity of X-ray beam
IAF	Intra-abdominal fat
IBD	Inflammatory bowel disease
IVA	Instant vertebral assessment
J	Transmission factor
K	R-value modified for the Hologic implementation of DXA technology using the calibration wheel
Lt	Left side of body or right on image
LM	Lean mass (g)
L1	First lumbar vertebra
L2	Second lumbar vertebra
L3	Third lumbar vertebra
L4	Fourth lumbar vertebra
L5	Fifth lumbar vertebra
L1+L2	Combined data for L1 and L2
L3+L4	Combined data for L3 and L4
m	Mass (g)
M	Mass per unit area or area density (g/cm^2)
MRI	Magnetic resonance imaging
MRTx	Male renal transplant study group
n	Number of lines in analysis region used for DXA WB sub-regional analysis
NHS	National Health Service
OST	Study group of females with osteoporosis
PMT	Photo-multiplier tube

PTH	Parathyroid hormone
pQCT	Peripheral quantitative computed tomography
q	Fat-to-lean area density ratio for soft tissue in a region adjacent to bone
Q	Fat-to-lean area density ratio in region when X-ray path also traverses bone
QC	Quality control
QCT	Quantitative computed tomography
QUS	Quantitative ultrasound
R	Ratio of soft tissue attenuation coefficients at the two energies used in DXA
RA	Radiographic absorptiometry
RCP	Royal College of Physicians
Rt	Right side of body or left on image
RM	Red bone marrow
ROI	Lumbar spine region of interest
SD	Standard deviation
SEE	Standard error in the estimate
SEM	Standard error in the mean
SERMs	Serum oestrogen receptor modulators
SNR	Signal to noise ratio
SOS	Speed of sound
SPA	Single photon absorptiometry
STB	Soft tissue box
STB1	Soft tissue box adjacent to central box placed over vertebrae
SXA	Single energy X-ray absorptiometry
t	Tissue thickness
T12	Thoracic vertebrae number 12
TBBM	Total body bone mineral
TBBMC	Total body bone mineral content (g)
TBBMD	Total body bone mineral density (g/cm^2)
TM	Total tissue mass (g)
Tx	Transplant

UC	Ulcerative colitis
UK	United Kingdom
V	Volume
VF	Vertebral fracture
W	Width of analysis regions used for DXA WB sub-regional analysis
WB	Whole body
WHO	World Health Organisation
YM	Yellow bone marrow
y	Age in years
Z	Atomic number
%fat	Percentage fat
σ	Area density (g/cm^2)
μ	Mass attenuation coefficient (cm^2/g)
μ_l	Linear attenuation coefficient (cm^{-1})
ρ	Physical density (g/cm^3)

Chapter 1
Introduction

1.1 Background and Aims

Osteoporosis is a skeletal disorder characterised by low bone density and decreased bone strength resulting in an increased risk of fracture. Common fracture sites are the hip, spine and forearm. Osteoporosis is a major cause of morbidity and even death in the elderly population (van Staa *et al*. 2001). Other consequences of osteoporosis are pain, height loss, spinal deformity, reduced mobility, loss of independence and low self esteem (Cooper 1997; van Staa *et al.* 2001; Osnes *et al*. 2004). An important goal in osteoporosis management is to predict fracture risk. A low bone mineral density (BMD) is one of the most important predisposing risk factors (Genant *et al.* 2000; Kanis *et al.* 2002; Siris and Delmas 2008; Compston and Rosen 2009). Dual-energy X-ray absorptiometry (DXA) is currently regarded as the gold-standard for

measuring BMD with high precision (Blake 2001). DXA BMD measurements are used to diagnose osteoporosis by comparing the patient's BMD with that for a reference population and applying the criteria developed by the World Health Organisation (WHO) (1994). An accurate measurement of BMD is therefore required. Once a diagnosis of osteoporosis is made, the aim is to prescribe the appropriate treatment to increase BMD in order to decrease fracture risk.

The accuracy of DXA is compromised by two assumptions: first, the body is composed of only two components (soft tissue and bone mineral) and second, the composition of soft tissue overlying bone is the same as that adjacent to bone. In this context, soft tissue includes muscle, fat, viscera, bone marrow, skin and the collagen matrix within bone. Actually this is everything that is not bone mineral. The presence of fat within the body and, in particular, the inhomogeneity of its distribution at a site of BMD measurement, will impact adversely on accuracy. Published work indicates that accuracy errors in lumbar spine BMD due to the non-uniform distribution of abdominal fat exist and can be significant (Roos *et al.* 1980; Gotfredsen *et al.* 1988; Hangartner and Johnston 1990; Hansen *et al.* 1990; Ho *et al.* 1990; Valkema *et al.* 1990; Tothill and Pye 1992; Tothill and Avenell 1994a; Formica *et al.* 1995; Svendsen *et al.* 1995; Svendsen *et al.* 2002; Bolotin *et al.* 2003). To improve the accuracy of DXA measurements, a method of correcting for the presence of fat is required.

The specific DXA scanner used in this work is the Hologic QDR-1000W absorptiometer. Information on soft tissue composition is potentially available within lumbar spine images providing a suitable tissue calibration is performed. However, it is not possible to extract this information from Hologic lumbar spine scans and so the distribution of abdominal fat in the region of the lumbar spine was obtained from DXA whole body (WB) scans.

The hypothesis for this thesis is that the accuracy of lumbar spine BMD measurements with DXA is compromised due to the non-uniform

distribution of abdominal fat and that it is possible to correct for this effect by measuring fat from WB DXA images. The aims of this work are to:

- Examine how the width of the soft tissue baseline region adjacent to the lumbar spine affects the reported BMD;
- Extract abdominal fat thickness profiles from WB images;
- Estimate the fat thickness in a region equivalent to the soft tissue baseline and over the lumbar vertebrae;
- Link the observed change in BMD as soft tissue baseline width increases with the fat thickness in the baseline at the corresponding width;

and ultimately to:

- Correct for the inaccuracy in lumbar spine BMD due to a difference in fat thickness in the baseline and over the vertebrae.

Historical data were used in this study with lumbar spine and WB images from previous studies being retrieved from the archive. All data were anonomysed for patient confidentiality. Ethical approval was granted by the Research Ethics Committee of the School of Engineering Cardiff University.

This chapter will discuss bone anatomy and physiology and the aetiology, diagnosis, consequences and treatment of osteoporosis. The development of methods to measure BMD and body composition will also be discussed.

1.2 Bone Structure and Physiology

The adult skeletal system consists of 206 bones with associated connective tissues including tendons, ligaments and cartilage. The skeleton provides shape and support, protects vital organs, allows body movements, produces blood cells, and stores minerals. Bone has an outer layer of tissue, the periosteum, under which is a layer of hard cortical bone (Fig.1.1). Cortical bone is also known as compact bone as

there are minimal spaces within the structure. In cortical bone the osteocytes and lamellae are orientated around blood vessels (Fig. 1.1). Osteocytes are osteoblasts that have been trapped in the bone matrix. The interior is composed of trabecular bone which has an irregular arrangement of trabeculae orientated along lines of mechanical stress within the bone to provide maximum strength. Trabeculae have layers of osteoblasts on the surfaces and each trabecula has several lamellae with osteocytes embedded between layers (Seeley *et al.* 1988). At the centre of bone is the medullary cavity filled with bone marrow containing fat cells, myeloid tissue, blood vessels, and lymphatic tissue. The majority of yellow marrow (YM) is fat whereas red marrow (RM) contains erythropoietic tissue which produces red blood cells. The RM:YM ratio varies with the location of the bone in the skeleton and during ageing the proportion of RM decreases as it is replaced by YM (Cristy 1981).

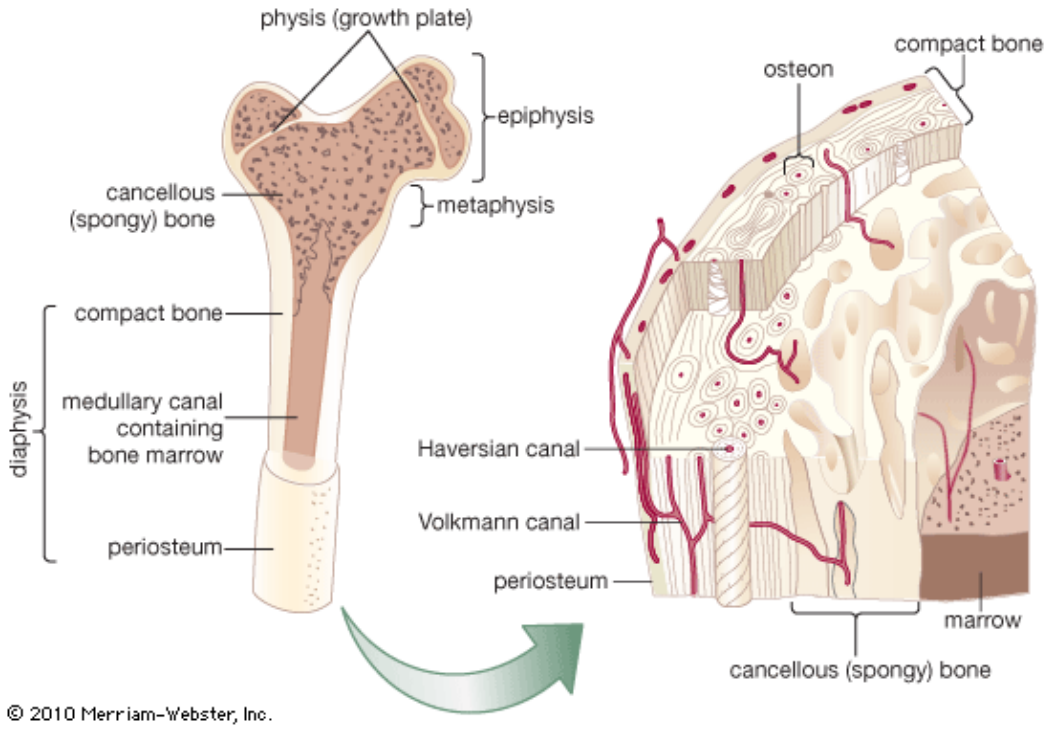

Figure 1.1 Structure of a long bone (femur) showing cortical or compact bone and trabecular or cancellous bone[1].

[1] Reproduced from Encyclopedia Britannica, www.britannica.com/EBchecked/media/66017/Internal-structure-of-a-human-long-bone-with-a-magnified

Approximately 70-80% of the skeleton is cortical bone and the remaining 20-30% trabecular bone (Blake *et al.* 1999). The ratio of trabecular to cortical in an individual bone depends on the type of bone. Bone tissue consists of bone mineral embedded in a supportive matrix which is predominantly collagen. Approximately 25% of the anatomical bone volume is bone mineral in the form of calcium phosphate crystals called hydroxyapatite $Ca_{10}(PO_4)_6(OH)_2$ (Blake *et al.* 1999).

Bone is a living tissue and its physiology involves a cycle of bone formation and resorption. Initially osteoclast cells are activated and fuse to become multi-cellular osteoclasts. These resorb bone creating a tunnel in cortical bone or a cavity on the surface of trabeculae thereby breaking down the bone structure (Fig. 1.2). Osteoclast cells are replaced by osteoblasts which make layers of osteoid to refill the cavity; eventually this osteoid will mineralise. Osteoid is newly formed organic matrix, mainly collagen, that has not mineralised. Over a period of months following filling of the cavity, the crystals of bone mineral get packed more tightly thus causing an increase in BMD. When osteoblasts are surrounded by bone matrix they are termed osteocytes. Once the bone surface is covered by lining cells there is a resting phase termed quiescence. The remodelling cycle lasts between 90 and 130 days (Compston and Rosen 2009).

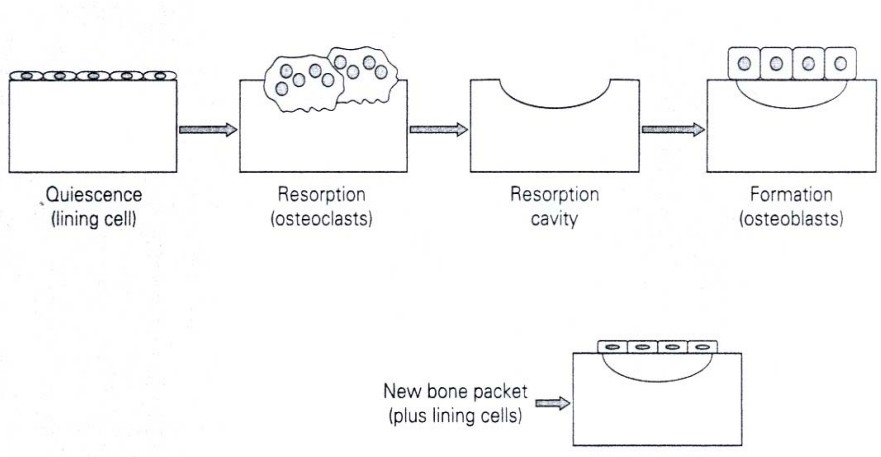

Figure 1.2 Bone remodelling cycle[2].

[2] Reproduced from Lane and Sambrook 2006.

During human growth, bone formation is the dominant process and so BMD increases during childhood reaching a peak between 20 and 30 y (Fig. 1.3). Peak BMD is determined by genetic factors, diet, physical activity and hormone levels (Table 1.1). During adulthood, resorption and formation should be coupled and so BMD remains constant. However, if there is an imbalance between resorption and formation during this period, bone loss will occur compromising the strength of bone. Age related bone loss occurs in both sexes due to normal or increased resorption and suppressed formation. Bone loss is accelerated in women following the menopause due to lack of oestrogen. There are many other causes of bone loss which can occur at any age (Table 1.1).

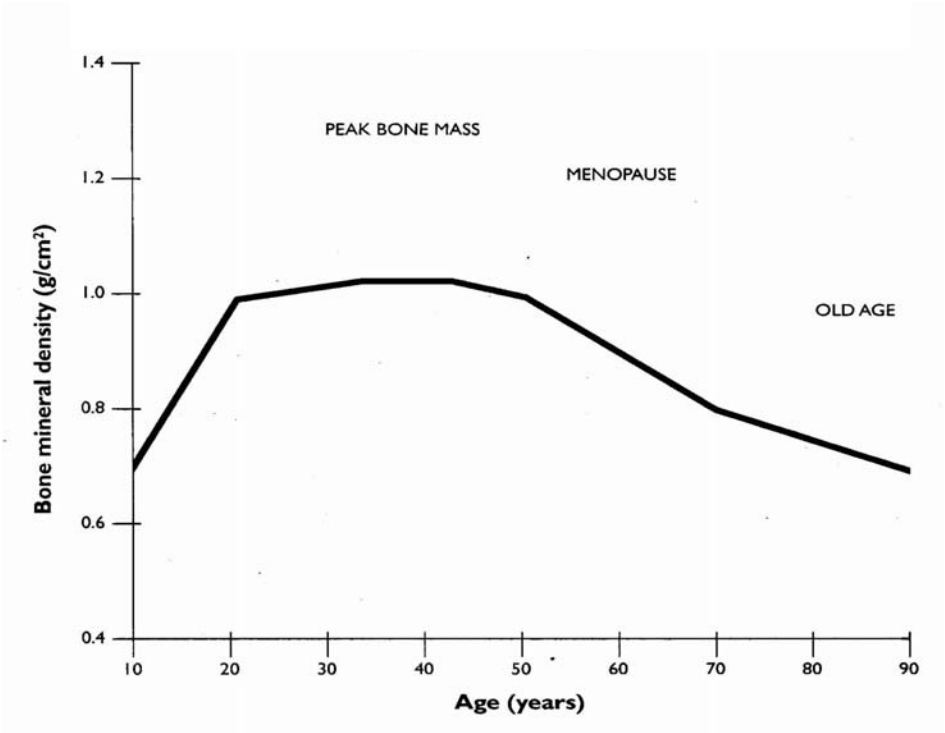

Figure 1.3 Variation in bone mineral density with age in women.

Peak BMD	Bone loss
Genetic factors	Oestrogen deficiency
Age reaching puberty	Immobility
Exercise levels	Nicotine consumption
Calcium intake	Excess alcohol consumption
Nicotine consumption	Decreased vitamin D
Chronic disease	Chronic disease
Alcohol consumption	Increased parathyroid hormone levels
Secondary osteoporosis	Secondary osteoporosis

Table 1.1 Determinants of peak BMD and bone loss. Summarised from Compston and Rosen (2009).

1.3 Osteoporosis

Osteoporosis is a disease characterised by low BMD and deterioration of the internal bone structure thus leading to enhanced bone fragility and an increase in fracture risk. As a result of osteoporotic fractures, patients may suffer increased mortality, pain, vertebral deformities, loss of height, abdominal protrusion interfering with the gastro-intestinal system and a general decrease in their quality of life. In osteoporosis, bone volume remains constant but there is cortical thinning and thinning or disappearance of the trabeculae (Fig. 1.4). There are primary and secondary risk factors for osteoporosis including those listed in table 1.2.

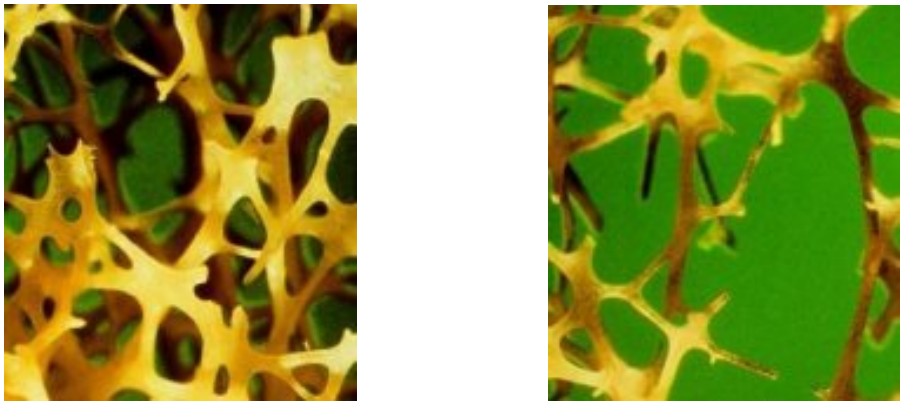

(a) (b)

Figure 1.4 Internal structure of a healthy bone with a continuous trabecular network (a) and an osteoporotic bone with loss of internal bone structure (b) (National Osteoporosis Society 2006).

Primary risk factors for osteoporosis	**Secondary causes**
Hypogonadism (premature menopause)	Endocrine disorders
Glucocorticoid (steroid) therapy	Malignant disease
Previous fracture	Connective tissue disorders
Maternal hip fracture	Drugs
Low BMI	Malabsorption disease
Delayed puberty	Chronic liver disease
Nicotine consumption	Chronic obstructive pulmonary disease
Excess alcohol consumption	Chronic renal disease
Excess caffeine consumption	Organ transplantation
Vitamin D deficiency	Immobility
Low calcium intake	Rheumatoid arthritis
Physical inactivity	Gastrectomy

Table 1.2 Primary and secondary risk factors for osteoporosis (Compston and Rosen 2009).

At the age of 50 y, one in two women (53.2%) and one in five men (20.7%) in the United Kingdom (UK) will suffer a fracture in their remaining lifetime as a result of osteoporosis (van Staa *et al.* 2001). Wrist or spine fractures are the most common in younger post-menopausal

women whilst hip fractures are more prevalent in the elderly. It is estimated that there are 250,000 fractures attributable to osteoporosis per year in the UK with the annual cost to the National Health Service (NHS) for care of patients with hip fractures being over £1.73 billion. It is estimated that by 2020 the annual cost of treating all osteoporotic fractures in post-menopausal women will be approximately £2.1 billion (Burge 2001). Prospective studies have estimated that only 1 in 4 vertebral fractures (VF) are clinically recognised (Ettinger *et al.* 1999) and this is a concern. Identification of VF is important for future fracture prediction as evidence shows the relative risk of a new VF is doubled if there is a previous VF and quadrupled if there is a previous VF plus low BMD (Compston and Rosen 2009). VF present as spinal deformities with height loss and the characteristic kyphosis commonly known as a "dowager's hump" (Fig. 1.5) and they may be accompanied by reduced mobility, loss of self-esteem and problems with the gastro-intestinal tract due to the spinal curvature. There is also an increased risk of a hip or any non-vertebral fracture following a VF (Black *et al.* 1999). Hip fractures can be traumatic with more than 20% of patients dying within a year following the fracture (Keene *et al.* 1993; Forsen *et al.* 1999). It has been reported that by 12 months after a hip fracture, 60% of patients will be limited in basic daily activities such as dressing and 80% will be unable to carry out slightly more active tasks such as climbing stairs or shopping (Cooper 1997).

Figure 1.5 The characteristic "Dowager's hump" resulting from vertebral deformities and fractures which are the consequence of osteoporosis[3].

[3] Reproduced from imag.ehowcdn.co.uk

1.3.1 Diagnosis of Osteoporosis

The gold-standard for BMD measurement is DXA. Clinical indications for bone densitometry using DXA are published by the Royal College of Physicians (RCP) (1999). It has been shown that a decrease in BMD equivalent to one standard deviation of the reference population is associated with a factor of 2 to 3 increase in fracture risk (Compston and Rosen 2009). To assist in the diagnosis of osteoporosis and assess fracture risk, the FRAX™ algorithm is often used; this is discussed in section 1.3.2. As well as BMD assessment, current DXA scanners can produce anterior-posterior (AP) and lateral images of the thoracic to lumbar spine with sufficient quality to diagnose VF (Genant *et al.* 2000). This instant vertebral assessment (IVA) is performed at a fraction of the radiation dose of a standard spinal radiograph and is acquired in approximately 10 seconds. The disadvantage of DXA for identification of VF is the relatively poor quality of the images for the thoracic vertebrae. It is also possible to use lateral spine DXA images to quantify vertebral body shape; this is known as vertebral morphometry (Blake *et al.* 1997). The aim of vertebral morphometry is to quantify the degree of deformity of the vertebral body and categorise the type of VF e.g. wedge, biconcave or crush fracture. A number of methods have been proposed to characterise the shape of the vertebrae by placing 6 points on the vertebral outline (Fig. 1.6).

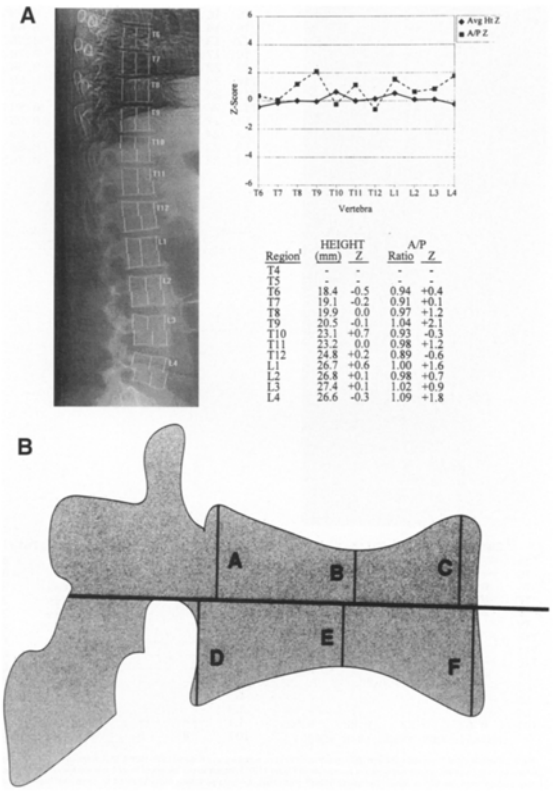

Figure 1.6 Vertebral morphometry to classify vertebral fractures. A shows a lateral DXA image with vertebral height markers and B shows how the heights are calculated. Taken from Blake *et al.* (1997). The Z-score is discussed in section 1.7 (page 23).

1.3.2 Management of Osteoporosis

The primary aim of osteoporosis management is to identify patients at risk of fracture and to reduce that risk. To aid fracture prediction, the FRAX™ algorithm was developed[4]. This is an on-line tool that estimates a 10 year fracture risk based on a selection of risk factors with or without femoral neck BMD. This can be found at WWW.shef.ac.uk/FRAX. The risk factors incorporated in this software are age, BMI, use of glucocorticoid therapy, previous fracture, a family history of hip fracture, smoking and alcohol consumption, and the presence of rheumatoid arthritis. Disadvantages of FRAX™ include failure to account for previously prescribed bone-protective drugs and the presence of other

[4] WWW.shef.ac.uk/FRAX

risk factors e.g. the number of previous fragility fractures. FRAX™ should not be used on patients who have received bone therapy or have other risk factors not included in the algorithm as no data for these populations were collected during development of the algorithm. There is therefore insufficient evidence for prediction of fracture risk in patients who have received treatment or those with risk factors not included in FRAX™. FRAX™ should not be used in place of clinical judgement.

Management of osteoporosis requires a multi-disciplinary approach. In the UK many NHS organisations have established a Fracture Liaison Service (FLS) that aims to identify those patients who present with a fracture who have, or are at risk of developing, osteoporosis. Once osteoporosis has been diagnosed, the aim is to alleviate symptoms of existing fractures and reduce the risk of further fractures.

There are many pharmacological agents available that have been shown to reduce the risk of vertebral fractures up to approximately 50% (Delmas *et al.* 1999; Ettinger *et al.* 1999; Harris *et al.* 1999; Meunier *et al.* 2004; Reginster *et al.* 2005). A significant decrease in the risk of non-vertebral fractures has also been shown. Patients are also likely to be given calcium supplements with or without vitamin D3. A major group of drugs are anti-resorptive agents i.e. ones that inhibit bone resorption. These include bisphosphonates such as Aledronate, Risedronate, Ibandronate, Zolendronate and Etidronate. After 3 annual infusions of Zoledronate, a reduction in vertebral fractures of 70% has been reported with a 41% reduction in hip fractures (Black *et al.* 2007). A newer class of drugs are selective oestrogen-receptor modulators (SERMs), which interact with the oestrogen receptor. An example is Raloxifene which has been shown to prevent bone loss, increase BMD and reduce the risk of vertebral fractures in postmenopausal women (Delmas *et al.* 1999; Ettinger *et al.* 1999).

Hormone replacement therapy (HRT) can protect against hip or spinal fractures. However, due to the associated risk of breast cancer, venous thromboembolism and stroke, it is not recommended for post-

menopausal women older than 60 y. The National Osteoporosis Society position statement on HRT (2011) stated that it may be beneficial in post-menopausal women younger than 60 y who do not have additional risk factors. Other anti-resorptive agents include calcitonin which increases calcium excretion from the kidney and acts on osteoclast receptors to increase BMD. Anabolic agents, e.g. parathyroid hormone (PTH), have been shown to increase bone formation and cause a significant and sustained increase in BMD (Compston and Rosen 2009). Strontium ranelate, which is believed to strengthen bone by altering its composition as the strontium atoms attach to the surface of the hydroxyapatite crystals (Marie *et al.* 2001), has been found to reduce the risk of vertebral and non-vertebral fractures in women (Meunier *et al.* 2004; Reginster *et al.* 2005). The future is likely to see an increase in the use of monoclonal antibodies such as Denosumab which inhibits osteoclast maturation thereby suppressing bone turnover and increasing bone density (Javaid 2011).

As well as bone medication, management of the osteoporotic patient includes lifestyle advice, pain relief, psychological and social care support. The risk of falling should be minimised as this increases with poor vision, postural instability, neuromuscular dysfunction, poor cognitive function, consumption of drugs and alcohol and frailty (Compston and Rosen 2009). Regular monitoring of BMD using DXA may be carried out to assess the patient's response to therapy, and possibly, to improve compliance with treatment.

1.4 Development of Bone Densitometry

In order to diagnose osteoporosis and to assess disease progression or response to therapy, an accurate and precise method of measuring BMD is of great importance. An early attempt to quantify bone mineral was radiographic absorptiometry (RA) in which the bone and an aluminium or ivory calibration wedge were imaged simultaneously on a single

radiographic film. BMD was calculated from the optical density of bone compared to that of the calibration wedge (Stein 1937; Mack *et al*. 1939). The precision of this technique was limited due to radiographic factors, film processing conditions, positioning of the anatomy and identifying bone regions for assessment; it was limited to the peripheral skeleton, particularly the hand. Radiogrammetry was developed to provide a morphometric assessment of tubular bones from projection radiographs. Originally the periosteal and endosteal diameters of the second metacarpal were measured (Barnett and Nordin 1960). With the introduction of digital radiography, radiogrammetry was extended to provide a fully automated method of estimating BMD from measurement of cortical thickness at five regions in the metacarpals, radius and ulna to estimate the mean bone volume per unit of projected area. This method is known as digital X-ray radiogrammetry (DXR) (Roshlom *et al.* 2001).

The earliest measurement of BMD using quantitative radiation absorptiometry was by single photon absorptiometry (SPA) applied to the peripheral skeleton (Cameron *et al.* 1968). SPA involved a radioactive source emitting single energy gamma photons, commonly I-125 emitting gamma rays at 30 keV or Am-241 emitting 60 keV gamma rays. The radiation beam was highly collimated to produce a narrow pencil-beam. A scintillation detector registered the photons transmitted through a particular site, usually the forearm. To correct for overlying soft tissue, the body part was surrounded by water and this limited the technique to the peripheral skeleton. SPA measurements assume that the soft tissue around bone is a homogeneous material of constant total thickness and that the attenuation due to soft tissue at the bone measurement site is equivalent to that of water. In reality this is not true as there is sub-cutaneous fat and deep tissue fat which makes the soft tissue baseline non-uniform.

To measure sites in the axial skeleton and to account for the attenuation of soft tissue, dual photon absorptiometry (DPA) was developed in 1965 (Reed 1966) and came into more widespread use in the 1980's. In DPA

the transmission of gamma radiation at two energies, usually 44 and 100 keV from Gd-153, was measured to account for the presence of soft tissue in the photon path through bone without the need for a constant total thickness. As the gamma rays originated from a radionuclide source, the activity was restricted for safety reasons and this limited the photon emission rate. This restriction resulted in long scan times and a poor signal to noise ratio (SNR) in the images. To improve image quality by reducing noise, a relatively wide collimator was required but this degraded the precision and spatial resolution. Due to radioactive decay the source needed to be replaced regularly.

Some of the limitations of SPA and DPA were overcome by generating photons from an X-ray tube leading to single energy X-ray absorptiometry (SXA) which was restricted to the peripheral skeleton, and dual energy X-ray absorptiometry (DXA) for both the peripheral and the axial skeleton. The higher photon flux resulted in faster scanning times and improved spatial resolution as a result of better collimation, while retaining a high SNR. X-ray tubes produce a spectrum of X-ray energies requiring the use of an energy selective detector in the form of a photo-multiplier tube (PMT).

The first commercial DXA scanner was introduced in 1987 by Hologic (Hologic Inc., Waltham, MA, USA) (Cullum *et al.* 1989; Stein 1990). The technique has established itself as the gold-standard for bone mineral density measurement due to it's high precision, low radiation dose, stable calibration and short scan times (Blake 2001). The radiation dose from DXA measurements is similar to that from the United Kingdom average daily background radiation (Fig. 1.7).

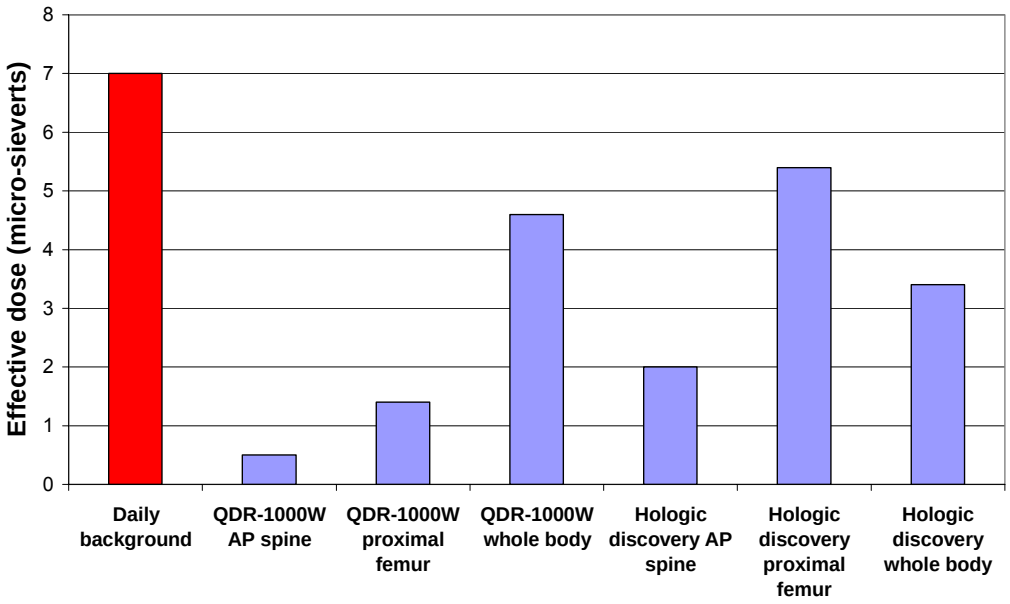

Figure 1.7 Comparison of radiation effective doses for typical scans performed on a pencil beam system (Hologic QDR-1000W) (Lewis *et al.* 1994) and a fan beam system (Hologic QDR 4500) (Blake *et al.* 1996) with the natural daily background radiation in the United Kingdom (Blake *et al.* 2006).

Computed tomography (CT) scanners were originally developed for cross-sectional body imaging but the technique was extended to measure BMD in a method known as quantitative CT (QCT) (Cann 1988; Fogelman and Blake 2000; Blake 2001). X-rays are collimated to a narrow fan beam shape and the X-ray tube and detectors rotate around the body. A cross-sectional digital image is reconstructed in which pixel values represent the linear attenuation coefficients of the corresponding voxels. The patient is scanned with a reference phantom and the patient's BMD is determined by comparing the attenuation of bone with that of known quantities of bone mineral and soft tissue equivalent materials within the phantom. There are also dedicated peripheral QCT (pQCT) scanners available for BMD measurement of the peripheral skeleton

The advantages of QCT over DXA are it gives a three-dimensional volumetric measurement and it separates trabecular and cortical bone. The disadvantages of CT compared to DXA are a higher radiation dose, increased cost and, at times, the limited availability of CT scanners. As

with DXA, the accuracy is affected by inhomogeneities in soft tissue distribution and fat content; it is also affected by fat in the bone marrow (Crawley *et al.* 1988; Kuiper *et al.* 1996). During aging, as the RM is replaced by the more fatty YM, the fat error increases whereas the BMD decreases (Gluer and Genant 1989). In an attempt to overcome these problems, the use of dual-energy QCT was investigated and this appeared to improve accuracy but degrade precision (Genant and Boyd 1977). Typically the accuracy of BMD measurements with single and dual energy CT are 5-15% (Blake *et al.* 1999) and 3-10% (Cann 1988) respectively. The precision for BMD of the spine has been quoted as 3% (Blake 2001).

The development of sequential CT has extended the single slice measurement to multiple slices and the invention of spiral CT has allowed construction of a 3D model of bone (usually the femur) providing information on trabecular structure (ICRU 2009) .

Quantitative ultrasound (QUS) techniques are based on the transmission of high frequency sound waves through whole bone i.e. combined trabecular and cortical plus organic material and bone marrow (Blake *et al.* 1999). The speed of an ultrasound pulse through bone can be measured from division of the width or length of bone by the time taken for the pulse to traverse the bone. Speed of sound (SOS) is dependent on the physical density and bulk modulus of bone, the latter being related to the tensile strength of bone. Thus SOS is related to bone strength. One disadvantage of QUS is that the theory is not well understood and so it is not possible to convert SOS directly into BMD. The precision of multi-site is SOS 1-2% (Blake 2001).

A second QUS measure is based on the attenuation of a broadband ultrasound pulse containing a spectrum of frequencies by bone. The frequency dependent attenuation through bone can be compared to the attenuation through the same length of water (Fogelman and Blake 2000, Blake *et al.* 1999). The relationship between relative attenuation in bone and frequency is linear between 0.2 and 0.6 MHz with the slope of this

line being called the broadband attenuation (BUA). As for SOS, BUA cannot be converted directly to BMD. Manufacturers have used a combination of BUA and SOS to predict BMD by measuring a skeletal site (e.g. the heel) by QUS and DXA.

Advantages of QUS over DXA are that it is non-ionising and the technology is relatively cheap and portable. The disadvantage is that measurements are affected by other materials and hence it is hard to define accuracy. The precision of BUA measurements of the calcaneus has been quoted as 2-5% (Blake 2001).

DXA is currently regarded as the gold-standard for BMD measurement. The precision for DXA AP spine BMD measurement is better than 1 % as discussed in section 1.8. A major problem with both QCT and QUS is that the measurements cannot be used in conjunction with WHO criteria which are used to diagnose osteoporosis as discussed in section 1.7.

1.5 Dual Energy-X-ray Absorptiometry Technology

DXA is a two-dimensional projection technique which measures BMD, bone mineral content (BMC) and bone area (BA) with the projected BA being in the direction on the X-ray beam. DXA measures integral trabecular and cortical bone. The main manufacturers of bone densitometers are currently GE, previously Lunar, and Hologic. A typical DXA system consists of an X-ray tube emitting photons that are collimated into a beam that passes through the patient's body and enter a detector (Fig. 1.8). The source, collimator and detector are mechanically connected and aligned on a scanning arm.

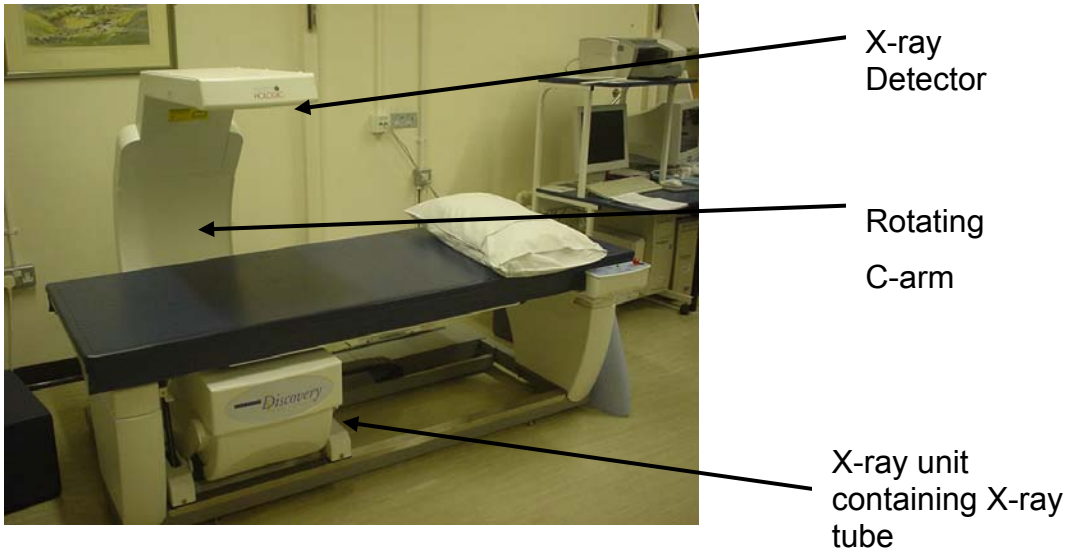

Figure 1.8 Basic components of an X-ray absorptiometer showing the Hologic Discovery A fan beam scanner.

X-rays of two energies are produced by either continuously switching the voltage of the X-ray tube between high and low values, known as kV switching, or by K-edge filtration. In K-edge filtration, the spectrum of X-rays produced by the X-ray tube is filtered into two narrow energy bands. The detector is usually a scintillation crystal coupled to a PMT or, in modern systems, a photodiode. When an X-ray interacts with a scintillating material the energy of the X-ray is converted into a scintillation consisting of many photons of light. A PMT or photodiode converts this scintillation into an electrical pulse. Systems using kV-switching, e.g. Hologic, operate in current-integrating mode where the total number of pulses from a PMT are integrated before being digitised. In contrast, K-edge filtration systems, e.g. GE(Lunar), use pulse counting with energy discrimination.

In early systems, the X-ray beam was collimated to form a thin pencil like beam which formed an image through a raster-scanning movement. In modern systems the beam passes through a slit collimator producing a fan shaped X-ray beam, which is detected by a linear array of detectors. The fan beam design allows simultaneous measurement of X-ray

transmission through many paths hence decreasing the scan time. With a pencil beam scanner the image is projected perpendicular to the plane of the patient couch, whereas with the fan-beam different parts of the image area will be projected at different angles (Fig. 1.9). Fan-beam geometry introduces inaccuracies and software is required to correct for mass magnification i.e. a mass element nearer the table is weighted more heavily than an identical mass element raised above the table (Griffiths *et al.* 1997). Numerous cross-calibration studies between pencil and fan beam scanners have been published highlighting differences in measurements (Bouyouecf *et al.* 1996; Barthe *et al.* 1997; Ellis and Shypailo 1998). Cone beam systems are also available which have a rectangular collimator that exposes an entire region during each exposure.

The measurement of BMD by DXA is discussed more thoroughly in chapter 2.

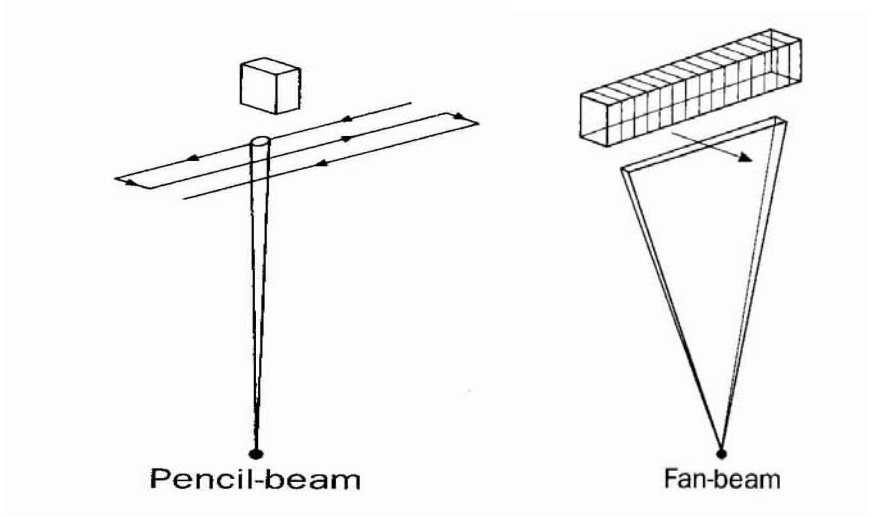

Figure 1.9 Comparison between pencil- and fan-beam geometry for DXA scanners (Blake *et al*. 1999).

1.6 Skeletal Sites for the Measurement of BMD

The skeletal sites chosen for BMD measurement are those prone to fracture, predictive of future fracture risk and useful for monitoring. Such sites are the lumbar spine (Fig. 1.10a), proximal femur (Fig. 1.10b) and forearm. Lumbar spine BMD measurements are usually made in the antero-posterior (AP) projection although it is also possible to measure BMD in the lateral projection (Blake *et al.* 1999). The best predictor of fracture risk at a particular site is the BMD at that location. However, measurements made at spine, hip, calcaneous or wrist can be related to fracture risk at any site (Compston and Rosen 2009, Marshall *et al.* 1996).

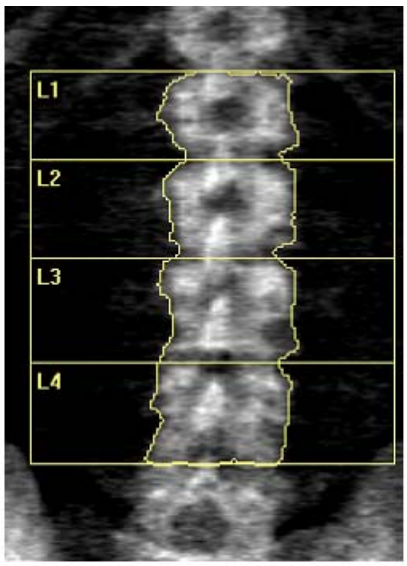

k = 1.148, d0 = 42.3
116 x 125

DXA Results Summary:

Region	Area (cm^2)	BMC (g)	BMD (g/cm^2)	T - Score	Z - Score
L1	10.57	10.71	1.013	0.8	1.0
L2	11.94	13.97	1.170	1.3	1.5
L3	13.34	14.86	1.115	0.3	0.5
L4	13.66	14.59	1.069	-0.4	-0.2
Total	**49.50**	**54.14**	**1.094**	**0.4**	**0.6**

Total BMD CV 1.0%, ACF = 1.018, BCF = 1.014, TH = 8.041

Figure 1.10a Lumbar spine DXA image showing analysis regions and an example of BMD, BMC, bone area results summary. T and Z-scores are discussed in section 1.7 (page 23).

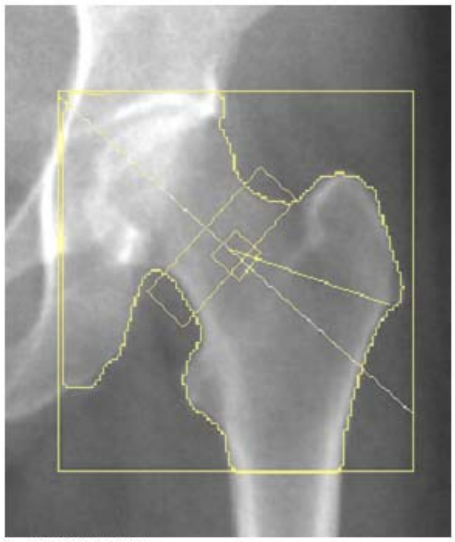

k = 1.159, d0 = 50.3
101 x 108

DXA Results Summary:

Region	Area (cm^2)	BMC (g)	BMD (g/cm^2)	T - Score	Z - Score
Neck	5.33	3.45	0.648	-1.8	-0.7
Troch	10.66	6.49	0.609	-0.9	-0.2
Inter	23.61	18.94	0.802	-1.9	-1.4
Total	**39.60**	**28.89**	**0.729**	**-1.7**	**-1.0**
Ward's	1.11	0.58	0.525	-1.8	-0.0

Total BMD CV 1.0%, ACF = 1.020, BCF = 1.019, TH = 4.781

Figure 1.10b Proximal femur DXA image with analysis regions and an example of BMD, BMC, bone area results summary. T and Z-scores are discussed in section 1.7 (page 23).

The lumbar spine is an ideal site for monitoring BMD change as it is composed of a high proportion of trabecular bone which has a high metabolic rate (Blake and Fogelman 1997b). As a result, trabecular bone exhibits a relatively fast turnover and the response to bone treatments or deterioration due to disease can be observed relatively soon with serial measurements. A disadvantage of monitoring changes in the spine is that an AP scan includes contributions from cortical bone and the spinous processes as well as the trabecular bone in the vertebral body. A further disadvantage is the susceptibility of the spine to degenerative changes with a falsely high BMD occurring at points of vertebral compression.

Aortic calcification and variations in abdominal fat over time may also influence BMD measurements of the spine. In the femur, the BMD of the femoral neck is important for fracture prediction as this is a common site of fracture.

1.7 Interpretation of DXA Results

Diagnosis of osteoporosis is based on the WHO classification using DXA measurements of the spine, hip or forearm. The patient's BMD is compared to the relevant reference population to calculate T and Z scores. The T-score compares the measured BMD with that of a young (30 year old) healthy population of the same gender whereas the Z-score is age and sex matched and therefore accounts for the expected decline in BMD with age.

$$\text{T-score} = \frac{\text{Subject's BMD} - \text{Young adult population mean BMD}}{\text{Young adult population standard deviation}}$$

$$\text{Z-score} = \frac{\text{Subject's BMD} - \text{Age matched population mean BMD}}{\text{Age matched population standard deviation}}$$

The WHO definition of osteoporosis is a T-score of ≤-2.5 at the spine, hip or forearm. When the T-score is between -2.5 and -1.0 the diagnosis is osteopaenia and when it is greater than -1.0 the BMD is classed as normal. Patients often undergo longitudinal measurements to monitor change in BMD. This may be due either to deterioration as a result of disease and medications or to improvement as a result of treatment. Measurements should be performed at a minimum interval of one year as true changes are unlikely to be detected in less than a year. A significant change is classed as a change in BMD of 2.8 times the precision of the technique. For example, Hologic quote the precision of lumbar spine L1 to L4 BMD measurements as a coefficient of variation of 1% and therefore a change in BMD of 2.8% would be needed to be classed as

statistically significant. During the menopause, women experience an average bone loss of 1% per year (Compston and Rosen 2009) and therefore the monitoring interval should not be less than about 3 years unless there are other risk factors involved.

1.8 Precision and Accuracy of DXA Lumbar Spine BMD Measurement

Errors in BMD measurement arise from a difference in soft tissue composition over bone and adjacent to bone, beam hardening, calibration method and in fan-beam scanners, scattered radiation. Random errors are introduced due to the instrument, the subject, the operator, the positioning of the patient and the variation in number of photons detected which is dependent on the tissue thickness of the patient. DXA scanners are usually calibrated assuming an abdominal thickness of 15 – 25 cm and errors may occur when scanning very thin patients (<10 cm) and the obese (>30 cm) (Cullum *et al.* 1989; Blake *et al.* 1992).

Accuracy and precision vary between manufacturers and also between different models produced by the same manufacturer (Sobnack *et al.* 1990; Laskey *et al.* 1991; Tothill *et al.* 1995). These discrepancies are due to inconsistencies in methods of generating the dual-energy X-ray beam, the calibration method, assumptions about fat distribution, the scan mode, processing software and the software algorithm used to identify bone edges. For example, the calibration of the Hologic QDR-1000W is based only on hydroxyapatite whilst the GE/Lunar scanners have a correction for intra-osseous fat (Gundry *et al.* 1990; Laskey *et al.* 1991).

This work concentrates on the accuracy of lumbar spine BMD measurements and in particular the uncertainties introduced by the non-uniform distribution of abdominal fat (Hansen *et al.* 1990; Tothill and Pye 1992; Tothill and Avenell 1994a; Svendsen *et al.* 1995; Svendsen *et al.* 2002). The clinical significance of the potential accuracy errors due to the

presence of fat is still under debate (Blake and Fogelman 2008). It is also likely that the thickness of fat overlying the proximal femur is different to that in the soft tissue baseline used to calculate femoral BMD. From a study using a GE Lunar scanner it has been concluded that an overlying fat panniculus, i.e. a dense fatty growth in the lower abdomen, may affect the measurement of proximal femur BMD and the authors recommend the retraction of the fat during scanning (Binkley *et al*. 2003).

The short-term precision of in-vivo DXA measurements is typically better than 1% for the AP lumbar spine, (Cullum *et al.* 1989; Laskey *et al.* 1991; Haddaway *et al.* 1992; Blake 2001), and 1-5% for the proximal femur (Laskey *et al.* 1991). The precision of BMD measurements is poorer for the hip due to more variability in positioning of the patient and defining the regions for analysis (Haddaway *et al.* 1992). Long-term precision has been reported to be double that for short-term measurements (Tothill and Hannan 2007).

The best method to assess the accuracy of BMC measurement is by comparing the BMC of a bone measured by DXA in-situ with the ash weight found by excising the bone, defatting and ashing. The BMD is found using the projected bone area from a radiograph. Using this method, errors of 5 to 10% have been reported (Ho *et al.* 1990; Svendsen *et al.* 1995). Accuracy and precision are degraded with larger soft tissue and fat thickness (Cullum *et al.* 1989; Laskey *et al.* 1991; Tothill *et al.* 1995), and when the actual BMD is low (Cullum *et al.* 1989; Tothill *et al.* 1995). Good accuracy and precision are vital to avoid misdiagnosis of osteoporosis and misinterpretation of treatment response.

1.9 Body Composition Analysis

Body composition measurements have been performed since the 1940's (Behnke 1942). Numerous techniques are available and many involve highly specialised equipment (Sheung and Huggins 1979). Body composition analysis (BCA) involves subdividing the body into conceptual

compartments with differing physiological or structural properties e.g. bone mineral, muscle, protein, fat, water (intra- and extra- cellular) and body cell mass. A number of methods have been proposed e.g. direct quantification of total body Ca, Na and N by neutron activation analysis, measurement of total body potassium (K) using a whole body counter and the use of isotope dilution for an in-vivo estimation of total body water and exchangeable K and Na. Probably the most widely used body composition model is a 4-compartment model which incorporates protein, water, bone mineral and fat (Heymsfield *et al.* 1990; Friedl *et al.* 1992). The measurement of bone mineral mass can be made using DXA.

Of interest to this work is measurement of fat mass (FM) by DXA. Fat content and distribution have also been measured using QCT, ultrasound and magnetic resonance imaging (MRI). Other methods of estimation of FM include anthropometry, underwater weighing, and from measurement of total body water and total body potassium (K).

1.10 Body composition Analysis with DXA

DXA measurements of bone mineral are based on the assumption that the body is composed of bone mineral and soft tissue whereas BCA subdivides the soft tissue into fat and fat free tissue mass. Fat free tissue incorporates bone mineral and lean tissue. Standard analysis of DXA WB images reports BMC, BMD, BA, lean tissue mass (LM) and FM for the arms, legs, trunk, head and total body (Fig. 1.11). Compared to other methods, BCA measurements with DXA are relatively quick, non-invasive and have good precision. In addition it is possible to make total body or regional measurements. The main limitation is that the composition of tissue overlying bone cannot be measured directly but is estimated by extrapolating the attenuation data from a bone free region of tissue adjacent to the bone. In order to do this, manufacturers make assumptions about the tissue distribution and this can introduce errors (Roubenoff *et al.* 1993; Tothill *et al.* 1994b; Tothill *et al.* 1994c; Nord

1998). Other limitations are a poor image quality with obese patients and an associated radiation dose although this is extremely small (Fig. 1.7). Variations in lean tissue hydration are no longer thought to affect measurements as body water attenuates X-rays similarly to lean tissue (Kelly *et al.* 1998; Nord 1998). Specific disadvantages with some DXA scanners include dependence of measurements on tissue thickness due to beam hardening, restrictions on patient size and, with fan-beam scanners, the magnification effect. BCA using DXA is discussed more thoroughly in chapter 2.

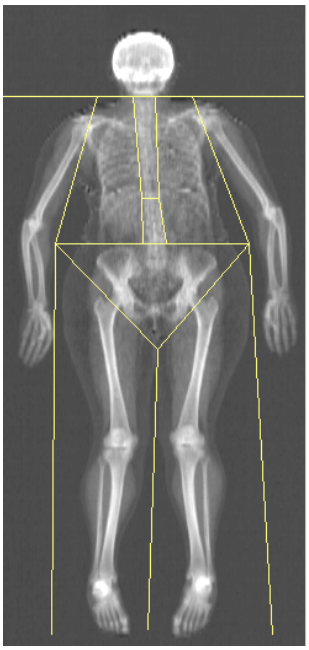

DXA Results Summary:

Region	BMC (g)	Fat (g)	Lean (g)	Lean+BMC (g)	Total Mass (g)	% Fat
L Arm	108.25	1867.5	2153.0	2261.2	4128.8	45.2
R Arm	115.56	1936.1	2334.0	2449.6	4385.6	44.1
Trunk	346.07	11654.3	20345.5	20691.6	32345.9	36.0
L Leg	282.32	5929.2	6939.2	7221.5	13150.7	45.1
R Leg	273.08	6343.5	6681.4	6954.4	13297.9	47.7
Subtotal	1125.29	27730.6	38453.0	39578.3	67309.0	41.2
Head	259.07	848.0	2909.9	3169.0	4017.0	21.1
Total	**1384.36**	**28578.6**	**41363.0**	**42747.3**	**71325.9**	**40.1**

Sub-Region	BMC (g)	Fat (g)	Lean (g)	Lean+BMC (g)	Total Mass (g)	% Fat
R1	133.85	4666.2	4393.8	4527.7	9193.9	50.8
R2	52.73	1450.3	1550.6	1603.3	3053.6	47.5
R3	179.79	4986.9	6910.2	7090.0	12077.0	41.3
Net	**364.67**	**11034.9**	**12749.3**	**13114.0**	**24148.9**	**45.7**

TBAR2492

Figure 1.11 A DXA whole-body scan showing the Hologic standard regions of interest used for analysis and an example of the results display. This image was acquired with the Hologic QDR-4500A fan beam scanner.

1.11 Summary

An accurate measurement of BMD is needed to ensure a correct diagnosis of osteoporosis. The underlying assumption in DXA is that the body is composed of uniform soft tissue and bone mineral and therefore the attenuation of X-rays by variable thickness of fat will introduce accuracy errors in measurements. The technology behind DXA and the stages involved in calculating lumbar spine BMD and FM will be discussed in the following chapter. A review of the published studies investigating the effect of a non-uniform fat distribution on lumbar spine BMD will also be presented.

Chapter 2
Accuracy of Lumbar Spine Bone Mineral Density Measurement by Dual Energy X-ray Absorptiometry

2.1 Background and Aims

The work presented in this thesis uses dual energy X-ray absorptiometry lumbar spine and whole body (WB) images to measure lumbar spine bone mineral density (BMD) and fat mass (FM) respectively. The principles behind DXA and the implementation by Hologic in their QDR-1000W absorptiometer will be discussed here. Also in this chapter are the findings of a literature review that was performed to answer the following questions:

- Does the width of the lumbar spine analysis box influence the reported BMD?
- Is there a difference in the soft tissue composition over the vertebrae and in an adjacent soft tissue region?
- Have the potential accuracy errors due to a non-uniform soft tissue distribution been quantified?
- Can the Hologic QDR-1000W WB sub-regional analysis tool be used to quantify the in-homogeneity in abdominal fat distribution in the region of the lumbar spine?

2.2 Principles of Bone Densitometry by Dual-Energy X-ray Absorptiometry

Bone densitometry techniques using X-rays or gamma radiation are based on measuring the attenuation of the radiation beams by body tissues. This section sets out the theory and associated assumptions behind DXA. At the X-ray energies used in DXA, attenuation in bone mineral and soft tissue is due to photoelectric absorption and Compton scattering. In Compton scattering the photon interacts with an atomic electron and is deflected with a loss of energy. Photoelectric absorption involves total absorption of the photon by the atom. For a mono-energetic narrow beam of radiation passing through a homogeneous material the attenuation is represented by equation 2.1 (Fig. 2.1).

$$I = I_0 \exp(-\mu_l t) \qquad (2.1)$$

where I_0 is the incident intensity, I is the intensity after passing through tissue of thickness t and μ_l is the linear attenuation coefficient of the tissue (cm^{-1}). μ_l is defined as the fractional change in the intensity of the incident beam per unit thickness of the attenuating material. The attenuation coefficient depends on the photon energy, tissue composition and the physical density (ρ) of the tissue.

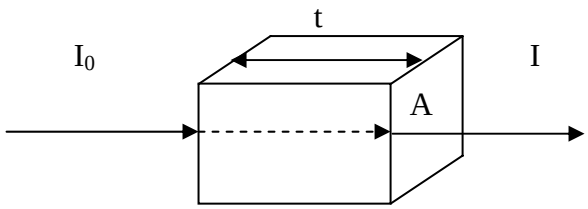

Figure 2.1 Attenuation of an X-ray beam by a block of tissue with physical density ρ, surface area A, mass m, thickness t and volume V.

The linear attenuation coefficient can be replaced by the mass attenuation coefficient μ (cm^2/g) where $\mu_l=\mu\rho$. In the human body, the path of a radiation beam traverses a variety of tissues each with a different attenuation coefficient. It is therefore necessary to sum the attenuation coefficients for all tissues in the X-ray path as in equation 2.2.

$$I = I_0 \exp-(\sum_{i=1}^{i=N} \mu_i \rho_i t_i) \qquad (2.2)$$

where *i* represents an individual tissue and N is the number of different tissues.

BMD measurement by dual-photon absorptiometry (DPA) and DXA is based on the simple assumption that the human body is composed of bone mineral and homogeneous soft tissue. In practice, soft tissue includes all non-mineral components including muscle, fat, skin, viscera, lung, bone marrow, and the collagen matrix within bone. The attenuation coefficient of fat differs from the other soft tissues; failure to account for this difference has the potential to result in measurement errors. The attenuation coefficient of bone mineral, i.e. calcium hydroxyapatite, is significantly greater than that of fat or other soft tissues due to the presence of phosphorus and calcium which have a relatively high atomic number (Fig. 2.2). The atomic numbers (Z) of calcium and phosphorous are 20 and 15 respectively whereas the components of the soft tissue have a lower atomic number; they are mainly carbon (Z=6), hydrogen

(Z=1), nitrogen (Z=7) and oxygen (Z=8). Fat has a larger hydrogen content than other lean soft tissues and therefore a lower mass attenuation coefficient. Adipose is loose connective tissue composed of mainly adipocytes which are cells that contain fat. Adipose is approximately 85% fat (Tothill and Pye 1992). Fat in a pure form is found in the liver and muscles whereas adipose is located beneath the skin as subcutaneous 'fat', around internal organs as visceral 'fat' and in the yellow bone marrow. Adipose tissue is also found in other locations referred to as adipose depots.

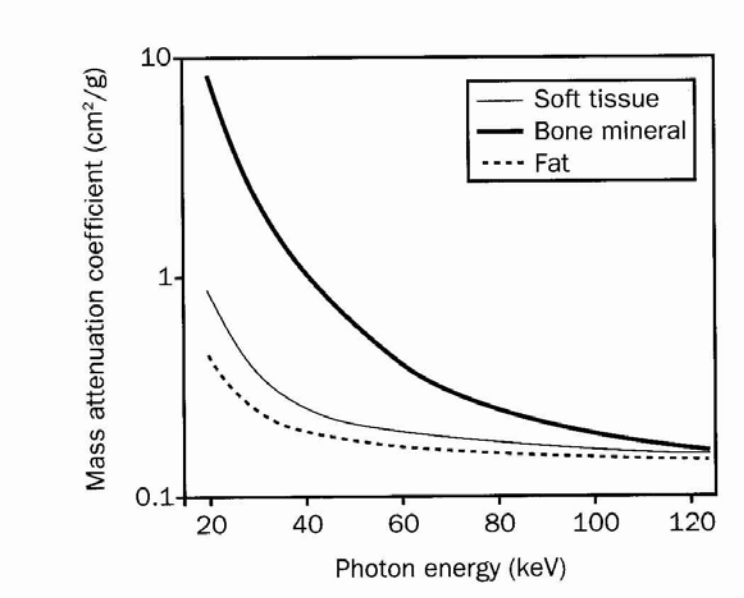

Figure 2.2 Dependence of the mass attenuation coefficient of bone mineral, fat and soft tissue on photon energy (Blake *et al.* 1999).

At a given energy the attenuation coefficient of bone mineral is constant as it has a constant composition whereas the attenuation coefficient of soft tissue is variable depending on the fat and lean mixture in the tissue. The total attenuation is dependent on tissue thickness and therefore will vary for both bone mineral and soft tissue as their thickness varies from point to point. If a mono-energetic X-ray beam travels through bone surrounded by soft tissue, the transmitted intensity is given by equation 2.3 where b and s represent bone mineral and soft tissue respectively; t_b

is the equivalent thickness of bone mineral in the X-ray path as if it had been isolated as a homogeneous layer, and t_s is the thickness of soft tissue in the X-ray path.

$$I = I_0 \exp -(\mu_s \rho_s t_s + \mu_b \rho_b t_b) \qquad (2.3)$$

From figure 2.1, the volume of an attenuating element is given by:

$$V = A \times t \qquad (2.4)$$

where A is the projected area perpendicular to the X-ray beam. The physical density is given by:

$$\rho = \frac{m}{V} \qquad (2.5)$$

Combining equations 2.4 and 2.5 gives the area density (M) i.e. mass per unit area as shown in equation 2.6.

$$M = \frac{m}{A} = \rho t \quad (2.6)$$

DXA is a two-dimensional projection technique and therefore BMD is an area density measurement not a volumetric density. Substituting for M in equation 2.3 gives:

$$I = I_0 \exp -(\mu_s M_s + \mu_b M_b) \qquad (2.7)$$

taking the natural logarithm of equation 2.7 gives:

$$-\ln\left(\frac{I}{I_0}\right) = \mu_s M_s + \mu_b M_b \qquad (2.8)$$

i.e. $\ln\left(\frac{I_0}{I}\right)$ which is the attenuation.

The logarithm of the ratio of the transmitted intensity, i.e. the attenuation, is denoted as J (equation 2.9) and can be substituted in equation 2.8 to give equation 2.10.

$$J = \ln\left(\frac{I_0}{I}\right) \qquad (2.9)$$

$$J = \mu_s M_s + \mu_b M_b \qquad (2.10)$$

Transmission measurements are made at two different photon energies which are selected to optimise the difference in the mass attenuation coefficients of bone mineral and soft tissue. The difference between the attenuation due to bone mineral and soft tissue is much less at higher photon energies than lower energies (Fig. 2.2). Having two X-ray beams generates two attenuation equations (2.11 & 2.12) where M_b and M_s are the area densities of bone and soft tissue respectively.

Low energy: $$J' = \mu_s' M_s + \mu_b' M_b \qquad (2.11)$$

High energy: $$J = \mu_s M_s + \mu_b M_b \qquad (2.12)$$

These simultaneous equations may be solved for M_b and M_s (equations 2.13 and 2.14).

$$M_b = \frac{J' - (\mu_s' / \mu_s)J}{\mu_b' - (\mu_s' / \mu_s)\mu_b} \qquad (2.13)$$

$$M_s = \frac{(\mu_b' / \mu_b)J - J'}{(\mu_b' / \mu_b)\mu_s - \mu_s'} \qquad (2.14)$$

The attenuation factors (J and J') are measured and both μ_b and μ_b' are known because of the fixed chemical composition of bone mineral. However, μ_s and μ_s' will vary depending on the tissue composition. Therefore a patient and site specific measurement of μ_s'/μ_s is needed to accurately compensate for the soft tissue overlying and within bone. This

is achieved by measuring the attenuation of the dual-energy X-ray beams through a bone-free region of tissue adjacent to the bone. The ratio of the soft tissue attenuation coefficients at the two energies is termed the R-value (equation 2.15) and depends on the soft tissue composition.

$$R = \frac{\mu'_s}{\mu_s} \qquad (2.15)$$

R will vary with the lean to fat ratio within soft tissue with an increase in fat reflected by a decrease in R. In calculating BMD it is assumed that the thickness and composition of the soft tissue in the bone free region is identical to tissue anterior and posterior to bone and within bone and therefore have identical R-values. As this is often not true there is a patient-specific error. R as defined in equation 2.15 can be substituted into equation 2.13 to give equation 2.16.

$$M_b = \frac{J' - R\ J}{\mu'_b - R\ \mu_b} \qquad (2.16)$$

In the bone free region M_b = 0 and therefore equations 2.11 and 2.12 become:

$$J' = \mu'_s M_s \qquad (2.17a)$$

$$J = \mu_s M_s \qquad (2.17b)$$

and so:

$$R = \frac{\mu'_s}{\mu_s} = \frac{J'}{J} \qquad (2.18)$$

Thus R is equal to the ratio of the soft tissue logarithmic attenuation values at the two energies (equation 2.18). Since J and J' are measured, R may be calculated. Substituting values of J, J', R, μ_b and μ_b' into equation 2.16 allows M_b to be calculated.

So far the measurement of M_b has been described for a single X-ray path through bone and soft tissue whereas measurements over a volume of bone are needed. This is achieved by making a linear series of measurements across the part of the patient that contains bone. The region of tissue adjacent to bone yet within the analysis region is known as the soft tissue baseline. The result is an attenuation profile for each of the X-ray beams (Fig. 2.3a). The high-energy absorption profile is multiplied by R then subtracted from the low energy profile to leave bone mineral (Fig. 2.3a). The Hologic QDR-1000W Utility Plot function gives a profile of the logarithmic transmission factors at the high and low energies for pixels in each scan line as shown in figure 2.3b (Blake *et al.* 1992). These data were not used in this work.

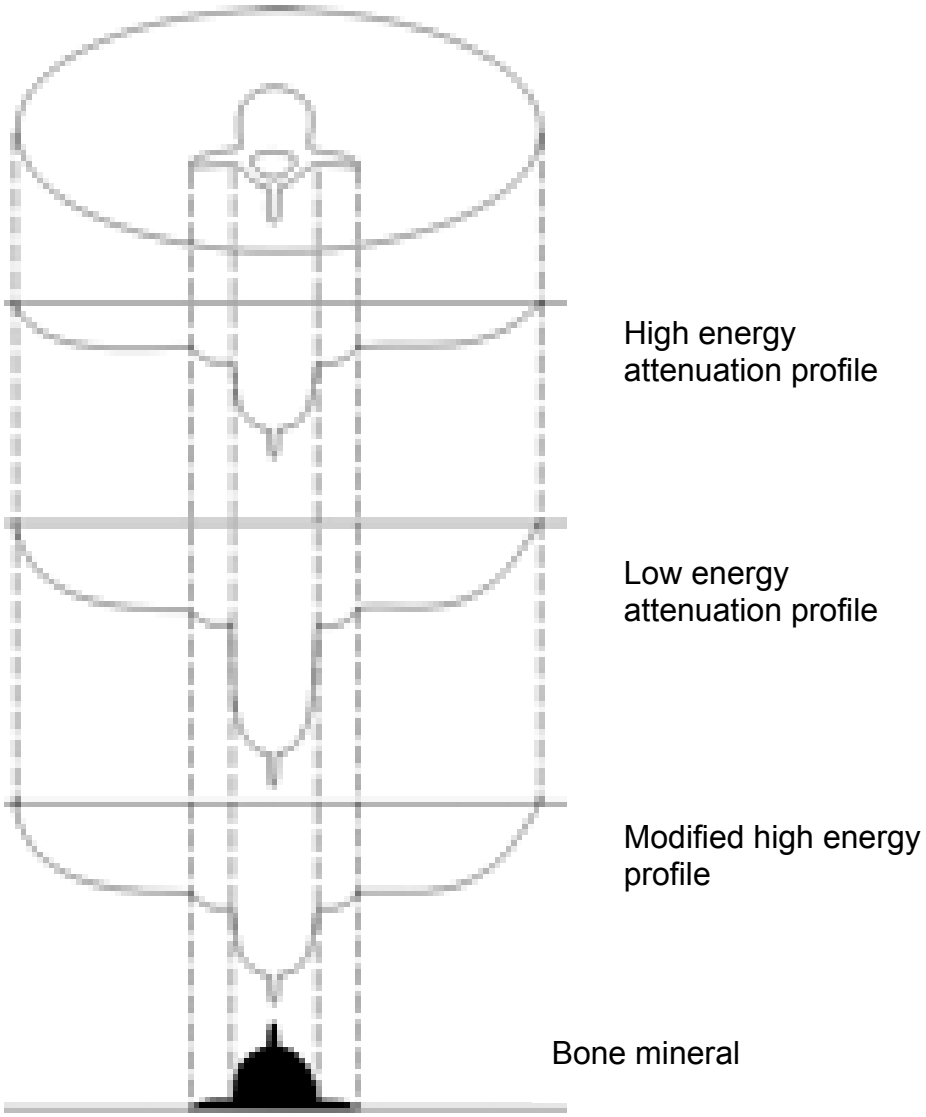

Figure 2.3a Principle of dual energy photon absorptiometry for measurement of bone mineral density (Wahner and Fogelman 1994).

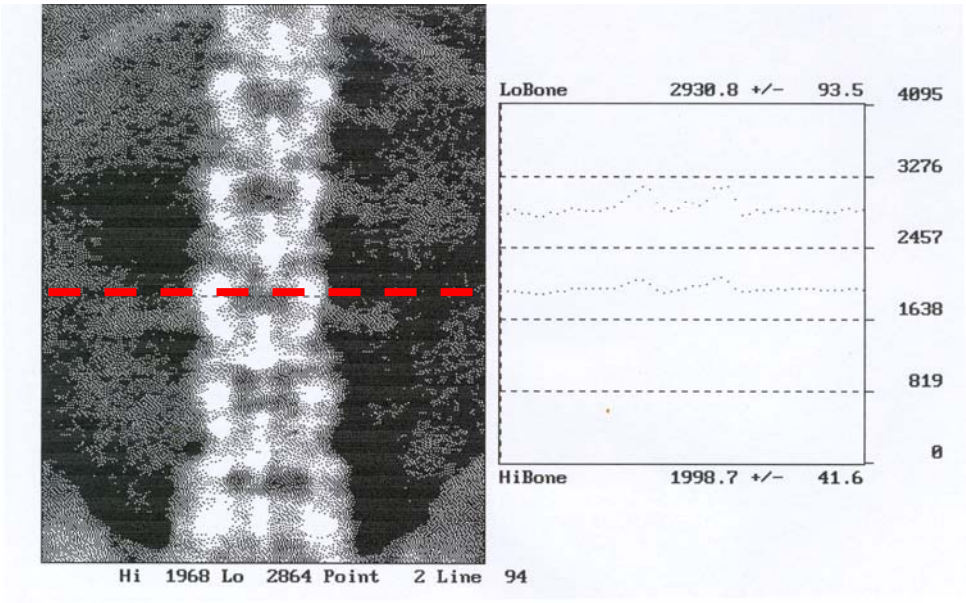

Figure 2.3b The Hologic QDR-1000W approach to measurement of bone mineral density. The high and low transmission factor profiles are shown for a single scan line (▬ ▬ ▬ ▬).

In practice the BMD values are displayed as a digital image with each pixel corresponding to a measurement point through the patient. In order to cover a larger section of bone numerous attenuation profiles are acquired along the length of the bone to form an image. The stages involved in BMD calculation are summarised in figure 2.4. Within the DXA algorithm R is estimated line-by-line over the image and averaged over soft tissue on either side of bone. An edge detection algorithm identifies the bone edge by applying a threshold value for BMD and designating pixels with a value greater than this as containing bone. The actual bone threshold used by Hologic for the QDR-1000W is unknown but it has been suggested that this value is 0.2 g/cm^2 as in in-vitro studies it has been found that no bone is registered below this (Mazess *et al.* 1991b; Nielsen *et al.* 1998; Tothill and Avenell 1998). The projected area of bone (cm^2) (BA) is the sum of the pixels within the bone edge. Within this area, the BMD of individual pixels is averaged and multiplied by the BA to calculate BMC.

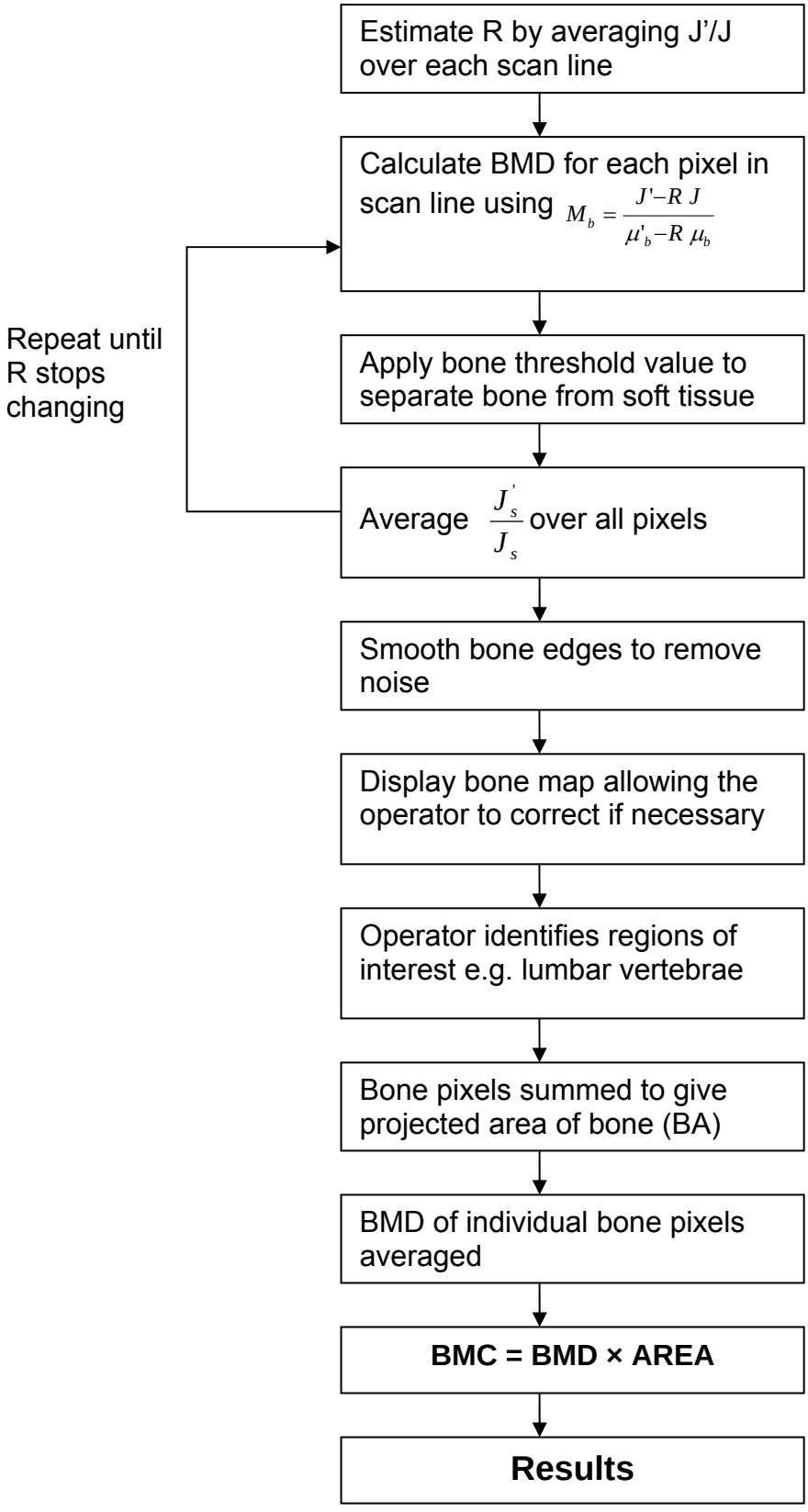

Figure 2.4 Stages involved in the calculation of BMD by dual energy X-ray absorptiometry modified from Blake *et al.* (1999).

2.3 Hologic QDR-1000W Dual-Energy X-ray Absorptiometer

The basic components of a DXA scanner were discussed in chapter 1 and for a Hologic scanner are shown in figure 2.5.

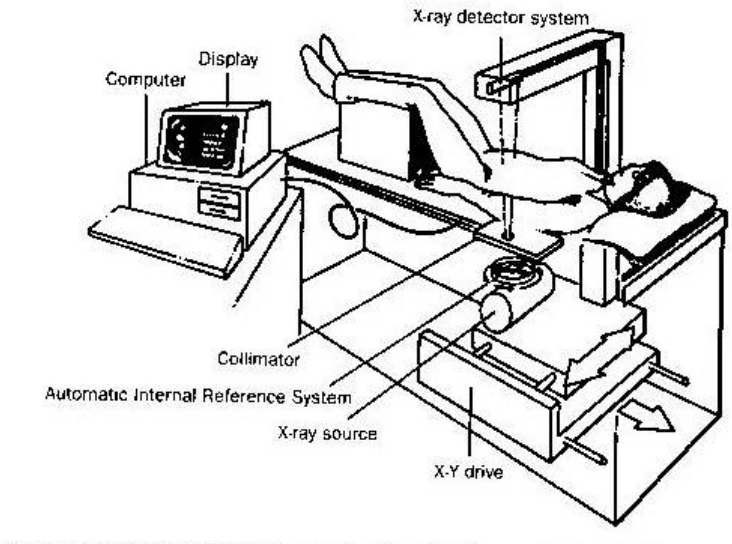

Figure 2.5 Components of a Hologic DXA scanner (Blake et al. 1999).

The Hologic QDR-1000W is a pencil beam scanner which acquires data line by line in a raster pattern. Dual-energy X-rays are produced by continuously switching the X-ray tube voltage between 70 kVp and 140 kVp giving X-rays of 45 and 100 keV (Fig. 2.6). The voltage is switched at the mains electrical supply frequency i.e. 50 Hz in the U.K.

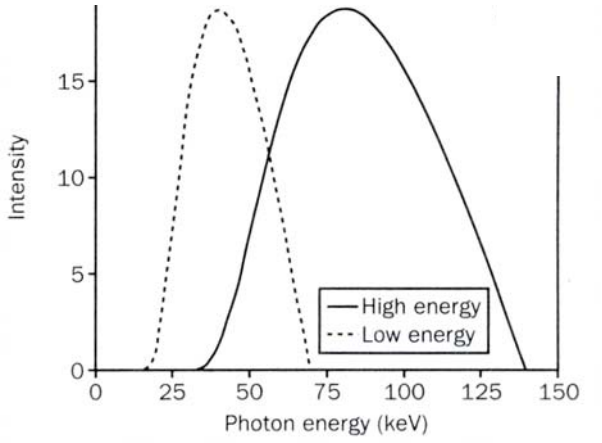

Figure 2.6 Typical X-ray spectra used for producing dual-energy X-rays with the kV-switching method (Blake *et al*. 1999).

There is inherent filtration of the X-ray beam due to the X-ray tube housing and also added filtration usually provided by aluminium filters. The disadvantage with this kV switching method is greater beam hardening where there is preferential attenuation of lower energy photons by body tissues leading to an increase in the average X-ray energy with penetration depth (Blake and Fogelman 1997b). As a result of beam hardening, the attenuation coefficients of bone and soft tissue decrease with body thickness leading to a false variation in measured BMD (Blake *et al.* 1992). Hologic overcome this problem by passing the beam through a spinning calibration wheel to measure energy dependent attenuation coefficients at each measurement point (Stein 1990; Blake *et al.* 1992). This wheel consists of an air gap, an epoxy resin filter equivalent to lean soft tissue and an epoxy resin & hydroxyapatite filter representing bone with a BMD of approximately 1 g/cm^2 (Fig. 2.7). Each sector is divided in two to account for the high and low energy cycles. The sector for the high energy beam contains a brass filter to preferentially remove lower energy photons thus hardening the beam and making it more monoenergetic before it enters the patient. Despite added filtration beam hardening will occur within the patient but attenuating the high energy beam will reduce this and the radiation dose will be decreased. Due to these filters each pixel in the image represents six transmission measurements for the three sectors at the two energies as shown in figure 2.8. The purpose of the calibration wheel is to ensure the calibration remains stable despite variations in soft tissue thickness between patients or scan site. The calibration will only be exact for a BMD equal to that of the bone equivalent material in the calibration wheel and a non-linear relationship exists for other BMD values. To overcome this Hologic use a linearity calibration phantom consisting of slabs of a bone mineral equivalent material in an acrylic block representing BMD values of 0.6, 1.0 and 1.6 g/cm^2 (Blake *et al.* 1992). The values from this factory calibration are used to derive calibration curves which are incorporated into an algorithm to correct BMD measurements. This linearity correction will only be accurate for regions of soft tissue with a thickness equivalent to that in linearity phantom.

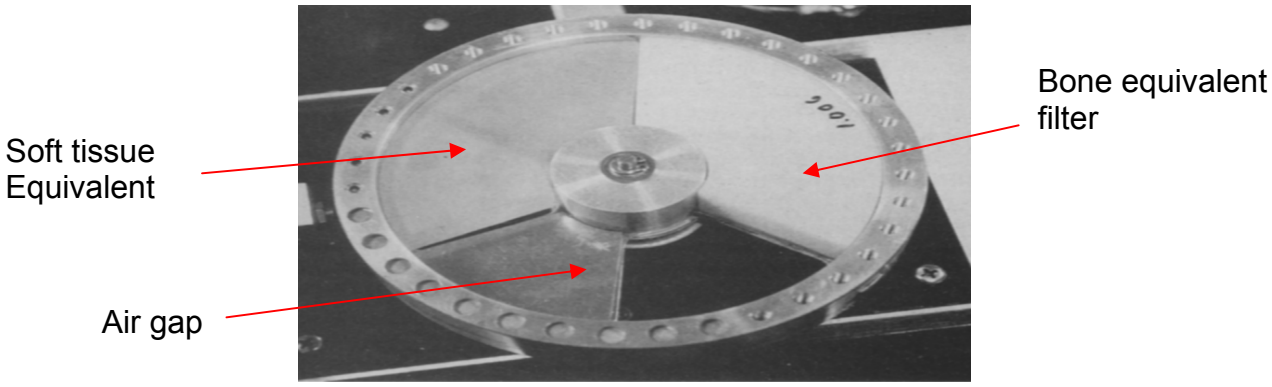

Figure 2.7 Hologic Calibration wheel showing sectors with bone and soft tissue equivalent materials and an air gap. Each sector has two segments – one with and one without a brass filter (Blake and Fogelman 1997b). The calibration wheel forms part of the automatic reference system in figure 2.5.

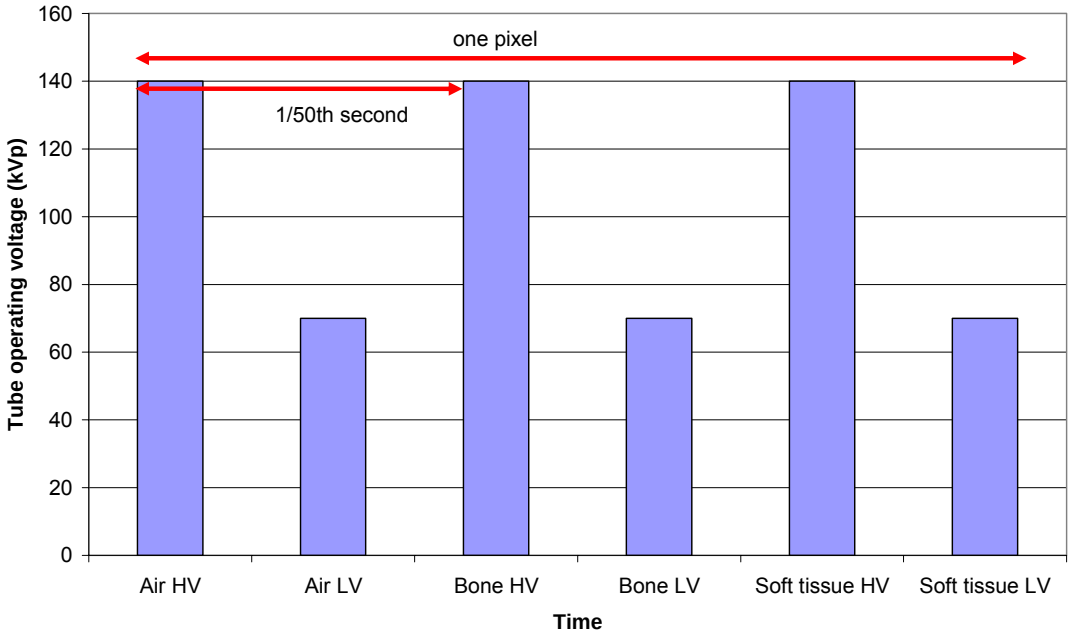

Figure 2.8 Voltage profile for Hologic scanner which produces the transmission information contained in each pixel. HV = high voltage, LV = low voltage.

In the QDR-1000W the photons transmitted through the body and calibration wheel are absorbed by a scintillation detector, a sodium iodide crystal, which converts the photon energy into optical radiation. The scintillation light is converted to an electrical signal by a photomultiplier tube (PMT) operated in current mode. A logarithmic amplifier produces an output signal proportional to the log of the transmission factor (J). The amplifier outputs are integrated for specified time periods. Suppose J', J'_b and J'_s represent the low energy attenuation factors for the air, bone and soft tissue sectors of the calibration wheel and J, J_b and J_s are those for the high energy. The change in the measured attenuation due to bone and soft tissue, accounting for the corresponding tissue calibration filters in the beam, are given by equations 2.19 and 2.20 respectively.

$$\Delta J'_{cb} = J'_b - J' \qquad (2.19a)$$

$$\Delta J_{cb} = J_b - J \qquad (2.19b)$$

$$\Delta J'_{cs} = J'_s - J' \qquad (2.20a)$$

$$\Delta J_{cs} = J_s - J \qquad (2.20b)$$

where the subscript c denotes the value measured with the calibration wheel. If M_{cb} and M_{cs} are the area densities of the bone mineral and soft tissue equivalent filters the effective attenuation coefficients are:

$$\mu'_b = \Delta J'_{cb} / M_{cb} \qquad (2.21a) \qquad \mu_b = \Delta J_{cb} / M_{cb} \qquad (2.21b)$$

$$\mu'_s = \Delta J'_{cs} / M_{cs} \qquad (2.22a) \qquad \mu_s = \Delta J_{cs} / M_{cs} \qquad (2.22b)$$

Replacing these in 2.13 gives:

$$M_b = \frac{(J' - (\Delta J'_{cs} / \Delta J_{cs}) J) M_{cb}}{\Delta J'_{cb} - (\Delta J'_{cs} / \Delta J_{cs}) \Delta J_{cb}} \qquad (2.23)$$

Let:

$$k = \frac{\mu_s^{'}}{\mu_s} = \frac{\Delta J_{cs}^{'}}{\Delta J_{cs}} \qquad (2.24)$$

$$Q = J^{'} - kJ \qquad (2.25)$$

$$d_0 = \Delta J_{cb}^{'} - k\Delta J_{cb} \qquad (2.26)$$

Using the substitutions 2.24 to 2.26 gives:

$$M_b = \left(\frac{Q}{d_0}\right) M_{cb} \qquad (2.27)$$

Equation 2.27 is the Hologic adaptation of equation 2.16 for a single X-ray path through bone. The modified R-value, k, is determined from the calibration wheel and so Q will be non-zero even for bone free regions. In theory, Q corrects for variations in soft tissue thickness and so should remain constant over soft tissue regions.

As discussed previously (section 2.2), a series of attenuation profiles are acquired over an area of bone and adjacent soft tissue, with the latter providing the soft tissue baseline. Once the bone pixels have been identified, Q_s for the baseline can be subtracted from Q for bone on the same scan line to calculate BMD as in equation 2.28. Equation 2.28 is equivalent to summation of the M_b values over all pixels in the image described earlier and it gives the total BMD value.

$$BMD = \left[\left(Q - Q_s\right) / d_0\right] BMD_{cal} \qquad (2.28)$$

Quantities k and d_0 are calculated by averaging over all points along the scan line. These parameters are dependent on the calibration and will vary with tissue thickness showing a decrease if the patient has gained weight. For the Hologic QDR-1000 a d_0 value less than 85 represents significant obesity. K and d_0 are displayed below the image on the DXA

report and should be examined to look for differences when performing serial measurements over time in the same patient.

For each scan site the Hologic QDR-1000W software has a variety of scan modes. The scan mode determines the speed of the scan with slower scan modes producing better quality images but with an increased radiation dose to the patient. The choice of mode depends mainly on abdominal thickness of the patient but faster scan modes are also used when the patient is unable to remain stationary. The QDR-1000W scan modes available for an AP lumbar spine scan include the Performance mode and Fast mode.

2.4 Calculation of Lumbar Spine BMD using the Hologic QDR-1000W Dual-Energy X-ray Absorptiometer

The lumbar spine usually has five vertebrae, denoted L1 to L5, and is located between the thoracic spine and the sacrum as shown in figure 2.9. Routine lumbar spine imaging is performed using an anterior-posterior (AP) projection with the patient supine and legs raised over a cushioned box as shown in figure 2.10. This position reduces lordosis and opens inter-vertebral spaces. The image should span L5 to T12 with L1 to L4 used for measurement as in figure 2.11. For a healthy lumbar spine the BMD, BA and BMC usually increase gradually from L1 to L4. For a healthy 30 year old caucasian female, the reference BMD used in the Hologic QDR-1000W software is 0.925±0.110 g/cm^2, 1.028±0.110 g/cm^2, 1.084±0.110 g/cm^2 and 1.116±0.110 g/cm^2 for L1, L2, L3 and L4 respectively. The combined L1 to L4 BMD is 1.047±0.110 g/cm^2. The ageing process and presence of vertebral fractures cause the distribution to become less uniform and the BMD results less reliable. Vertebrae with areas of abnormally high density, for example due to osteophytes or compression fractures, should be excluded from analysis.

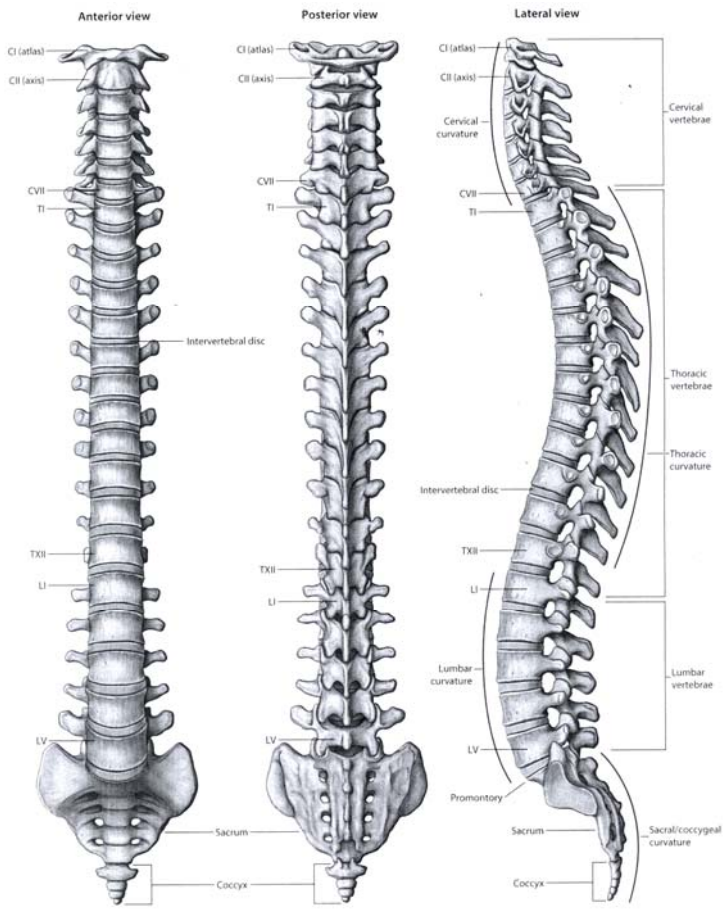

Figure 2.9 Anterior, posterior and lateral views of the human spine (Drake *et al.* 2008).

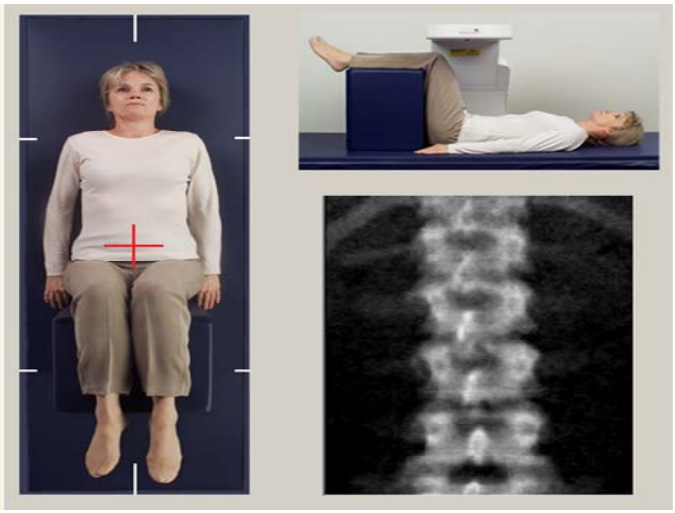

Figure 2.10 Position of patient for a DXA lumbar spine scan[3].

[3] Reproduced from Hologic work station

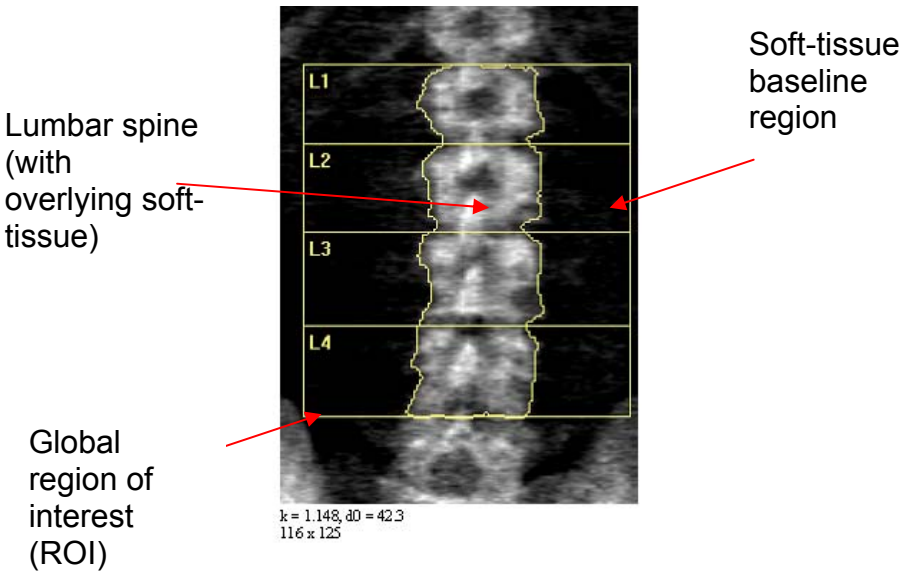

Figure 2.11 Analysis of a Hologic QDR-1000W AP lumbar spine image.

The attenuation of soft tissue overlying the spine cannot be directly measured and so is estimated from the ratio of the attenuation coefficients for the two X-ray beams in bone free regions adjacent to the vertebrae as in equation 2.18 (Fig. 2.11). The general method of BMD calculation is outlined in figure 2.4. In practical terms, the QDR-1000W lumbar spine software identifies what it believes to be soft tissue and displays it in blue. The average of all the soft tissue attenuation values within these pixels is calculated and subtracted from each pixel in the global region of interest (ROI). Only pixels left with a positive value are considered to be bone and displayed in yellow. The software automatically fills in any non-yellow pixels within the bone outline and removes any isolated yellow pixels outside the bone edge.

The method of soft tissue correction described above may not recognise bone with a relatively low BMD producing an incomplete bone map. The software will label any missed out bone as soft tissue consequently increasing the area density of the baseline and also the soft tissue attenuation coefficient. Hence there will be over-subtraction when compensating each bone-containing-pixel for the attenuation of overlying soft tissue. Thus some bone pixels with low BMD will not be recognised

as bone. The result is a falsely low BA and BMC producing a low BMD result.

The operator can manually paint in what they perceive to be bone to correct the bone map. However, the added tissue will not be recognised as bone and will still contribute to the soft tissue baseline. Painting in bone may reduce the measured BMD further as the BA will increase without an increase in BMC (Hipgrave 2010; Kelly 2010). Modern scanners have an “auto-low density” feature which is activated if the BMD is low and adjusts the bone threshold algorithm (Kelly 2006). When the bone map is incomplete including more soft tissue in the global ROI may improve the accuracy of the bone map because more sampling points are used in the soft tissue baseline. This is the recommended approach rather than painting in bone.

After the bone has been identified and the soft tissue correction applied, markers are placed in the inter-vertebral spaces (Fig. 2.11). The BMD of individual vertebrae is calculated from averaging the BMD of all bone containing pixels over the BA to give the average BMD. The BMC is calculated from multiplication of BMD by BA.

2.5 Effect of Changes in Soft Tissue on Hologic QDR-1000W Lumbar Spine BMD Measurements

The relative amount of fat and lean tissue within soft tissue varies throughout the body. The DXA technique does not account for the difference between the thickness and/or composition of soft tissue anterior and posterior to bone and that in the bone-free baseline region. It is therefore likely that the presence of fat will affect the accuracy and precision of BMD measurements. The influence of soft tissue depth and composition on lumbar spine BMD measurements has been investigated in-vivo and in-vitro by others (Hangartner and Johnston 1990; Laskey *et al.* 1991; Blake *et al.* 1992; Martin *et al.* 1993; Tothill *et al.* 1995; Barthe *et al.* 1997; Yu *et al.* 2012). Results from published studies investigating the

dependence of BMC and/or BMD on soft tissue distribution vary depending on scanner type and software version (Sobnack *et al.* 1990; Laskey *et al.* 1991; Tothill *et al.* 1995; Barthe *et al.* 1997; Tothill and Avenell 1998). Also, for in-vitro studies the phantom design will affect measurements and therefore influence the conclusions drawn from the study.

In order to account for three body components, i.e. fat, bone mineral and lean tissue, each with an unknown tissue thickness, three equations are required (Kotzki *et al.* 1991). Attempts at using triple energy photon absorptiometry to account for fat were unsuccessful due to the high photon flux that was necessary to achieve sufficient precision. This required a radionuclide source with a relatively high activity introducing concerns over radiation safety (Farrell and Webber 1990). A continuous X-ray spectrum can be used to measure bone mineral accurately and remove the dependence on soft tissue fat content or body thickness. However, the penalty with this technique is a lower precision compared to DXA (Swanpalmer *et al.* 1998). Another approach that has been used to improve the accuracy of DXA BMD measurements involved two transmission equations, as in the standard DXA technique, and the addition of a third equation for the total path length of the X-ray beam within the body (Michael and Henderson 1998). The total path length represents the sum of the X-ray path length through fat, lean tissue and bone mineral. These three equations allowed resolution of a three-component model thus removing the dependence of BMD measurements on soft-tissue composition. Using Monte Carlo modelling, Michael and Henderson (1998) showed that the accuracy of BMD measurements was improved using this method as lean and fat were considered separately; however, the precision was poorer than that of the standard DXA technique.

It is common to perform longitudinal BMD measurements to monitor changes in BMD. A change in the patient's body mass index (BMI) between scans may be related to a change in soft tissue thickness and/or

the relative amounts of fat and lean within the tissue. Potentially such changes could give a false result for changes in BMD and it is therefore important to distinguish true BMD changes from those due to tissue changes. The manufacturer's calibration is performed assuming a certain tissue thickness, which is 16 cm for the Hologic linearity phantom (Blake *et al.* 1999), and therefore errors will be introduced for different tissue thickneses (Blake *et al.* 1992).

Studies have been published that show there are apparent changes in lumbar spine BMD due to weight change with many reports of BMD decreasing with weight loss (Martin *et al.* 1993; Svendsen *et al.* 1993c; Ramsdale and Bassey 1994; Tothill and Avenell 1998). There have been unexpected observations of changes in BMC exceeding those for BMD due to an increase in BA. These findings suggest that some of the change in lumbar spine BMD during weight loss may be due to this anomaly (Tothill and Avenell 1998). In these studies, a change in BA was not thought plausible physiologically or anatomically. When a correlation between BMC and BA has been observed it has been concluded that changes in BMD are underestimated (Peel and Eastell 1995; Tothill and Avenell 1998). Assuming BMC is measured accurately, these anomalous observations are likely to be the result of the inaccurate identification of the bone edge as discussed previously. As the number of bone containing pixels increases, the BA will increase and therefore it is logical that the BMC increases. This was confirmed by studies that measured a higher BMD with a user defined rectangular ROI to demarcate bone instead of relying on the edge detection algorithm (Tothill and Avenell 1998).

The work in this thesis will focus only on the magnitude of errors in lumbar spine BMD introduced by the non-uniform distribution of abdominal fat.

2.6 Effect of a Non-Uniform Distribution of Abdominal Fat on Lumbar Spine Bone Mineral Density Measurements with DXA

The measurement of lumbar spine BMD by DXA assumes that fat is distributed uniformly across the abdomen. This assumption is violated due to the presence of fat around organs, variations in subcutaneous fat thickness and the presence of fat within yellow bone marrow (YM). There are also fat depots throughout most body tissues including muscle. Within the abdomen there is intra-abdominal fat, sometimes called visceral fat, located inside the abdominal cavity between organs. Visceral fat is composed of fat depots and includes the perirenal depots around the kidneys. In the region of the lumbar spine there are a variety of structures so the fat and lean composition of the soft tissue in the baseline, used for BMD calculation, is unlikely to be identical to that overlying the spine (Fig. 2.12). This will influence the accuracy and precision of BMD measurements.

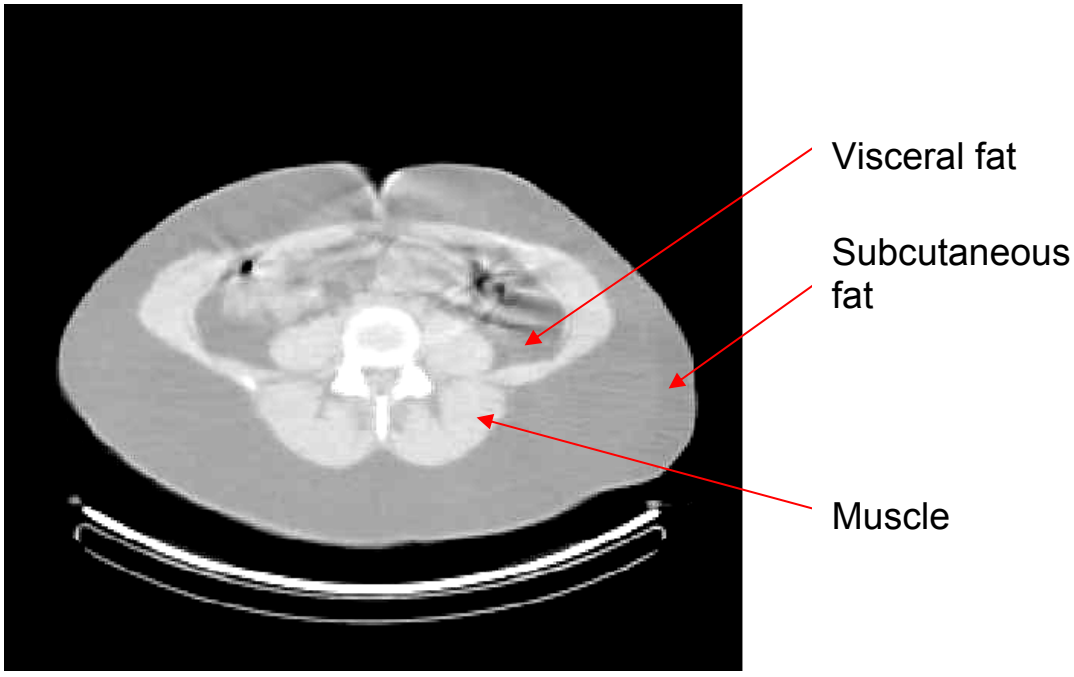

Figure 2.12 Abdominal CT scan at the level of L4 to L5. Acquired at the University Hospital of Wales Cardiff.

If the thickness of fat within the soft tissue adjacent to the lumbar spine is greater than in soft tissue overlying it, the BMD will be overcorrected by the software and reported falsely high. Similarly, if there is less fat in the bone free region, there is an under-correction and the BMD is reported lower than the true value. This has been demonstrated in phantom studies using the QDR-1000 and QDR-1000W. Hansen *et al.* (1990) showed for the Hologic QDR 1000 that when using lard to simulate fat: (1) a simultaneous change in fat over and adjacent to a bone does not significantly affect BMD results; (2) an increase in fat thickness adjacent to the bone increases lumbar spine BMD; and (3) an increase in fat thickness over bone decreases BMD. Similar observations have been reported by others (Cullum *et al.* 1989; Hangartner and Johnston 1990). For the Hologic QDR-1000W, the expected change in BMD due to fat, whilst keeping the combined lean and fat thickness constant, has been reported as 0.044 g/cm^2 per cm of fat (Hangartner and Johnston 1990) which was similar to the value of 0.043 g/cm^2 measured by Tothill and Pye (1992).

For Hologic scanners it appears that increasing the width of the global lumbar spine ROI causes an increase in the reported BMD for in-vitro and in-vivo studies (Hansen *et al.* 1990; Tothill and Pye 1992). This increase is the consequence of more soft tissue falling within the baseline thus changing the average tissue composition and subsequently the attenuation value used for soft tissue compensation.

Computed tomography (CT) images of the abdomen provide cross-sectional images from which it is possible to directly measure fat thickness and quantify the difference over and adjacent to the vertebrae. From abdominal CT scans it has been shown there is a higher amount of fat in the baseline region than over the vertebrae (Tothill and Pye 1992; Tothill and Avenell 1994a; Formica *et al.* 1995; Svendsen *et al.* 1995; Svendsen *et al.* 2002). There have been different ways of expressing this difference as shown in table 2.1. The usual anatomical sites for acquisition of CT images used to investigate fat distribution appear to be

L4-L5 and T12-L1. There are reports that the distribution of fat is less uniform at the level of L4-L5 than T12-L1 due to the variety of body structures within that region (Svendsen *et al.* 2002).

Reference	Quantity used to determine in-homogeneity in abdominal fat	Difference between quantity in soft tissue in baseline region and soft tissue anterior & posterior to vertebrae (Baseline – over vertebrae)
Farrell and Webber (1989)	Percentage fat measured from CT images	4.4% (range: -2.7% to 18.7%)
Tothill and Pye (1992)	Fat thickness measured from CT images	6.7±8.1 mm (men) 13.4±4.7 mm (women)
Formica *et al.* (1995)	Area of fat (cm^2) from QCT images	6.3 cm^2 (Pre-menopausalwomen) 7.5 cm^2 (Post-menopausal women)
Tothill and Avenell (1994a)	Fat thickness from CT images for L2 to L4 level	Men = 14±9 mm Women = 17 ± 9 mm
Svendsen *et al.* (2002)	Percentage fat from CT images at the L4-L5 level	Baseline: 7.5% After weight loss: 10.4%
Svendsen *et al.* (1995)	Percentage fat from CT images for 1^{st} to 4^{th} inter-vertebral space	6.5%

Table 2.1 Quantification of the difference in fat between bone and non-bone regions at the level of the lumbar vertebrae using CT images.

A simultaneous change in fat thickness over and adjacent to the spine during weight loss is unlikely to affect the accuracy due to a non-uniform fat distribution. Tothill and Avenell (1994a) showed using CT scans that the amount of fat over the vertebrae relative to that in the baseline does not change significantly during weight loss. These findings suggest that the error due to non-uniform fat deposition will remain constant and hence not introduce further errors into follow-up BMD measurements used for monitoring (Tothill *et al.* 1994a). Other researchers have shown that the change in soft tissue during weight loss causes a minor theoretical decrease in lumbar spine BMD at L4-L5 level (Svendsen *et al.* 2002).

Measurement of FM and percentage fat (%fat) within soft tissue is possible from DXA WB scans and will be discussed in section 2.7. Formica *et al.* (1995) used the Lunar DPX DXA system to measure %fat in regions adjacent to the vertebrae to estimate the fat in the soft tissue baseline used in spine AP scans. However, to estimate the error in BMD due to an inhomogeneous fat distribution CT measurements of fat were used.

Errors in BMD and BMC measured with DPA resulting from the presence of fat have been estimated to be between 3 and 10% (Roos *et al*. 1980; Gotfredsen *et al*. 1988). For DPA measurements, the fat content in the capsules of the kidneys has proved to cause a non-systematic inaccuracy (Roos *et al.* 1980). Also with DPA, Valkema *et al.* (1990) reported errors of 0.7% and 1.5% in BMC for healthy and osteoporotic patients respectively due to variations in the soft tissue baseline.

Bone mineral equivalence (BME) factors (BEF) have been measured for the Hologic QDR-1000 to convert the difference between the thickness of fat within bone regions and non-bone regions into an error in BMD measurement. Svendsen *et al.* (1995) used the BEF measured by Hangartner and Johnston (1990) in an equation which incorporated the abdominal thickness to estimate the theoretical error in spinal BMD. The error in lumbar spine BMD, at the L4 to L5 level, due to the fat distribution

was estimated to be -0.105±0.014 g/cm^2 and -0.129±0.012 g/cm^2 for a group of subjects pre- and post- weight loss respectively. Also using this method an accuracy error of 0.03 g/cm^2 (or 3-4%) for the AP spine BMD was estimated.

Using CT images to quantify the inhomogeneity in fat at the level of the lumbar spine, Tothill and Pye (1992) reported that BMD would be overestimated by 0.029 g/cm^2 in men and 0.057 g/cm^2 in women with the error exceeding 0.1 g/cm^2 in 10% of the CT images examined.

Bolotin *et al.* (2003) devised a series of simulations using phantoms composed of an array of materials to replicate bone material, red marrow (RM), YM and extra-osseous fat and lean in various amounts and configurations. By simulating a non-uniform extra-osseous fat distribution, they demonstrated that inaccuracies as high as 20-50% can occur in certain situations e.g. when the BMD is low or for elderly patients.

2.7 Body Composition Analysis using DXA

DXA scanners have the capability of performing a scan of the whole body (Fig. 1.12 and 2.14). FM, LM, and bone mineral can be measured from the X-ray attenuation data contained in these images. To acquire a WB scan, the patient lies supine on the scanning couch with arms and legs next to the body. Careful preparation of the patient is necessary to remove any metallic or high density articles of clothing or jewellery which would cause a false result. The Hologic QDR-1000W acquires the scan in a raster pattern with a calibration phantom, such as that shown in figure 2.13 placed next to the patient. The calibration method is discussed later.

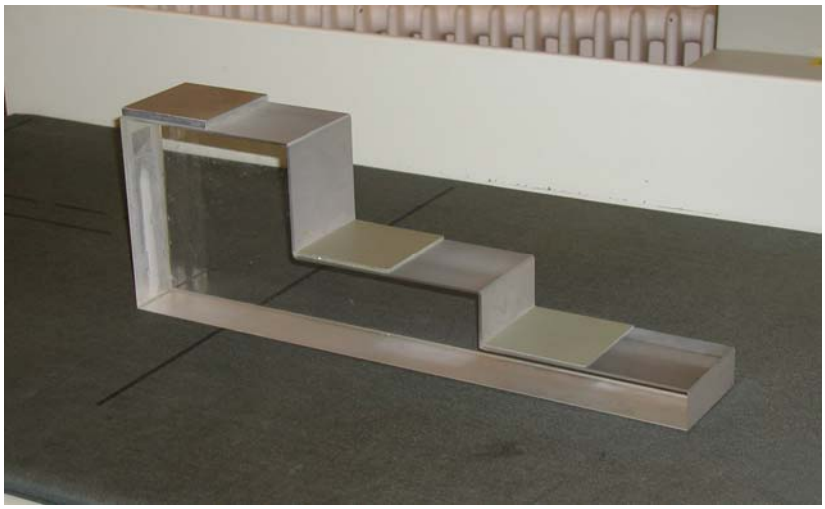

Figure 2.13 Calibration phantom which is placed next to the patient to perform a whole body scan for the Hologic QDR-1000W.

The software reports FM, LM, percentage fat (%fat), BMC, BA, BMD and the summed FM, LM and BMC for the total body or specific regions. An example of results is shown in chapter 1 (Fig. 1.11). The QDR-1000W also has a sub-regional analysis facility to allow the user to place analysis regions of any size at any location (Fig. 2.14). Long term stability of FM and LM measurement has been assessed by others from repeatedly scanning a series of frozen meat samples with a known fat content. Over an 11 month period, the precision of FM and non-fat mass was found to be 4.2% and 0.5% respectively (Blake et al. 1999). Routine quality control checks for FM and LM were not carried out on the QDR-1000W scanner in Cardiff. As the patient and a calibration phantom were scanned simultaneously, it was assumed the calibration remained stable over time.

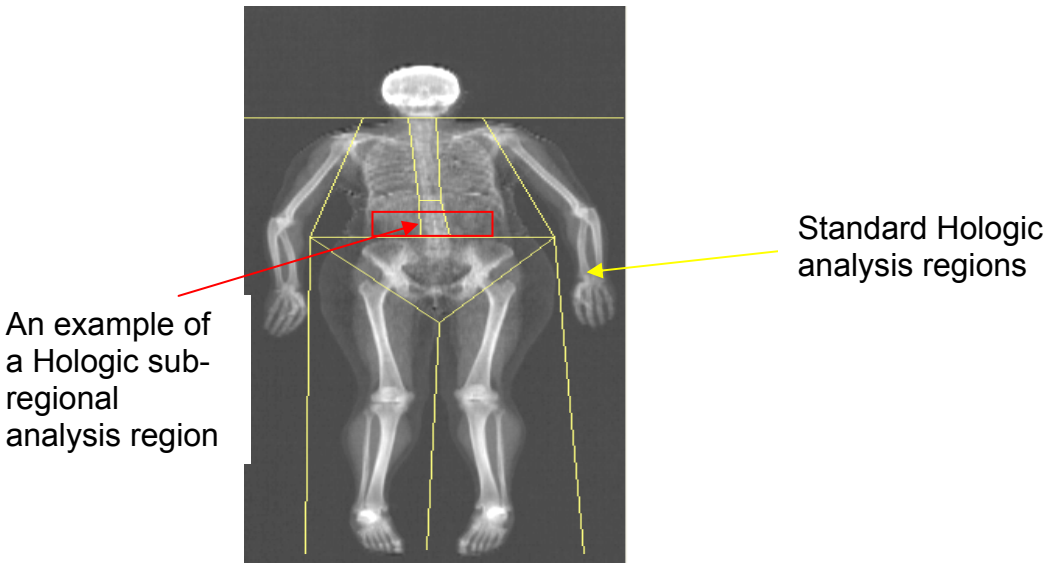

Figure 2.14 A Hologic QDR-1000W whole body image showing the standard analysis regions and an example of a sub-regional analysis box for measurement of abdominal soft tissue composition.

The basis for body composition analysis (BCA) is the DXA algorithm discussed previously for regional BMD calculation. The method is discussed more fully by Blake *et al.* (1999) and only summarised here.

As with lumbar spine BMD measurement, J is the logarithmic attenuation factor, M is the area density (g/cm^2), μ is the mass attenuation coefficient and b and s represent bone mineral and soft tissue respectively. Measuring the transmitted intensities and solving the simultaneous equations allows measurement of M_b and M_s (equations 2.13 & 2.14).

These equations calculate total body bone mineral (TBBM) but not the properties of soft tissue. However, in bone free pixels $M_b = 0$ with equations 2.13 & 2.14 becoming equation 2.29. The two X-ray energies used in DXA can be used to decompose soft tissue into fat and lean for body regions that do not contain bone. However, the difference in the attenuation coefficients of fat and lean is much less than between bone mineral and soft tissue and so additional calibration is needed.

$$M_s = \frac{J'}{\mu_s'} = \frac{J}{\mu_s} \qquad (2.29)$$

As the R-value is the ratio of soft tissue attenuation coefficients, denoted as R, then:

$$R = \frac{\mu_s'}{\mu_s} = \frac{J_s'}{J_s} \qquad (2.30)$$

The software initially identifies pixels containing bone, tissue and air. In the non-bone regions the R-value represents the combined fat and lean composition of the tissue. The calibration process is complex due to the beam hardening effect which causes the relationship between R and tissue composition to be dependent on tissue thickness.

To calibrate the Hologic QDR-1000W an acrylic/aluminium step phantom is used which has a primary calibration to fat, in the form of stearic acid, and a lean material (water). The calibration is performed in accordance with the standards proposed by Nord and Payne (1990). Each of the six steps in the phantom contain a different combination of acrylic and aluminium to represent the physiological range of tissue thickness and composition found in the human body (Kelly *et al.* 1998). The acrylic is equivalent to 68% fat and 32% lean and the water is equivalent to 8.6% fat and 91.4% lean. The ratio of low to high attenuation pairs through the phantom gives a series of R-values which are used to form calibration curves, examples of which are shown in figure 2.15. The R-value is plotted on the vertical axis and the high energy attenuation, which is proportional to tissue mass, is plotted on the horizontal axis (Blake *et al.* 1999). The calibration grid consists of a series of six lines each with a constant fat and lean composition. From the measurements of J and R for each of the bone-free pixels in the image, %fat can be calculated. In regions containing bone, the soft tissue composition cannot be measured directly and therefore the composition adjacent to the bone must be measured and interpolated linearly across the bone (Kelly *et al.* 1998). In a projection image of the body, approximately 40% of the pixels contains

bone and soft tissue and 60% of pixels soft tissue only. The stages involved in BCA analysis are summarised in figure 2.16.

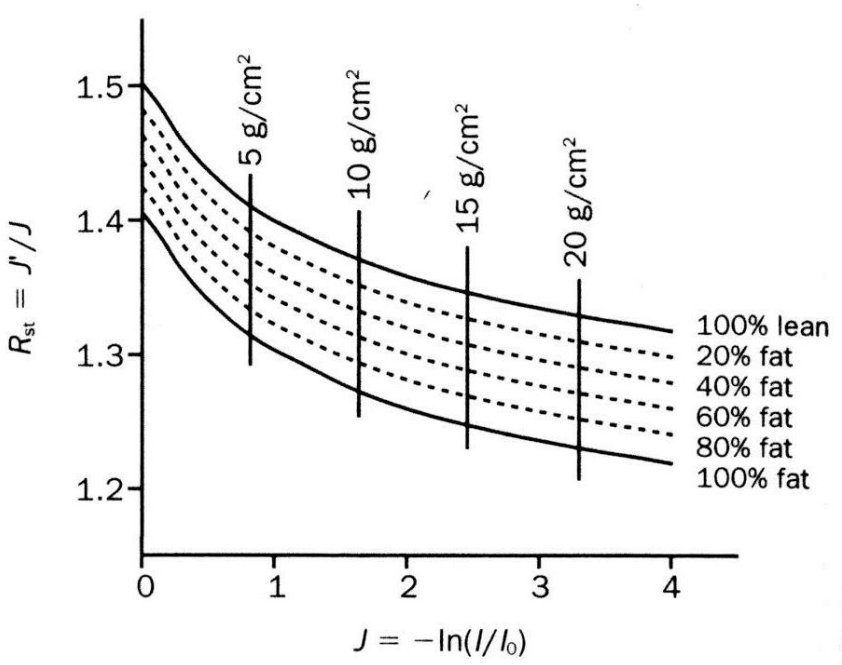

Figure 2.15 Calibration curves used for body composition measurement by DXA (Blake *et al.* 1999).

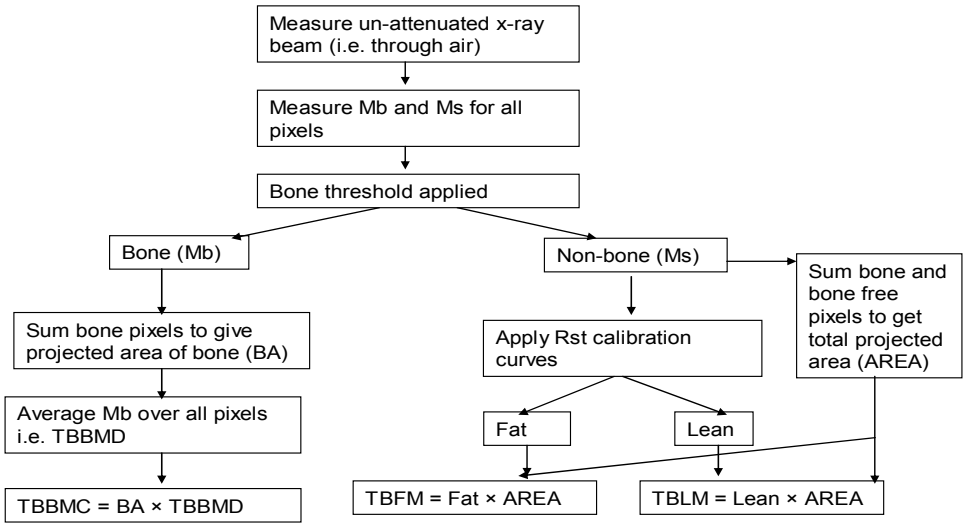

Figure 2.16 Stages in algorithm based on description in Blake *et al.* (1999).

2.8 Precision and Accuracy of Body Composition Measurements with DXA

Published work indicates that the accuracy and precision of BCA measurements are dependent on the manufacturer, scanner model, and software version (Mazess *et al.* 1991a; Tothill *et al.* 1994b; Tothill *et al.* 1994c; Laskey 1996; Tothill *et al.* 1997; Tothill *et al.* 1999; Tothill 2005). A detailed review has been carried out by Nord (1998). These differences are likely to be attributable to variations in the soft tissue distribution models used by each manufacturer (Tothill *et al.* 1999). Significant inconsistencies in BCA measurements have been found when upgrading from a pencil beam to fan beam system (Ellis and Shypailo 1998; Tothill *et al.* 2001). Each standard WB analysis region has a corresponding soft tissue distribution assumption. In regions containing a large proportion of bone, e.g. thorax, the accuracy of the BCA results is limited (Roubenoff *et al.* 1993; Nord 1998; Blake *et al.* 1999). The long term precision of total body BCA measurements made with the QDR-1000W has been quoted as 0.6% for TBBMD, 0.5% for non-fat mass, 0.4% for total body mass and 4.2% for FM (Blake *et al.* 1999). Short term precision is expected to be better than long term precision. For BMD measurements, the long term precision has been reported as double that for short-term measurements (Tothill and Hannan 2007).

The accuracy and precision for in-vitro studies using standard WB software will depend on the phantom design and the body region which is used for analysis. This is due to the fat distribution model within that region (Tothill *et al.* 2001). The most reliable results are likely to be for an anthropormorphic shaped phantom which fills all the analysis regions, such as that designed by Shypailo *et al.* (1998).

The accuracy of changes in TBBMC and TBBMD due to weight change is a matter of debate with conflicting results depending on scanner and software version (Tothill *et al.* 1997; Tothill *et al.* 1999). There are reports of changes in TBBMD being positively correlated with changes in weight (Compston *et al.* 1992; Tothill *et al.* 1999; Tothill 2005), TBBMC

correlating with weight change (Tothill *et al.* 1997; Tothill 2005) and also the unexpected observation of the TBBMD increasing with loss of weight due to an increase in BA (Tothill *et al.* 1997). It has been suggested that some of the observed changes in TBBMD measurements during weight change using Hologic systems are false and the results will vary depending on the software version used for analysis (Tothill *et al.* 1999). This is supported by the observations of the reported BA changing even when this is not plausible (Tothill *et al.* 1997; Vestergaard *et al.* 2000).

The current study focuses on lumbar spine BMD, WB scans are used only for the measurement of FM. Therefore the influence of fat on TBBMD will not be discussed further in this work.

2.9 Precision and Accuracy of Fat Mass Measurement with DXA

Compared to bone mineral measurements, relatively little data is available for the accuracy and precision of FM measurements using the Hologic QDR-1000W. However, the long term precision of FM has been estimated to be 4.2% for the QDR-1000W (Blake *et al.* 1999).

In an attempt to assess the accuracy of FM measurements, Jebb *et al.* (1995) observed that the amount of fat detected by DXA was dependent on tissue depth and questioned the validity of WB algorithms. The accuracy with which DXA measures simulated changes in FM are variable. Milliken *et al.* (1996) found the Lunar DPX-L underestimated fat added to the trunk by approximately 50% which was similar to the observations by Snead *et al.* (1993) using the Hologic Enhanced Whole Body software version 5.50. When repeating the work of Snead *et al.* using version 5.64 of the WB software, Kohort (1998) found the QDR-1000W accurately quantified fat placed over the trunk and thighs of a human subject. Tothill *et al.* (1994c) also demonstrated how later versions of software can improve results.

It is difficult to assess in-vivo accuracy as techniques used to validate DXA have associated errors. Numerous studies exist that validate in-vivo

BCA measurements by DXA against other methods such as skinfold thickness, bioelectric impedance, the four-compartment model and direct tissue analysis. These other methods of BCA are reviewed in depth elsewhere (Sheung and Huggins 1979). Of the methods available, the 4-compartment model is likely to be the most accurate as it accounts for fat, water, protein and mineral (Prior *et al.* 1997). It has been found that the amount of fat measured with the Hologic QDR-1000W correlates well with estimates from a 4-compartment model. These results lead the authors to conclude that body fatness estimates by DXA are accurate (Prior *et al*. 1997). Of concern are reports that for both in-vivo and in-vitro studies, the Hologic QDR-1000W underestimates fat when the actual fat proportion is low (Arngrimsson *et al.* 2000; Tothill *et al.* 2001). Compared to other methods of BCA, DXA is a relatively simple method of measuring total and regional body composition.

2.10 Can Whole Body Fat Mass Data be used to Quantify the Inhomogeneity in Abdominal Fat in the Region of the Lumbar Spine?

In this investigation, the distribution of abdominal fat will be quantified from DXA WB images using the Hologic QDR-1000W sub-regional analysis tool which is an extension of the enhanced whole body analysis protocol.

Abdominal fat has been measured by others from WB scans acquired with DXA by defining analysis regions from the superior border of L2 to the inferior border of L4 or that of the iliac crest and extending across the width of the body (Formica *et al.* 1995; Bertin *et al.* 2000; Kamel *et al.* 2000; Park *et al.* 2002). These studies measured the total fat within this region and not the homogeneity of the fat distribution and therefore are different to the work presented in this thesis.

The precision and accuracy of BCA measurements in the thorax are likely to be compromised due to the ribs as soft tissue overlying bone cannot

be directly measured. This was supported by Park *et al*. (2002) who observed, for the Lunar scanner, a degradation in precision of FM measurement due to the ribs. The authors report that the coefficient of variation for the FM in a region extending across the abdomen from L2 to L4 and to the upper iliac crest was smaller than that for regions extending from lower costal to upper iliac (Park *et al.* 2002). When using sub-regional analysis to measure abdominal fat distribution, bony structures should be avoided whenever possible.

CT images have been used to validate abdominal fat measured by DXA (Svendsen *et al.* 1993b); however the limitation with this comparison is that CT measures adipose tissue whereas DXA measures fat. Also, DXA does not distinguish between intra-abdominal fat (IAF) and subcutaneous fat. In one such study it was concluded that when compared to CT measurements, DXA could be used to determine abdominal adiposity (Glickman *et al.* 2004).

In order to compensate lumbar spine BMD for overlying soft tissue, ideally the abdominal FM and lumbar spine BMD should be measured from a single scan. There have been publications showing abdominal fat can be estimated from AP lumbar spine scans, acquired with Lunar DPXL scanner (Suh *et al.* 2002; Leslie *et al.* 2010). The advantage of this method is that the BMD of the spine and the abdominal FM are measured simultaneously from a single radiation exposure with the patient in the same position to improve the accuracy of matching the soft tissue region used for lumbar spine analysis with that extracted from a WB image.

No published work has been found that assesses the accuracy or precision of the Hologic QDR-1000W WB sub-regional analysis tool for quantification of abdominal fat distribution.

2.11 Summary

A review of relevant literature indicates the assumptions inherent in the DXA technique are not valid. A difference in soft tissue composition in the X-ray path through the bone from that in an adjacent soft tissue region has been proven.

The use of DXA for body composition studies using the standard software supplied by the manufacturer has been questioned (Roubenoff *et al.* 1993). However, as this work uses the Hologic sub-regional analysis tool it is likely that the soft tissue distribution assumptions incorporated into the software will not influence the FM measurements.

Published reports of attempts at quantifying the inhomogeneity in abdominal fat and estimating the potential errors in BMD have used CT scans. Therefore an entirely new method of extracting the abdominal fat profile from a WB DXA image is required.

Initially validation studies were carried out to investigate the possibility of combining lumbar spine BMD measurements and the FM from WB scans with a view to quantifying the impact of the in homogeneity in abdominal fat on BMD measurements.

Chapter 3

Validation of Hologic QDR-1000W Lumbar Spine and Body Composition Software to Measure Fat Thickness in the Baseline of the Lumbar Spine ROI from WB Images

3.1 Introduction

In this chapter techniques that will be used for the research itself will be validated. This includes the influence of the lumbar spine ROI width on bone mineral density (BMD) measurements of a phantom and the use of DXA whole body (WB) scans for sub-regional body composition analysis (BCA) and the possibility of linking data from lumbar spine and WB scans.

DXA lumbar spine BMD measurements are dependent on machine calibration. Quality control (QC) checks are performed to check calibration, precision and detect drifts in performance before failure allowing precautionary measures to be taken.

Lumbar spine BMD measurement is dependent on the thickness of fat and lean tissue within a baseline region adjacent to the vertebrae as shown in figure 2.11. The width of this region of interest (ROI) can be set

by the user, however, Hologic recommend a default width of 11.5 (119 lines) for the QDR-1000W. For a precise BMD measurement, the ROI must include sufficient soft-tissue to provide a bone-free baseline. It has been reported that, for the QDR-1000W, the BMD appears to increase as the width of the ROI increases due to the composition of soft tissue within the baseline changing (Hansen *et al.* 1990; Tothill and Pye 1992). As a foundation to the current work it was decided to investigate the effect of the ROI width using a phantom with a fixed BMD and uniform soft-tissue baseline.

As discussed in previous chapters, it has been proven that there is an inhomogeneity in abdominal fat thickness which potentially introduces errors in DXA lumbar spine BMD measurement. So far the inhomogeneity in abdominal fat has only been quantified from CT scans (Tothill and Pye 1992; Tothill and Avenell 1994a; Formica *et al.* 1995; Svendsen *et al.* 2002).

To investigate a link between reported BMD and fat thickness in the soft tissue baseline in the current work, a method of quantifying fat thickness was required. Soft tissue attenuation data is potentially available within lumbar spine images but a calibration to separate fat and fat-free tissue, such as that using the step phantom for WB scans, is needed. To overcome this problem for the Hologic QDR-1000W scanner, the soft tissue composition in a region equivalent to the lumbar spine baseline was extracted from WB scans.

The validity of extracting abdominal fat thickness from WB scans is dependent upon the accuracy of the Hologic WB sub-regional analysis software which reports BMD, BMC, BA, FM, LM and percentage fat (%fat) within a user defined area.

The accuracy and precision of the standard Hologic QDR-1000W software has been assessed by others, as discussed in chapter 2, and is not the aim of this work. No publications were found that test the sub-regional analysis software and therefore that was one aim of this chapter.

The area density of fat is derived from the division of reported FM by the area of the analysis region. The fat thickness is then calculated by dividing this area density by the physical density of fat which was taken to be 0.95 g/cm^3. Hologic quote dimensions in terms of “lines” and supply line-spacing and point resolution conversion factors to convert lines into metric units. The accuracy of the area measurement is therefore dependent on these factors.

A source of uncertainty in the proposed method to investigate the influence of abdominal fat on lumbar spine BMD is the accuracy of matching the soft-tissue region chosen from WB scans with the soft tissue baseline within the lumbar spine ROI. Also, combining data from two separate scans poses problems as they involve different patient positioning, scan modes and software algorithms.

The aims of this chapter were:

- To demonstrate that, for BMD measurements, the DXA scanner was stable over the period of the study.
- To determine the effect of the width of the lumbar spine ROI on measured lumbar spine BMD, BMC and BA.
- To investigate the minimum width of ROI that produces a complete lumbar spine bone map.
- To determine the accuracy of dimensions quoted by the WB sub-regional analysis software and subsequently confirm the value of the point resolution and line spacing factors.
- To investigate the linearity and accuracy of WB body composition measurements using the sub-regional analysis software.
- To investigate the validity of combining the data from lumbar spine and WB images.

3.2 Quality Control for DXA Bone Mineral Density Measurements

3.2.1 Method

Routine QC checks are performed on the Hologic QDR-1000W at the University Hospital of Wales (UHW) with the Hologic QDR-1 spine phantom (Serial no. Q-946) shown in figure 3.1. This consists of a model of vertebrae L1 to L4 moulded from hydroxyapatite mixed in epoxy resin embedded in a homogeneous epoxy resin block. The vertebrae have a nominal BMC of 57.5 ± 0.4 g, BA of 54.2 ± 0.4 cm^2 and BMD of 1.061 g/cm^2. The material surrounding the vertebrae acts as the soft tissue baseline. The phantom was scanned and analysed in accordance with manufacturer's instructions.

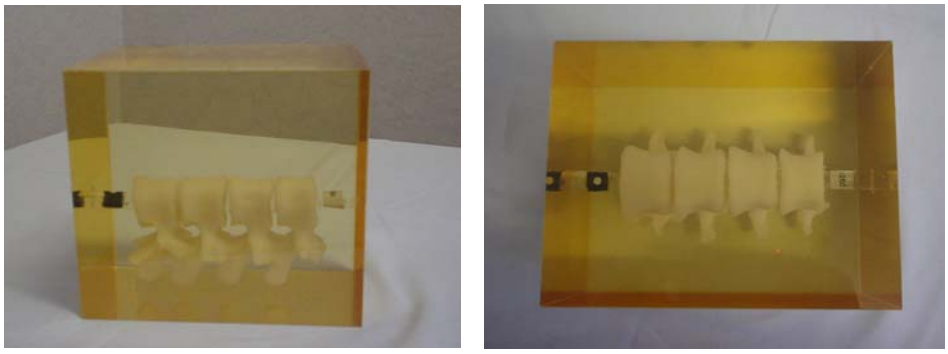

Figure 3.1 Hologic spine phantom used for routine quality control checks and used in the current work to examine the influence of ROI width on BMD measurements.

QC scans of the Hologic spine phantom acquired before each scanning session were retrieved from the archive to cover the time scale over which the in-vivo scans used in this work were performed. Spine phantom images were analysed using the standard Hologic software. BMD, BMC and BA results were plotted and regression analysis performed on the data.

3.2.2 Results

Figures 3.2 and 3.3 show the QC plot for phantom L1 to L4 BMD extracted from the archive for 1992 to 1998. The central horizontal line represents the mean BMD when the system was calibrated by the manufacturer. The dashed lines represent the upper and lower limits which are set to indicate ±1.5% of the mean value at calibration. The precision of measurements, represented by the coefficient of variation (CV%), was 0.3%. Corresponding graphs for BMC and bone area (BA) are given in Appendix A with the results summarised in table 3.1. Regression analysis indicated that there were no significant trends with time for BMD, BMC and BA (Table 3.1). As DXA is a two-dimensional projection technique, an increase in projectional area would lead to a decrease in BMD. If there is an actual increase in bone size, there would be an increase in projected BA but a greater increase in BMC. This would result in a false increase in BMD due to this artefact of the DXA technique.

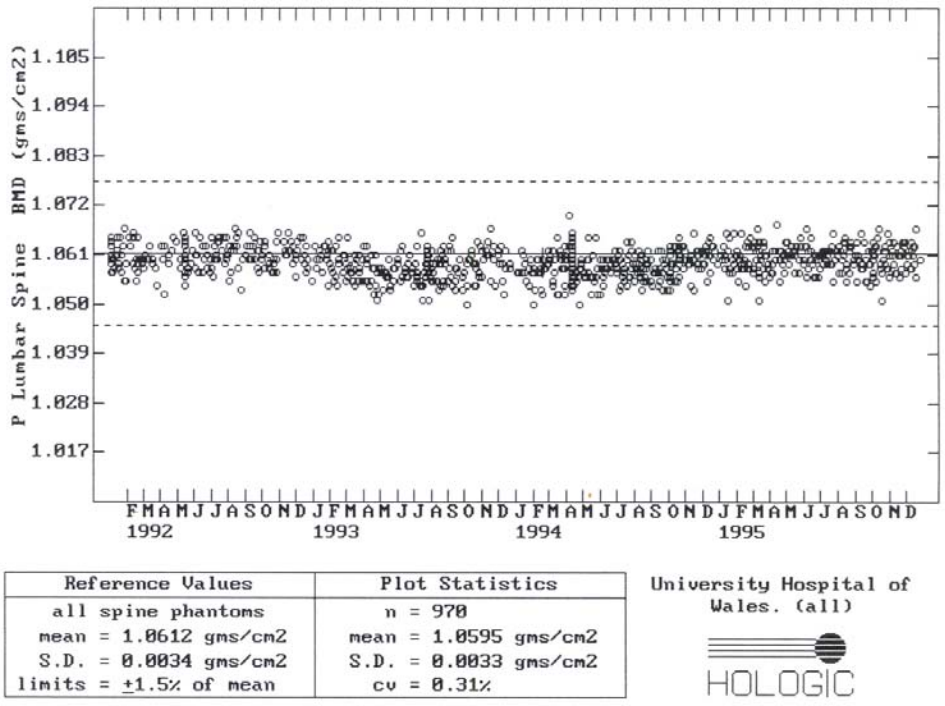

Figure 3.2 Quality control plot for L1 to L4 BMD of the Hologic spine phantom between 1992 and 1995.

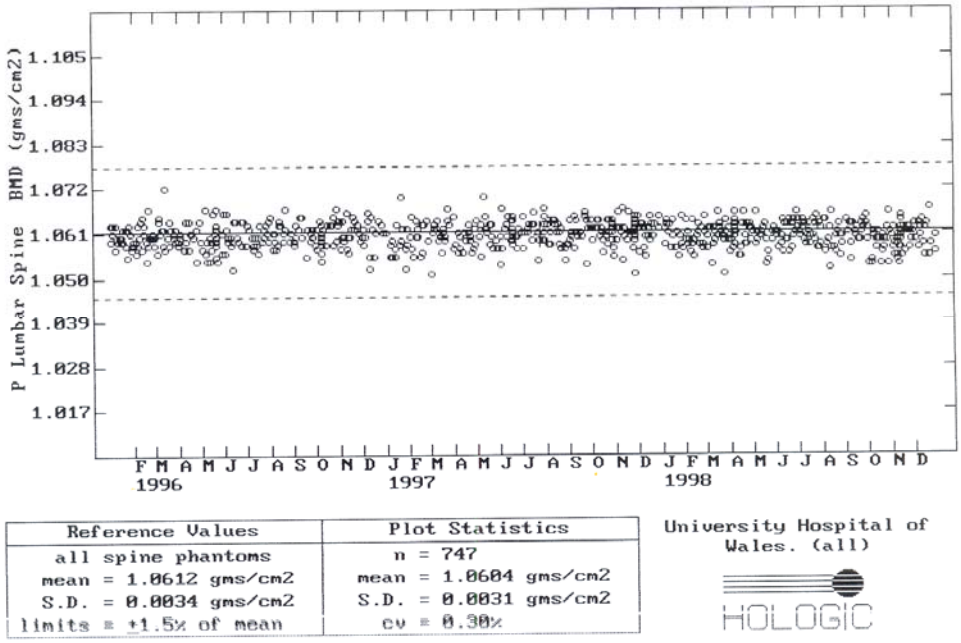

Figure 3.3 Quality control plot for L1 to L4 BMD of the Hologic spine phantom between 1996 and 1998.

	BMD		BMC		BA	
	1992 - 1995	1996- 1998	1992 - 1995	1996- 1998	1992 – 1995	1996- 1998
Mean	1.0595 g/cm^2	1.0604 g/cm^2	57.4971 g	57.4472 g	54.2702 cm^2	54.1754 cm^2
SD	0.0033 g/cm^2	0.0031 g/cm^2	0.2050 g	0.2161 g	0.1891 cm^2	0.1957 cm^2
CV	0.31 %	0.30%	0.36%	0.38%	0.35%	0.36%
Rate of change	-0.02 ± 0.01 %	0.01 ± 0.02 %	-0.00 ± 0.01 %	-0.03 ± 0.03 %	0.01 ± 0.01 %	-0.04 ± 0.03 %

Table 3.1 Summary of BMD, BMC and BA quality control results from the Hologic QDR-1000W between 1992 and 1998.

3.2.3 Discussion

The BMD QC plots confirm that the calibration of the Hologic QDR-1000W was stable over the time period from which the in-vivo scans used in this study were collected. In-vitro long term precision in BMD was 0.3% which, as expected, is better than the 1% quoted for in-vivo lumbar spine scans. The precision of BMC and BA measurements was also low.

3.3 Effect of ROI Width on Measured In-vivo Lumbar Spine BMD

3.3.1 Method

Prior to analysing in-vivo lumbar spine scans, the influence of ROI width on BMD measurements of the Hologic spine phantom with a fixed BMD and a homogeneous baseline needed to be determined. As the baseline tissue is homogeneous and of constant thickness the BMD should remain constant as the ROI width increases. Any change in measured BMD was considered to be an artefact.

Twenty scans of the spine phantom acquired with the lumbar spine performance mode over the same time period as the in-vivo scans used in future work were retrieved from the archive. The scans were analysed using the standard Hologic lumbar spine software (Version 4.74P). Each image was analysed five times with ROI widths of 8.3 cm (86 lines) to 12.2 cm (126 lines) increasing in approximately 1 cm (10 line) steps. The maximum width possible was 126 lines and therefore to work in 10 line steps 86 lines was chosen as the starting width. The reported BMC, BMD and BA were recorded. A linear regression model was fitted to the data. Repeated measurement analysis was performed to investigate the differences in linear relationships. For all statistical tests, a p-value <0.05 was considered significant.

A quadratic and a logarithmic model were compared with the linear model for combined L1 to L4 measurements. The goodness of fit was compared using a SPSS curve estimation test based on the least squares

method. The R^2 value and the significance value for each fit were compared for each model.

3.3.2 Results

Figures 3.4 to 3.6 show that for four individual vertebrae the reported BMD, BMC and BA of the spine phantom increased consistently as ROI width increased. In all cases the gradient of the regression line was significantly different to 0 ($p<0.05$). The correlation coefficient indicated a significant positive correlation between BMD, BMC and BA with ROI width ($p<0.05$). The relative increase in BMC exceeded the relative increase in BA resulting in a net increase in BMD (Fig. 3.4). It was apparent from visualisation of the bone map during analysis that the bone edge generated by the software moves further outwards from the vertebrae as the ROI increases. Repeated measurement analysis confirmed the ROI width had a significant effect on BMD, BMC and BA for all vertebrae ($p<0.001$). The BMD, BMC and BA were significantly different for each vertebrae. Overall there was a significant interaction between the regression lines for BMD. However, when looking at pairs of vertebrae there was no significant interaction between the slopes for L2 and L3. The interaction between the regression slopes for BMC was significant ($p<0.001$). For BA, overall the slopes were significantly different indicating an interaction $p<0.001$. However, when looking at individual pairs, the regression slope for L1 was significantly different to L2, L3 and L4 but there was no significant difference between the other slopes ($p<0.001$).

The Pearson's correlation coefficient indicated a significant correlation between changes in BMC and BA ($p<0.001$) for all vertebrae.

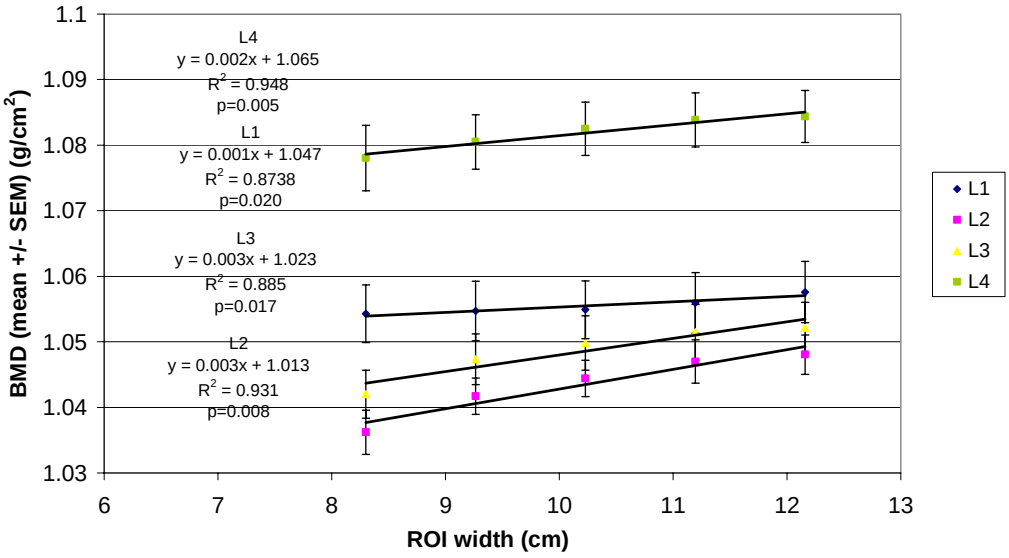

Figure 3.4 Relationship between measured BMD with ROI width. Linear regression analysis gave a SEE of L1= 0.001 g/cm^2, L2=0.001 g/cm^2, L3=0.002 g/cm^2, L4=0.001 g/cm^2. Errors in gradient: L1 = < 0.001 g/cm^2 per cm; L2= <0.001 g/cm^2 per cm, L3=0.001 g/cm^2 per cm, L4= <0.001 g/cm^2 per cm. Error bars represent ± 95% CI for the 20 data sets.

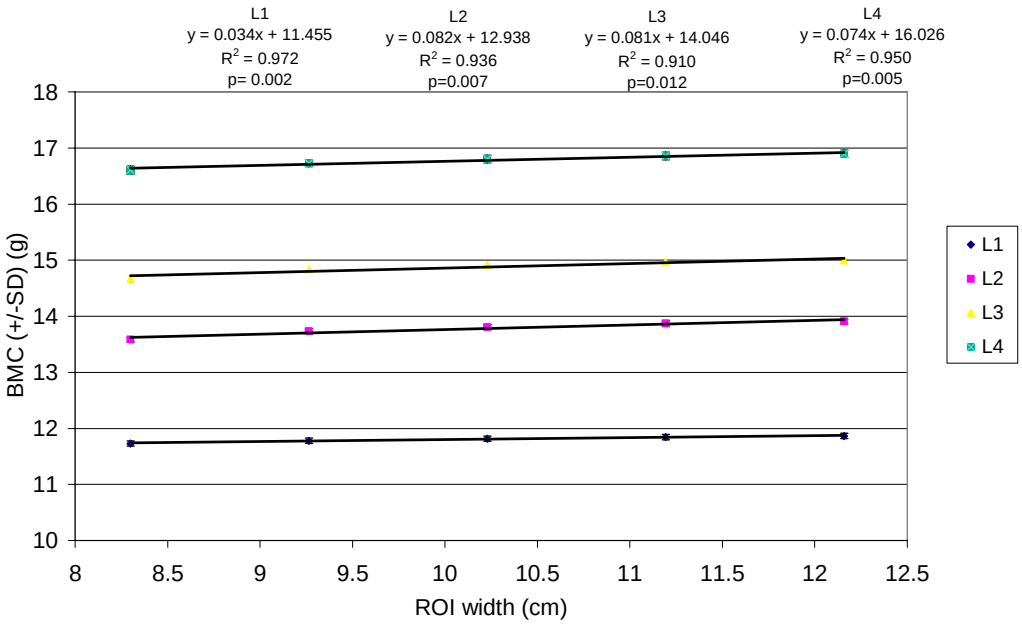

Figure 3.5 Relationship between measured BMC with ROI width. Linear regression analysis gave a SEE of L1= 0.01 g, L2= 0.04g, L3=0.05 g, L4=0.03 g. Errors in gradient: L1 = <0.01 g per cm; L2=0.01 g per cm, L3=0.02 g per cm, L4=0.01 g per cm. Error bars represent ± 95% CI of the 20 data sets.

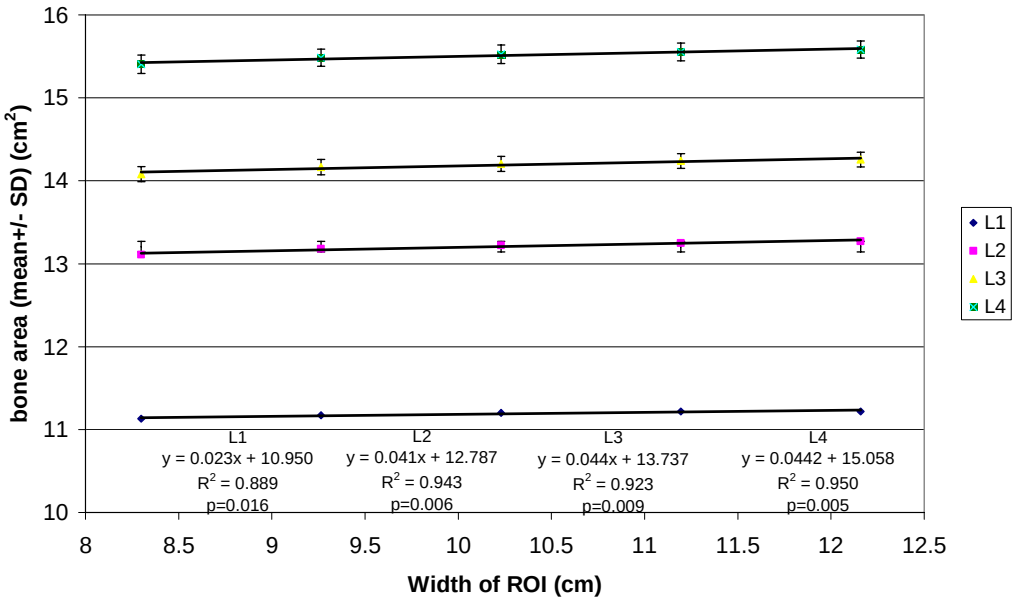

Figure 3.6 Relationship between measured BA with ROI width. Linear regression analysis gave a SEE of L1= 0.01 cm^2, L2= 0.02 cm^2, L3=0.02 cm^2, L4=0.02 cm^2. Errors in gradient: L1 = 0.01 cm^2 per cm; L2= 0.01 cm^2 per cm, L3=0.01 cm^2 per cm, L4=0.01 cm^2 per cm. Error bars represent ± 95 % CI for 20 data sets.

Figure 3.7 shows the linear and quadratic fits for the total BMD (a), BMC (b) and BA (c) data with the 95% CI of the line superimposed. The R^2 values for the BMD data were 0.951 for the linear fit, 0.972 for the logarithmic fit and 0.997 for the quadratic model. The R^2 values for BMC were 0.939, 0.963 and 0.997 for the linear, logarithmic and quadratic models respectively. For BA, R^2 values were 0.934, 0.958 and 0.997 respectively. These results indicate the quadratic model gives the best fit to the BMD, BMC and BA for combined L1 to L4 data. Significance testing using the SPSS curve estimation analysis confirmed all fits were significant ($p<0.05$). This was also the case for BA with R^2 of 0.934, 0.958 and 0.997 respectively. As there was no statistical difference between the quadratic and linear fits, a linear fit was used to derive a correction factor for in-vivo data for mathematical simplicity. Also, with the linear model the ROI width that gave a BMD close to the actual BMD was 11.6 cm which was similar to that recommended by Hologic as the default ROI (11.5 cm).

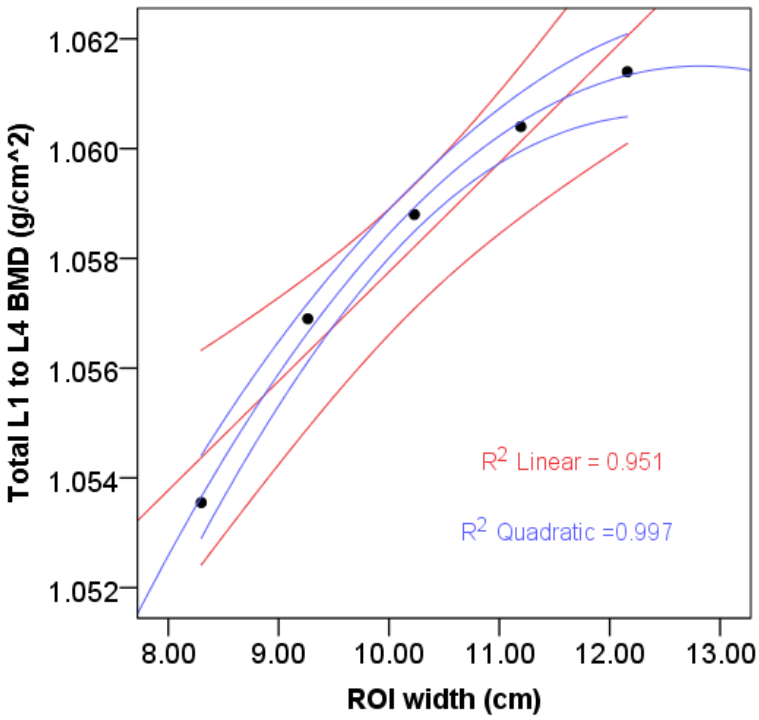
Total L1 to L4 BMD (g/cm^2)
1.062
1.060
1.058
1.056
1.054
1.052
8.00
9.00
10.00
11.00
12.00
13.00
ROI width (cm)
R2 Linear = 0.951
R2 Quadratic =0.997

(a)

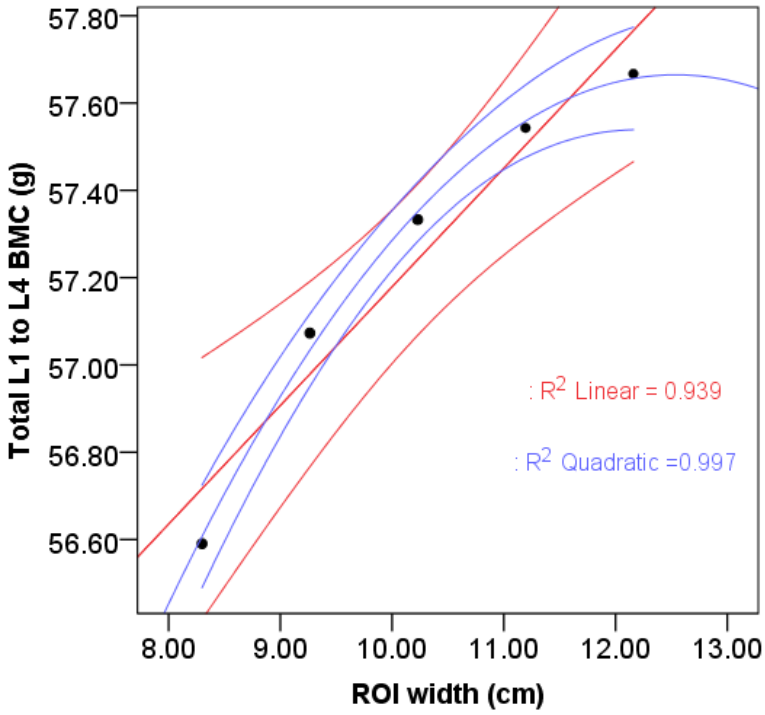
Total L1 to L4 BMC (g)
57.80
57.60
57.40
57.20
57.00
56.80
56.60
8.00
9.00
10.00
11.00
12.00
13.00
ROI width (cm)
: R2 Linear = 0.939
: R2 Quadratic =0.997

(b)

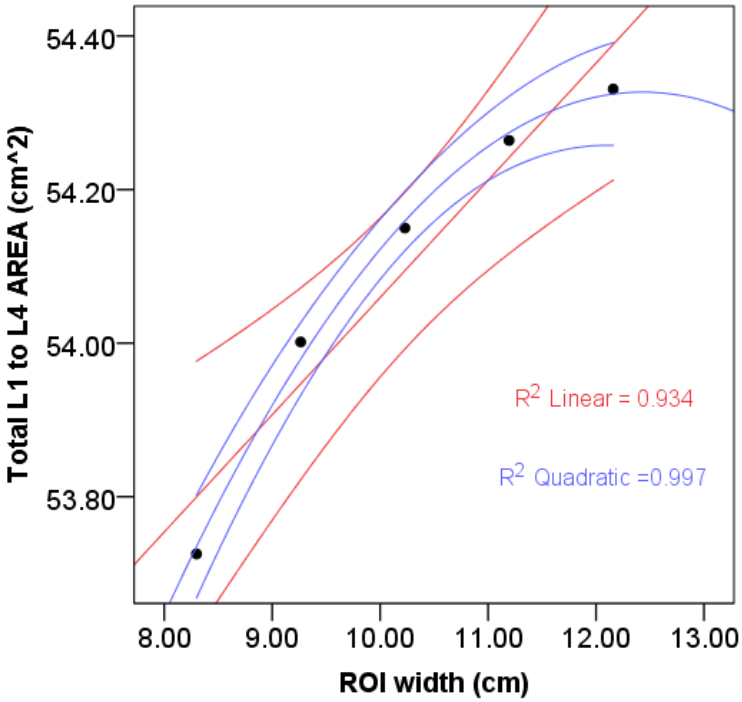

(c)

Figure 3.7 Variation in total L1 to L4 BMD (a), BMC (b) and BA (c) of the phantom as width of lumbar spine ROI increases showing a linear (red) and quadratic (blue) model with the corresponding 95% CI of the line.

3.3.3 Discussion

The results presented here confirm the observations of Tothill and Pye (1992) that there is an apparent increase in BMD of the Hologic spine phantom as the ROI width increases. This phenomenon was also observed in-vivo by Hansen *et al.* (1990) for the QDR-1000 who found that the BMD of 30 women appeared to decrease by approximately 3.5% as the ROI width decreased by 6 cm. In order to explain these findings the stages in the lumbar spine algorithm need to be considered. This is discussed in chapter 2 sections 2.2 and 2.4 and summarised in figure 2.4. As discussed, an edge-detection algorithm is responsible for determining the bone edge by setting a BMD threshold to separate the bone mineral from soft tissue. Any bone mineral not identified as bone will be classed as soft tissue and therefore elevate the area density of the soft-tissue in

the baseline resulting in an over-subtraction from the bone map subsequently causing an underestimation of BMC. Changes in reported BMD as the ROI is widened would not be expected when scanning a phantom with homogeneous soft tissue in the baseline.

The BMD BMC and BA of healthy vertebrae usually increases from L1 to L4. As the phantom is supposed to mimic the spine, it was surprising that the BMD of L1 was reported to be higher than that of L2 or L3. This was not the case for BMC or BA and therefore it is likely that the relatively small BA of L1 causes the BMD to be greater than L2 or L3. The correlation between BMC and BA has been noted by others (Tothill and Avenell 1998) and it is logical that an increase in BA results in more pixels being recognised as bone resulting in a higher BMC. A correlation between BMD and BA has also been reported (Yang *et al.* 1997).

The observed changes in BMD, BMC and BA with width are relatively small but statistically significant and highlight the importance of ensuring consistency in the ROI width. As these changes occur with a homogeneous baseline it is likely that the changes in-vivo will be greater due to the variety of tissues within the abdomen at the level of the lumbar vertebrae.

Tothill and Pye (1992) used the observed variation in phantom BMD to derive a correction factor for in-vivo data. For the data presented in the current work, the gradient of the linear regression model was used to compensate changes in BMD, BMC and BA measurements for changes in ROI width when baseline is homogeneous. The correction factors are summarised in table 3.2. When examining in-vivo data in chapter 4 it was decided to concentrate on L3 and L4 as this was where the largest errors in BMD are likely to occur due to a greater inhomogeneity in fat distribution at this level. This was confirmed in Chapter 5.

	Gradient of regression line	
	L3	L4
BMD (g/cm^2/line)	0.0002	0.0002
BMC (g/line)	0.0078	0.0071
BA (cm^2/line)	0.0043	0.0043

Table 3.2 Factors derived from phantom data to compensate BMD, BMC and BA for changes due to increasing the ROI width when the baseline is homogeneous.

3.4 Effect of ROI Width on In-vivo Lumbar Spine Bone Map

3.4.1 Method

The attenuation due to soft-tissue in the baseline of the lumbar spine ROI will affect the bone map as discussed in 3.3.3. There must be sufficient soft tissue within the baseline to provide a precise value for the attenuation of high and low energy X-ray beams to obtain the R value in a bone free region. If the ROI is too narrow the bone map may be incomplete. As the ROI increases to include more soft-tissue, the software can make a more realistic measurement of the attenuation of baseline soft tissue to subtract from the global tissue map to identify the bone edge. The Hologic-QDR1000W software allows the user to paint in missing bone to match the visible bone edge. However, it has been noted that painting in bone visually corrects the bone map but the software does not recognise this tissue as bone mineral. The reported BA increases but without a corresponding increase in BMC thus reducing BMD (Hipgrave 2010; Kelly 2010). As some bone mineral is still considered as soft tissue this results in the BMD decreasing further in addition to the decrease due to BA increasing.

The Hologic lumbar spine software was tested to determine the smallest ROI width that gives a complete bone map. Twenty lumbar spine scans

were retrieved from the archive and analysed with ROI widths between 6.4 cm (66 lines) and 12.2 cm (126 lines). The minimum width was chosen to give as little soft tissue as possible within the ROI whilst allowing the analysis program to run.

To examine the effect of painting in bone, the BMD, BMC and BA measured from a scan showing an incomplete bone map with a ROI of 6.4 cm (66 lines), were compared with the measurements after re-analysing and painting in bone to match the perceived bone edge. The results were also compared to those recorded using a ROI of typical width used for clinical measurements i.e. 11.5 cm (119 lines). A one-way ANOVA test was used to test if the results were different. A Bonferroni test indicated where the differences occurred. A p-value <0.05 was classed as significant.

3.4.2 Results

In 17 out of 20 scans analysed the bone map was incomplete at 6.4 cm (66 lines) and incomplete in 3 of 20 cases at 7.3 cm (76 lines). An example of an incomplete bone map is shown in figure 3.7. With ROI width increased to 8.3 cm (86 lines), the edge detection algorithm identified the edge of the vertebrae on all images.

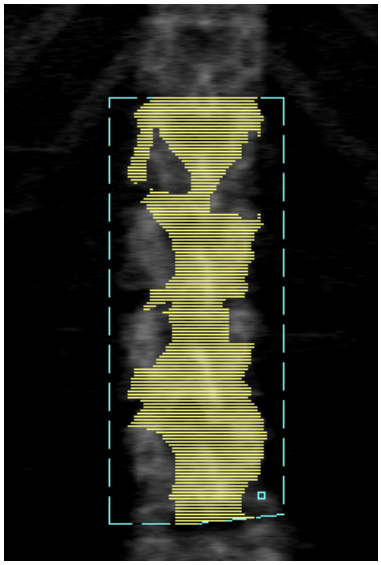

Figure 3.7 Screen printout of an incomplete bone map.

Figure 3.8 compares the average BMD, BMC and BA for a measured with an incomplete bone map at 6.4 cm, the first complete bone map (8.3 cm) and when using a standard ROI of 11.5 cm. It is evident that when the ROI is too narrow and the bone map incomplete the BMC, BMD and BA are all underestimated. An ANOVA Bonferroni post hoc test confirmed there is a significant difference in the BMD, BMC and BA measured with a 6.4 cm ROI and that measured with a 8.3 or 11.5 cm ROI ($p<0.001$). The difference between the BMD, BMC and BA measured with a 8.3 cm and 11.5 cm ROI was not significant ($p = 1.000$).

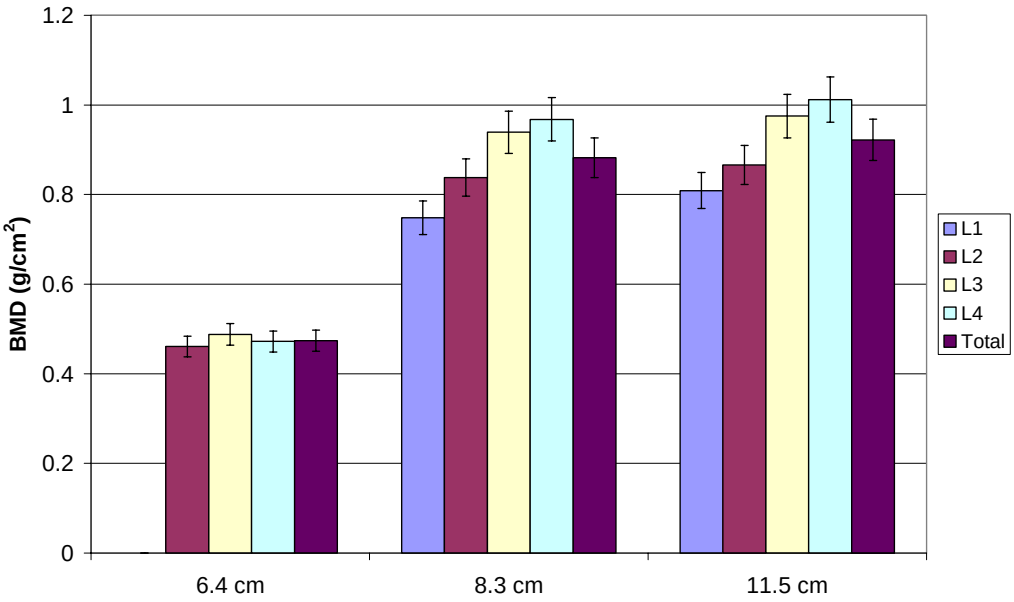

(a)

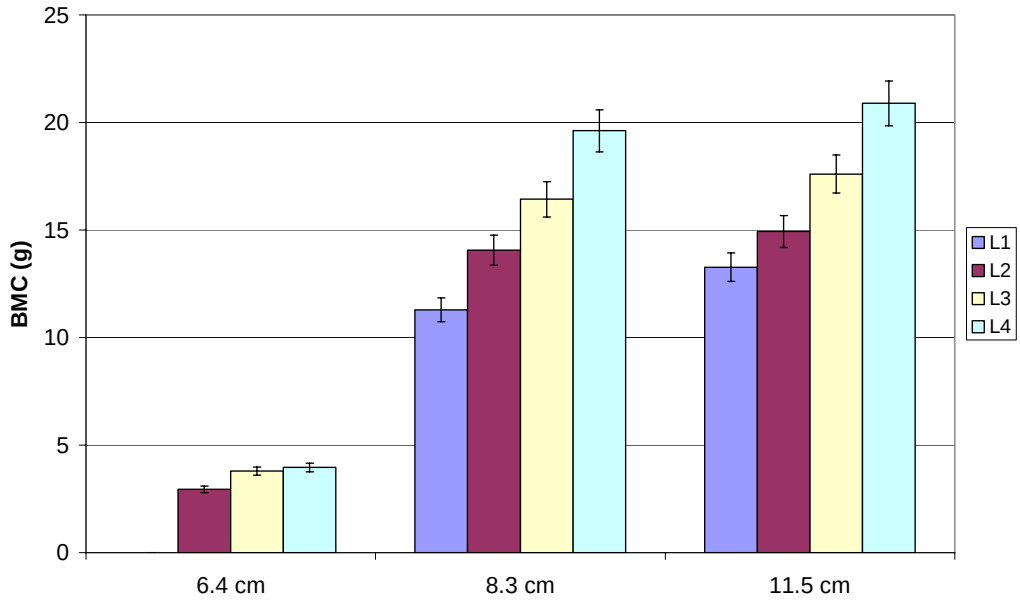

(b)

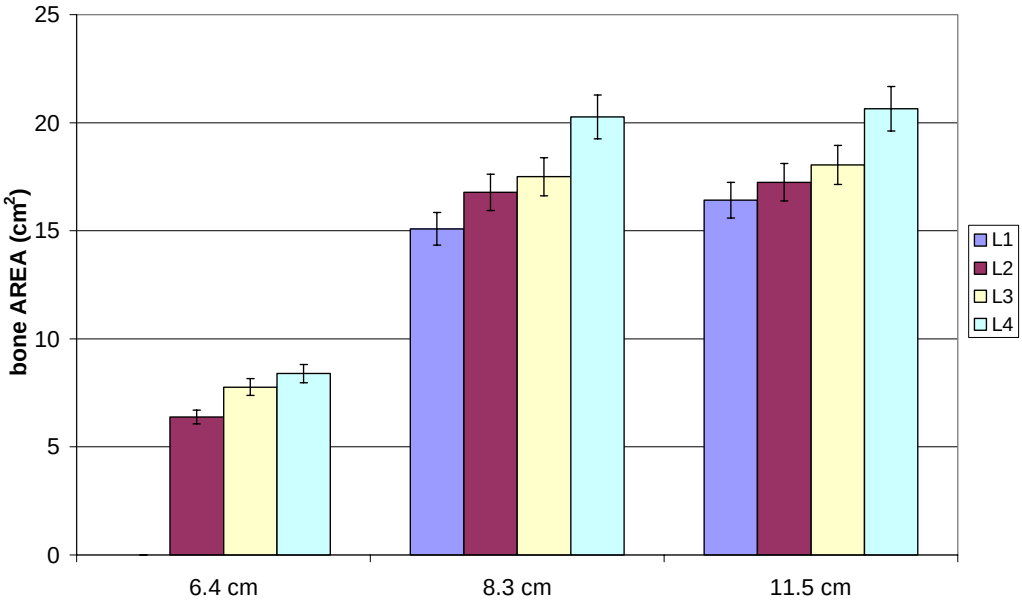

(c)

Figure 3.8 Comparison of the BMD (a), BMC (b) and BA (c) reported for an incomplete bone map for a ROI width of 6.4 cm (66 lines), for the first complete map at a width of 8.3 cm (86 lines) and for a standard width ROI of 11.5 cm (119 lines). The BMD and BMC of L1 at 6.4 cm (66 lines) was 0 and the BA for L1 was 0. Error bars represent 95% CI of data.

The results shown in table 3.3 confirm that an incomplete bone map will produce false results and painting in bone appears to falsely reduce BMD. This is due to the relatively large increase observed in BA compared to BMC.

	Percentage difference between pre and post manually painting in bone to visually complete the bone map (%)		
	AREA	BMC	BMD
L1	85.0	18.3	-36.1
L2	46.9	4.3	-28.9
L3	61.1	16.5	-27.7
L4	51.0	-4.7	-36.9
Combined L1 to L4	58.3	7.1	-32.3

Table 3.3 Difference in reported BMD, BMC and BA after painting in bone to visually complete bone map to match perceivable edge of vertebrae.

Occasionally the software identified soft tissue with a relatively high density as bone or included ribs in the bone map. In such instances part of the bone map may need to be deleted. Only bone or high density tissue that would be deleted using the standard width ROI was removed.

3.4.3 Discussion

The aim of this work is to examine the effect of the soft tissue baseline on the reported BMD. As the bone map was unreliable with a ROI width less than 8.3 cm (86 lines) it was decided to use this as the smallest width of ROI for further lumbar spine in-vivo investigations.

It is unlikely that a ROI width smaller than 8.3 cm (86 lines) would be used for clinical measurements. The BMD, BMC and BA measured for an 8.3 cm ROI were not significantly different to those with a standard ROI of 11.5 cm. The results produced from an incomplete bone map will be

unreliable but it is a concern that when the bone map is painted-in manually the BMD is reduced further. The results confirm reports that the BA increases but that the added bone is not recognised - hence the little variation in BMC. Due to these findings, no bone was painted in during analysis of in-vivo spine images in subsequent work.

3.5 Accuracy of ROI Dimensions Reported by the Hologic Whole Body Analysis Sub-regional Software

3.5.1 Method

One of the measurements that will influence the accuracy of the proposed method for quantifying abdominal fat thickness distribution is the area of the regions used to analyse tissue. This is calculated from the width and height of the region which is quoted in lines and converted to metric units, (cm), using the point spacing and line resolution factors supplied by Hologic. These factors have different values for the WB and lumbar spine scans due to different pixel sizes in these images. To validate these factors for the WB sub-regional software, a WB scan was performed of two stainless steel rods (6×6×150 mm) placed 5 cm apart on a 1 cm Perspex slab in horizontal and vertical orientations in turn.

Each image was initially analysed using the enhanced WB analysis protocol (Version 5.73). The sub-regional analysis tool was then used to place a rectangular region on the image of the rods with the edges aligned with the centre of each rod as shown in figure 3.9.

Figure 3.9 Orientation of stainless steel rods placed on 1 cm Perspex on the scanning couch to check point resolution (A) and line spacing (B) factors.

The separation of these lines as reported by the software was compared to the actual distance between the rods (D) calculated using equation 3.1, thus allowing the calculation of point resolution and line spacing using equations 3.2 and 3.3 respectively.

$$D = \text{Separation of rods} + (2\times(\text{rod width}/2)) \quad (3.1)$$

$$\text{Point Resolution} = D_H / A \quad (3.2)$$

$$\text{Line Spacing} = D_V / B \quad (3.3)$$

where D_H and D_V are the actual distance between the centre of the rods in the horizontal and vertical planes respectively.

3.5.2 Results

When fitting a rectangular analysis box on the image, the smallest increment possible for altering the height and width was two lines and hence the associated errors were ± 0.1 cm in the horizontal direction and ± 0.7 cm vertically. As shown in table 3.4, the point resolution and line spacing factors quoted by Hologic agree with those measured within the error margin. These factors were therefore confirmed to be correct.

	Actual separation of rods (± 0.1 cm)	Measured separation of rods on image (± 2 lines)	Measured value of conversion factor (cm/line)	Hologic Value of conversion factor (cm/line)
Horizontal (x)	7.1	35	0.2029±0.0119	0.2047
Vertical (y)	15.6	13	1.2000±0.1848	1.303

Table 3.4 Comparison of the line spacing and point resolution factors quoted by Hologic for WB images with those measured from imaging metal rods on Perspex using WB mode and analysing the images using the Hologic sub-regional software.

3.5.3 Discussion

The line spacing and point resolution conversion factors quoted by Hologic were confirmed and therefore can confidently be used to convert the dimensions of regions used to quantify FM and LM from “lines”, or pixels, to cm.

3.6 Linearity of Hologic QDR-1000W Sub-regional Analysis Body Composition Measurements

3.6.1 Method

The linearity of body composition analysis (BCA) measurements with various width analysis regions was tested by scanning 5 cm thickness of Perspex. The Perspex was placed on the couch to coincide with the trunk region of the WB standard analysis regions. The image was analysed with the Enhanced WB software and sub-regional tool. Analysis regions of constant height 16.9 cm and widths increasing from 0.6 cm (3 lines) to 14.1 cm (69 lines) in 0.4 cm increments were placed within the image of the Perspex. FM, LM, total tissue mass (TM) and percentage fat (%fat) within each region was recorded.

3.6.2 Results

Figure 3.10 shows the reported FM, LM and TM of 5 cm Perspex increased linearly as the area of the analysis box increased. The correlation coefficient was 1 indicating a perfect correlation. All the gradients were significantly different to 0 ($p<0.001$).

The results in figure 3.11 were unexpected as in a phantom the %fat should remain stable. The variation in %fat with width is likely to be due to poorer precision with small analysis regions and the ability of the software to accurately measure tissue in such small regions. As the width of the analysis region increased, the %fat appeared to become more constant. The mean %fat over all ROI widths was 63.2 ± 0.1%.

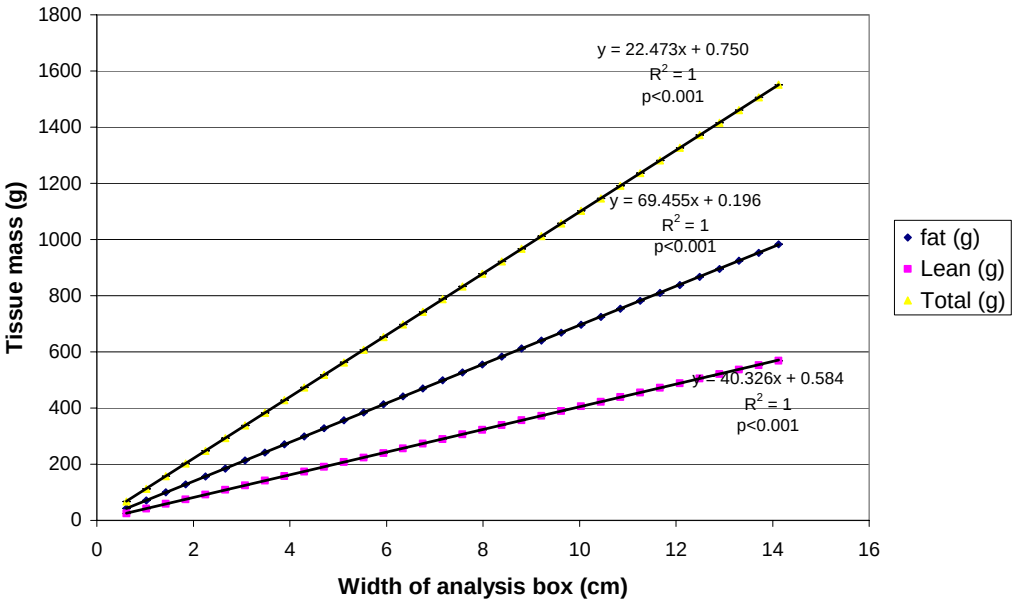

Figure 3.10 Variation in reported body composition parameters for 5 cm Perspex as the area of the analysis box increases. 95% CI were used as error bars but they do not show up due to y-axis scale. The 95% CI are ±0.042 g for fat, ±0.041 g for lean tissue and ±0.048 g for total tissue mass.

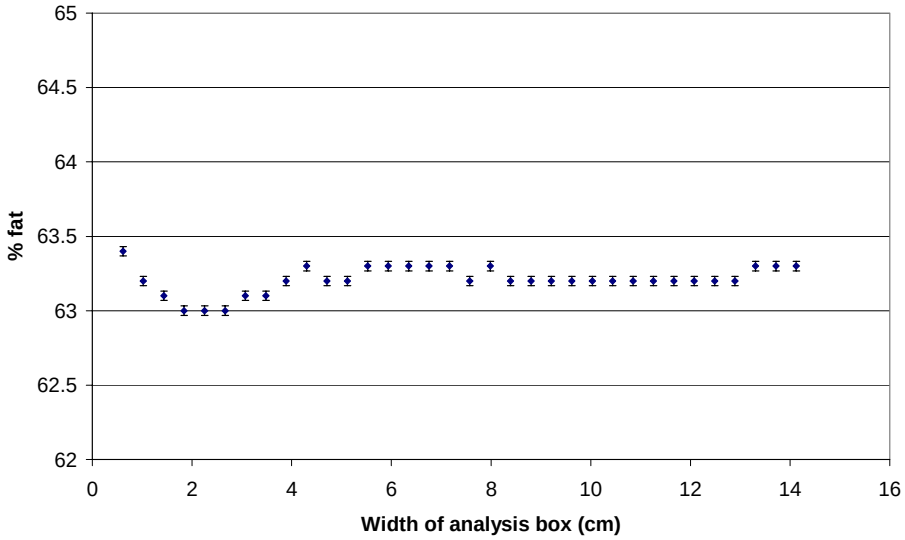

Figure 3.11 Percentage fat reported for 5 cm of Perspex analysed using various size analysis regions (mean ± 95% CI).

3.6.3 Discussion

These results provide confidence that the BCA measurements are linear as the width of the analysis region increases. This is important as various size regions will be used to quantify in-vivo abdominal fat thickness. It is acknowledged that the regions of analysis used here are relatively small compared to those used within the standard software but are comparable to those that will be used to quantify abdominal fat thickness.

Another confirmation that the software reports accurate results was demonstrated by the %fat of the Perspex being in close agreement with the value for Perspex measured by Tothill *et al.* (2001) i.e. 64%. However, this was slightly lower than the nominal value of 68%.

In theory the %fat should remain constant as the analysis region increases; this can be assumed to be the case because the standard deviation of the measurements is satisfactorily low. The %fat measurements become more stable as the width of the analysis region increases as there is more tissue to sample.

3.7 Assessment of Whole Body Sub-regional Analysis Software for Measurement of Fat

3.7.1 Method

The uniformity of in-vivo abdominal fat thickness will be measured by extracting the FM in small analysis regions, termed soft tissue boxes (STB), placed on WB images across the abdomen at the level of the lumbar vertebrae as shown in chapter 5 figure 5.1. An accurate FM measurement is therefore vital.

To assess the accuracy of FM measurement the various combinations of Perspex and lard listed in table 3.5 were scanned using the WB mode. Perspex was used to support the lard. The lard/Perspex combinations were placed to coincide with the trunk region of the scan. Prior to

scanning, the lard was weighed and the dimensions of the blocks of lard were measured with a ruler, after removing the wrappers. The physical density of the lard was calculated using equation 3.4.

Various size STB were placed within the image and the FM, LM, TM and %fat recorded for each region. The area density of fat beneath the regions was calculated using equation 3.5 and compared with the actual area density determined from the physical characteristics of lard.

$$Physical\_density = \frac{mass}{volume} \qquad (3.4)$$

$$Fat\_area\_density = \frac{FM}{\left[\left(H \times 1.303\right) \times \left(W \times 0.2047\right)\right]} \qquad (3.5)$$

where H and W are the height and width of the STB respectively, 0.2047 is the point resolution in cm/line and 1.303 the line spacing factor in cm/line.

1	1 cm Perspex
2	1 cm Perspex + 1 block of lard
3	1 cm Perspex + 2 blocks of lard
4	1 cm Perspex + 3 blocks of lard

Table 3.5 Combinations of Perspex and lard scanned with whole body mode to test the accuracy of the body composition parameters reported by the Hologic QDR-1000W WB sub-regional analysis software.

It was uncertain whether the soft tissue under the boundary line of the STB was recognised and included in the measurement. To test this, the physical density of lard was used to calculate the FM that would be

expected under an area equivalent to that with and without the border line.

3.7.2 Results

The physical density of the lard blocks was calculated by weighing and measuring to be 1.03±0.03 g/cm^3, 0.99±0.03 g/cm^3 and 1.00±0.03 g/cm^3 for 1,2 and 3 blocks respectively. The average physical density of lard calculated from the FM reported by DXA was 1.03 ± 0.05 g/cm^3.

When scanning 1 cm Perspex alone the FM, LM and %fat was 0. There was a close agreement between the actual area density of lard and the DXA measured value for 1 and 3 blocks of lard with the percentage difference being -0.84% and 0.04% respectively. Such a close agreement was not found for 2 blocks of lard i.e. 6.39%.

The FM and LM reported by the software increased linearly as the width of the STB increased as seen in figure 3.12.

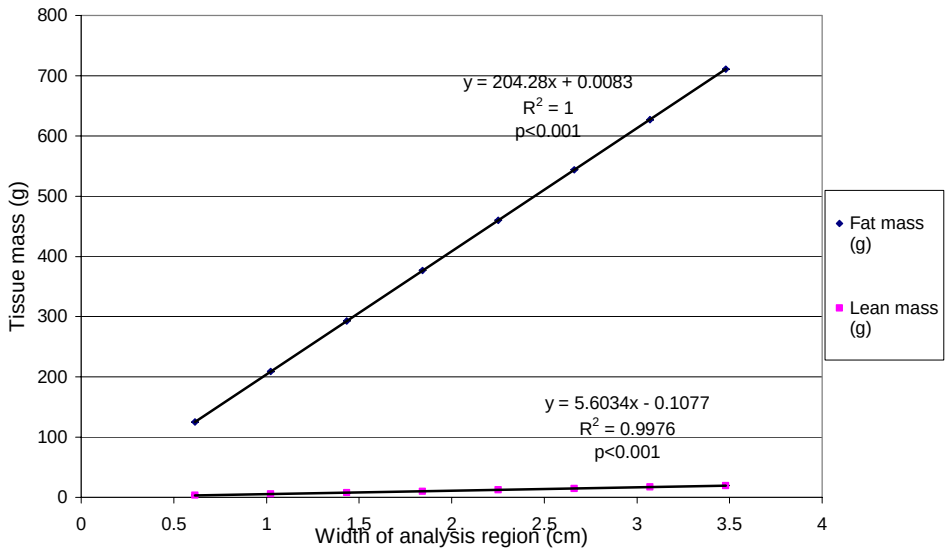

Figure 3.12 Relationship between fat mass and lean mass DXA measurements with area of analysis region when scanning 3 blocks of lard on 1 cm Perspex. SEE: FM=0.3 g, LM = 0.3 g. Standard error in gradients: FM = 0.11 g/cm, LM = 0.11 g/cm. Both gradients were significantly difference to 0 ($p<0.001$). 95% CI are plotted as error bars but due to y-axis scale they are not visible. 95% CI: FM = 0.27 g and LM=0.27 g.

The true percentage fat of lard is 99.8% but as the lard is placed on 1 cm Perspex with a nominal %fat of 68% this would lower the total %fat reported by DXA. Figure 3.13 shows that the %fat measured for 1 block of lard was lower than for 2 and 3. The measurement errors for data shown in figure 3.13 were derived from the precision of repeated measurements. The relatively large errors for 1 block of lard reflect the measurements are less precise when the amount of lard is lowest.

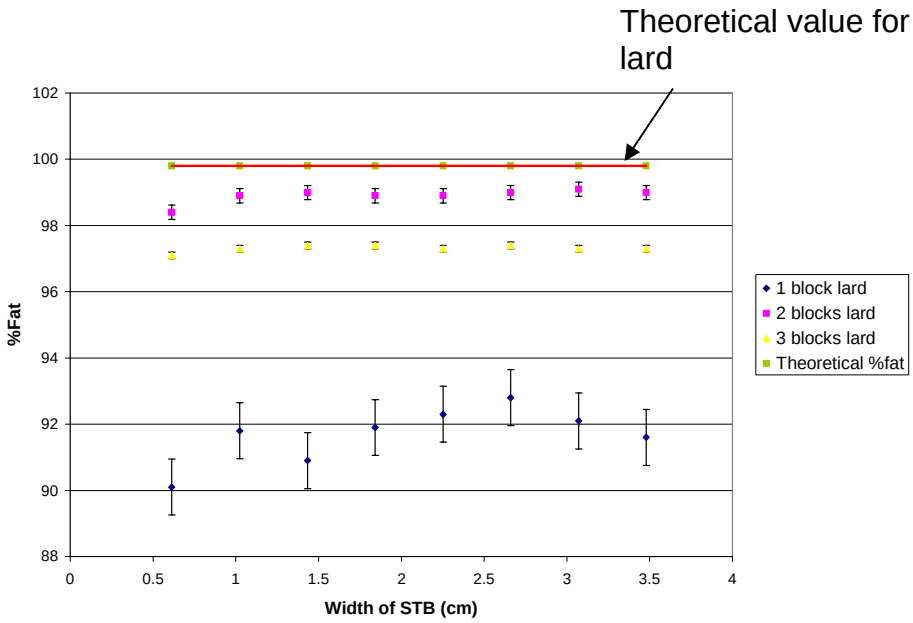

Figure 3.13 Variation in percentage fat (%fat) reported by the DXA sub-regional analysis when analysing images of 1, 2 and 3 blocks of lard on 1 cm Perspex.

The results in table 3.6 show that the reported FM was 6.4% different to that expected when basing calculations on an area including the boundary line but 27.0% different without accounting for the boundary. This suggests that the soft-tissue under the border lines is accounted for in DXA sub-regional measurements.

Width of ROI	Height of ROI	AREA (cm^2)	Area density of fat from physical parameters (g/cm^2)	Expected fat mass for area (g)	Fat mass reported by software (g)
17	9	40.81	5.86	257.6	236.5
15	7	28.06	5.86	172.6	236.5

Table 3.6 Comparison of fat mass reported by Hologic software with that calculated from the physical parameters of lard using areas including and excluding the boundary of the region of interest.

3.7.3 Discussion

Available literature indicates that the accuracy and precision of body composition measurements by DXA are dependent on the scanner type and the software version (Tothill *et al.* 1994b; Tothill *et al*. 1994c; Diessel *et al.* 2000). For in-vitro studies the results will depend on the design of the phantom and, when using the standard WB analysis software, the position of the phantom relative to the analysis regions as the software has different assumptions about tissue distribution within each body region (Tothill *et al.* 2001). The standard Hologic WB analysis regions will not be used in this work and therefore it is assumed these assumptions will not influence the measurements. The position of the phantom on the scanning couch was consistent for all scans. Due to the discrepancies between the results from different manufacturers and software versions it is not plausible to compare any results obtained with other scanners with the work presented here.

Phantom designs described in literature use various materials to simulate body tissues. Among these are water, polyvinylchloride, meat or muscle to represent fat-free mass; ethanol, polyethelene, acrylic, vegetable oil, paraffin wax, or lard to represent fat; and aluminium or actual bone for bone (Jebb *et al.* 1995; Shypailo *et al*. 1998; Diessel *et al*. 2000; Tothill *et al.* 2001). It is appreciated that the blocks of lard used in this work are a very simplistic way of assessing the accuracy of DXA FM measurement

and no inference can be made about true accuracy of in-vivo measurements.

There does not appear to be any published work describing extraction of abdominal fat profiles from Hologic QDR-1000W WB images using the sub-regional analysis software. However, sub-regional analysis has been used to estimate visceral and intra-abdominal FM within a region encompassing the a large section of the abdomen at the level of the lumbar vertebrae and to validate DXA measurements against CT, MRI or other measures of anthropometry (Kamel *et al.* 2000; Park *et al.* 2002).

The physical density of the lard calculated from the actual mass and volume was higher than the actual physical density of fat i.e. 0.9 g/cm^3 but the value calculated from the DXA FM and that calculated using the weight and physical dimensions are in good agreement. This value is also higher than the density of body fat i.e. 0.9007 g/cm^3 at 37˚C (Blake *et al*. 1999). It is uncertain why the area density of fat calculated from the FM measured by DXA for 1 and 3 blocks are closer to the actual value but not for 2 blocks. Ideally each block of lard would have been scanned individually and the measurements with all 3 blocks scanned in various combinations. This was not possible as each time the lard was handled the shape changed due to the lard becoming soft. The discrepancy between 1,3, and 2 blocks highlights the potential variability in results, however, the largest difference between DXA FM measurements and the FM expected from the physical characteristics of the lard was approximately 6% which is consistent with the findings of Jebb *et al.* (1995) when comparing DXA FM and direct fat analysis. When compared with other errors inherent in the proposed method to develop abdominal fat thickness profiles, for example the error introduced by combining data from different types of images, this 6% error was considered acceptable for proceeding with in-vivo measurements.

Analysis of the Perspex alone measured the FM, LM and %fat to be 0 but it is likely that when adding the lard the Perspex influenced the measurements. This was found by Jebb *et al.* (1995) when using a

polypropelyne tank as the basis of a phantom. The %fat reported with 1 block of lard is lower than that with 2 or 3 blocks which is possibly consistent with the reports that the QDR-1000W underestimates low fat proportions in-vitro and in-vivo (Jebb *et al.* 1995; Prior *et al.* 1997; Tothill *et al.* 2001). These findings may be due to the assumptions about fat distribution used by the manufacturer in the software. Using the Hologic Enhanced Whole Body software version 5.50, Snead *et al.* (1993) found that lard added to the trunk region of the body was measured as 55% fat but accurately measured as 96% fat in limbs. However, when repeating this work using an updated version of the Hologic software (version 5.64), Kohort (1998) found the lard was correctly measured as being 96% fat in the trunk and limbs. Using version 5.55, Tothill *et al.* (2001) reported low fat proportions were underestimated and measurements in the trunk region were more variable. These reports imply that problems in early versions of the software have been rectified by Hologic. As the Enhanced WB software version 5.73 is used in this work, it can be assumed that the body composition measurements in the region of the trunk are accurate.

Another possible explanation for different values for one block of lard is the presence of inhomogeneities within the lard block such as air bubbles.

It is also possible that at smaller thickness of lard the Perspex has more influence on measurements. In a more realistic study, Jebb *et al.* (1995) found that the FM of a 55 kg sample of pork meat, analysed within the trunk region of software, was underestimated by 6-8% compared to direct analysis and suggested that the validity of the WB algorithms is questionable. As maybe expected, the accuracy and precision of %fat measurements was poorer with smaller STB and lower quantities of fat. Caution must be taken when comparing the current results with published findings as different methods were used to obtain the data. No results have been found to compare directly with those presented in the current validation investigation.

A disagreement between phantom and in-vivo measurements was reported by Yu *et al*. (2012). In-vitro, the BMD was found to increase as the fat thickness increased but in-vivo lumbar spine BMD decreased as fat thickness increased. This report highlights the need for caution when interpreting results from phantom studies.

The total tissue thickness has also been shown to affect the accuracy of fat measurement with the %fat being overestimated at extremes of depth (<10 cm and >25 cm) (Jebb *et al.* 1995). The blocks of lard used in this study were 5.7, 5.7 and 5.8 ± 0.1 cm in height and therefore the blocks plus the Perspex ranged from 6.7 to 18.2 cm.

As very small STB are used, the error introduced in the results if the tissue under the border is not included will be large and therefore it was important to establish that this tissue is incorporated in the measurement.

It was not the aim of this work to quantify the absolute accuracy of FM measurements but to assess the sub-regional software. It is recognised that the methods used here are a crude test of the software but the results are useful in confirming that (1) there was no significant difference between the DXA measured area density of fat and that calculated from the physical dimensions; (2) FM, LM and TM measurements are linear as the area of STB increases; and (3) the software reports tissue composition under border of STB.

The method of obtaining the abdominal fat profile from WB scans tests the software to its limits but the results presented here, along with a review of relevant literature, do not give any reason why FM data extracted from WB scans using the sub-regional analysis software cannot be used to derive abdominal in-vivo fat profiles.

3.8 Combination of Measurements from DXA Whole Body and Lumbar Spine Images

3.8.1 Method

When using body composition data from DXA WB images to estimate the fat thickness in the baseline of lumbar spine scans, it is assumed that the regions of tissue are identical on each scan. To test this, the height and width of the lumbar spine on both images were compared.

Archived lumbar spine studies were retrieved for 50 subjects, scanned as part of an inflammatory bowel disease (IBD) study. The lumbar spine image was analysed using the standard protocol. The global ROI was placed over L1 to L4 and the width narrowed until the edges touched the perceived outline of each vertebrae in turn. The width of each vertebrae was recorded and converted to metric units by multiplication with the point spacing factor i.e. 0.0965 cm/line for the lumbar spine image. The height of L1 to L4 was measured by placing the superior and inferior borders of the global ROI in the T12 and L4-L5 inter-vertebral space.

WB images from the same subjects were analysed with the Hologic Enhanced WB software plus the sub-regional analysis tool. The image contrast was varied to achieve the clearest picture of vertebrae and a rectangular region of interest was placed around L1 to L4. When it was not possible to place the boundary of the STB in the inter-vertebral space, either part of adjacent vertebrae could be included or some vertebrae of interest omitted. For consistency it was decided that the former method be adopted.

3.8.2 Results

The average width of each vertebra measured from lumbar spine images is shown in table 3.7. It was not possible to measure individual vertebrae on the WB images and so the width of the L1–L4 and L3-L4 combinations was assumed to be equivalent to the L4 width as this was the widest vertebra. The mean width of L4 from WB scans was 4.3 ± 0.2 cm (mean ±

SD). A paired t-test showed a significant difference between the width of L4 measured on lumbar spine images and L3 and L4 combinations from WB images ($p<0.001$).

A paired t-test indicates a significant difference ($p<0.001$) in the height of L1 to L4 as measured on each scan. The actual L1 to L4 height was 15.1±1.3 cm on the WB scan and 13.8 ± 0.7 cm on the lumbar spine image.

Frequently the boundary of the analysis region on WB images needed to be moved less than 2 lines to coincide with the edge of the vertebra or inter-vertebral space thus giving an error of 1 line equivalent i.e. ± 0.2 cm and 1.3 cm for the height and width respectively.

Vertebra	Width measured from lumbar spine image Mean ±SD (cm)
L1	4.1 ± 0.3
L2	4.1 ± 0.3
L3	4.4 ± 0.3
L4	4.9 ± 0.4

Table 3.7 Width of lumbar vertebrae measured from lumbar spine DXA image.

3.8.3 Discussion

The width of the vertebrae are within the normal range for anatomical dimensions of the spine confirming that the measurements reported by the software are plausible (Busscher *et al.* 2010). The results of a paired t-test indicate the widths and heights are significantly different. The lumbar spine measurement will be more accurate as it is usually possible to place the superior and inferior boundaries of the ROI within the T12 to L1 and L4 to L5 inter-vertebral space respectively. In contrast, on WB images it is often difficult to identify the inter-vertebral space and even

when identified, it is not always possible to place the border of the analysis region into the space. When the analysis region could not be placed exactly in the inter-vertebral space, the edge was placed such that part of an adjacent vertebra was included e.g. top of L5 or bottom of T12. This is the likely explanation for the height measured from WB images being larger than that measured from the lumbar spine scan. Possible reasons for a difference in width are (1) the resolution of the WB image makes defining the edge of vertebrae difficult and (2) the width of the analysis region increases in two line increments. As a result of the latter the region was frequently larger than the vertebrae and included some soft-tissue.

3.9 Conclusions

The calibration of the Hologic QDR-1000W used in this work remained stable over the time period of this study and the long term precision was acceptable.

This work has shown the importance of the width of the soft-tissue baseline when analysing lumbar spine scans as even in a phantom study where the BMD is fixed and the soft-tissue baseline is homogeneous, the BA, BMC and BMD appear to increase as the width of the ROI increases.

These findings suggest that the smallest width of ROI that gives a complete bone map is 8.3 cm (86 lines) and therefore results reported with regions smaller than this may be unreliable. Painting in bone to complete a bone map introduces further inaccuracies and therefore it was decided not to paint in bone during in-vivo analysis.

The measurements in this chapter indicate that the line spacing and point resolution factors for the Hologic WB sub-regional analysis software are correct.

The results presented in this chapter form a base for further in-vivo BCA as they confirm the measurements reported by the Hologic WB sub-

regional analysis tool are linear as the area of the analysis region increases. Also, the accuracy of the FM measurements appears to be acceptable for levels expected in the body and the tissue under the border of the STB is accounted for in measurements.

Despite a statistical test showing a significant difference between the height and width of the spine, the actual differences were considered small enough, in relation to other potential errors involved in combining WB and lumbar spine data, to proceed with further in-vivo work.

Chapter 4

Dependence of Dual-Energy X-ray Absorptiometry Lumbar Spine Bone Mineral Density Measurement on Width of Analysis Region

4.1 Introduction

Bone mineral density (BMD) measurements of the lumbar spine by dual-energy X-ray absorptiometry (DXA) are routinely used to diagnose osteoporosis. An accurate measurement of BMD is of clinical importance as the patient BMD is compared with a reference population to obtain T-scores which are used to diagnose osteoporosis based on The World Health Organisation (WHO) criteria as discussed in section 1.7.

When analysing lumbar spine images, the analysis region incorporates the vertebrae plus a region of soft tissue adjacent to the spine as shown in figure 2.11. This is termed the global region of interest (ROI) in this work. It has been observed both in-vitro and in-vivo that the lumbar spine BMD reported by Hologic scanners appears to increase as the width of the ROI increases (Hansen *et al.* 1990; Tothill and Pye 1992). These findings were confirmed in-vitro using the Hologic spine phantom in chapter 3. The next stage was to investigate the effect of the ROI width on in-vivo lumbar spine images.

The aims of this chapter are:

- To investigate the influence of the width of the lumbar spine ROI on the reported in-vivo BMD.
- To investigate the effect of applying a correction factor to in-vivo BMD measurements based on changes in BMD observed when spine phantom images are analysed with increasing ROI widths.

4.2 Study Population

To develop a method for quantifying the effect of a non-uniform distribution of abdominal fat on lumbar spine BMD, lumbar spine and whole body (WB) DXA data were extracted from scans of patients who had previously participated in a study of BMD and body composition in inflammatory bowel disease (IBD). WB scans are not performed routinely on patients undergoing BMD assessment or for the majority of research studies and hence there was limited data available. The IBD study group was chosen as it contained the largest number of participants of a single gender that had lumbar spine and WB scans.

Evidence shows that patients with IBD have an increased incidence of osteopaenia and osteoporosis (Dinca *et al*. 1999; Arden and Cooper 2002) and it has been reported that IBD patients have a 40% increase in fracture risk (Bernstein *et al.* 2000). Low BMD has also been shown to occur in children with IBD (Gokhale *et al.* 1998). Reduced BMD in IBD is multi-factorial with links to calcium deficiency, vitamin D deficiency, malnutrition, malabsorption, systemic inflammation and use of corticosteroids. BMD is expected to decrease more rapidly in steroid treated patients (Dinca *et al.* 1999). Literature suggests that bone metabolism is different in Crohn's Disease (CD) and ulcerative colitis (UC) (Dinca *et al.* 1999) with reports of a higher prevalence of osteoporosis in CD than UC (Gokhale *et al.* 1998).

Lumbar spine and WB scans for 50 IBD subjects previously scanned with the Hologic QDR-1000W bone densitometer were retrieved from the archive. The mean age of the subjects was 50±11y (±SD) and the mean body mass index (BMI) was (23.95±4.66) kg/m^2. All subjects were female and Caucasian. The advantage of using only females was to give a more homogeneous study population with similar fat distribution. The information recorded at the time of the scan indicated that 13 subjects had UC, 18 CD, 2 proctitis and 17 unspecified IBD. The average BMD of this group with the standard ROI width was 0.977 ± 0.156 g/cm^2. Further detail on the characteristics of this group is given in chapter 7 table 7.1. The IBD group covers a wide range of ages and the average BMD is within the normal range. A considerable number of patients attending for a BMD assessment have osteopaenia or osteoporosis and hence the data obtained from the IBD group may not be directly applicable to these patients. However, a group with confirmed osteoporosis is investigated in chapter 7.

4.3 Influence of the Width of Soft Tissue Region used for Lumbar Spine Analysis on BMD Measurement

4.3.1 Method

The DXA scans used in this work were acquired at the University Hospital of Wales in Cardiff on the Hologic QDR-1000W. During the time period over which the lumbar spine scans used in this thesis were acquired, the image width used in Cardiff was wider than that recommended by Hologic. The Cardiff scan width was 15.05 cm (156 lines) compared to 12.45 cm (129 lines) recommended by Hologic. This increased scan width allowed BMD measurements to be made with a greater range of analysis ROI widths for the purpose of the current investigation. Hologic software places the lateral borders of the default ROI 10 lines within the edge of the scan field.

Fifty lumbar spine scans were analysed with the standard Hologic QDR-1000W lumbar spine software (Version: 4.74P). The scans were analysed

eight times with the ROI equivalent in height to L1 to L4 and with widths increasing from 8.3 cm (86 lines) to 15.1 cm (156 lines) in 0.97 cm (10 line) steps (Fig. 4.1). The smallest ROI was determined by assessing the quality of the bone map with various widths of ROI as reported in chapter 3. The narrowest ROI that gave a complete bone map for all images was 86 lines and hence this was the narrowest ROI used in this study.

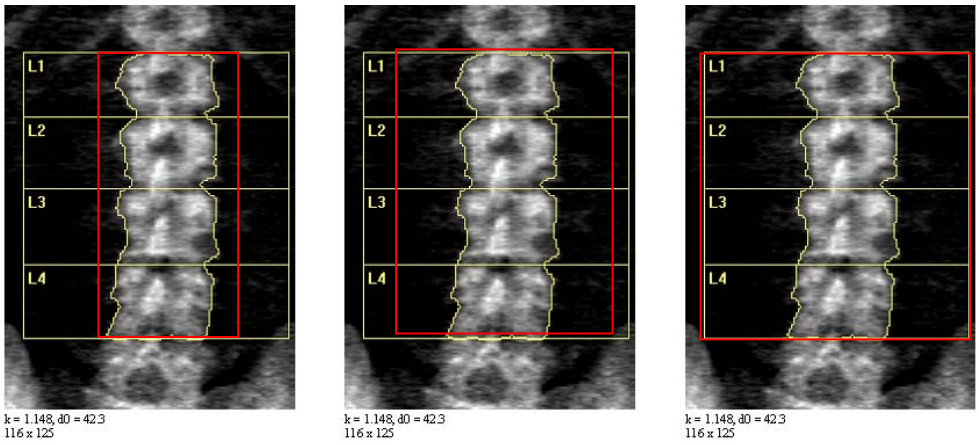

Figure 4.1 Analysis of lumbar spine images to investigate the width of the ROI on the reported BMC, BMD and BA. Eight widths of ROI were used but the principle is demonstrated here with three. The yellow largest ROI represents the standard width whereas the red ROI is variable for this study.

At each width the BMD, BMC and BA for individual vertebrae and the total of L1 to L4 were recorded. The data were averaged over the 50 subjects and analysed with a linear regression model using the SPSS statistics software version 12.0.1. Repeated measures analysis was performed to investigate (1) the relationship between BMD, BMC and BA with ROI width, (2) the difference in BMD, BMC and BA between the vertebrae and (3) the interaction between ROI width and vertebral level. A one-way ANOVA test was used to compare the difference in BMD, BMC and BA between the largest and smallest ROI. For all statistical tests a p-value < 0.05 was classed as significant.

To establish the intra-observer variability, a single lumbar spine scan was analysed thirty times and also scans from thirty individuals were analysed

twice on separate days. The inter-observer reproducibility was measured by two observers independently analysing thirty spine scans.

Due to the similarity between the regression line gradients for changes in BA and BMC with ROI width of L1 and L2 and also L3 and L4, it was considered appropriate to combine the BMD for these pairs of vertebrae. Also, combining data for adjacent vertebrae enabled the BMD results to be compared to fat and lean measurements from the WB images. It was found when analysing WB images in later work that it was not possible to isolate accurately individual vertebrae due to the size and resolution of the images. The combined BMD for pairs of vertebrae is denoted by L1+L2 and L3+L4 in this thesis and calculated using equations 4.1 and 4.2. Repeated measures analysis was used to check for an interaction between the combined L1+L2 and L3+L4 BMD with a significance level of $p<0.05$.

$$BMDL1+L2 \equiv \frac{(BMCL1+BMCL2)}{(AREAL1+AREAL2)} \qquad (4.1)$$

$$BMDL3+L4 \equiv \frac{(BMCL3+BMCL4)}{(AREAL3+AREAL4)} \qquad (4.2)$$

4.3.2 Results

When the lumbar spine ROI width is increased from 8.3 cm to 15.1 cm there is an apparent increase in BMD, BMC and BA for L2, L3 and L4 but a decrease in all parameters for L1 (Figs. 4.2, 4.3, 4.4, 4.5). Linear regression analysis indicated that all changes are significant ($p<0.05$). Significance in this context means that the gradient of the slope is significantly different to zero, which would occur if there were no true change in BMD, BA or BMC. The error bars on figures 4.2 to 4.4 represent the 95% CI of the data.

Repeated measures analysis on data in figures 4.2 to 4.4 indicated that in general, the ROI width had a significant effect on BMD, BMC and BA ($p<0.001$). The only exception was for the L1 and L2 BMC and BA. There

was a significant difference in BMC and BA between the four vertebrae ($p<0.001$). A Bonferroni post hoc test revealed there was no significant difference between the BMD of L2 and L3 ($p = 0.073$) and L3 and L4 ($p = 0.452$) but there was a significant difference for all other pairs of vertebrae. A significant interaction was found between the vertebral levels and ROI width for BMD, BMC and BA ($p<0.001$).

An ANOVA test on data in table 4.5 showed the difference between the BMD, BMC and BA measured with the largest and smallest ROI were significant ($p<0.001$). A Bonferroni post-hoc test revealed that changes in BMD, BMC and BA for L3 and L4 were not statistically significant ($p=1.00$). The changes for all other combinations of two vertebrae were statistically significant ($p<0.001$).

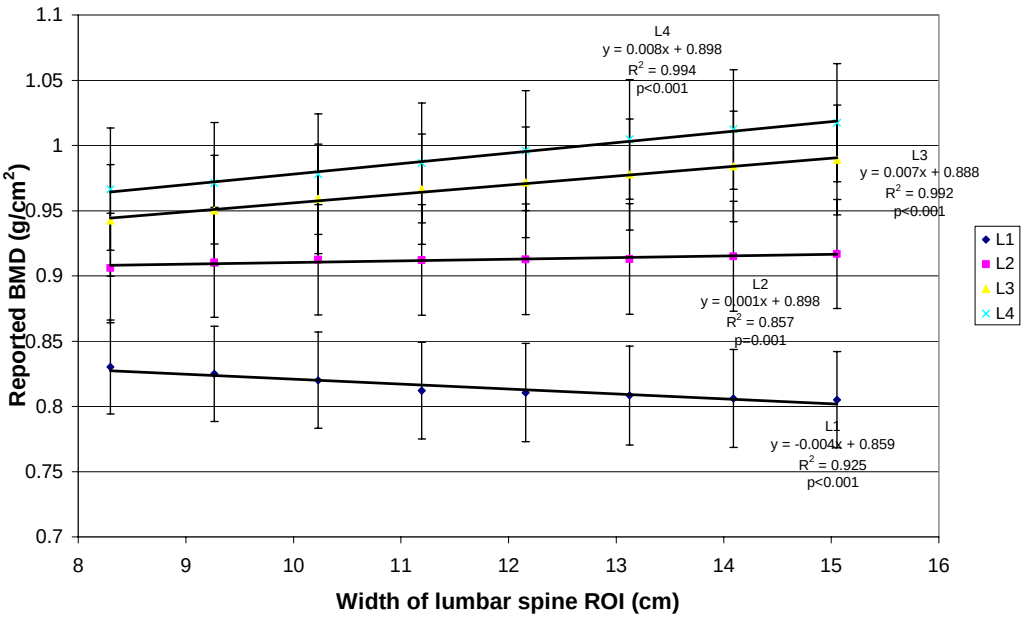

Figure 4.2 Relationship between measured lumbar spine BMD and the width of the lumbar spine ROI. Data are the average (± 95% CI) for 50 IBD subjects. SEE: L1 = 0.003 g/cm^2, L2 = 0.001 g/cm^2, L3 = 0.002 g/cm^2, L4 = 0.002 g/cm^2. Errors in slope were <0.001 g/cm^2 per cm for all vertebrae.

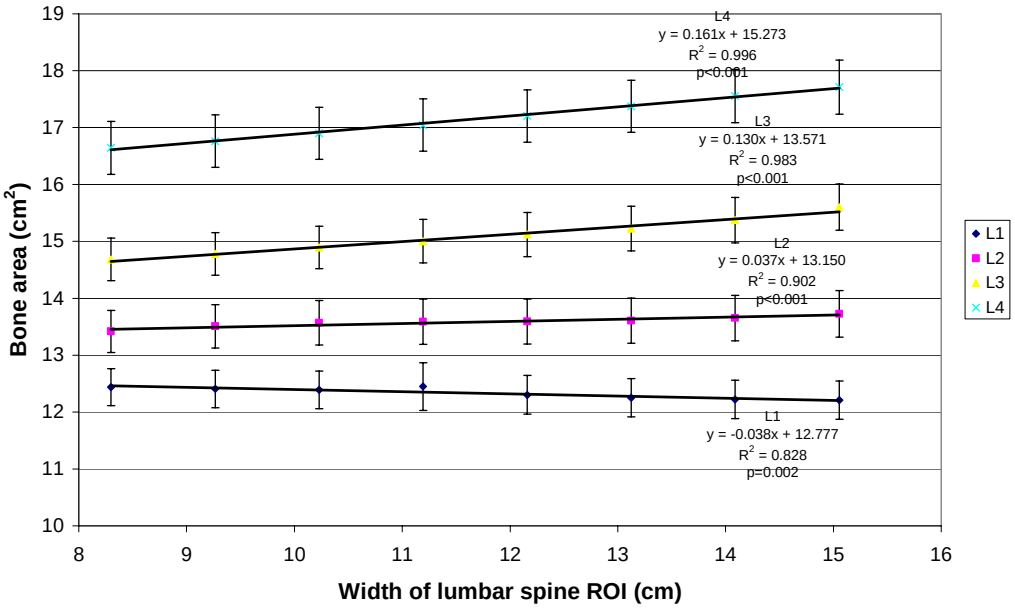

Figure 4.3 Relationship between measured lumbar spine BA and the width of the lumbar spine ROI. Data are the average (± 95% CI) for 50 IBD subjects. SEE: L1=0.044 cm^2, L2 = 0.031 cm^2, L3 = 0.044 cm^2, L4 =0.025 cm^2. Errors in slope were L1 ± 0.007 cm^2 per cm, L2 ±0.005 cm^2 per cm, L3± 0.007 cm^2 per cm, L4 ± 0.004 cm^2per cm.

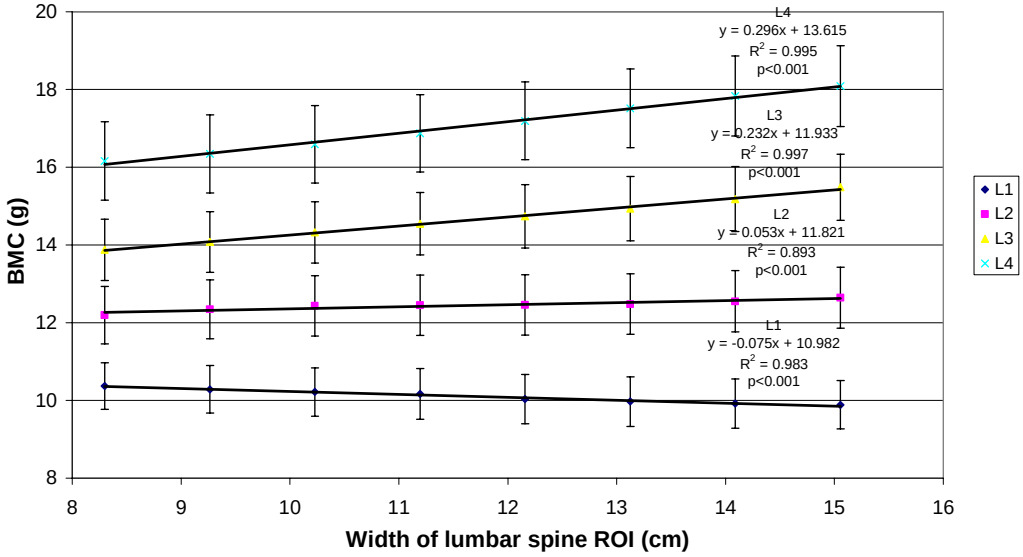

Figure 4.4 Relationship between measured lumbar spine BMC and the width of the lumbar spine ROI. Data are the average (± 95% CI) for 50 IBD subjects. SEE: L1=0.025 g, L2 = 0.047 g, L3=0.034 g, L4 = 0.053 g. Errors of the slopes were L1 ± 0.004 g/cm, L2±0.008 g/cm, L3±0.005 g/cm and L4±0.008 g/cm.

It can be seen from figure 4.5 that the changes in BMC between extremes of ROI widths are approximately a factor of two greater than those for BA for the L2, L3 and L4 vertebrae.

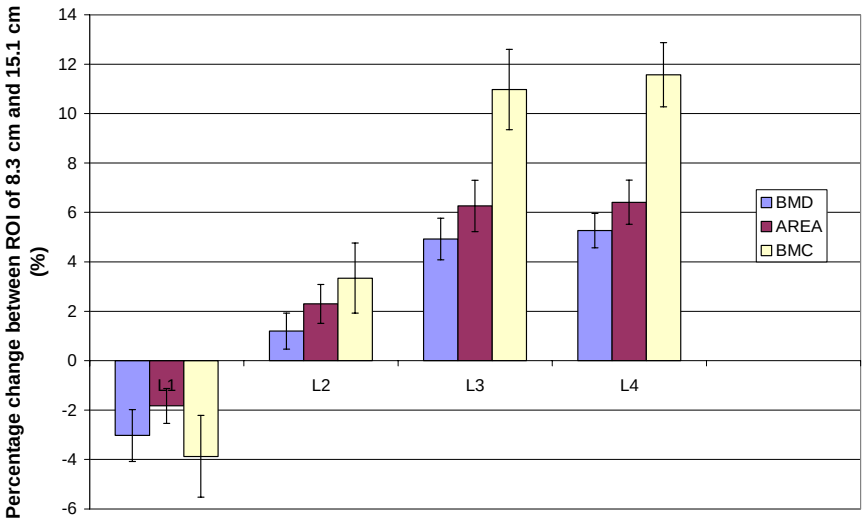

Figure 4.5 Change in measured BMD, BMC and BA observed with an increase in the lumbar spine ROI from 8.3 cm to 15.1cm. Data are averaged over all scans for the 50 IBD subjects. Error bars represent ± 95% CI.

Figure 4.6 shows that when combining BA and BMC for L3+L4 using equation 4.2, the resultant BMD increased by 5.1% as the width of the ROI increased from 8.3 cm to 15.1 cm. However, for L1+L2 there was little variation probably due to the changes in L1 and L2 being in opposite directions (-0.6%). Repeated measures analysis indicated the ROI width had a significant effect on L1+L2 and L3+L4 BMD ($p<0.001$). The L3+L4 BMD was significantly higher than L1+L2 ($p<0.001$). There was a significant interaction between ROI width and vertebrae ($p<0.001$) for the L1+L2 and L3+L4 BMD. The gradient of the L1+L2 BMD regression line in figure 4.6 was significantly different to that for L3+L4 ($p<0.001$).

When analysing 30 lumbar spine scans twice, the coefficient of variation (CV%) for the combined L3+L4 BMD, calculated from combining the BMC and BA, was 0.22%. When two observers independently analysed 30 scans the CV% was 0.39%. The error bars on figure 4.6 are the 95% CI for the data.

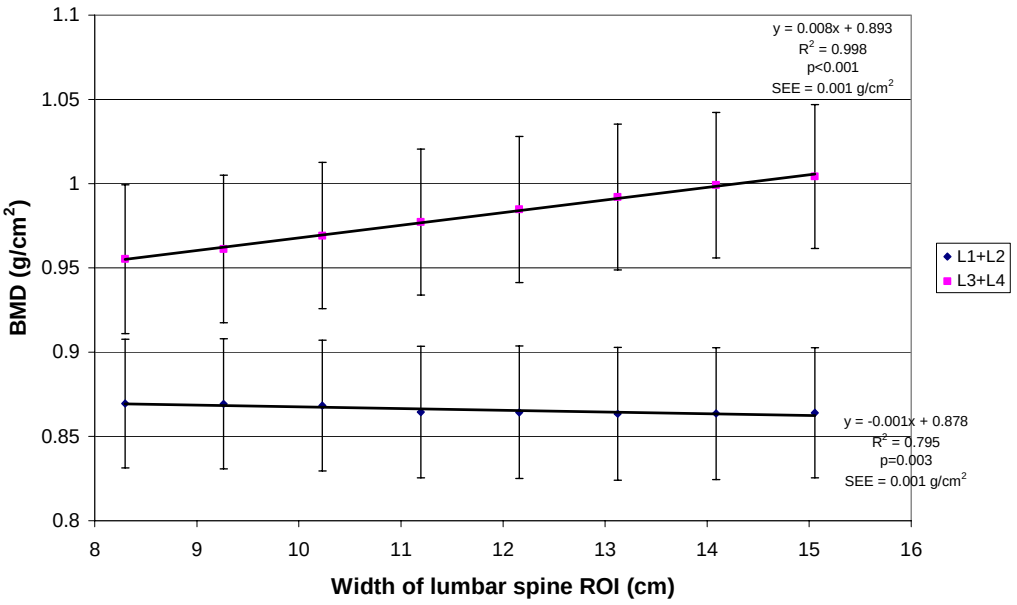

Figure 4.6 Relationship between measured combined L1+L2 and L3+L4 BMD and the width of the lumbar spine ROI. Data are the average (± 95% CI) for 50 IBD subjects. Errors in slope are <0.001 g/cm^2 per cm for L1+L2 and L3+L4.

As can be seen in figure 4.7, there was a significant correlation between the BA and BMC of both L3 and L4 as ROI width increased which was confirmed by a significant Pearson's correlation coefficient ($p<0.05$).

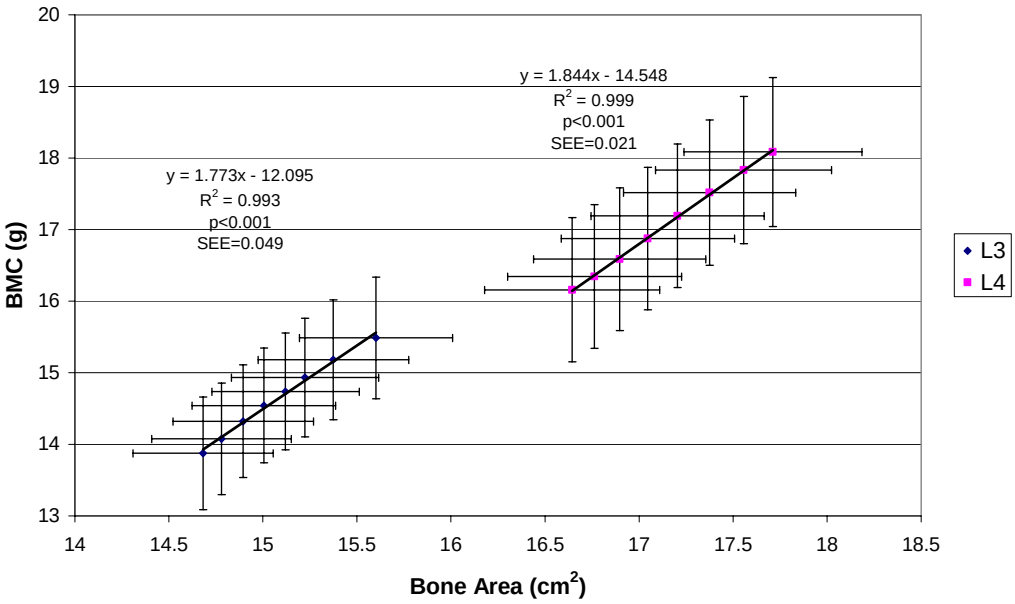

Figure 4.7 Relationship between BMC and BA and the width of the lumbar spine ROI for L3 and L4. Data are the average for 50 IBD subjects. Errors for slope of regression lines are ±0.059 g/cm^2 for L3 and ±0.021 g/cm^2 for L4. Error associated with each data point is ±95% CI.

4.3.3 Discussion

It is evident from these results that there is a dependence of BMD, BMC and BA on lumbar spine ROI width and a significant interaction between the vertebral level and ROI width for BMD, BMC and BA ($p<0.001$). Real changes in these parameters are not plausible as a single lumbar spine image was repeatedly analysed with the only variable being the ROI width. These findings are not unexpected based on the existing literature. The BMD, BMC and BA appear to increase for L2, L3 and L4 as the ROI width increases. In contrast there is a decrease in all parameters for L1. A Bonferroni post-hoc test revealed the changes in BMD, BMC and BA between the largest and smallest ROI were not significantly different for L3 and L4 ($p<0.001$) which supported the decision to combine data for L3 and L4 in further work. The linear regression and repeated measures analysis indicated that the dependence of L1+L2 and L3+L4 BMD on ROI

width is significant ($p<0.001$) with a significant interaction between the vertebral level and ROI width.

It is probable that the dependence of the measured BMD, BMC, BA on ROI width is linked with the accuracy of the algorithm used to identify the edge of the vertebrae i.e. the edge detection algorithm. The bone edge is identified by applying a threshold value for BMD to all the pixels within the image as summarised in figure 2.4. Only pixels with a value greater than this threshold are designated as containing bone. As the ROI width increases and more tissue is included in the soft tissue baseline, it is plausible that the R-value will change. The R-value is discussed in section 2.2. As the fat content of the soft tissue adjacent to the spine and within the ROI increases, R will decrease.

As BMC is calculated from multiplication of BMD by BA, as discussed in section 2.4, it is logical that an increase in BA, will result in an increase in BMC. As the changes in BMC observed in this work are approximately a factor of two greater than those in BA this explains the resultant change in BMD (Fig. 4.5).

It is likely that the increase in BMC, BMD and BA observed for L2 to L4 in the current study are due to an increase in the amount of fat in the baseline as the ROI width increases. This can be explained another way; BMD is over corrected as the average thickness of fat in the baseline increases and this is reflected as an increase in the area density of the soft tissue baseline. Subsequently, when applying the bone threshold value to each pixel in the image, more pixels are included in the bone map and hence BA increases.

When analysing lumbar spine scans using the Hologic QDR-1000W software, the areas identified as bone, i.e. the bone map, and soft tissue can be visualised by the operator at the relevant stages of the BMD calculation. Tissue considered as bone is coded in yellow and soft tissue used for the baseline correction is coloured in blue. Throughout this work, the bone map and soft tissue regions were closely inspected for each

width of ROI and any anomalies noted. Visual inspection of the bone map confirmed an increase in the number of pixels containing bone as the width of the ROI increased. The consequence of this was an increase in the reported BA. At the largest ROI widths, the lateral processes were sometimes included in the bone map and occasionally ribs and tissues with a relatively high density were designated as bone. No bone was added to the bone map and regions were only deleted when tissue classed as bone was obviously not bone and when it would be deleted in a clinical situation. Any alterations to the bone map were kept consistent when analysing images for each ROI width.

Further evidence that the QDR-1000W BMD results depend on the accuracy of the automatic edge detection algorithm comes from studies in which a region around the vertebrae is defined manually thus removing dependence on the automatic edge detection algorithm (Tothill and Avenell 1998). One such study involved a series of scans from individuals that were acquired over a period of time being analysed using a manually defined inner-rectangular region to designate the bone edge (Tothill and Avenell 1998). It was found that using this region, larger changes were observed in the reported BMD than when relying on the automatic edge detection algorithm. These findings support the theory that BMD is underestimated due to changes in BA which is determined by the software defining the bone outline.

The reason for the inconsistency in the trend of results between L1 and the other vertebrae is unclear. One possible explanation is that the amount of fat in the soft tissue baseline adjacent to L1 decreases as the ROI width increases, whereas for L2 to L4 the amount of fat increases. When analysing the images of the Hologic spine phantom using increasing widths of ROI, there was an increase in BMD, BMC and BA for all the vertebrae. The discrepancy between the in-vivo and phantom observations is probably due to the fact that the thickness of baseline soft tissue within the phantom is uniform and equal for all vertebrae. Whilst the changes seen in L1 BMD are small, the data shows a gradual

decrease as the ROI is widened and a significant interaction between the regression lines for L2, L3 and L4 BMD. The results are therefore unlikely to be due to inaccuracy or lack of precision.

It was encouraging that the inter and intra observer reproducibility for combined L3+L4 BMD measurements are less than the precision of 1% quoted by Hologic for lumbar spine BMD measurement, and are therefore considered acceptable. Precision was assessed for the combined L3 and L4 measurements as this was the data used in further work.

The larger variation in BMD of L3+L4 relative to L1+L2 as the ROI width increased is likely to be due to the greater inhomogeneity in the abdominal fat distribution within the ROI at the L3+L4 level. This theory would be consistent with other research which showed a greater difference in the amount of fat in the soft tissue baseline compared to that in the tissue over the vertebrae at the L4-L5 level compared to the T12-L1 level (Svendsen *et al.* 2002). There is a significant interaction for variation in L1+L2 and L3+L4 BMD with ROI width. However, the regression gradient for L1 BMD is negative but positive for L2 BMD hence there will be a cancellation effect when combining the BMD of L1 and L2.

The results of this study corroborate the work of others. Hansen *et al.* (1990) showed that for the QDR-1000, the reported lumbar spine BMD decreased by approximately 3.5% when reanalysing images from 30 postmenopausal women six times and gradually narrowing the ROI in 1 cm steps. Tothill and Pye (1992) observed an increase in in-vivo L2 to L4 BMD of approximately 2% when increasing the width of the ROI from 8.5 cm to 12.5 cm. To compare these published findings with those from the current study, these changes can be expressed as decreases of 0.5% and 0.7% per cm decrease of ROI width for Tothill and Pye (1992) and Hansen *et al.* (1990) respectively, whereas for the current data the uncorrected L3+L4 BMD decreased by 0.7% per cm.

The findings of the current study support the theory proposed by Tothill and Avenell (1998) who observed a dependence of BA on BMC and

concluded that changes in BMD between scans may be anomalous depending on changes in BA. This suspected anomaly was confirmed by observations of a correlation between changes in reported BMC and BA with repeated scans performed on the same individual even when a change in BA is not realistic. In the Tothill and Avenell study (1998), the observations were made when analysing repeat scans performed at intervals of up to five years in which a change in BMD between scans may have occurred. However, similar findings were found when only including scans from patients in whom a true change in BMD, BMC or BA was unlikely. Real changes in BA are unlikely to be significant over the time scales of many longitudinal studies. An increase in vertebral cross-sectional area of 25-30% between 20 to 80 years old has been measured in a group of men but not women (Mosekilde and Mosekilde 1990).

The Tothill and Avenell study (1998) is not directly comparable to the current one as they looked at a series of images for individual patients whereas in the current study, the same scan was repeatedly analysed each time and including more soft tissue included in the baseline. Despite the difference in study design, the apparent changes in BMD reported in this study are consistent with the theory that they are, at least in part, due to changes in BA. A strong correlation was found between changes in BA and BMC as the width of the ROI increased thereby increasing the area of soft tissue in the baseline when there is no true change in BA (Fig. 4.7a, b).

These anomalous changes in BA and BMC have been corroborated by others for pencil beam absorptiometers (Yang *et al.* 1997; Nielsen *et al.* 1998). Similarly, for the Hologic-4500A fan beam densitometer an underestimation in BMD due to a correlation between changes in BA and BMC has been reported (Tothill and Hannan 2007).

For the adult population, the variation in lumbar spine width is small and therefore the vertebrae will occupy approximately the same fraction of the ROI for all patients. However, in children there is a greater variation in spine width dependent on the size of the child and therefore the fraction

of the ROI that the spine occupies will vary. The results of a preliminary study showed that for an adult population, the standard width ROI used in Cardiff was on average 2.8 times the width of the lumbar spine whereas for a paediatric sample this ranged between 2.4 and 3.2 centred around 2.8 (Pettit *et al.* 2005). For the IBD subjects included in the present study the standard width ROI was on average 2.4 times the width of L4.

The present results highlight the importance of standardising the width of the ROI to include the same region of soft tissue within the baseline. However, even with standardising the width of the ROI, the fat thickness in the baseline region may change over time thus introducing accuracy and precision errors in BMD.

The effect of the ROI width on the BMD of L3+L4 is more pronounced than for L1+L2 and therefore it was decided to concentrate on the L3+L4 data in future work.

4.4 Correction of In-vivo Lumbar Spine BMD Measurements with In-vitro Data

4.4.1 Method

It was shown in chapter 3 that there is an apparent increase in BMD, BMC and BA of vertebrae embedded in the Hologic spine phantom as the width of the ROI increased. These changes must be an artefact. The region of the phantom representing soft tissue has a uniform composition and therefore changes in BMD are not expected as the ROI increases if the average area density of the tissue remains constant. To determine in-vivo changes in BMD, BMC and BA due to a non-uniform fat distribution as ROI width increased the measured BMD, BMC and BA must be corrected for the changes observed in the phantom study when varying the ROI width. It is assumed that the artefact applies to in-vivo data in the same way as it does in-vitro.

The in-vivo L3 and L4 BMC and BA, measured in section 4.2, were corrected using the gradient of the linear regression lines for BMC and BA of the Hologic spine phantom as the ROI width increased. The regression lines and correction factors are presented in chapter 3 table 3.2. The corrected BMC and BA were subsequently combined, using equations 4.1 and 4.2 to obtain the corrected L3+L4 BMD. This will be termed the phantom corrected BMD in this thesis. The reference width for correction was 11.5 cm (119 lines) as this was the width recommended by Hologic and it was within the range generally accepted for clinical practice (Wahner and Fogelman 1994). It was assumed that for a width less than 11.5 cm BMD, BMC and BA is underestimated and that for a width greater than 11.5 cm they are overestimated. Based on this fact, the correction factors calculated using equation 4.3 were added and subtracted respectively to the reported BMD. Repeated measures analysis, with a significance level of $p<0.05$, was used to test for an interaction between the uncorrected and corrected BMC, BMD and BA with ROI width.

$$\text{correction factor} = n \times \text{gradient (change/line)} \qquad (4.3)$$

where n is the number of lines from the reference width i.e. 119 lines.

4.4.2 Results

As shown in table 4.1, compensating the L3 and L4 BMC and BA for the change in these quantities observed when analysing phantom images reduced the dependence of BMC and BA on the ROI width. This was quantified by examining regression line gradients for BMC and BA plotted against the ROI width. Repeated measures analysis on data in table 4.1 confirmed a significant effect of ROI width on the corrected and uncorrected BMC and BA for L3 and L4 ($p<0.001$). The uncorrected and corrected BMC and BA were not significantly different as $p>0.950$ in all cases. The gradient of the regression lines for corrected data were

significantly different than those for uncorrected data with a significant interaction between the uncorrected and corrected data and ROI width.

	Gradient of regression line for uncorrected measurements	Gradient of linear regression line for corrected data
L3 BMC (g/cm)	0.23±0.01	0.15±0.01
L4 BMC (g/cm)	0.30±0.01	0.22±0.01
L3 BA (cm^2/cm)	0.13±0.01	0.09±0.01
L4 BA (cm^2/cm)	0.16± <0.01	0.12± <0.01
L3+L4 BMD (gcm^{-2}/cm)	0.008± <0.001	0.005± <0.001

Table 4.1 Comparison of gradients of regression lines for L3 and L4 BMC and BA and combined L3+L4 BMD before and after correcting with phantom data.

Figure 4.8 shows that when combining the corrected BMC and BA to give the L3+L4 BMD, the change in BMD between extremes of ROI width reduced from 5.1% to 3.6%. Repeated measures analysis showed there was a significant effect of ROI width for corrected and uncorrected L3+L4 BMD ($p<0.001$) but there was no significant difference in the absolute BMD ($p=0.994$). There was a significant interaction between the slopes in figure 4.8 indicating the gradients of the regression lines are significantly different ($p<0.001$). The corrected L3+L4 BMD results were used in subsequent analysis.

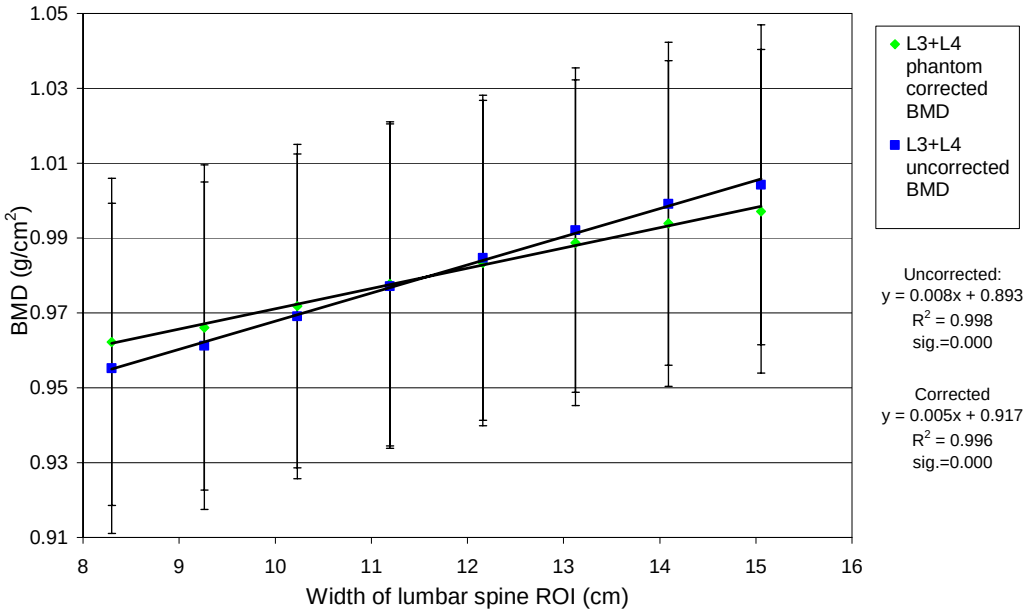

Figure 4.8 Relationship between the corrected and uncorrected L3+L4 BMD and the width of the lumbar spine ROI. Data are the average for 50 IBD subjects. SEE: uncorrected = 0.001 g/cm^2 and corrected BMD = 0.001 g/cm^2. Standard error of slope is <0.001 g/cm^2 per cm for both uncorrected and corrected BMD. Data points represent mean ± 95% CI.

4.4.3 Discussion

The current study found that correcting the in-vivo L3 and L4 BMC and BA with the phantom data prior to calculating L3+L4 BMD reduced the change observed when increasing the ROI width. The phantom correction is based on changes which are observed with a homogeneous soft tissue baseline. The residual error in BMC, BA and BMD after accounting for this change when increasing the ROI width is likely to be due to the in-homogeneity in the distribution of fat in the abdomen at the level of the lumbar vertebrae. It is acknowledged that the change in the gradient is relatively small compared to the 95% CI of the data shown as error bars in figure 4.8. However, repeated measures analysis confirmed there was a significant interaction between the slopes ($p<0.001$).

A limitation of this study is that the reference width used to correct BMC and BA is 11.5 cm and therefore it is assumed that the BMD measured

with this ROI is the true value. In reality this is unlikely to be the case. DXA is considered as the “gold-standard” for BMD measurement but the current results show that accuracy errors can occur due to the analysis procedure. As with any studies involving in-vivo BMD measurements, it is not possible to determine the true BMD for the subjects. The only way of assessing accuracy is in a cadaver study such as that by Svendsen *et al.* (1995) where the BMD of bones measured in-situ is compared to that measured following excision.

It is unlikely that in practice ROI widths less than 11.5 cm and greater than 12.5 cm would be used, but the results presented here imply that even small changes in the width can cause changes in BMD. For example, the corrected BMD was 0.002 g/cm^2 lower with a ROI slightly smaller than the standard ROI, i.e. 11.2 cm, and for a slightly wider ROI of 13.1 cm the BMD was 0.009 g/cm^2 higher. Such changes are very small and are unlikely to affect the diagnosis. Changing the ROI width between scans could introduce an accuracy error and an error in the rate of change of BMD used to monitor disease progression or the effectiveness of a therapeutic drug.

A similar attempt at correcting in-vivo lumbar spine BMD data were made by Tothill and Pye (1992). A correction factor was applied to lumbar spine in-vivo data based on changes in BMD observed when repeatedly analysing images of the Hologic spine phantom whilst increasing the width of the ROI. When correcting BMD of L2 to L4, the difference between the values reported for ROI widths of 8.5 cm and 12.5 cm decreased from 0.0176 g/cm^2 to 0.0116 g/cm^2. For L3 and L4 separately the corrected difference was 0.0182 and 0.0194 g/cm^2 respectively (Tothill and Pye 1992). In the current work, the difference between the uncorrected L3+L4 BMD for similar widths of ROI was larger than that found by Tothill and Pye (1992) (0.030 g/cm^2). When correcting the BMD this difference was 0.021 g/cm^2. These values can be expressed as a change in BMD of 0.5% per cm and 0.3% per cm for the Tothill and Pye (1992) uncorrected and corrected data respectively. Whereas, for the

current work correcting the data decreased the change in BMD from 0.7% per cm to 0.5% per cm. Differences may be due to slight differences in the actual ROI width and the vertebrae examined.

It can be concluded from the data presented here that compensating in-vivo BMD results for changes in BA and BMC observed in a phantom with a homogeneous baseline will remove some of the dependence of BMD on ROI width.

The purpose of this entire study is to examine the influence of a non-uniform distribution of fat on BMD results and therefore the corrected L3+L4 results will be used in subsequent work.

4.5 Conclusions

There is a dependence of BMD, BMC and BA on lumbar spine ROI width which is an artefact associated with the amount of soft tissue within the baseline region. Changes in BA are strongly correlated with changes in BMC which supports the theory that changes in BMD may be anomalous depending on changes in BA. Compensating the in-vivo BMD measurements for the changes observed in a phantom study decreased the dependence on ROI width but there remains a residual increase in combined L3+L4 BMD.

Chapter 5
Quantification of the Distribution of Abdominal Fat in the Region of the Lumbar Vertebrae from DXA Whole Body Images

5.1 Introduction

Measurement of lumbar spine BMD by DXA requires knowledge of the attenuation of the dual energy X-ray beams due to the soft tissue anterior and posterior (AP) to the vertebrae. This cannot be measured directly so the attenuation due to soft tissue in an adjacent bone free region is used to provide this information. The measured BMD will only be accurate if the attenuation by the soft tissue in these two regions is identical. Relative differences in the fat thickness over and adjacent to the vertebrae will potentially lead to the BMD being measured falsely high or low (Hangartner and Johnston 1990; Hansen *et al.* 1990).

From a review of the existing literature there appears to be two approaches to investigate the affect of abdominal fat distribution on the accuracy of lumbar spine BMD. These are firstly, the measurement of fat thickness from CT images and, secondly, the calculation of the relative thickness of fat and lean tissue within baseline soft tissue (Bolotin *et al.* 2003).

From Hologic QDR-1000W DXA whole body (WB) images it is possible to quantify abdominal fat and lean tissue distribution using the sub-regional analysis tool. This approach allows the lumbar spine BMD and the FM and LM to be collected from separate scans but which are acquired with the same technology. Whilst DXA WB images have been used to

measure FM in regions covering a large width of the abdomen, it is believed that this work is the first to use the Hologic QDR-1000W sub-regional analysis software to quantify abdominal fat and lean distribution by forming profiles of fat and lean tissue thickness using very small soft tissue analysis regions.

This chapter describes the development of a method to quantify the distribution of abdominal fat using WB images acquired with the Hologic QDR-1000W DXA scanner.

5.2 Method

For the 50 IBD subjects discussed in section 4.2, WB scans acquired on the same day as the lumbar spine scan used in chapter 4 were analysed using the Hologic Enhanced WB software (version 5.73). Although the goal of this work is to correct lumbar spine BMD for the non-uniform distribution of fat in individuals, an initial approach was to combine the data for the 50 subjects. In doing this it is assumed the outcome would be representative of many patients attending for a DXA scan. The images were checked for artefacts, e.g. metal on clothing, jewellery, body piercings, or internal implants. Prior to analysing the images, the display was optimised to give good contrast between soft tissue and bone. The sub-regional analysis software allows the user to place up to 7 analysis regions of any size at any position on the image. The BMD, BMC, BA, LM, FM and %fat was reported for the tissue within each region.

Initially an analysis region was placed over the vertebrae at the level of L1+L2 which was termed the central box (CB) (Fig. 5.1). Adjacent to the CB were placed regions of the same height and a width of 3 lines (0.6 cm) which is the smallest achievable with the software. These regions were called soft tissue boxes (STB). The STB were placed so that neighbouring boxes overlapped by one line to ensure no tissue was omitted. It was shown previously in 3.6 that tissue under the border of the sub-regional analysis box is accounted for. Fifteen STB were placed on

each side of the CB to cover approximately 7 cm each side of the spine. This width corresponded to the maximum width of the lumbar spine ROI used in section 4.3 i.e. 15.1 cm as shown in figure 5.1. For each STB the FM, LM and BMC were recorded. The analysis described above was repeated with the height of the CB and STB equal to L3+L4.

To allow comparison between different size analysis regions, the area density of fat in the CB and STB was calculated using equation 5.1.

$$Fat\_Area\_Density(g/cm^2) = \frac{Fat\_Mass\_in\_STB(g)}{Area\_of\_STB(cm^2)} \qquad (5.1)$$

FM was reported by the software and the area of each STB was calculated using equation 5.2.

$$STB\_AREA(cm^2) = (Width \times 0.2047) \times (Height \times 1.303) \qquad (5.2)$$

where the height and width are in lines, 0.2047 cm/line is the point resolution factor and 1.303 cm/line is the line spacing factor. The distance of the centre of each STB from the central axis (CA) of the spine was calculated using equation 5.3.

$$Distance\_from\_CA(cm) = [(0.5 \times width\_of\_CB) + ((2 \times no.\_of\_STB) - 1)] \times 0.2047 \qquad (5.3)$$

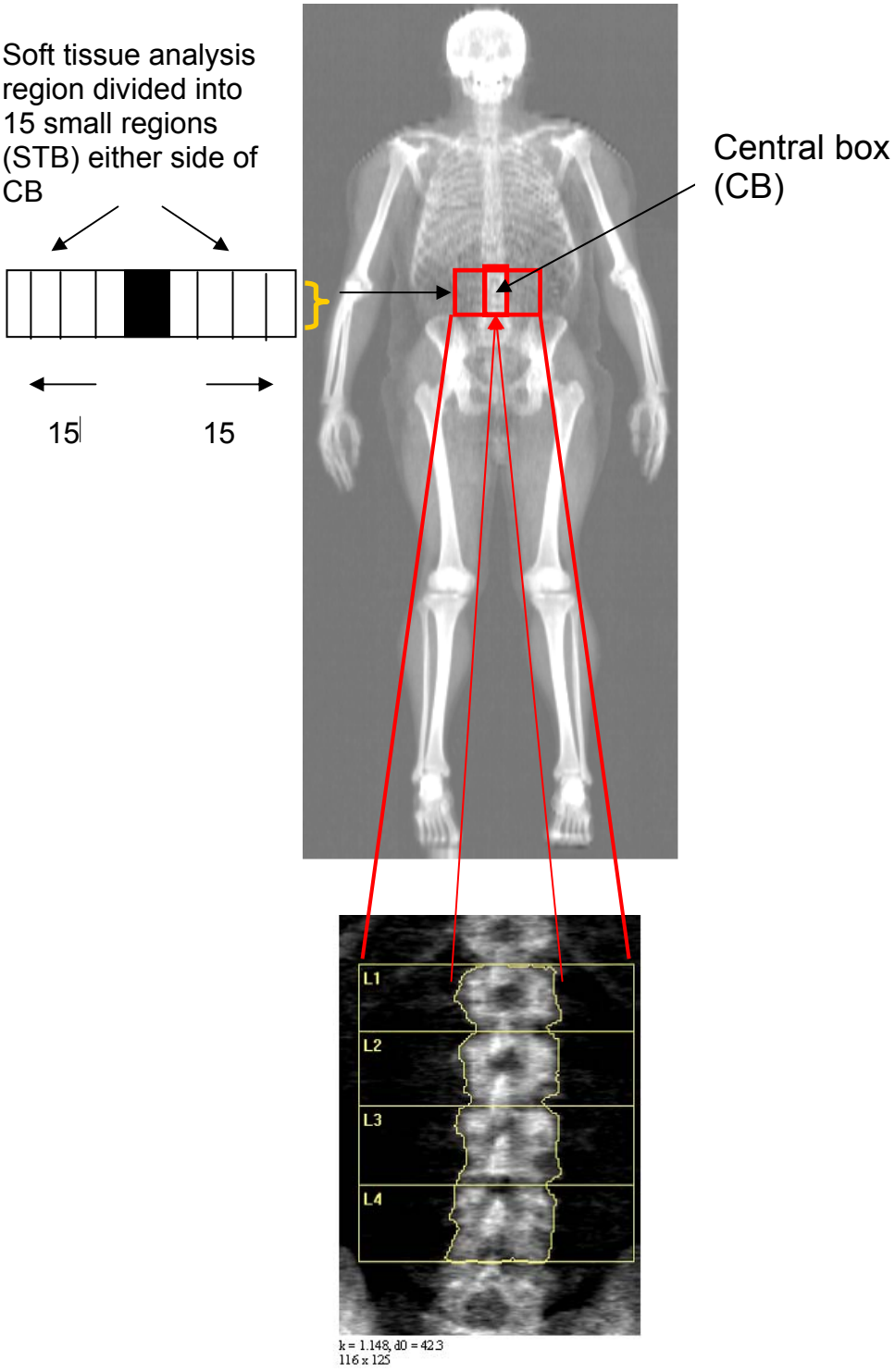

Figure 5.1 Comparison of DXA lumbar spine ROI used for BMD measurement and the equivalent soft tissue region on DXA whole body image. The soft tissue region is divided into 15 small analysis regions (STB) each side of central box (CB) which is placed over the spine. Only 4 STB each side of spine are shown. Example is shown for L1 to L4.

The area density of fat was converted into a fat thickness using equation 5.4.

$$t = \sigma / \rho \qquad (5.4)$$

where:

t= fat thickness (cm)

σ = area density of fat (g/cm^2)

ρ = physical density of fat (g/cm^3).

When discussing fat thickness in relation to DXA studies, the quantity represents the thickness of fat expected if all the fat that the X-ray beam traverses is condensed into a single layer. The physical density of fat was assumed to be equivalent to that of stearic acid (0.95 g/cm^3) as this is the material used by Hologic in calibrating the system for body composition studies. Lean and bone mineral are also considered as being condensed into single layers for DXA measurements.

The accuracy and precision of this method was limited due to the small size and poor resolution of the images and the fact that it was not always possible to place the superior and inferior borders of the STB in the inter-vertebral spaces. In these instances, the border was placed to include part of the adjacent vertebrae and not to exclude any of the vertebrae of interest e.g. to include part of T12 rather than exclude part of L1. The difference between FM measured with a CB and STB of height 5 lines and 7 lines was investigated where the 7 line region included part of an adjacent vertebra. When it was not possible to accurately match the lateral borders of the CB to the spine width, the width was chosen to include a small amount of soft tissue thus potentially incorporating the lateral processes of the spine.

To assess precision, the inter- and intra-observer variability of placing the CB and STB were calculated by one user analysing thirty scans twice and one scan thirty times and two observers independently analysing 30 scans.

The FM over the vertebrae is estimated by interpolation of the FM in a region of soft tissue adjacent to the bone. The validity of this assumption was tested by looking at the correlation between FM in the CB and that in the STB immediately adjacent to the spine.

To examine how the BMI affects the degree of inhomogeneity, abdominal fat thickness profiles were plotted for a lean and obese subject. These profiles were normalised to the fat thickness within the CB. The image display was optimised to identify the border between lean tissue and subcutaneous fat and the width of each at the level of L1 to L4 was measured by placing a region across the body. This measurement was described as the total body width and fat width in subsequent work.

5.3 Results

Fat thickness profiles derived from DXA WB images shown in figure 5.2 confirm that fat is distributed non-uniformly across the abdomen at the level of the lumbar vertebrae used to measure BMD.

At the L1+L2 level the fat thickness was relatively constant up to about 6 cm from the centre of the spine. The deviation of the fat thickness from that in the CB was less than 10% up to 6.7 cm and 5.4 cm on the right side (Rt) and left side (Lt) respectively. Extending laterally outwards there was an increase of 19% and 26% on the Rt and Lt respectively up to 7.9 cm from the centre of the spine. In comparison, at the L3+L4 level the fat thickness varied less than 2% up to 2.6 cm from the centre of the spine and less than 10% up to 4.2 cm. Following a minimum in fat thickness symmetrically at 3.5 cm there was an increase of 26% on the Rt and 28% on the Lt. Figure 5.3 shows the L3+L4 fat thickness profile with the scale expanded and with the SEM for the error bars. Also superimposed on figure 5.3 is the region that would be contained within a standard lumbar spine BMD ROI of 11.5 cm.

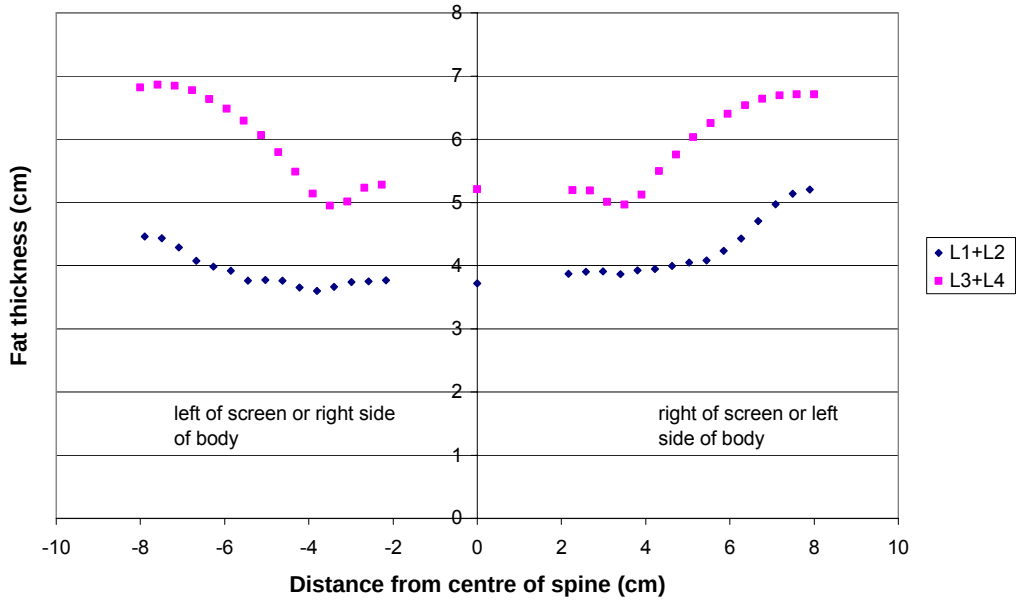

Figure 5.2 Comparison of abdominal fat thickness distribution at the L1+L2 and L3+L4 levels. Data are for the average of 50 IBD patients. Error bars were removed to allow a clearer comparison.

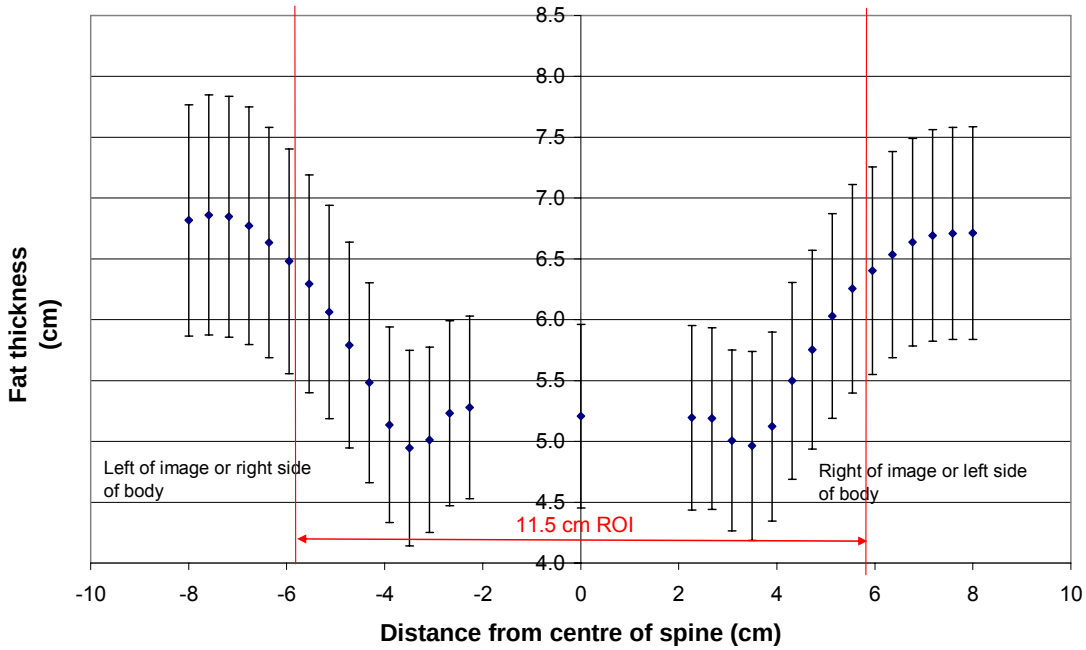

Figure 5.3 Variation in abdominal fat thickness at the level of L3+L4 with distance from the centre of lumbar spine for 50 IBD patients (± 95% CI).

There was a wide range in fat thickness measured for the CB over the vertebrae ranging from 1.2 cm to 12.0 cm. For the individual STB the minimum fat thickness measured was 0.4 cm and the maximum was 14.6 cm.

When analysing a WB image from a single individual using the method described here, the difference between the FM measured with an analysis region of height 5 lines and 7 lines was 18% for the CB and for the small STB it ranged from 1.5% to 34.0% (average 18.2%). This changed the fat thickness in CB by 0.43 cm. The intra-observer variability, expressed as the coefficient of variation (CV%), for measuring fat thickness within the STB was 15% (0 to 38%) and the inter-observer variability was 17% (0 to 39%).

Figure 5.4 shows a significant positive correlation between the fat thickness in the CB and that in the first STB adjacent to the spine. The gradient of the regression line was close to 1 which is expected if the fat thickness is the same in both regions. A paired t-test showed there was no significant difference between the mean fat thickness within the CB and the STB immediately adjacent to the CB; the mean±SD values were 5.21±2.72 cm compared to 5.24± 2.72 cm with p=0.284.

Figure 5.5 shows that the abdominal fat thickness distribution at the level of L3+L4 for a subject with a BMI of 17 kg/m^2 varies relatively more than that for a subject with a BMI of 40 kg/m^2. The difference in fat thickness between individual STB and the CB ranged from -21% to 115% for the lean subject and -15% to 22% for the obese subject. The absolute fat thickness in the CB was 2.1 cm and 12.0 cm for the lean and obese subjects respectively. The FM measured within the CB was almost 8 times greater for the obese subject being 446.5 g compared to 56.8 g. The width of lean tissue across the body at the L1 to L4 level was only 0.8 cm different for the two subjects but the difference between the fat and total body width was 10.2 cm and 5.7 cm for the obese and lean subjects respectively. Fat thickness profiles from individual subjects

within the IBD group were compared with BMI and variation in BMD with ROI width in chapter 6.

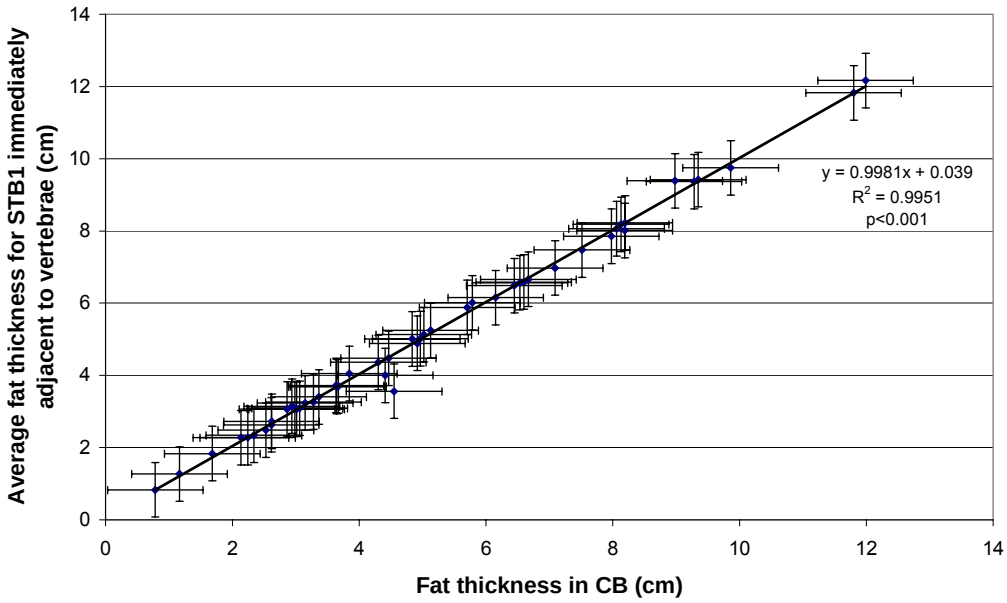

Figure 5.4 Relationship between fat thickness measured for the CB over the vertebrae and the first STB adjacent to the vertebrae (mean ±95%CI). Standard error of gradient is ±0.01 and SEE = 0.192 cm.

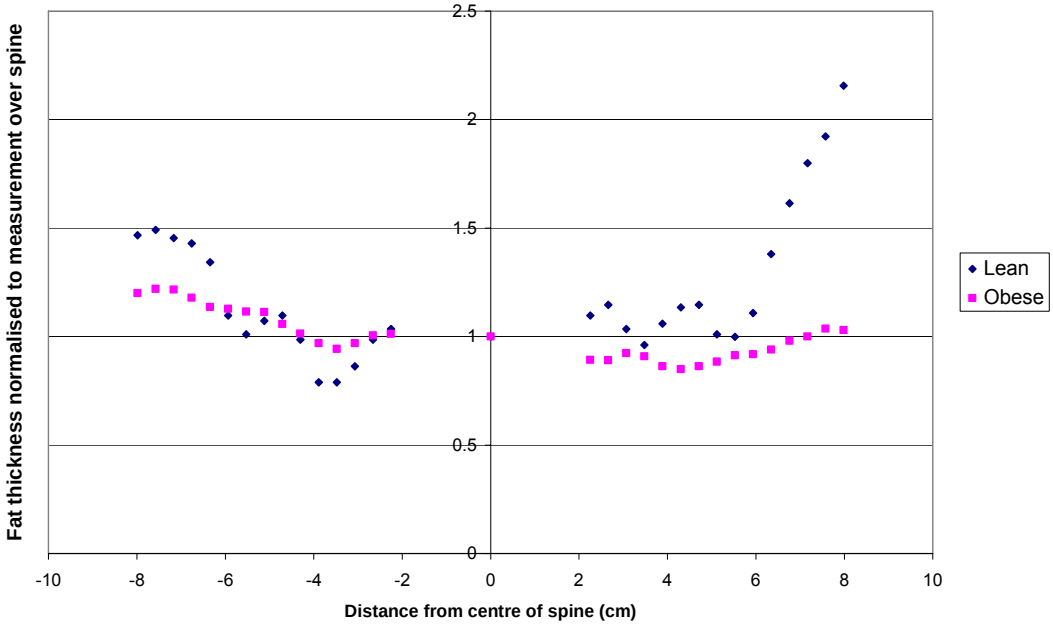

Figure 5.5 Comparison of abdominal fat thickness profiles from a lean (BMI = 17 kg m^{-2}) and an obese (BMI = 40 kg m^{-2}) subject.

5.4 Discussion

It is evident from the results presented here that the abdominal fat distribution is more uniform at the L1+L2 level than at the L3+L4 level. Abdominal fat thickness profiles, derived using FM extracted from DXA WB images, appear to contain sufficient detail to quantify the inhomogeneity in fat thickness at the level of the lumbar vertebrae (Fig. 5.2). The number of data points in the profile is governed by the width of the smallest STB, i.e. 3 lines (6 mm) which gives a fat thickness measurement every 4 mm as the STB overlap by 1 line. Advantages of WB DXA over CT for quantifying FM include a lower radiation dose to the patient, data are obtained from scans acquired using the same technology and the scans can be performed relatively quickly during a single visit by the patient.

In this work, FM was converted into a fat thickness using the physical density of stearic acid as this is used by Hologic in calibrating the system and also included in the standards proposed by Nord and Payne (1990). These standards are widely used in body composition analysis (BCA) methods as they span range 0 to 100% fat with stearic acid being equivalent to 100% fat.

The limitation of this method to quantify the inhomogeneity in abdominal fat thickness is the ability to match the borders of the CB and STB with the spaces between vertebrae of interest. This could lead to errors in FM measurements of up to 39% in individual cases (average 17%) for the STB. Even though these errors appear large, it is the shape of the profile that is of interest in this work and not the absolute fat thickness. If the height of the CB and all STB are equal, quantification of inhomogeneity will not be affected. Assuming the width of the CB represents the vertebral width, the spine width measured from WB scans was close to that measured from lumbar spine scans and within the range of normal anatomical widths expected for the lumbar vertebrae (Busscher *et al.* 2010). This finding was important as it confirmed that L1 to L4 were correctly identified on WB images.

The anatomy and tissue distribution within the abdomen in the region corresponding to the L1+L2 and L3+L4 vertebrae was compared to that found on CT images in the literature and shown in figures 5.6, 5.7 and 5.8. The exact location of organs, muscles and other tissues within the abdomen will vary slightly between individuals and therefore only approximations of their position relative to the lumbar spine can be made.

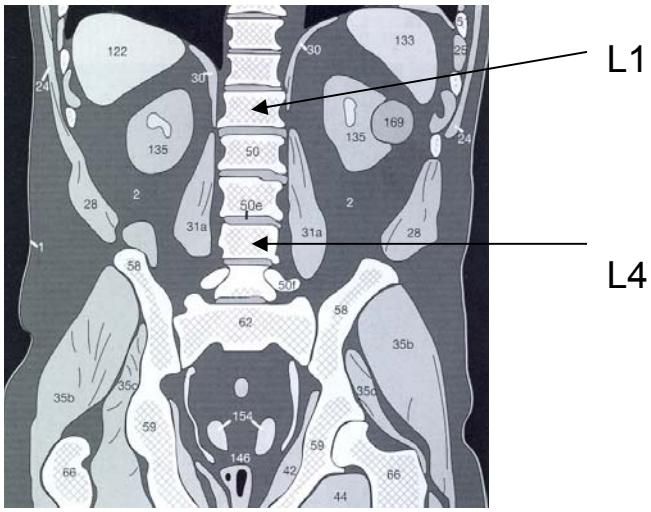

Figure 5.6 Schematic diagram of an abdominal CT image in the coronal plane showing the position of the lumbar vertebrae in relation to psoas muscles (31), kidneys (135), liver (122), spleen (133) and fat (2) (Hofer 2007).

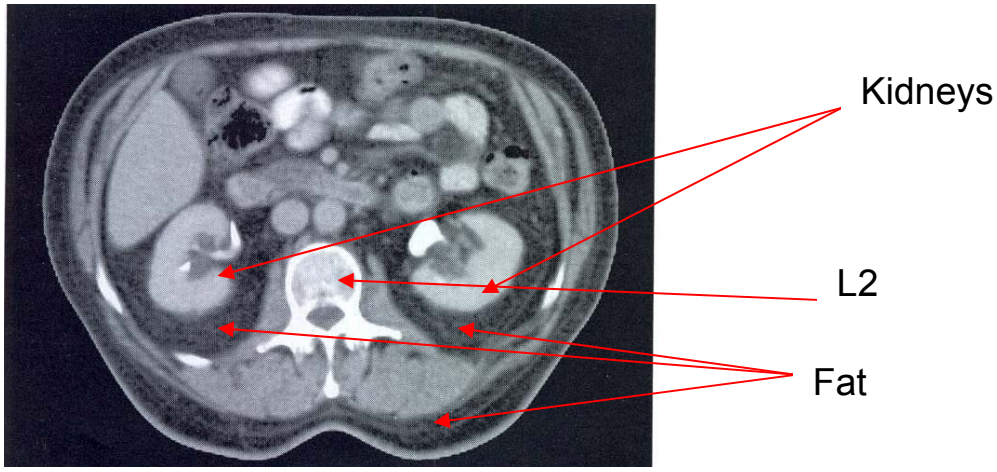

Figure 5.7 Transverse CT image of the abdomen at the level of L2 showing the distribution of fat and position of the kidneys in relation to the lumbar vertebrae (Hofer 2007).

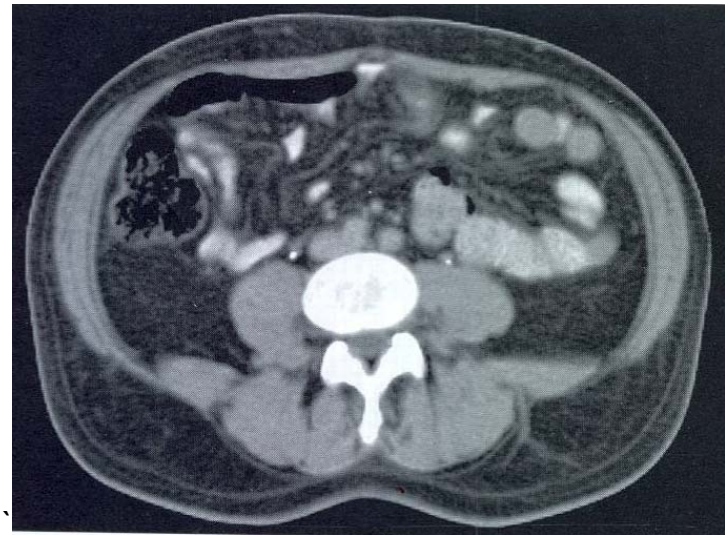

(a)

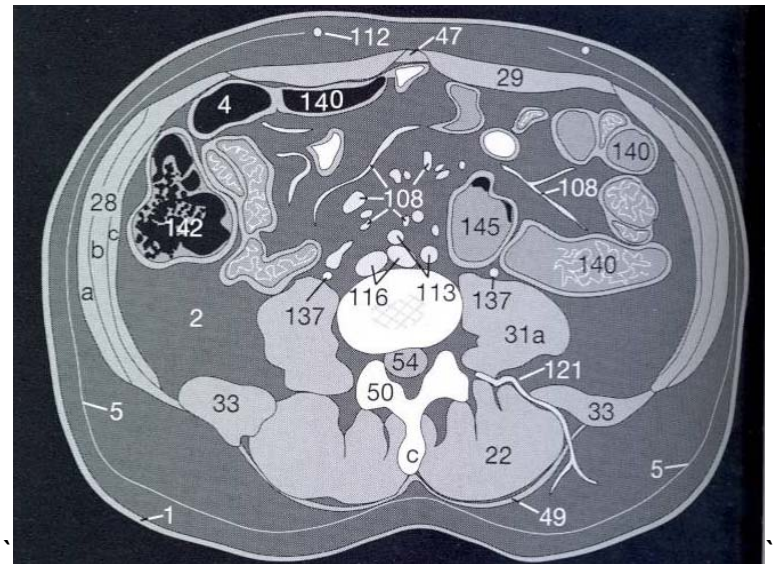

(b)

Figure 5.8 CT axial image of the abdomen at the level of L3 to L4 showing the distribution of fat (2), position of the psoas muscles (31), erector spinae muscle (22), colon (145) and ileum (140) in relation to L4 (50) (Hofer 2007).

It appears from the profiles that fat thickness in soft tissue adjacent to L1+L2 is similar to that over the vertebrae up to approximately 6 cm from the centre of the spine. If the ROI width were 11.5 cm, i.e. extending 5.8 cm laterally from the centre of the spine on each side of the body, this

finding suggests that accuracy errors in L1+L2 BMD introduced by fat distribution are likely to be small. This suggestion would be in accord with the relatively small changes in L1+L2 BMD observed when increasing the width of the ROI discussed in chapter 4. The corresponding CT scan shows that there is approximately the same total fat thickness within the abdomen either side of L1+L2. Also at the level of L1+L2, the kidneys are located symmetrically about the vertebrae and therefore may fall within the region of the L1+L2 profile shown in figure 5.2.

At the L3+L4 level the psoas muscles lie either side of the lumbar vertebrae and, as muscle is lean tissue, these are likely to be the reason for the observed decrease in the fat thickness (Figs. 5.2 & 5.3). Also contributing to this region are the longissimus dorsi and lliocostalis lumborum muscles posterior to the spine and the rectus abdominal muscles anterior to vertebrae (Fig. 5.8). The psoas muscles do not extend to L1+L2 which is a likely explanation for the more uniform fat distribution.

There are many organs within the abdomen at the L3+L4 level including the colon and ileum (with fat distributed between them) and also abdominal muscles. The DXA fat thickness profiles extend up to approximately 8 cm each side of the centre of the spine and therefore the profile for L3+L4 is likely to extend into the region containing a larger thickness of fat around the colon and ileum. Assuming the default ROI width is 11.5 cm at L3+L4, the baseline soft tissue will incorporate muscle tissue and fat. Whilst the kidneys are unlikely to be at this level, the fat capsule surrounding them (peri-renal fat) may be present in the baseline. The pattern of fat distribution lateral to L3+L4, seen from CT images, is asymmetrical but the total thickness appears to be equal each side of the body which is consistent with the shape of the profiles.

It was assumed that the schematic representation of the CT image of the abdomen at the level of L4, shown in figure 5.8b, is drawn to scale and the distance from the centre of the vertebrae to the lateral edge of the external oblique muscle is equivalent to the average lean width of the

abdomen. The variation in lean width is smaller than the total body width due to subcutaneous fat which varies with BMI. Revisiting the WB images, the average lean width at the L1 to L4 level for the IBD subjects was 25.9±2.2 cm whereas the average total body width was 32.4±3.9 cm. Applying the assumptions above, the distance of mid-point of psoras muscle from the centre of the vertebrae equates to approximately 4 cm which coincides with the minima on the DXA profile. It is accepted that this measurement is not accurate but it serves to identify features observed in the DXA fat thickness profiles.

The overall shape of the fat thickness profile extracted from WB scans is comparable to that published by Tothill and Pye (1992) from superimposing a fat profile on an abdominal CT scan. The minimum fat thickness on this profile also corresponded to the location of the psoas muscles and there was an increase in fat thickness when moving laterally through colon etc and interspersed fat. Tothill and Pye (1992) measured the fat thickness over the L2 to L4 vertebral area from CT images to be 5.81±2.80 cm for men and 4.77±2.14 cm for women, which are similar to those found in this work i.e. 5.2±2.7 cm. In another study, the average fat thickness over the L2 to L4 vertebral area was measured to be 2.9±2.3 cm (Tothill and Avenell 1994a). It should be noted that there appears to be substantial variation from one individual to another in fat thickness over the vertebrae. This is reflected in the large SD seen for the mean fat thickness in work by Tothill and Pye (1992), Tothill and Avenell (1994a) and measurements presented in this thesis. The fat distribution profiles presented here are for data averaged over 50 subjects whereas in reality the distribution of fat can vary considerably between individuals. It was interesting that fat thickness distribution for a leaner patient showed a relatively greater degree of inhomogeneity (Fig. 5.5). The structure within the fat profile for the lean subject is likely to be due to the distribution of the visceral or deep body fat between the organs and muscles. The abdominal girth of the population can vary significantly dependent on the thickness of subcutaneous fat. Variation in the distribution of internal fat in the abdomen on the other hand, is likely to be less marked and should

remain relatively constant over time in a healthy adult individual. The subcutaneous fat of the obese subject, resulting in a larger total body width, is likely to obscure the detail seen in the fat thickness profile for the thinner patient. Fat thickness profiles for individuals will be less smooth; however, it is encouraging that there is still sufficient detail to quantify the degree of in-homogeneity in fat distribution as shown in chapter 8 (Figs 8.18 and 8.19).

Published studies indicate that the precision of the Hologic QDR-1000W to measure total body %fat and FM in-vivo using the standard WB software is good and in some cases better than 2 % (Herd *et al*. 1993; Pritchard *et al.* 1993; Braillon *et al.* 1998). Published work assessing the absolute accuracy of the QDR-1000W for FM measurement is limited, but studies validating DXA measurements against other methods show a good agreement (Prior *et al.* 1997). In one study to assess the accuracy of FM measurement, Jebb *et al.* (1995) found that the Hologic QDR-1000W underestimated FM in a 55 kg meat sample by 6-8% compared to direct analysis. Based on these results they concluded that the QDR-1000W underestimates soft tissue mass measurements. In another study, using a Lunar DPX scanner, Svendsen *et al.* (1993a) found the SEE for total body fat of pigs measured by DXA verses direct chemical analysis was 2.9% for percentage fat or 1.9 kg of FM. It should be noted that considerable differences in BCA measurement algorithms exist between manufacturers and software versions (Tothill *et al.* 1994b; Tothill *et al.* 1994c). It was shown in chapter 3 that the maximum difference between the area density of lard measured by DXA and that calculated from the physical dimensions of lard was 6.4 % for a range of thickness of lard. In all measurements the DXA measurement was lower. The most realistic measurement in chapter 3 for fat thickness encountered in the human body was for a depth of 10 cm where the DXA measurement was 0.8% lower than the true value.

A review of relevant literature failed to find any published data on the accuracy or precision of the Hologic WB sub-regional analysis software.

Using it in this work to form a fat thickness profile tests the algorithm to the limits as the analysis regions are very small as are the measured tissue masses. The accuracy of the QDR-1000W algorithm to measure low FM using the standard WB software has been questioned (Tothill *et al.* 2001). Therefore the measurement of quantities as low as 1.7g FM, which was the lowest recorded for the STB, may also not be accurate. However, the data presented by Tothill *et al.* (2001) was acquired with the QDR-1000W enhanced WB software version 5.55 whereas version 5.73 is used in the present work. It has been shown that upgrading the WB software from version 5.55 to 5.64 makes measurement of FM more accurate (Snead *et al.* 1993; Kohort 1998). It has been shown in an in-vitro study that FM measured by the QDR-1000W is dependent on the total tissue thickness and it is possible that errors in FM will occur at extremes of tissue depth (Jebb *et al.* 1995).

It was shown in chapter 3 that BCA measurements with smaller STB were less accurate and precise than those with wider STB indicating that there is likely to be an error associated with using the former. This is difficult to quantify in-vivo. However, data presented in chapter 3 showed that the percentage fat of Perspex^{TM} measured by DXA with a region of width 0.6 cm was only 0.2% different to that measured with a 14 cm analysis region. In this validation study, the absolute FM reported for the smallest region was 42.9 g which is much greater than values for some STB and therefore this is not a true test of measuring a low FM. Due to the un-physiological nature of this validation study, no inference can be made regarding the accuracy of in-vivo FM measurements.

The only measure of quality that can be used in validating this method is the precision i.e. reproducibility, of measuring fat thickness in soft tissue regions. As expected, this was poorest for the inter-observer reproducibility with an average CV% of 17%. This precision is worse than that quoted for measurements of fat from the standard WB software due to the difficulty in positioning very small analysis regions on an image where the vertebrae are small. Also, the image resolution can be poor

when there is considerable soft tissue attenuation making identification of L3+L4 difficult. For the purpose of this work, the error in measuring fat thickness using the proposed method was considered to be ±17% to represent the precision. A limitation of DXA for BCA measurements is that only total tissue mass can be measured for pixels containing bone and the proportions of fat and lean must be estimated by interpolation of the measurements adjacent to the bone. If the algorithm used to do this is accurate, it is expected that the FM within the CB should be identical to that immediately adjacent to the spine. This was confirmed in this work (Fig. 5.5).

Quantifying the difference betwfseen the fat thickness over bone and in the adjacent soft tissue baseline from WB images is likely to be valuable in estimating the inaccuracy in lumbar spine BMD. It was shown in section 4.3 that the influence of the lumbar spine ROI width on BMD measurement is more pronounced for L3+L4 than L1+L2 and therefore only the BMD and FM data for L3+L4 was used in subsequent work.

5.5 Conclusions

The distribution of abdominal fat is non-uniform at the level of the lumbar vertebrae used for BMD measurement by DXA. It is possible to quantify the inhomogeneity in fat distribution from fat thickness profiles derived from FM measurements made on DXA WB images. These results highlight the importance of careful selection of ROI width to include soft tissue in the baseline region which has an average fat thickness which is the same as that over the vertebrae. The results presented in this section, for L3+L4 level, will be used to quantify the difference in fat thickness in the baseline of the ROI compared to over the vertebrae and ultimately to estimate accuracy errors in BMD measurement due to the non-uniform distribution of fat.

Chapter 6

Quantification of Fat Thickness within the DXA Lumbar Spine ROI from DXA WB Images and the Relationship to the Measured Lumbar Spine BMD

6.1 Introduction

Lumbar spine BMD measurement by DXA is dependent on the composition of soft tissue adjacent to bone within the global ROI which is used to compensate for the effect of soft tissue over the vertebrae. It was shown in chapter 4 that there is a systematic increase in in-vivo L3+L4 BMD with an increase in ROI width. In general the accepted width for the ROI is 11.5 cm to 12.0 cm (Wahner and Fogelman 1994). However, it has been suggested that narrower widths may produce more accurate BMD results but at the expense of precision (Tothill and Pye 1992). To ensure good precision the ROI must include sufficient soft tissue to allow scope for small changes in soft tissue composition over time.

The majority of published studies investigating the inaccuracy of BMD have quantified fat thickness over bone and in the baseline from CT scans. However, as shown in chapter 5, it is possible to quantify the distribution of abdominal fat at the level of the lumbar vertebrae using DXA WB images.

This chapter is the focal point of the thesis and describes a method to quantify the influence of abdominal fat on lumbar spine BMD measured

with the Hologic QDR-1000W DXA scanner. This will be achieved by estimating the average fat thickness in soft tissue regions equivalent to those used for lumbar spine BMD analysis from fat thickness profiles derived in chapter 5 (Fig. 5.1). Subsequently, the difference between fat thickness in the baseline region and that over the vertebrae will be converted into a bone mineral equivalence (BME). Finally the lumbar spine BMD changes measured for various width ROI will be compared with the BME of changes in fat thickness within the baseline of equivalent width ROI.

6.2 Quantification of Fat Thickness within Baseline Region used for Lumbar Spine BMD measurement from DXA Whole Body Images

6.2.1 Aim

The aim of this section was to combine the FM in individual STB, that form the fat thickness profile in figure 5.3, to calculate the average fat thickness within regions corresponding to the soft tissue baselines used for measurement of L3+L4 BMD described in chapter 4. It is acknowledged that combining FM from small STB may be less precise than obtaining FM from a wider analysis region which matches the width of the lumbar spine ROI. However, it was decided to use small STB in this work to highlight the variation in fat thickness across the abdomen in more detail as in chapter 5 figures 5.2 and 5.3.

6.2.2 Method

The FM within individual STB placed on WB images at the L3+L4 level on each side of the vertebrae in chapter 5 was summed using equations 6.1 and 6.2.

$$SnR = FM\_right(g) = Fat\_in\_STB1 + \left(\frac{2}{3} \times \left(Fat\_in\_additional\_STB\right)\right) \quad (6.1)$$

$$SnL = FM\_left(g) = Fat\_in\_STB1 + \left(\frac{2}{3} \times \left(Fat\_in\_additional\_STB\right)\right) \quad (6.2)$$

where SnR represents the total FM in n strips on the right side (Rt) of the body and SnL for the left (Lt). STB1 is the STB next to the vertebrae. Only two-thirds of the fat in additional STB needs to be added to previous strips as the STB overlapped by one line. It was shown in chapter 3 that the tissue under the boundary lines is accounted for in the FM measurement. Next the FM on the Lt and Rt of the vertebrae was summed for 2,3,…n STB. Figure 6.1 outlines the stages involved in summation of the FM to equate to lumbar spine baseline regions.

Due to the overlap of the STB, the total width of the soft tissue region was calculated from equation 6.3.

$$Softtissue\_width(cm) = \left(\left(2 \times width\_of\_STB1\right) + 4\left(n-1\right)\right) \times 0.2047 \quad (6.3)$$

where *STB1_width* is the width of the first STB next to the box covering the vertebrae (CB) which is 3 lines, n is the number of STB and 0.2047 cm/line is the Hologic point resolution factor to convert lines into cm for WB images. The total area of the soft tissue region is given by equation 6.4.

$$Softtissue\_area(cm^2) = \left[\left(\left(2 \times width\_of\_STB1\right) + 4\left(n-1\right)\right) \times 0.2047\right] \times \left[Ht\_in\_pixels \times 1.303\right] \quad (6.4)$$

where 1.303 cm/line is the line spacing conversion factor.

The FM was converted into an area density using equation 5.1 and this was translated into fat thickness using equation 5.4. The average fat thickness for the tissue within the combined STB was plotted against the width of ROI on a lumbar spine scan that would contain an equal area of soft tissue as a baseline region (Fig. 5.1). This width is equivalent to the width of the combined STB (equation 6.3) plus the CB accounting for one line overlap. The fat thickness in the baseline regions used in the lumbar spine analysis in chapter 4 was calculated by interpolating from a graph of fat thickness against ROI width and assuming a linear change in fat thickness between consecutive points. The data were analysed with linear regression analysis using SPSS with a level of $p<0.05$ used to indicate statistical significance.

The fat thickness within the baseline at each width of lumbar spine ROI was compared to the fat thickness in the CB. This was considered a valid approach as it was proved in chapter 5 that there was not a significant difference between the FM for the CB and the STB next to the spine. The difference in fat thickness between the tissue within the baseline of the Hologic recommended ROI width (11.5 cm) and the CB was also calculated.

Linear regression analysis was used to investigate a link between the difference in baseline and CB fat thickness for a 11.5 cm ROI and (a) the BMI, (b) trunk width and (c) the lateral thickness of the subcutaneous fat layer. The relationship was considered significant for $p<0.05$.

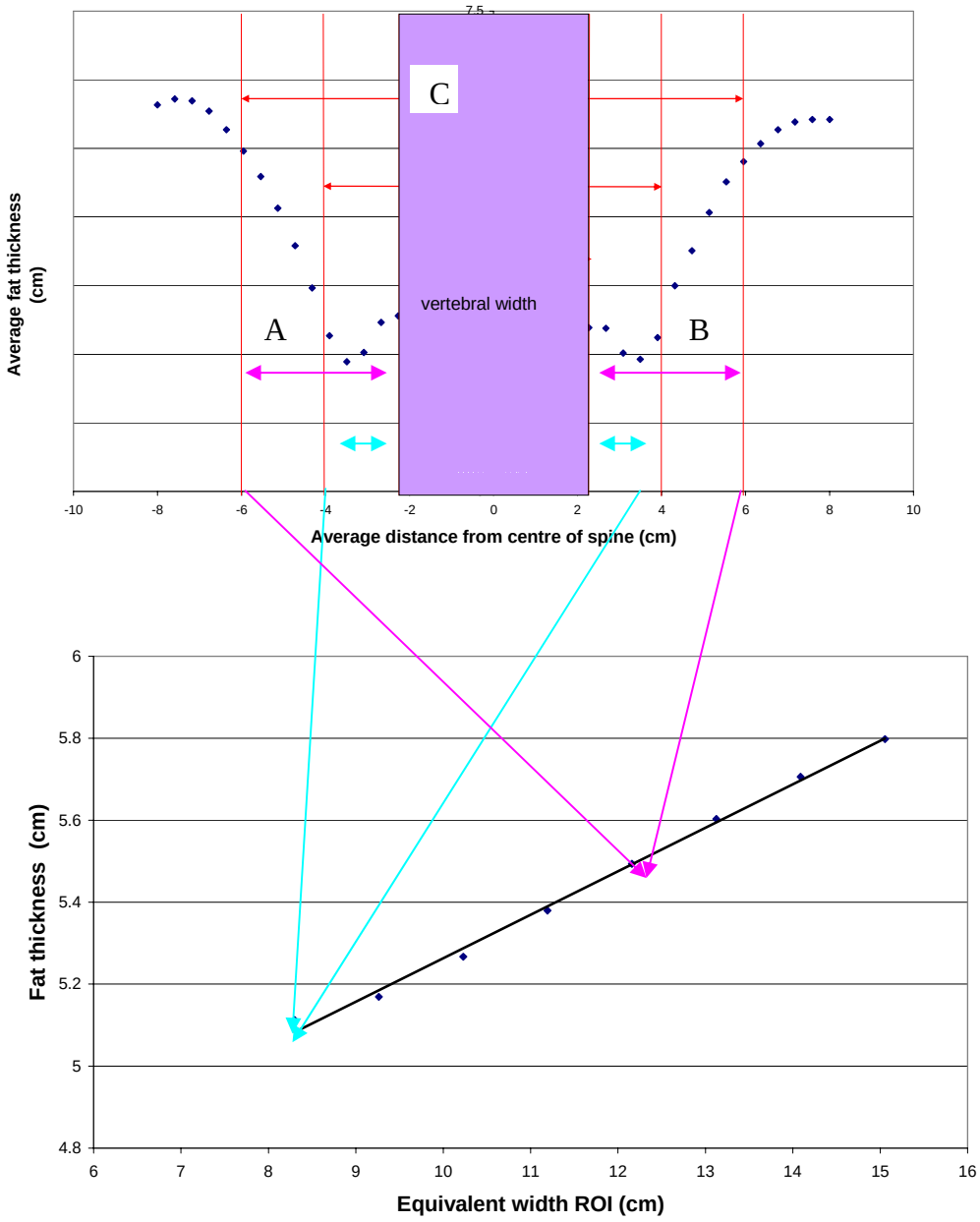

Figure 6.1 Schematic representation of the stages involved in determining the average fat thickness within soft tissue regions corresponding to the baseline region used in lumbar spine BMD measurement. The central box on profile represents the width of the vertebrae. Each point on the lower graph represents a different ROI width used for lumbar spine BMD measurement. Examples are given for a ROI of approximately 8 cm and 12 cm. For example consider the 12 cm ROI, initially the average fat thickness within ROI is calculated individually for each side of vertebrae in regions A and B and then summed to give the average fat thickness within the total ROI – region C i.e. A+B. Error bars were removed from the graph to make process clearer, however, the same graph is shown in figure 6.3 with results of error analysis.

6.2.3 Results

Figure 6.2 shows that the average fat thickness in a region adjacent to the spine measured from WB images initially decreased and then increased as the width of the region extended laterally.

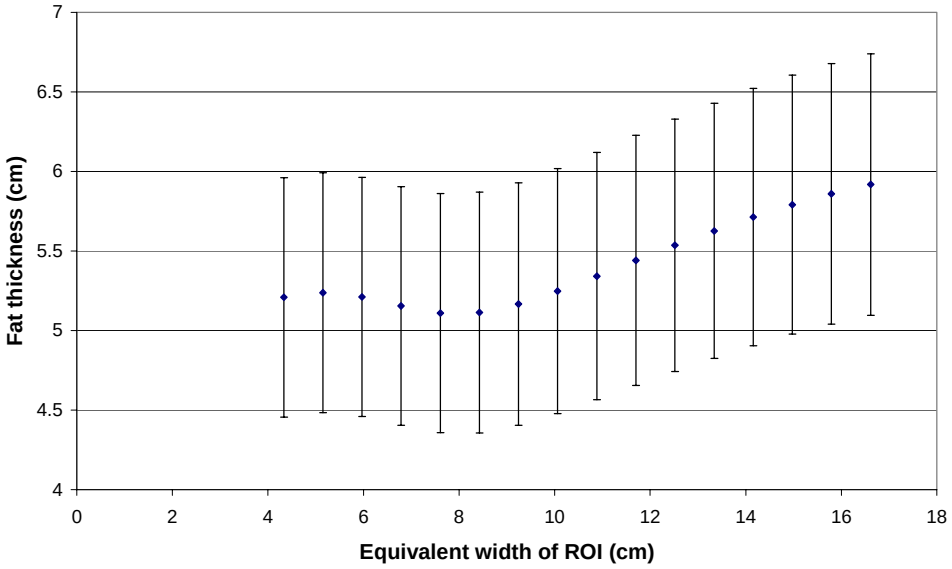

Figure 6.2 Relationship between the average fat thickness in the soft tissue regions adjacent to L3+L4 and the width of the lumbar spine ROI that would contain an equivalent area of soft tissue as the baseline. The data are averaged over 50 IBD subjects (± 95% CI).

The fat thickness in regions equivalent to those used for the soft tissue baseline in lumbar spine measurements discussed in chapter 4 was extracted by interpolating between the data points on figure 6.2. Figure 6.3 shows a positive correlation between the fat thickness within the baseline, as measured from WB images, and the equivalent lumbar spine ROI width.

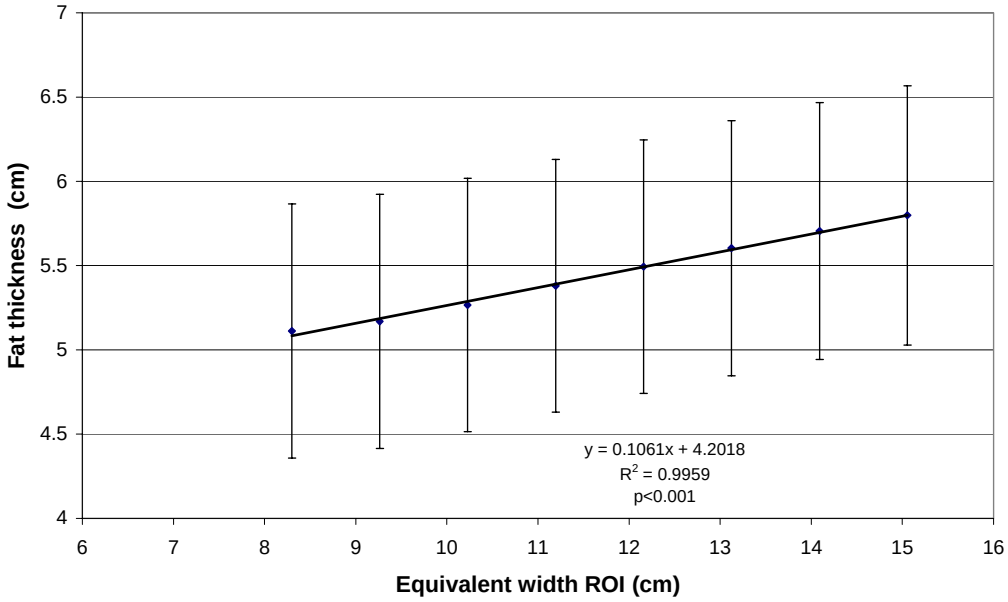

Figure 6.3 Average fat thickness in soft tissue regions adjacent to L3+L4 that are equivalent to those used as a baseline region for lumbar spine BMD analysis in chapter 4. The data are averaged over 50 IBD subjects (± 95% CI). SEE = 0.017 cm and standard error in gradient is 0.003 cm fat per cm.

The average fat thickness in the baseline of each ROI was compared to that in the CB over the vertebrae. For the 50 subjects it was evident that the width of lumbar spine ROI that contains an equal fat thickness over the vertebrae and in the baseline was 9.5 cm (Fig. 6.4). There was a significant positive correlation ($p<0.001$) between ROI width and the difference in fat thickness over and adjacent to the spine as shown in figure 6.4.

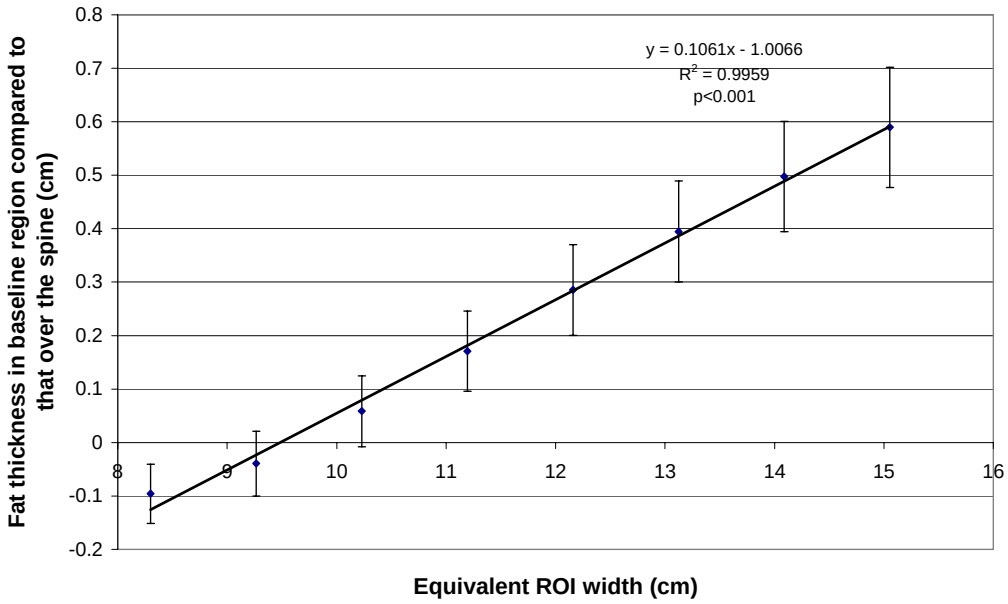

Figure 6.4 Fat thickness in the baseline soft tissue relative to that over vertebrae measured from WB images for ROI widths equivalent to those used in the measurement of L3+L4 BMD. Linear regression analysis shows that a ROI width of 9.5 cm would give an equal fat thickness in the soft tissue baseline and over vertebrae. (± 95% CI). Data are averaged over 50 IBD subjects. SEE = 0.017 cm and standard error of gradient is 0.003 cm fat per cm.

Figure 6.5 shows the difference between the fat thickness within the baseline of a 11.5 cm ROI and that in the CB over L3+L4 ranged from -0.69 cm to 0.84 cm. In terms of percentage, the average fat thickness in the soft tissue baseline was approximately 4% higher than over the spine at the L3+L4 level when averaging over 50 data sets. This was in close agreement with the average fat differences for all individuals which was 3.4 ± 6.1%. The histogram representing individual cases shows a wide range of fat thickness in baseline relative to that within the CB across the study population (-15.5% to 18.5%). However, figure 6.6 shows a significant linear relationship between the fat thickness in the CB and baseline ($p<0.001$). A paired t-test indicated the fat thickness within the baseline of a 11.5 cm ROI was significantly different ($p<0.001$) to that over the vertebrae.

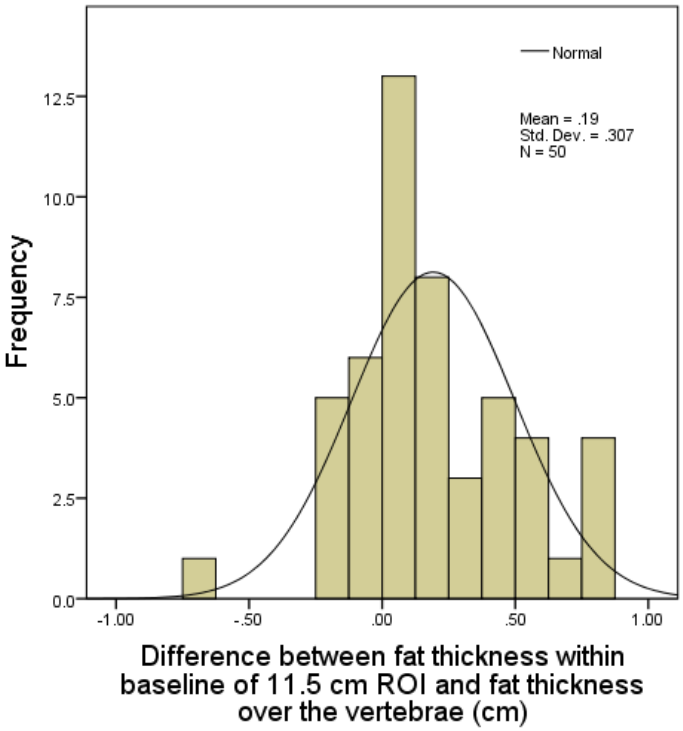

Figure 6.5 Difference between the fat thickness over the spine and the average within the baseline of a 11.5 cm ROI at the level of L3+L4 for 50 individual IBD patients. Expressed as a percentage difference the average difference was 3.4 ± 6.1 % i.e. the fat thickness in the baseline was 3.4% greater than over the vertebrae (range = -15.5% to 18.5%).

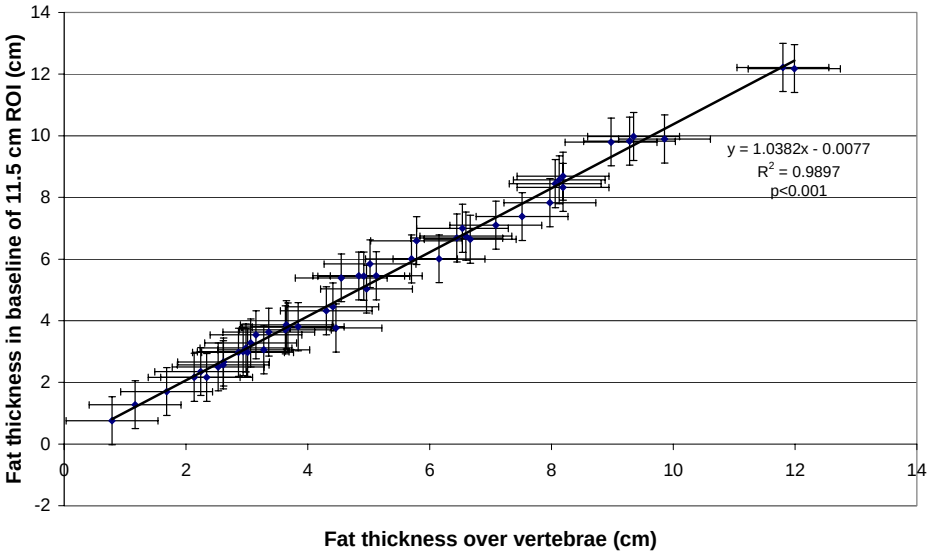

Figure 6.6 Relationship between the fat thickness in the baseline of a ROI with width recommended by Hologic and that over the vertebrae at the level of L3+L4 for 50 subjects (±95% CI). SEE = 0.292 cm, standard error of gradient = 0.015 cm per cm.

Linear regression analysis confirmed there was not a significant link between the inhomogeneity in fat within a 11.5 cm ROI and the BMI, trunk width or width of subcutaneous fat layer ($p<0.05$).

6.2.4 Discussion

The results in 6.2.3 confirmed the observations of others which lead them to conclude that there is a greater thickness of fat in the soft tissue adjacent to the vertebrae than over the vertebrae for lumbar spine ROI widths generally used for clinical BMD measurements (Tothill and Pye 1992; Tothill and Avenell 1994a; Formica *et al.* 1995; Svendsen *et al.* 2002). This is likely to result in the BMD being over corrected producing a falsely high result as the DXA software assumes there is a greater thickness of fat over the spine than is actually the case. The increase in average fat thickness observed as the width of the ROI increased strengthens the existing evidence for the apparent increase in BMD being due to a systematic increase in fat thickness within the baseline. The abdominal fat thickness has been quantified in the present work to follow on from the work of others. However, it is acknowledged that in reality the presence of lean tissue needs to be addressed. When discussing changes in fat thickness it is assumed that the attenuation due to lean tissue remains constant which may not be true. For example, during aging some of the lean muscle tissue within the abdomen is replaced by fat and therefore the thickness of lean tissue decreases with an associated increase in fat. In theory the relative thickness of fat and lean tissue in the soft tissue baseline should be equal to that within the tissue actually attenuating X-ray photons in the region containing bone. In reality it is the attenuation of these tissue regions that must be identical to ensure an accurate BMD result. The same attenuation could be provided by numerous compositional mixes of fat and lean. Making the assumption that the fat thickness must be equal, the current data suggests the width of the ideal ROI to optimise accuracy of BMD measurement is 9.5 cm for the IBD study sample. This width is 2 cm smaller than that recommended for the Hologic QDR-1000W. Tothill and Pye (1992) suggested that

reducing the ROI width below their preferred value of 12.5 cm could minimise the “fat error” in lumbar spine BMD measurements. Reducing the amount of soft tissue in the baseline region would degrade the precision of measurements. With a relatively narrow baseline region, changes in the fat thickness could have a significant impact on BMD. On the other hand, with a larger region, there is more tissue to calculate the average attenuation giving more measurement points. Repositioning a patient may cause a slight change in abdominal fat distribution and therefore the ROI should be wide enough to account for small deviations in fat distribution to keep the average fat thickness in the baseline constant. It would be expected therefore that the influence of soft tissue changes would possibly be less significant for a wide ROI. Reducing the ROI width below that recommended by the manufacturer is not advisable in clinical practice.

Other attempts at quantifying the thickness of fat in the baseline relative to that over vertebrae have used a single large region adjacent to vertebrae. However, it is believed that using small STB provides more detail on fat distribution and allows quantification of fat thickness within any width ROI.

The fat thickness within the soft tissue baseline of a standard ROI of 11.5 cm was 4% or 2 mm greater than that over the vertebrae. This was similar to the 4.4% average difference reported by Farrell and Webber (1989) from measurements on a CT image. These authors reported a wide range of fat thickness differences between subjects ranging from -2.7% to 18.7% as was found in the current work (Fig. 6.5). Two studies by Tothill *et al.* (1992; 1994a) found that for a 12.5 cm ROI, the difference in fat thickness adjacent to the L2 to L4 vertebrae compared to that over the vertebrae ranged from 6.7±8.1 mm to 17±9 mm for various study populations. The equivalent measurement for the IBD data were smaller with a difference of 3.2 ± 0.2 mm.

The large variability in absolute and relative fat thickness measurements observed between individuals was also shown in some published data

(Farrell and Webber 1989; Tothill and Pye 1992). The level at which the difference between fat thickness over spine and in the baseline becomes significant to BMD accuracy errors is, as yet, unknown. The statement that ideally needs to be completed as this work progresses is “If the difference in fat thickness between the baseline and vertebral region is greater than X% then the error in BMD due to the fat distribution is likely to be significant and hence the results should be treated with caution”.

In an attempt to filter out those patients in whom the inhomogeneity in fat thickness within the lumbar spine ROI is great enough to cause a considerable error in BMD, the links with trunk width, subcutaneous fat width and BMI were investigated. Unfortunately there was no significant link between any of these measurements and the relative difference in fat between baseline and CB for a standard (11.5 cm) ROI. It appears that, based on current findings, it is not possible to identify patients in which a correction for a non-uniform fat distribution is necessary based on body size.

The current findings highlight that, in some individuals where there is a greater inhomogeneity in fat distribution, there is a need to quantify the difference in fat thickness between bone and non-bone regions. However, due to the wide variation in results between individuals a single correction factor would not be viable. The influence of changes in fat distribution on BMD may also be highly variable as shown by Yu *et al.* (2012). It is suggested that ideally in clinical practice, any correction for fat distribution must be tailored to the individual in order to improve the accuracy of BMD results. It is believed that the method used in this work to quantify fat thickness using DXA WB images could be valuable in optimising the accuracy of BMD measurements.

To estimate the accuracy error due to the fat distribution the bone mineral equivalence (BME) of the fat within the ROI will be calculated in the next section.

6.3 Relationship between Fat Thickness in Baseline Region of the ROI used for Lumbar Spine BMD measurement and the Lumbar Spine BMD Measured by DXA

6.3.1 Aims

Initially the relationship between the measured lumbar spine BMD and the average fat thickness within the baseline soft tissue region, calculated from WB scans, was investigated. Subsequently the inaccuracy in L3+L4 BMD due to the relative difference between the fat thickness within the baseline and that over the vertebrae was estimated.

6.3.2 Method

The L3+L4 phantom corrected lumbar spine BMD measured with ROI widths from 8.3 cm to 15.1 cm was plotted against the average fat thickness within the corresponding baseline region as estimated from DXA WB scans. The BMD data were presented in section 4.4 and the fat thickness in section 6.2. A graph was also produced of the corrected L3+L4 BMD and the difference between the fat thickness in the baseline and CB for each ROI width.

The difference between the BMD measured for each ROI width and that expected with a uniform fat distribution, which was assumed to be the "true BMD" was plotted against the difference in the fat thickness in the baseline of an equivalent ROI compared to that over the spine i.e. the CB measurement.

The average fat thickness in the baseline of each ROI was compared to that in the baseline of the smallest ROI as the ROI width increased. This analysis investigated the effect of gradually increasing the width of the ROI, e.g. (96 pixels – 86 pixels), (106 pixels – 86 pixels) etc., to include more soft tissue within the baseline.

Using equation 6.5, the difference in fat thickness between different baseline regions was converted to an equivalent bone mineral density,

termed the bone mineral equivalence (BME) in g/cm^2, by multiplication with a bone equivalence factor (BEF) in units of g/cm^2 per cm of fat.

$$BME = t \times BEF \qquad (6.5)$$

The BEF was taken from work by Tothill and Pye (1992) who measured this for the Hologic QDR-1000 using stearic acid to be 0.050 g/cm^2 of bone mineral per cm of fat. The BME of difference in fat thickness within the baseline of each ROI relative to the smallest ROI was plotted against the observed difference in the measured lumbar spine BMD for the corresponding ROI widths.

All these plots were analysed with linear regression analysis with $p<0.05$ used to identify statistical significance.

6.3.3 Results

Figure 6.7 shows there is a significant linear relationship between the fat thickness within the baseline and the phantom corrected L3+L4 BMD measured for equivalent width ROI ($p<0.001$). The Pearson's correlation coefficient indicated a significant positive correlation (0.997). Effectively the data in figure 6.7 represents an increase in fat within the baseline soft tissue hence the BMD appears to increase by 0.051 ± 0.001 g/cm^2 per cm fat.

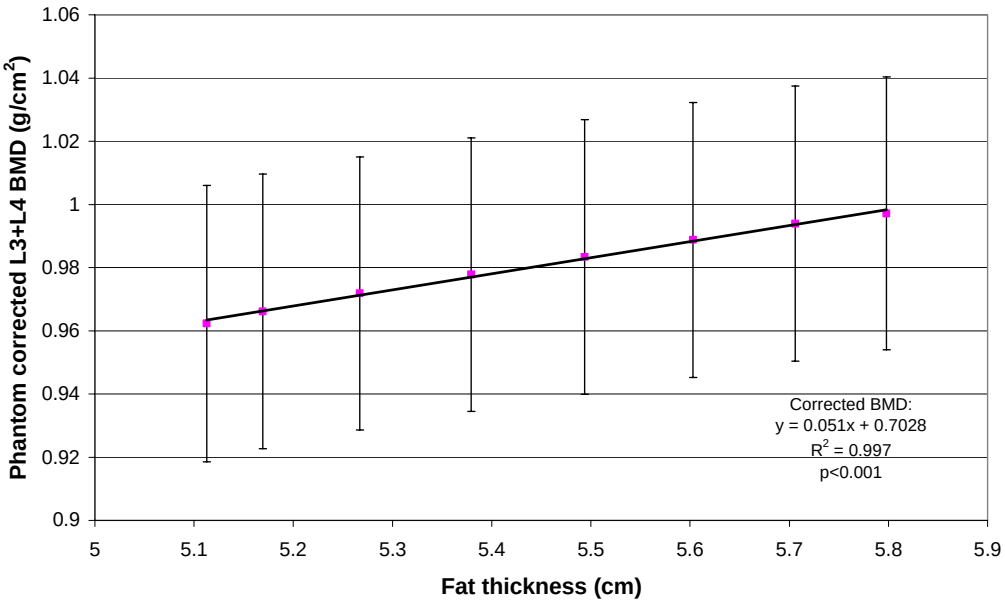

Figure 6.7 Relationship between fat thickness within the soft tissue baseline extracted from DXA WB scans and the phantom corrected L3+L4 BMD for equivalent ROI width. Each data point represents a different width of ROI from 8.3 cm to 15.1 cm. Data are for the L3+L4 level and averaged over 50 subjects. BMD is mean ± 95% CI. SEE = 0.001 g/cm^2 and error in gradient is 0.001 g/cm^2 per cm fat.

It was assumed that the "true" value of BMD occurs when the fat thickness in the baseline is equal to that over the vertebrae and the attenuation due to lean tissue remains constant. A linear regression model fitted to the data in figure 6.8 indicates the "true" average BMD for the IBD study population is 0.968 ± 0.001 g/cm^2.

If this is value is the "true" BMD then the data in figure 6.9 suggests that errors in BMD up to 2.6±0.1% for a difference in fat thickness between the baseline and over the vertebrae of 0.5 cm could potentially occur in this subject group.

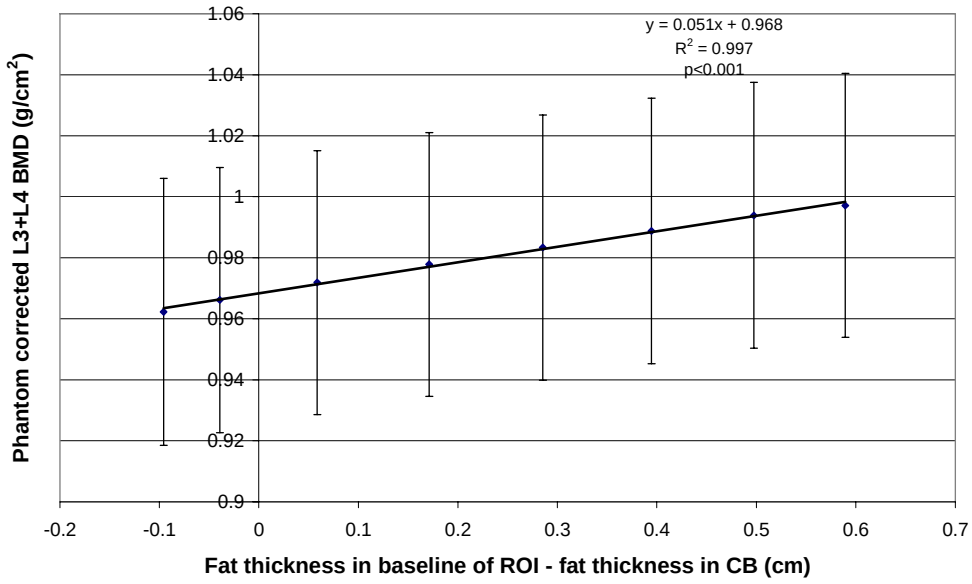

Figure 6.8 Relationship between the fat thickness in baseline relative to that to in the CB over spine and the reported L3+L4 BMD for average of 50 IBD subjects. SEE = 0.001 g/cm^2, error on slope = 0.001 g/cm^2 per cm. Corrected BMD is mean ± 95% CI.

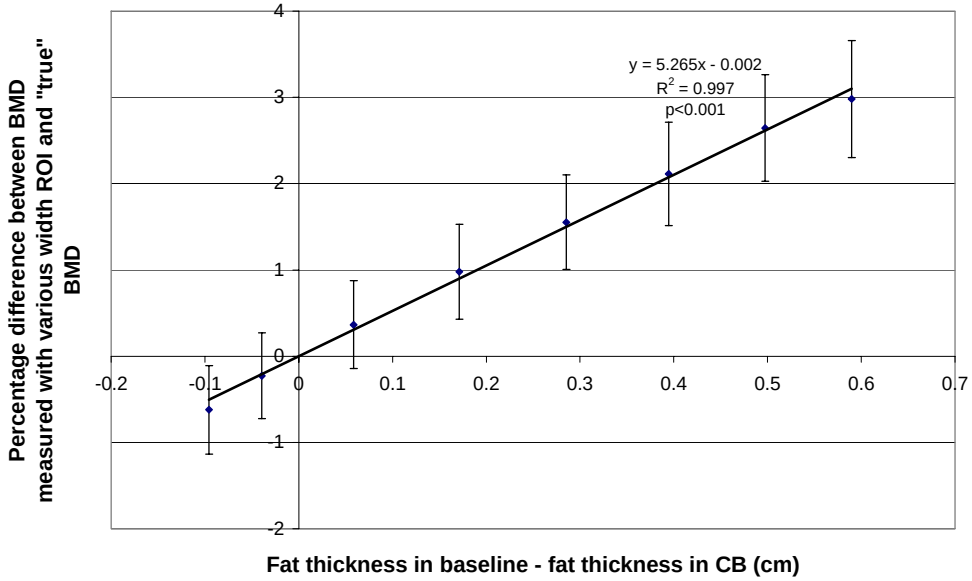

Figure 6.9 Relationship between the fat thickness in the baseline relative to that over the vertebrae and the potential errors in L3+L4 due to a non-uniform fat distribution. Errors in BMD estimated by assuming true BMD is 0.968 g/cm^2. Data are for L3+L4 level and averaged over 50 IBD subjects. SEE 0.085% and error of gradient is 0.128% per cm. Errors represent mean ± 95% CI.

For the phantom corrected L3+L4 BMD at the two extremes of ROI width (8.3 cm to 15.1 cm), the difference in fat thickness within the baseline was calculated to be 0.69 cm. Using the Tothill and Pye (1992) BEF in equation 6.4 this converts to a BME of 0.034±0.018 g/cm^2 (mean ± SD). The actual difference in phantom corrected L3+L4 BMD from measured lumbar spine scans was 0.035±0.018 g/cm^2.

Figure 6.10 shows a significant positive relationship between the BME of the difference in fat thickness within the baseline of different width ROI and the measured phantom corrected BMD for equivalent width ROI. A paired t-test showed the BME of the difference in fat thickness was significantly different to the difference in actual BMD measurements ($p<0.001$).

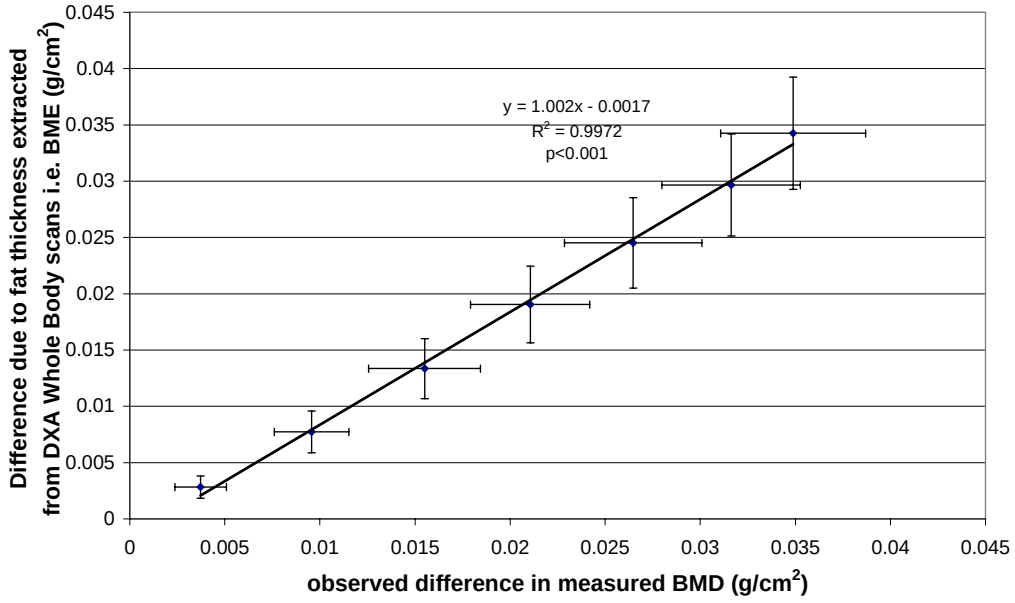

Figure 6.10 Relationship between the observed difference in phantom corrected L3+L4 BMD and the bone mineral equivalence (BME) of the difference in fat thickness within the baseline of equivalent width ROI. The data are average over 50 subjects with IBD. SEE = 0.001 g/cm^2, error of gradient = 0.024 g/cm^2 per g/cm^2. Error bars represent ± 95% CI.

6.3.4 Discussion

The results presented in section 6.3 provide further evidence that the fat thickness within the baseline of the ROI influences DXA L3+L4 lumbar spine BMD measurements. The present findings show that a 1 cm change in fat thickness within the baseline relative to that over the vertebrae results in an apparent change in BMD of 0.051 ± 0.001 g/cm^2. This value can be classed as the bone equivalence of human fat, or BEF, and is in accord with that published by others. Tothill and Pye (1992) measured a BEF of 0.049 g/cm^2 per cm of lard and 0.050 g/cm^2 per cm stearic acid for the Hologic QDR-1000. For the Lunar DPX scanner, Hangartner and Johnston (1990) observed that fat, in the form of Lucite, placed over a bone equivalent material, reduced the measured BMD by 0.051 g/cm^2 per cm of fat and an increase in fat in the soft tissue region increased the BMD by the same amount. The equivalent value published in that work for the Hologic-1000 was 0.044 g/cm^2. Cullum *et al.* (1989) using the QDR-1000, measured that 3 mm fat over a bone like material decreased BMD by 1%; however, the authors do not state the reference BMD. To relate to the current work, a 3 mm relative change in fat thickness between the baseline and over the vertebrae gives an apparent 1.6% decrease in BMD. The BEF derived in the current work is based on changes in human abdominal fat thickness whereas these other BEF are from in-vitro phantom studies using fat and bone mineral substitutes. With regard to clinical lumbar spine BMD measurements, it is likely to be the in-vivo value which is most accurate. The Tothill and Pye (1992) BEF factor was used in subsequent work in this thesis as this is in published, peer reviewed work whereas the value from DXA WB measurements requires validation. The BEF calculated from DXA WB and lumbar spine data were derived using the published value for physical density of stearic acid to convert to area density of fat into a fat thickness. Stearic acid has a physical density close to fat and whilst other fat substitutes could have been used, it is stearic acid that is used by Hologic in calibrating the DXA scanner for BCA. The value of BEF measured from WB scan data was

encouraging as it was deduced using a much different method to those for existing published values.

For a change in BMD to be significant, it should be 2.8 times the precision of the measurement technique which, for the Hologic QDR-1000W lumbar spine BMD is 1%. The average phantom corrected L3+L4 BMD measured with a standard width ROI of 11.5 cm was 0.979 g/cm^2 for this study population and therefore the BMD at ±2.8% was 1.006 g/cm^2 and 0.952 g/cm^2. The fat thickness within the baseline that correspond to these values are 6.0 cm and 4.9 cm respectively with the fat thickness in the baseline of the standard ROI being 5.4 cm. This suggests that a 0.5 cm change in fat thickness between the bone and baseline region has potential to cause a significant change in BMD.

The term “true” BMD in the context of this part of the study refers to a BMD measurement that is free from accuracy errors caused by a non-uniform distribution of abdominal fat. Assuming an accurate BMD measurement occurs when the fat thickness in the baseline is equal to that over the vertebrae, results indicate the “true” BMD would be 0.968 g/cm^2. This is slightly lower than the BMD of 0.979 g/cm^2 measured with the ROI width recommended by Hologic but such a difference is unlikely to be of clinical significance.

Comparing the measured BMD for all ROI widths with the “true BMD”, errors up to approximately 3% can occur when the fat thickness in baseline is 6 mm greater than that over the spine (Fig. 6.8). It was pleasing that the errors from the DXA WB method were in good agreement with those estimated by Tothill and Pye (1992). These authors found that for a fat difference of 6.7±8.1 mm the L2 to L4 BMD was overestimated by approximately 3%, and with a fat difference of 13.4±4.7 mm approximately 6%. The same values of fat thickness differences would give errors in BMD of 3.5±0.1% and 7.1±0.1% using the data for the IBD group in this work (Fig. 6.8).

The only true method of assessing accuracy errors in BMD due to the presence of fat surrounding bone is to compare the BMD of vertebrae measured in-situ with that following excision from the body and removing the inter-vertebral fat. There are valuable studies of this kind involving DPA measurements of BMD. In such studies, Wahner *et al.* (1985) found that the error in vertebral BMD due to surrounding soft tissue was approximately 3% and Gotfredsen *et al.* (1988) reported an error of approximately 10%. Whilst DPA measurements of BMD are not directly comparable to DXA, the magnitude of the accuracy errors are worthy of comment to compare with those seen in the current work.

Unfortunately there are relatively few studies of the accuracy of DXA using cadavers. The most extensive study is that by Svendsen *et al.* (1995) who measured the SEE for AP spine BMD to be 5.3% and deduced a random accuracy error of approximately 3-4%. Other accuracy studies have involved comparing in-vitro and true values e.g. that by Ho *et al.* who found a 8.9% soft tissue accuracy error in vertebral BMC measurement (Ho *et al.* 1990) and Sabin *et al.* (1995) who found the Hologic QDR-2000 systematically underestimated AP L2-L4 BMC by 14% compared to ash measurements giving a root mean standard error of 4.9%. Using phantom simulations, Bolotin *et al*. (2003) concluded that lumbar spine BMD errors up to 10% can occur in certain patient groups, e.g. the osteoporotic and elderly, due to a non-uniform distribution of fat.

In clinical practice, DXA operators focus on ensuring good precision of BMD measurements as, currently, there is no straight forward method of correcting for inaccuracy. Comparing the average fat thickness in the baseline of a 11.5 cm ROI with that over the spine and using the data in figure 6.9 would imply an error of approximately 1.1% in the BMD with relation to the “true” value. The “true” value is that expected if the fat thicknesses in baseline and over vertebrae are equal. It can be assumed therefore that there is a systematic error of 1.1% in BMD measurements with a 11.5 cm ROI width. Whilst a very small error may be introduced when using a standard ROI width of 11.5 cm for clinical measurements, it

is important to keep the width constant to avoid errors in longitudinal BMD results. At each bone densitometry centre, the true value is assumed to be that measured with the standard ROI width used at that centre.

It appears from DXA WB and spine measurements that a relative change of 1 cm in fat thickness between the baseline and over spine is likely to result in a 5.2% change in BMD. Hence if the fat thickness in the baseline changes by 5 mm between scans, there would be a false change in BMD of 2.6% in longitudinal measurements. The extremes of ROI width used in this work are unlikely to be used in clinical practice as the accepted width is 11.5 to 12 cm; hence the likely errors are below the level for the LSC.

Soft tissue accuracy errors have been discussed since the 1960's (Cameron *et al*. 1968). However, their effect on the interpretation of T-scores is still not fully understood. Blake and Fogelman (2008) reviewed the importance of accuracy for the clinical interpretation of DXA scans and concluded errors are unlikely to have a major impact on the clinical use of DXA. The authors used a model proposed by Kiebzak *et al*. (2007) to define the 95% confidence interval of a single T-score and a gradient of risk model for fracture risk. Bolotin (2007) expressed an opposing view claiming that errors due to the non-uniform distribution of soft tissue composition can make BMD results unreliable. The impact of the potential BMD accuracy errors found in this work on T-score measurement can be estimated from equation 1.1 assuming that the average BMD of a normal population is 1.0 g/cm^2 and the population SD is 0.1 g/cm^2.

The maximum difference in fat thickness between the largest and smallest ROI was equivalent to a bone mineral density of 0.034±0.018 g/cm^2 which converts to a change in T-score of 0.34. An error in T-score of 0.3 is unlikely to cause a misdiagnosis unless the patient's BMD is on a boundary between osteopaenia and osteoporosis. T-scores are calculated on an individual basis and therefore no conclusion should be drawn from this average data set. Figure 6.5 shows that in some subjects there is potential for the BME of fat differences to relate to larger more

significant changes in T-score. The analysis performed in this chapter will be repeated on an individual level in chapter 8.

A number of important limitations need to be considered when predicting the inaccuracy in BMD using the proposed methods. Sources of error include:

(1) Assumption of “true” BMD from fat thickness distribution.

It was assumed that the “true” BMD occurs when there is an equal fat thickness in bone and non-bone regions. This assumption was made neglecting the presence of lean tissue or the relative lean to fat mixture. Without a “gold-standard” for BMD in-vivo measurements this is possibly the most viable assumption.

(2) Study population

The data so far is based on the lumbar spine WB scan data for the average of 50 female subjects with IBD. Other study populations need to be considered and these should include male subjects as the distribution of abdominal fat is likely to vary with gender. Evidence of a wide deviation in abdominal fat distribution between individuals has been provided and therefore a single BMD correction factor which applies to all patients is not viable.

The average (± SD) L3+L4 BMD with the default ROI was estimated as 0.979 ± 0.156 g/cm^2 (range: 0.651 to 1.510 g/cm^2). There have been many publications indicating that BMD errors increase when the actual BMD is low and therefore a group with low BMD should be considered.

The average age of the study group was 50±11 y and BMI was 23.91 ± 4.32 kg/cm^2. Age is a relevant factor as during aging the thickness of lean tissue decreases and is replaced by fat tissue. Subject populations with different ages will be investigated in chapter 7.

(3) Assumption that fat thickness within CB represents that over the spine

The fat thickness within the CB is only an estimate of that over the spine based on the soft tissue attenuation measurement immediately next to the spine. A true fat thickness measurement over the spine would account for inter-vertebral fat within the yellow bone marrow as well as the extra-osseous fat.

(4) Data are collected from two different DXA scans

In addition to differences in software for the WB and spine scans, there is a difference in the position of the patient for each scan. Lumbar spine scans are acquired with the patient's legs raised over a cushioned box such that the legs are at right angles to the body (Fig. 6.11a), whereas, for a WB scan the patient lies flat (Fig. 6.11b). Changing position is likely to alter the abdominal fat distribution. Without performing a WB scan on a patient in the two positions and examining the fat thickness profiles, it is difficult to assess the significance of the position on fat distribution. A discrepancy in data may also occur due to difficulty in alignment of the lumbar spine baseline region with the soft-tissue region chosen on the WB image. Due to the size of the WB image on the monitor and the poor image resolution, placement of the soft-tissue regions corresponding to the lumbar vertebrae on the WB scan was difficult. The most viable method of assessing the accuracy of matching the regions was to compare the height and width of the vertebrae measured with on both scans. The results of this are discussed in chapter 3.

(5) Bone mineral equivalence factor

The BEF factor used in this work was found by performing a literature review to find reliable data obtained using the Hologic QDR-1000 (Tothill and Pye 1992). Ideally the BEF should have been measured on the scanner used to collect the FM and BMD data. However, the scanner had been decommissioned before this was possible.

(a) (b)

Figure 6.11 Patient position for a lumbar spine scan (a) and a WB DXA image (b). The WB image shown is for the Hologic Discovery fan beam scanner whereas for the QDR-1000W scanner a soft tissue calibration phantom would be placed next to the subject.

The current work was based on BMD measurements obtained by gradually increasing the width of the ROI to include more soft tissue and comparing the BME of fat thickness within the baseline, estimated from WB scans, and the reported lumbar spine BMD. The findings for the IBD group suggest that converting the difference between the fat thickness within the baseline for various width ROI into a BME is a good predictor of the difference observed in the measured lumbar spine BMD measurements with equivalent ROI. For a perfect model, the gradient of the linear regression line in figure 6.10 would be 1 and the y-intercept 0. Hence, a gradient of 1.002 ±0.024 g/cm^2 per cm and a y-intercept of -0.002±0.001 g/cm^2 was encouraging. At the extremes of ROI width, the BME of the difference in fat in the baseline of these ROI was 0.034±0.018 g/cm^2 (±SD) whereas the actual change observed for L3+L4 BMD with these ROI was 0.035 ± 0.014 g/cm^2 (±SD).

Whilst the present results are encouraging, the data must be interpreted with caution as the findings may not be transferable to other subject populations or be suitable for individual patients. In clinical practice, if the difference between the fat thickness over spine and in baseline was

measured from a WB scan, the BMD error could be estimated from the BEF or from the data in figure 6.8. This would involve making the major assumption that the “true” BMD is correct. Existing reports and current data shows there will be a vast range of fat thickness differences expected in a typical population. It was found in section 6.2 that the deviation between fat thickness in the baseline relative to CB for this study population ranges from -0.69 cm (-15.5%) to 0.84 cm (18.5%). Thus using the linear regression model in figure 6.9, the error in BMD will range from -3.6% to 4.4%. These errors are not dissimilar to those published by others as discussed elsewhere but they are smaller than those published by Bolotin *et al.* (2003) for cases of extremely low BMD and a considerable difference in fat in baseline relative to over spine.

WB measurements on individuals could be simplified by measuring the FM in a single STB each side of the lumbar vertebrae and comparison with that in a region over spine. Whilst this offers less detail in fat distribution, it could be a crude method of assessing relative difference in fat across the ROI used to calculate lumbar spine BMD.

In order to employ the proposed method to estimate the inaccuracy in BMD, the patient would require a WB scan along with the lumbar spine scan. It is therefore not anticipated that this technique would be applied to the general patient population presenting for BMD assessment. However, it allows an appreciation of the magnitude of potential errors due to a non-uniform distribution of fat within scan ROI. The current findings suggest that, for this study group, the impact of a non-uniform distribution of fat on T-scores is likely to be minimal. However, it may be advisable that a WB scan is performed for patients where there is a significant change in abdominal girth between scans to gain an accurate measure of BMD improvement or deterioration. The emphasis of this work is on the accuracy of BMD results but soft tissue accuracy errors will also make precision worst if the magnitude of the accuracy error changes between repeated scans.

In theory BCA data could be obtained from lumbar spine scans as the attenuation of soft tissue adjacent to the spine is required to calculate lumbar spine BMD. A method of calibration would be required to separate fat from lean tissue as in WB scans. GE-Lunar scanners make lumbar spine scan soft tissue data available to the user but Hologic do not.

6.4 Conclusions

It appears that fat thickness profiles formed using data extracted from DXA WB images can be used to predict the inaccuracy in lumbar spine BMD measurements resulting from a non-uniform fat distribution. It can be concluded that there is a greater thickness of fat in the baseline soft tissue region than over the vertebrae for ROI widths generally used in clinical practice. For the IBD group, reducing the ROI width to approximately 9.5 cm would minimise the accuracy errors due to soft tissue distribution. As there is a large variation in fat thickness in the baseline and over the vertebrae, any correction for fat distribution should ideally be made for individual patients.

The findings suggest that errors in L3+L4 BMD will be introduced if there is a considerable difference between the average fat thickness within the baseline and overlying the spine. The BME of 1 cm of abdominal fat was shown to be 0.05 g/cm^2. For the IBD group, errors in BMD of up to 3% can occur for a 6 mm difference in fat thickness between baseline and over spine. One noteable finding from these results is that a small systematic error in BMD is expected using the ROI width recommended by Hologic when assuming the “true” BMD occurs when fat is uniformly distributed throughout the scan ROI.

The strong relationship between the observed change in phantom corrected L3+L4 BMD as the ROI increases and the BME of fat within the baseline suggests that errors in BMD can be predicted from data extracted from WB images. Conversion of the difference in baseline fat thickness between the largest and smallest ROI used in this work gave a

BME of 0.034±0.018 g/cm^2, whereas the actual change in BMD measured from lumbar spine scans using the corresponding ROI width was 0.035 ±0.014 g/cm^2 (± SD) i.e. approximately a 3% difference.

The original approach used here appears to corroborate published data in this area of research. The proposed model of predicting BMD accuracy errors from WB FM data works for this study population when averaging data over a group of similar subjects but the analysis performed in chapters 4, 5 and 6 needs to be repeated in different study populations and also in individual subjects.

Chapter 7

Quantification of the Fat Thickness within the DXA Lumbar Spine ROI from DXA Whole Body images and the Relationship to the Measured Lumbar Spine BMD for Various Patient Populations

7.1 Introduction

The work presented in this thesis so far has outlined a method to predict the inaccuracy in lumbar spine BMD measurement by quantifying the fat thickness within the baseline of lumbar spine ROI from DXA WB images. It appears that this is a novel approach.

The method was developed using lumbar spine and WB images from a group of 50 subjects with inflammatory bowel disease (IBD) and averaging data over the entire group. However, there was a wide variation in the difference between fat thickness in the baseline and over the spine. The apparent change in BMD as the ROI width increased, as shown in chapter 4, was successfully predicted from the bone mineral equivalent (BME) of the fat thickness within the baseline for the IBD population. However, this may not be the case with different patient

groups or for individual subjects. There was difficulty selecting study populations as data were required from a WB scan as well as the routine lumbar spine scan. From available studies, the groups with the largest number of subjects other than the IBD group were patients with confirmed osteoporosis and renal transplant (Tx) patients. The osteoporosis group (OST) was a good population to study as existing publications indicate that BMD accuracy errors and precision are worst when the actual BMD is low (Sobnack *et al.* 1990; Laskey *et al.* 1991). The renal Tx group was the only group with sufficient numbers of male and female subjects which allowed comparison of abdominal fat distribution between genders. Renal Tx usually involves placing an additional kidney within the lower abdomen. The male and female renal Tx groups were termed MRTx and FRTx respectively in this work.

In this chapter the analysis performed on lumbar spine scans and WB scans for the IBD subjects in chapters 4, 5 and 6 was repeated on the OST, MRTx and FRTx populations. The analysis concentrated on the L3+L4 level only. A comparison of the results is given here with a full data set provided in appendix B, C and D for the OST, MRTx and FRTx subjects respectively.

7.2 Methods

7.2.1 Study Populations

Lumbar spine and WB scans from 10 female patients with confirmed osteoporosis were retrieved from the archive, all of these OST patients had a clinical diagnosis of osteoporosis at the time of the scans.

Spine and WB images performed approximately 3 months post renal Tx for 20 male and 20 female patients were also retrieved.

All lumbar spine and WB images were free from artefacts.

Comparison of these study populations with the IBD groups is shown in table 7.1. A one-way ANOVA test was used to compare the characteristics of the study populations. A Bonferroni post hoc test was used to compare the mean age, BMD, BMI and weight as Levene's test confirmed equal variances for the data. A p-value < 0.05 indicated a significant difference. The mean age of the OST group was significantly greater than the FRTx group (p=0.017), however, the difference between the other populations was not significant. There was no significant difference in BMI between the populations. As expected, the BMD of the OST group was significantly lower than the other groups (p<0.001) with no significant difference between the three other populations. The mean weight of the MRTx group was significantly higher than the OST (p=0.003) and IBD (p<0.001) groups but not the FRTx group (p=0.057). There was no significant difference in weight between the IBD group compared to the FRTx (p=0.556) and OST (p=1.000) populations or between the OST and FRTx groups (p=1.000).

	IBD	OST	MRTx	FRTx
BMD with 11.5 cm ROI mean±SD (g/cm^2)	0.977±0.155	0.682 ±0.114	1.003±0.144	0.978±0.237
BMD Range (g/cm^2)	0.651 - 1.510	0.566-0.884	0.781-1.193	0.629-1.694
Age mean±SD (y)	50±11	59±10	49±12	45±14
Age Range (y)	17-70	42-76	29-68	23-68
Height mean ± SD (m)	1.6±0.6	1.6±0.1	1.7±0.8	1.6±0.6
Weight mean±SD (kg)	60.0±11.3	56.7.5±10.1	78.9±12.9	67.5±15.5
BMI mean±SD (kg/m^2)	24±4	23±4	26±4	27±6
BMI range (kg/m^2)	17-40	18-32	21-33	18-38

Table 7.1 Comparison of BMD, age, height, weight and BMI of subjects within the IBD, OST, MRTx and FRTx study populations.

7.2.2 Quantification of Errors in Lumbar Spine BMD using Fat Thickness Measured from DXA WB images

The influence of ROI width on measured lumbar spine BMD was investigated using the method described in chapter 4. Fat distribution within the baseline of the ROI and over the vertebrae was quantified from WB images as outlined in chapters 5 and 6. The process of relating the lumbar spine BMD and WB measurements is summarised in figure 7.1. Differences between data for the study populations were investigated

using a one-way ANOVA test and, when necessary, a relevant post hoc test. When appropriate, general linear model repeated measurement analysis was used to investigate linear regression interactions. For all statistical tests a p-value < 0.05 was considered significant.

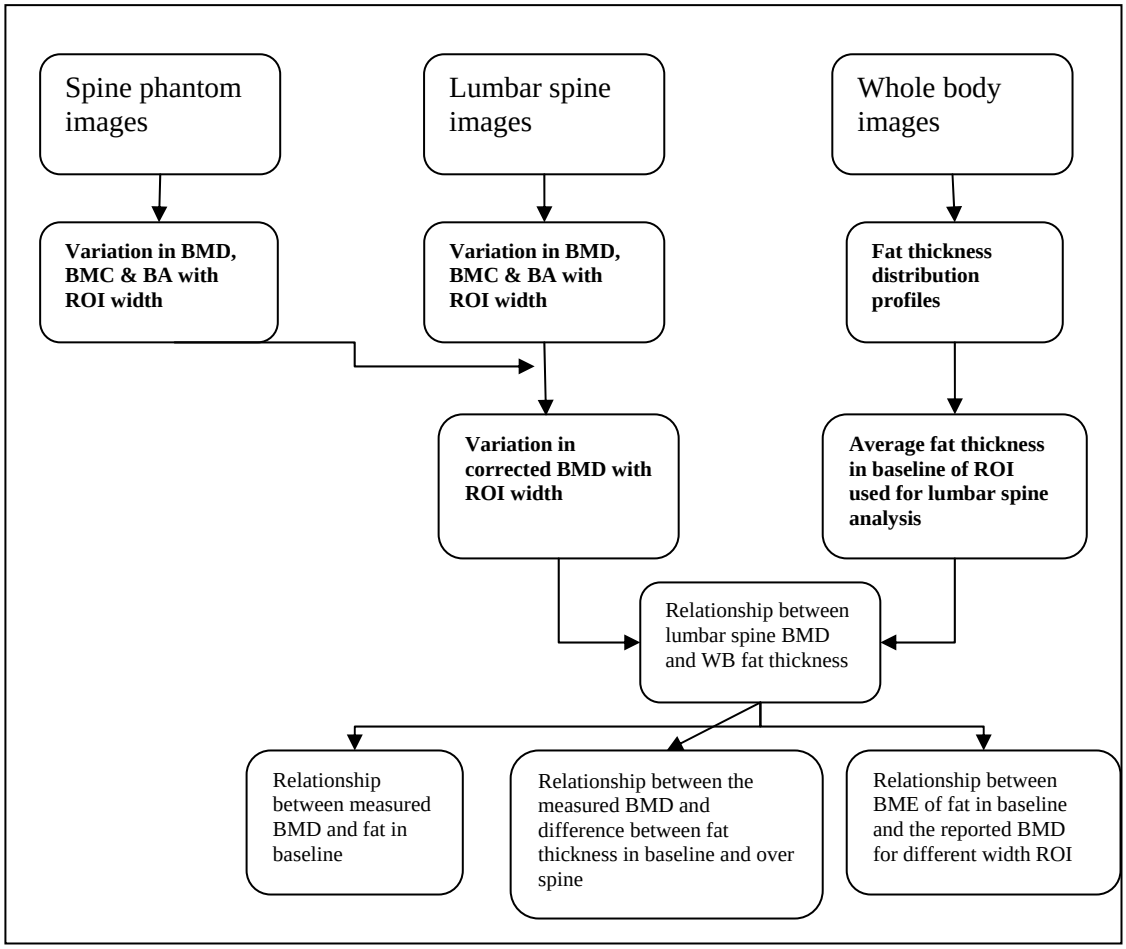

Figure 7.1 Summary of stages involved in predicting accuracy errors in lumbar spine BMD using fat thickness measured from DXA WB scans.

7.3 Influence of Lumbar Spine ROI Width on Reported BMD

7.3.1 Results

The gradients of the linear regression model for the relationship between BMD, BMC and BA and the ROI width are shown in tables 7.2, 7.3 and 7.4. Figures 7.2 to 7.4 and results in table 7.2 indicate there was a similar trend in the variation of BMD with ROI width for the three populations. For all groups there was a very small decrease in BMD for L1, a small increase for L2 and a greater increase for L3 and L4. For the latter, the gradient of the regression lines were significantly different to 0 and therefore represent real changes. Repeated measurement analysis showed that for all groups the ROI width had a significant effect on the BMD, BMC and BA ($p<0.001$). However, pairwise comparisons showed that for individual vertebrae, the ROI width did not have a significant effect on BMC for L1 in any group ($p=0.112$).

There was a significant difference between the BMD of individual vertebrae for the OST group ($p=0.026$) but not for the FRTx ($p=0.292$) or MRTx groups ($p=0.266$). The BMC and BA of L1 to L4 was significantly different for each group ($p<0.001$). However, pairwise comparisons for the OST and FRTx groups revealed the BMC was not significantly different for consecutive pairs of vertebrae. For the FRTx group, there was a significant difference in BA between the vertebrae for all pairs of vertebrae except L1 compared to L2 ($p=0.400$), L2 compared to L3 ($p=1.000$) and L3 compared to L4 ($p=0.389$). For the MRTx group, there was a significant difference in BMC between L1 and L3 ($p=0.007$) and between L1 and L4 ($p<0.001$) only.

There was a significant interaction between vertebrae and width for BMC, BMD and BA ($p<0.001$) for L1 to L4. However, when looking at pairs of vertebrae for the OST group, there was no significant interaction between the BMD data for L1 compared to L2 ($p=0.058$) and L3 compared to L4 ($p=0.303$) indicating that the gradients were not significantly different. For the FRTx group, there was no interaction between the slopes for L3 compared to L4 ($p=0.159$) or L2 compared to L3 ($p=0.096$). Paired

analysis for the MRTx group showed that the gradient of the L2 regression line was not significantly different to that for L4 (p=0.076). The same was true of L3 compared to L4 (p=0.491) showing no interaction.

For BMC, in the OST group there was no significant interaction between regression lines of L1 compared to L2 (p=0.1000) and L3 compared to L4 (p=0.321) showing that the gradients were not significantly different. For the MRTx group, there was no significant interaction for L2 compared to L4 (p=0.063) and L3 compared to L4 (p=0.512). For the FRTx group, all interactions were significant except that for L3 compared to L4 (p=0.097).

For the variation in BA with ROI width for the OST group, there was no significant interaction for L1 with L2 (p=0.253) and L3 with L4 (p=0.720) with all other pairs having significant interaction (p<0.001). For the FRTx and MRTx groups, the interaction between gradients was only significant for L1 compared to L3 and L1 compared to L4. This confirmed that the regression gradients for all other pairs of vertebrae were not significantly different.

Repeated measurement analysis was also used to investigate the interactions between groups for individual vertebrae and ROI width for BMD, BMC and BA. There was a significant interaction between the regression gradients for the four subject groups for L1 (p=0.024) and L2 (p=0.005) but not L3 (p=0.113) and L4 (p=0.386). This indicated the regression gradients for L3 and L4 were not significantly different over all subject populations. A more detailed analysis showed that for L1, the only significant interaction in slopes was between the IBD and MRTx groups (p=0.004); the slopes of all other groups were not significantly different.

Repeated measurement analysis on BMC data showed for all vertebrae except L4 (p=0.693) there was a significant interaction between the regression gradients for all study populations (p<0.001). Paired comparisons showed that for L1 the interaction was only significant for IBD group compared to MRTx group (p<0.001) and the IBD group compared to the FRTx group (p=0.047). For L2 and there was no

interaction between gradients for the IBD and OST (L2: p=0.279; L3: p=0.409), IBD and FRTx (L2: p=0.188; L3 p=0.445) and OST compared to FRTx groups (L2: p=0.147, L3: p=0.739).

In general, for BA there was a significant interaction between the study population and ROI width for L1, L2 and L3 but not L4 (p=0.863). Paired comparisons for L1 showed a significant interaction between IBD and MRTx, OST and MRTx and MRTx and FRTx groups. For L2, only the interactions of IBD with MRTx and OST with MRTx were significant. For L3, the only significant interaction was between the IBD and MRTx populations (p=0.011).

The regression gradients are more variable across the groups for BMC and BA. As with BMD, changes in L3 and L4 BMC are greater than those in L1 and L2 with a decrease in L1 for all groups except MRTx. The BA also increased significantly for L3 and L4. Comparing the percentage change in BA with BMC changes, the resultant increase in BMD is expected. Changes in L1 and L2 BA are very small and in some groups non-significant. A full set of BMC and BA graphs for the OST and renal Tx groups are shown in appendices B to D.

Study Population	Gradient of BMD regression line (g/cm^2 cm^{-1})			
	L1	L2	L3	L4
IBD	-0.004±<0.001	0.001±<0.001	0.007±<0.001	0.008±0.001
OST	-0.003±0.001	0.001±<0.001	0.008±<0.001	0.010±<0.001
MRTx	-0.002 ± 0.001 (p=0.123)	0.005±0.001	0.009±<0.001	0.008±<0.001
FRTx	-0.002±<0.001	0.002±<0.001	0.005±<0.001	0.008±<0.001

Table 7.2 Gradients of linear regression model for the relationship between the measured lumbar spine BMD and ROI width for subjects with IBD, osteoporosis and male and female patients 3 months post renal transplant. The gradients were significantly different to 0 ($p<0.05$) unless otherwise stated. Results expressed as gradient ± standard error in gradient.

Study Population	Gradient of BMC regression line ($g\ cm^{-1}$)			
	L1	L2	L3	L4
IBD	-0.08±<0.01	0.05±0.01	0.23±0.01	0.30±0.01
OST	-0.05±0.02	0.02±0.01	0.21±0.01	0.26±0.01
MRTx	0.07±0.03 (p=0.060)	0.23±0.02	0.36±0.01	0.32±0.01
FRTx	-0.03±0.01	0.09±0.01	0.22±0.01	0.29±0.01

Table 7.3 Gradients of linear regression model for the relationship between the measured lumbar spine BMC and ROI width for subjects with IBD, osteoporosis and male and female patients 3 months post renal transplant. The gradients were significantly different to 0 ($p<0.05$) unless otherwise stated. Results expressed as gradient ± standard error in gradient.

Study population	Gradient of bone area regression line (cm^2 cm^{-1})			
	L1	L2	L3	L4
IBD	-0.04±0.01	0.04±0.01	0.13±0.01	0.16±<0.01
OST	-0.04±0.01	0.00±0.01 (p=0.976)	0.13±0.01	0.15±0.01
MRTx	0.09±0.02	0.15±0.01	0.20±<0.01	0.17±0.03
FRTx	0.00±0.01 (p=0.844)	0.06±0.01	0.13±<0.01	0.17±0.01

Table 7.4 Gradients of linear regression model for the relationship between the measured lumbar spine bone area and ROI width for subjects with IBD, osteoporosis and male and female patients 3 months post renal transplant. The gradients were significantly different to 0 ($p<0.05$) unless otherwise stated. Results expressed as gradient ± standard error in gradient.

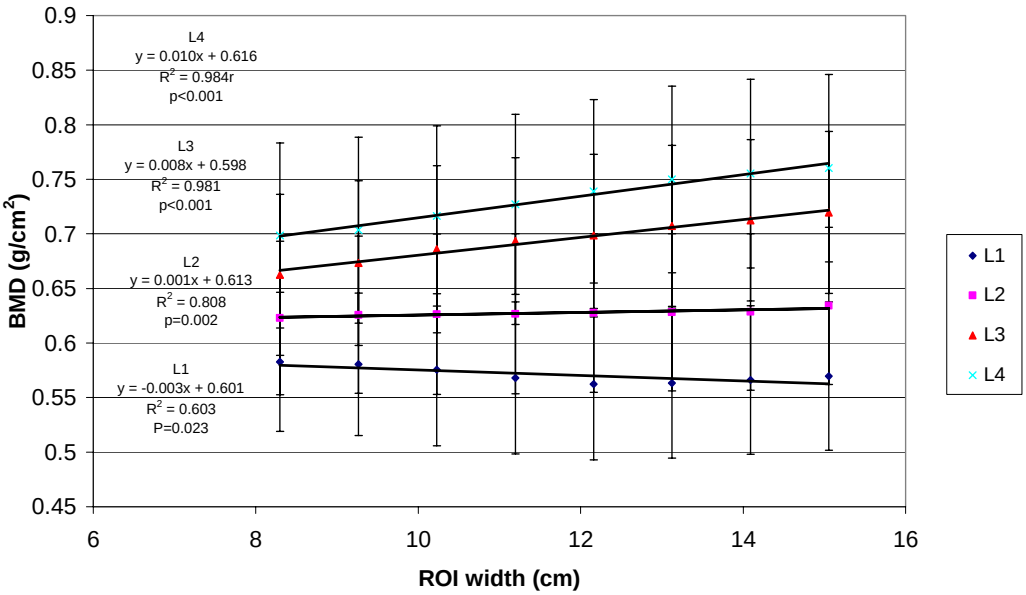

`Figure 7.2 Relationship between measured lumbar spine BMD and the width of the lumbar spine ROI are the average (± 95% CI) for 10 subjects with confirmed osteoporosis. SEE: L1= 0.005 g/cm^2, L2=0.002 g/cm^2, L3=0.003 g/cm^2, L4=0.003 g/cm^2.

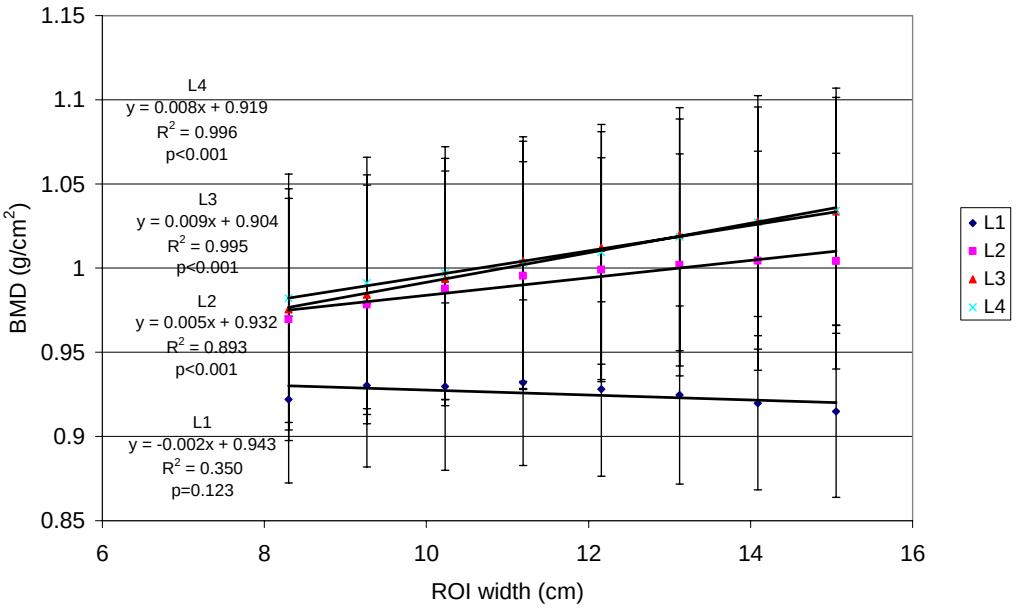

Figure 7.3 Relationship between measured lumbar spine BMD and the width of the lumbar spine ROI. Data are the average (±95% CI) for the 20 male renal Tx patients. SEE: L1=0.005 g/cm^2, L2=0.005 g/cm^2, L3=0.002 g/cm^2, L4=0.001 g/cm^2.

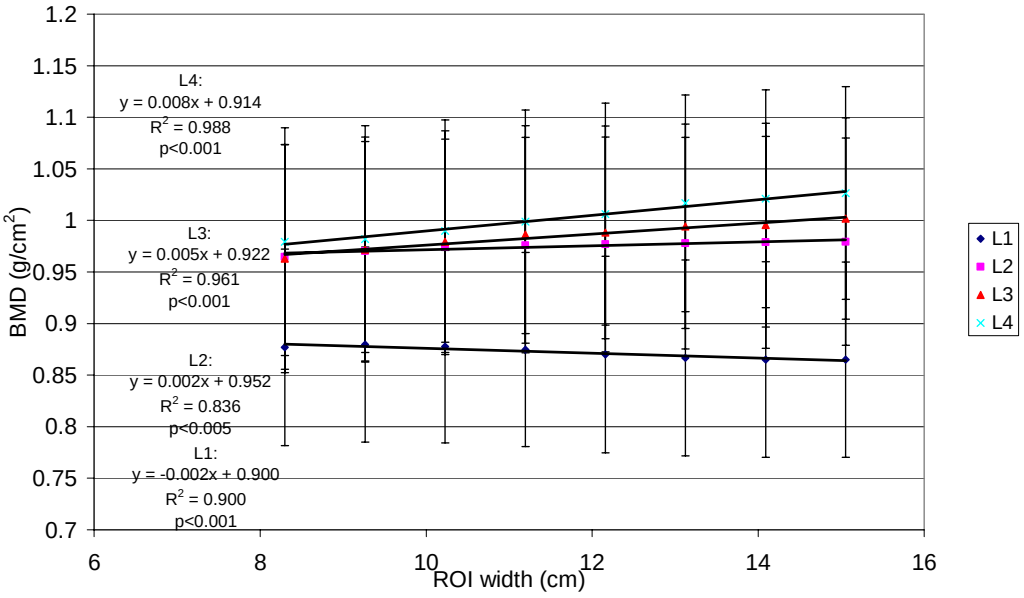

Figure 7.4 Relationship between measured lumbar spine BMD and the width of the lumbar spine ROI. Data are the average (± 95% CI) for female renal Tx patients. SEE: L1=0.002 g/cm^2, L2=0.002 g/cm^2, L3=0.003 g/cm^2. L4=0.002 g/cm^2.

For all study populations the Pearson's correlation coefficient confirmed that there was a significant ($p<0.01$) positive correlation between changes in BMC and BA for L3 and L4 (table 7.5).

	Pearson's Correlation Coefficient	
	L3	L4
IBD	0.997	1.000
OST	0.999	0.992
MRTx	1.000	1.000
FRTx	0.998	0.999

Table 7.5 Results of test for correlation between BMC and BA. Pearson's correlation coefficient indicate a significant correlation between BMC and BA for L3 and L4 at the $p<0.001$ level.

Table 7.6 and figures 7.5 to 7.7 show that in all groups when combining the BMD for pairs of vertebrae, the gradient of the linear regression model was significantly different to 0 for L3+L4 in all groups ($p<0.001$) but only in the IBD and MRTx groups for L1+L2. Repeated measurement analysis confirmed that in all groups the ROI width had a significant effect on the BMD of L1+L2 and L3+L4 ($p<0.001$). There was a significant interaction between the vertebral pairs and ROI width ($p<0.001$) indicating that the slopes are significantly different. Over all ROI widths, the BMD of L1+L2 was significantly lower than that for L3+L4 for the OST group ($p<0.001$) but there was no significant difference for the IBD ($p<0.001$), MRTx ($p=0.313$) or FRTx ($p=0.355$) groups.

	L1+L2		L3+L4		Corrected L3+L4	
	Gradient	R^2	Gradient	R^2	Gradient	R^2
IBD	-0.001±<0.001 (p<0.05)	0.795	0.008±<0.001	0.9976	0.005±<0.001	0.9961
OST	-0.001±<0.001 (p=0.339)	0.153	0.009±<0.001	0.988	0.006±<0.001	0.976
MRTx	0.002±0.001 (p=0.035)	0.550	0.008±<0.001	0.999	0.006±<0.001	0.9988
FRTx	-3×10^{-5}±<0.001 (p=0.911)	0.002	0.007±<0.001	0.991	0.004±<0.001	0.983

Table 7.6 Gradient of linear regression model for the relationship between the measured lumbar spine BMD and ROI width. The regression line gradient was significant at the p<0.001 unless otherwise stated. Results expressed as gradient ± error in gradient.

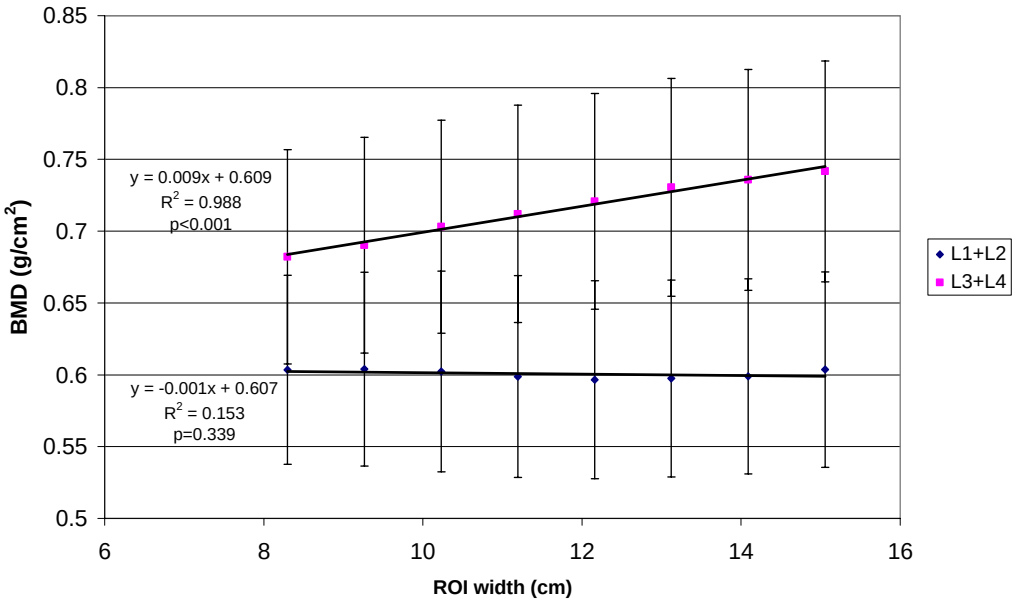

Figure 7.5 Relationship between the combined L1+L2 and L3+L4 BMD and the width of the lumbar spine ROI. Data are the average (± 95% CI) for the 10 subjects with confirmed osteoporosis. SEE: L1+L2 = 0.003 g/cm^2, L3+L4 = 0.003 g/cm^2.

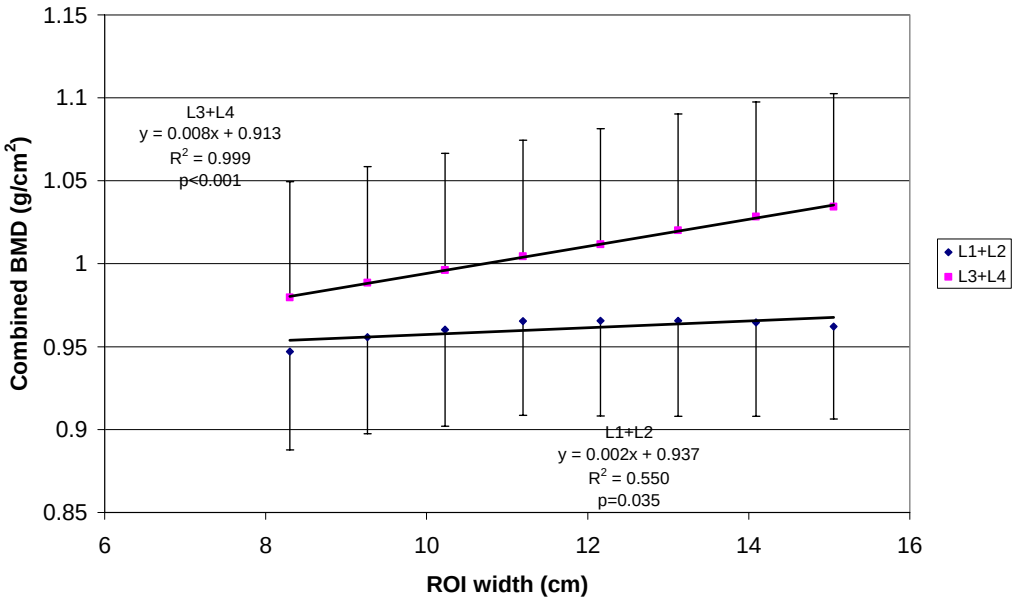

Figure 7.6 Relationship between combined L1+L2 and L3+L4 BMD and the width of the lumbar spine ROI. Data are the average (± 95% CI) for 20 male renal transplant patients. SEE: L1+L2 = 0.005 g/cm^2, L3+L4 = 0.001 g/cm^2. For clarity only the negative error bars are displayed on L1+L2 data and positive error bars on L3+L4.

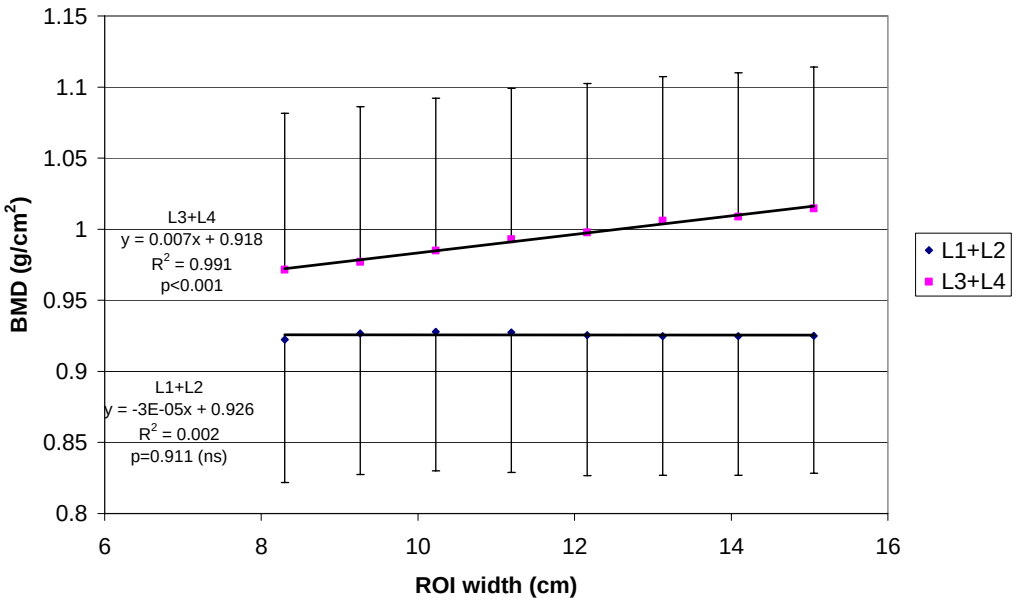

Figure 7.7 Relationship between combined L1+L2 and L3+L4 BMD and the width of the lumbar spine ROI. Data are the average (± 95% CI) for 20 female renal transplant patients. SEE: L1+L2 = 0.002 g/cm^2, L3+L4 = 0.002 g/cm^2. For clarity only the negative error bars are displayed on L1+L2 data and positive error bars on L3+L4.

Table 7.6 also shows that correcting the L3+L4 BMD using phantom data reduced the dependence of BMD on ROI width in all groups. Repeated measurement analysis showed a significant interaction between the data for uncorrected and corrected BMD in the OST group ($p=0.014$) and IBD group ($p<0.001$) but not for the FRTx ($p=0.131$) or MRTx ($p=0.148$) groups. However, there was still a significant increase in corrected BMD with the gradient of the regression model being significantly different to 0 ($p<0.01$) in all groups and repeated measurement analysis confirmed ROI width has a significant effect on both the uncorrected and corrected BMD ($p<0.001$). As expected, there was no significant difference between the corrected and uncorrected BMD for all groups (OST: $p=0.995$; MRTx: $p=0.997$; FRTx: $p=0.997$).

7.3.2 Discussion

Whilst there are differences in the average L1 to L4 BMD between subject groups, the changes in BMD, BMC and BA as the ROI width increased was similar and consistent with those seen for the IBD group in Chapter 4. In general the changes in BMD, BMC and BA for both L1 and L2 are small with the error in the gradient relatively large compared to the actual gradient. However, changes in BMD, BMC and BA for L3 and L4 are all significant. Repeated measurement analysis confirmed that ROI width had a significant effect on BMD, BMC and BA for L1 to L4 in all study populations. Consistently, there was no significant interaction between the L3 and L4 regression gradients for variation in BMD, BMC and BA with ROI width, indicating that the regression lines were not significantly different. This finding strengthens the argument for combining data for L3+L4 in this work. The ROI width had a similar effect on BMD, BMC and BA for L4 in all study populations with the effect varying between groups for other vertebrae.

In the FRTx and OST groups, the change in L1+L2 BMD is non-significant. The results therefore confirm that there is a greater dependence of combined L3+L4 BMD on the width of the ROI than for

L1+L2 and reinforces the decision to concentrate on L3+L4 measurements in this work.

As discussed in chapter 4, it is suspected by others that changes in BMD are, at least in part, attributable to the apparent false changes in BA (Yang *et al*. 1997; Tothill and Avenell 1998). A strong correlation between the BA and BMC for both L3 and L4 observed here provides further evidence that changes in BMD are dependent on the relationship between BA and BMC.

As with the IBD group, the phantom correction reduces the dependence of BMD on ROI width but there remains a residual significant increase in L3+L4 BMD as the ROI is widened. Correcting the BMD data changed the gradient significantly in the OST and IBD groups, which justifies the need for compensating for changes seen in the phantom. Due to the similarity of changes in L3 and L4 BMD, BMC and BA as the ROI increases across all study populations investigated, it can be concluded that this is a real phenomenon which occurs in all individuals.

7.4 Quantification of Abdominal Fat Thickness Distribution using DXA Whole Body Images

7.4.1 Results

An ANOVA test showed that the mean estimated fat thickness over the spine was not significantly different between the four study populations ($p=1.000$). The fat thickness profiles for all the subject groups showed similar features with the positions of the minimum and maximum coinciding to within 1 cm (Table 7.7.1 a, Figs 7.8, 7.9, 7.10). An ANOVA test confirmed that there was no significant difference in the position of maximum and minimum fat thickness between study populations ($p<0.05$) Table 7.7.1b shows that the fat thickness within individual STB varied less than 5% from the thickness over the spine up to 4.6 cm from the centre of the spine. A Bonferroni ANOVA post hoc test showed that the width of the spine, represented by the CB, was significantly larger for the

group composed of male subjects than the three female groups (p=0.015, 0.001, 0.001) (Table 7.7.1 a).

	Mean (± SD) fat thickness over spine (cm)	Position of minimum (cm)		Position of maximum (cm)		Increase in thickness min to max (%)		Mean (± SD) width of vertebrae (cm)
		Rt	Lt	Rt	Lt	Rt	Lt	
IBD	5.2±2.7	3.5	3.5	7.6	7.6	26	28	4.3±1.3
OST	5.0±3.7	3.0	2.6	7.1	7.1	21	34	4.2±0.2
MRTx	6.2±2.7	3.6	3.6	7.7	8.1	38	35	4.6±0.3
FRTx	5.0±3.2	3.4	3.4	6.7	7.5	29	30	4.1±0.3

(a)

	Distance from spine at which fat thickness deviates less than 10% from that over vertebrae (cm)	Distance from spine at which fat thickness deviates less than 5% from that over vertebrae (cm)
IBD	4.2	3.9
OST	4.3	3.9
MRTx	4.8	4.4
FRTx	5.0	4.6

(b)

Table 7.7.1 (a) Comparison of features within fat thickness profiles from IBD, osteoporotic and renal transplant patients (Rt = right of body/left on screen); (b) deviation of fat thickness from the thickness of fat estimated to be over the spine – where asymmetrical the maximum distance was recorded.

The individual fat thickness profiles shown in figures 7.8 to 7.10 were plotted on a scale to enhance features. However, when normalising the fat thickness to that in the CB as shown in figure 7.11, it can be seen that the profile for the OST group does not show such a pronounced minimum as the other groups. A paired t-test showed that for all groups except the FRTx group, the fat thickness over the vertebrae was not significantly different to that in the soft tissue region placed next to the vertebrae (STB1) (p=0.5).

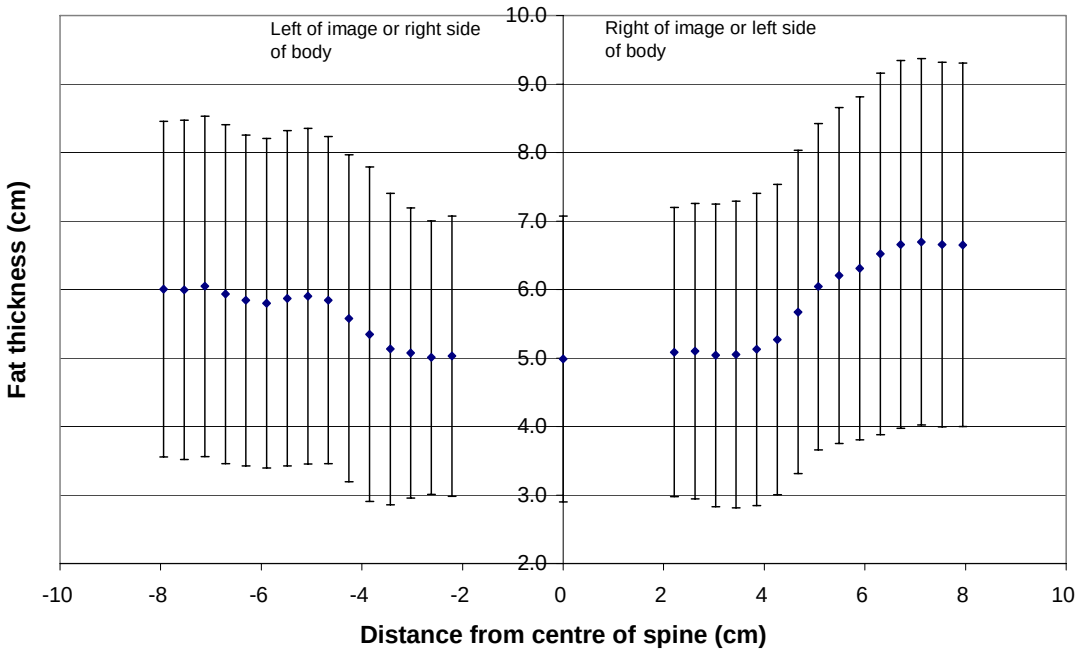

Figure 7.8 Average variation in fat thickness at the level of L3+L4 with distance from the central axis of lumbar spine for 10 patients with confirmed osteoporosis (± 95% CI).

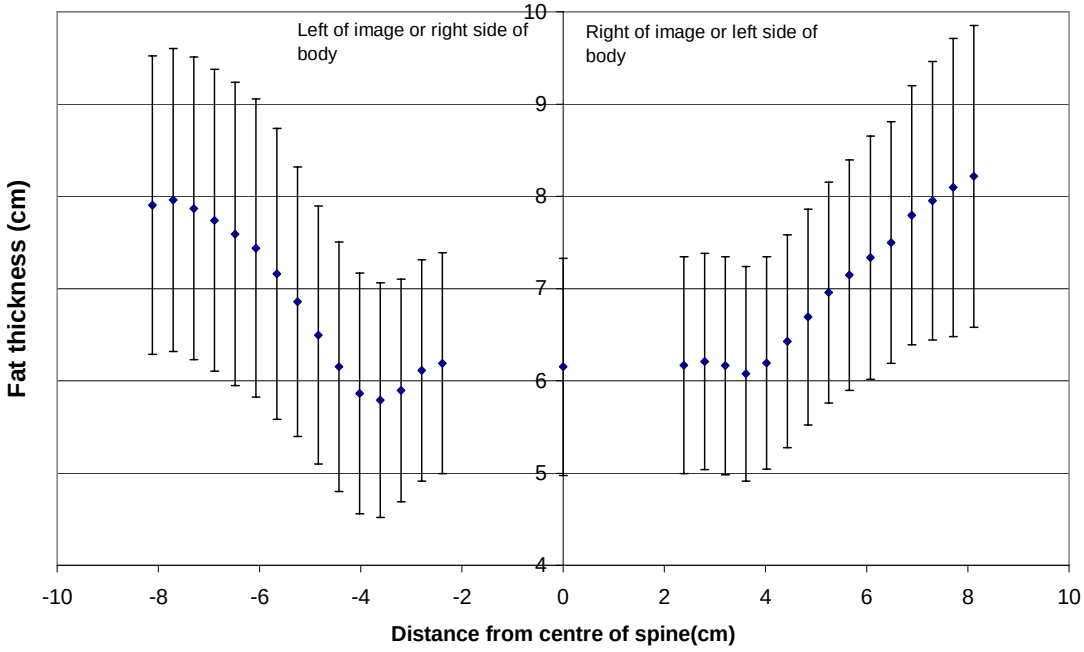

Figure 7.9 Average variation in fat thickness at the level of L3+L4 with distance from the central axis of lumbar spine for 20 male patients 3 months post renal transplant (± 95% CI).

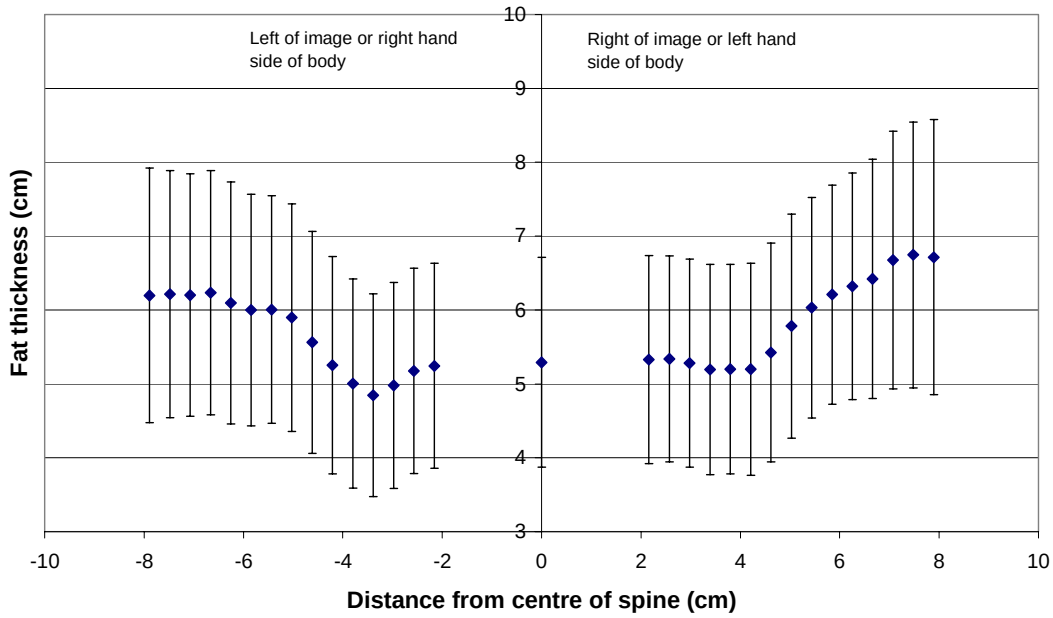

Figure 7.10 Average variation in fat thickness at the level of L3+L4 with distance from the central axis of lumbar spine for 20 female patients 3 months post renal transplant (± 95% CI).

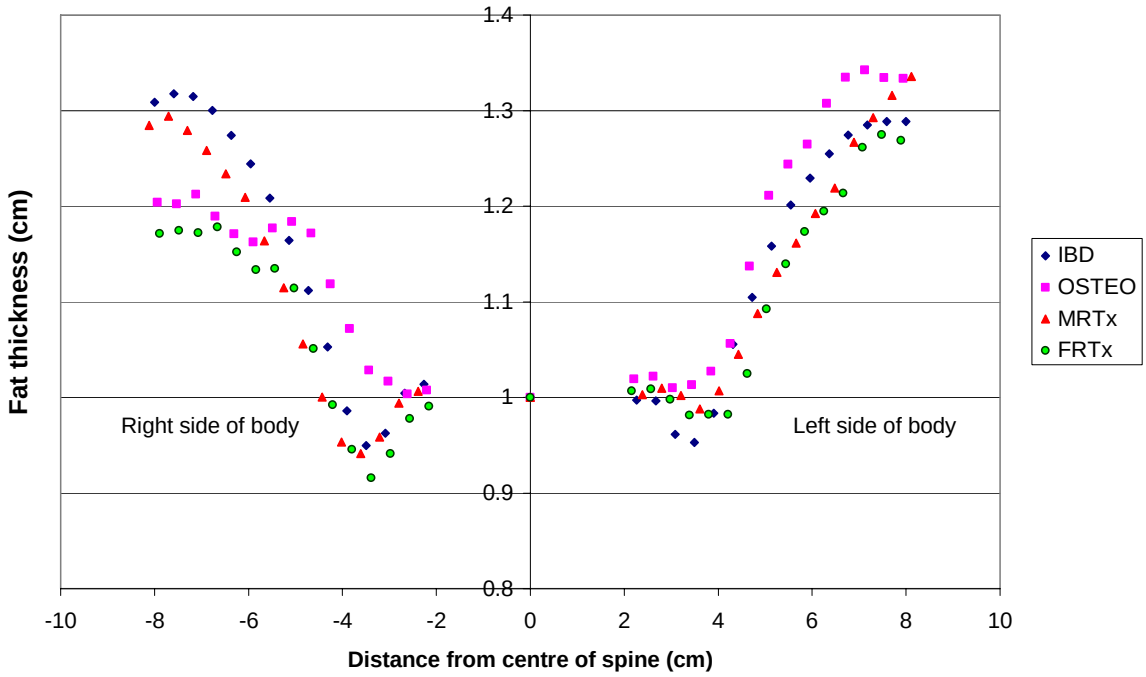

Figure 7.11 Comparison of fat thickness profiles from subjects with IBD, osteoporosis and a group of male and females three months post renal transplant. Fat thickness at all points is normalised to that over the vertebrae.

7.4.2 Discussion

The features within the abdominal fat thickness distribution profiles for the L3+L4 level are similar for all groups and are in keeping with that observed for the IBD group. A full discussion of the features in the profile in relation to the abdominal anatomy seen on published CT scans can be found in chapter 5. The profiles for the FRTx and OST groups are less symmetrical than for the other groups with a lower fat thickness on the RHS. The most noticeable difference between the groups is the lack of a minimum in fat thickness for the OST group. As discussed in chapter 5, the minimum fat thickness is likely to occur at the location of the psoas muscles (Fig. 5.8). A possible explanation for the absence of the minima in the OST group is due to the mean age of this group being significantly higher than the other groups as confirmed by an ANOVA test. During aging muscle tissue can decrease and be replaced by fatty tissue. As the mean age of the OST group is at least 9 y greater than other groups, with a higher age range (42 – 76), it is plausible that these subjects have a lower proportion of muscle adjacent to the spine relative to other groups. The youngest in the OST group is 42 y whereas the other groups are composed of a considerable number of subjects in 20 to 40 y range.

Renal Tx involves placing an additional kidney low down in the abdomen just above the pelvic brim near to the skin surface as shown in figure 7.12. It is therefore possible that the additional kidney may fall within the region of the soft tissue baseline at the L3+L4 level which could cause the fat thickness profile to be asymmetrical. There does not appear to be any evidence of this for MRTx patients but it could explain the asymmetry in the FRTx profile.

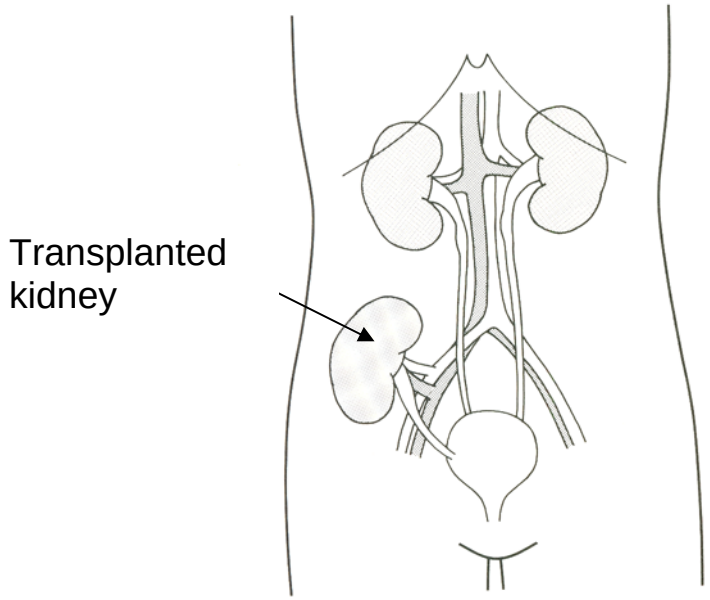

Figure 7.12 Location of transplanted kidney (Allen and Chapman 1994).

As expected, the variation in fat thickness measurement, reflected by the 95% CI, increases as the number of subjects within the study population decreases. However, even the profile obtained from the OST group composed of only 10 subjects shows enough detail to quantify the inhomogeneity in fat thickness. When quantifying the uniformity of fat distribution within the lumbar spine ROI, it was found that for a 10% deviation in fat thickness relative to that over the vertebrae, the ROI width would be 12.7 cm, 12.8 cm, 14.2 cm and 14.1 cm for the IBD, OST, MRTx and FRTx respectively. For a 5% deviation, ROI widths should be less than 12.1 cm, 12.0 cm, 13.4 cm and 13.3 cm for these groups. Hence, if the standard width ROI was 11.5 cm there would be less than 5 % deviation in the fat thickness at any point within the baseline from the fat thickness over the vertebrae. The CB for the male group is larger than for the female groups which is plausible as, in general, the vertebrae are wider in males (Busscher *et al*. 2010).

The average fat thickness over the L3+L4 vertebrae in all groups is similar to published data based on CT measurements and that measured for the IBD group. There was no significant difference between the fat thickness in the CB for the four study populations. Tothill and Pye (1992)

measured a fat thickness over the vertebrae to be 5.81±2.80 cm for men and 4.77±2.14 cm for women. In the current work, BMI is highest for the MRTx and FRTx patients and lowest for the OST group, which is reflected in the fat thickness measurements. An ANOVA test proved the difference in BMI between the groups was not significant. Further confirmation that the Hologic WB algorithm estimates the fat thickness over the vertebrae by interpolating the value for tissue next to bone was provided here, as fat thickness for STB next to spine was not significantly different to that in CB. The results in this section confirm that fat thickness measurements from DXA WB analysis presented in this work are sensible and plausible.

7.5 Quantification of Fat Thickness in Soft Tissue Baseline used for DXA Lumbar Spine Analysis from DXA Whole Body Images

7.5.1 Results

Figure 7.13 shows there was a significant positive correlation between the fat thickness in the region corresponding to the soft tissue baseline within the lumbar spine ROI and the width of the ROI for all groups. The gradient of the linear regression model was significantly different to 0 in all cases being 0.085±0.002 cm cm^{-1}, 0.100±0.006 cm cm^{-1}, and 0.077±0.003 cm cm^{-1} for the OST, MRTx and FRTx groups respectively. Repeated measurement analysis on data in figure 7.13 confirmed that the ROI width had a significant effect on the average fat thickness in the baseline region for all subject groups ($p<0.001$). Comparing the IBD data from figure 6.3 with the other study groups in figure 7.13, confirmed that there was no significant interaction between regression gradients for each group and the ROI width, indicating that the gradients were not significantly different ($p=0.249$). Over all ROI widths, fat thickness in the baseline was not significantly different between the groups ($p=0.648$) as

reflected by the considerable overlap of the ±95% CI error bars for each group in figure 7.13.

For all subject groups there was a greater average fat thickness in the baseline of a 11.5 cm ROI than over the vertebrae (Table 7.7.2). Multiple comparisons revealed this difference in fat thickness was only significant between the OST group and FRTx group (p=0.030). Differences in fat thickness were converted to a BME of 0.010 g/cm^2, 0.020 g/cm^2, 0.005 g/cm^2 and 0.015 g/cm^2 for the IBD, OST, MRTx and FRTx groups respectively.

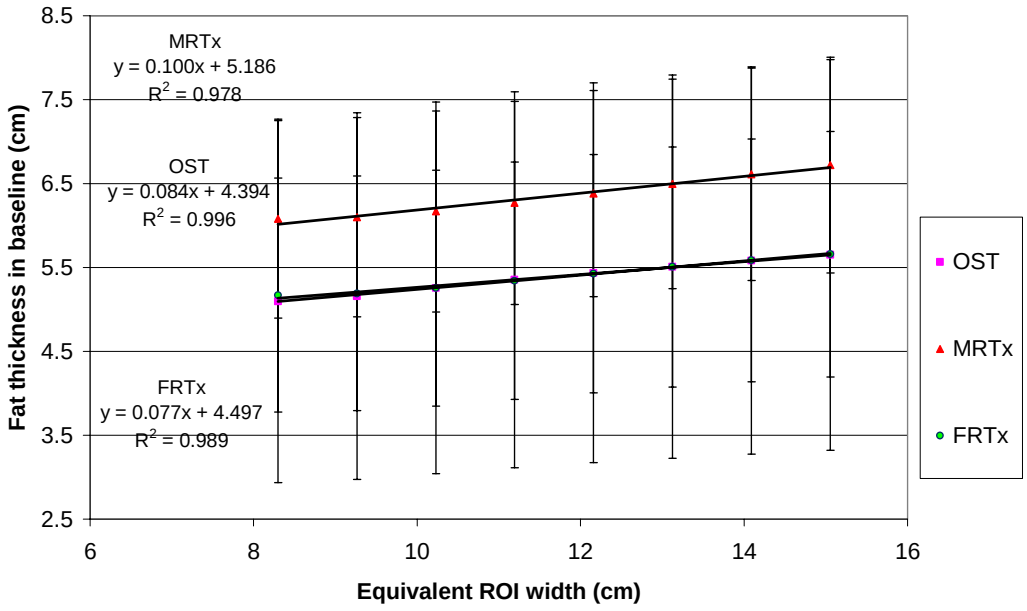

Figure 7.13 Average fat thickness (±95% CI) in soft tissue regions adjacent to L3+L4 that are equivalent to those for used for lumbar spine BMD analysis. Comparison of between subjects width osteoporosis (OST) and those 3 months post renal transplant (MRTx and FRTx). SEE: OST=0.133 cm, MRTx=0.038 cm, FRTx=0.021 cm. Gradients of regression line were significantly different to 0 for all groups with p<0.001. Standard errors in gradients: OST=0.002 cm per cm, MRTx=0.006 cm per cm, FRTx=0.003 cm per cm.

	Average fat thickness in CB (±SD) (cm)	Fat thickness in baseline of 11.5 cm ROI (± SD cm)	Difference (%)	ROI with equal fat thickness over and in baseline (cm)
IBD	5.2 ±2.7	5.4±2.8	3.8	9.5
OST	5.0±3.8	5.4±3.6	7.4	7.0
MRTx	6.2±2.7	6.3±2.8	3.0	9.7
FRTx	5.3±3.2	5.4±3.2	5.5	10.4

Table 7.7.2 Comparison of the fat thickness over the spine and in the baseline of the ROI as measured from DXA WB scans for subjects width IBD, osteoporosis (OST) and those 3 months post renal transplant (MRTx and FRTx).

Figure 7.14 shows that the fat thickness in the baseline was lower than that over vertebrae for ROI widths of 8.3 cm and 9.3 cm for the MRTx group and widths of 8.3 cm, 9.3 cm and 10.8 cm for the FRTx group. In contrast, fat thickness in baseline was higher than that over the vertebrae for all ROI widths in the OST group. Using a linear regression model for data in figure 7.14, the ROI width which would give an equal fat thickness in the baseline and over the vertebrae was 7.0 cm, 9.7 cm and 10.4 cm for the OST, MRTx and FRTx groups respectively. A one-way ANOVA test showed there was no significant difference between these “ideal” ROI widths ($p=0.117$). There was a strong positive correlation between the ROI width and the relative difference in fat thickness over and adjacent to the spine in all cases reflected by a Pearson’s correlation coefficient of 0.996, 0.978 and 0.989, for OST, MRTx and FRTx groups, and gradient of regression line significantly different to 0 ($p<0.001$). A similar relationship was seen for the IBD group with a correlation coefficient of 0.998. Paired t-tests on data from individual groups showed that the average fat thickness in the baseline of a 11.5 cm ROI was significantly higher than that over the vertebrae for the IBD ($p<0.001$), OST ($p=0.002$) and MRTx ($p<0.001$) groups. However, for the FRTx group, the average thickness of fat in the baseline was not significantly different to that in the CB ($p=0.092$).

Repeated measurement analysis on data in figure 7.14 and figure 6.4, confirmed that the ROI width had a significant effect on the difference between baseline and CB fat thickness ($p<0.001$). There was no significant interaction between the regression gradients for each group ($p=0.249$) confirming they were not significantly different. Over all ROI widths, the difference between fat in baseline and that in the CB did not vary significantly between groups ($p=0.994$), which is consistent with the overlap in error bars in figure 7.14.

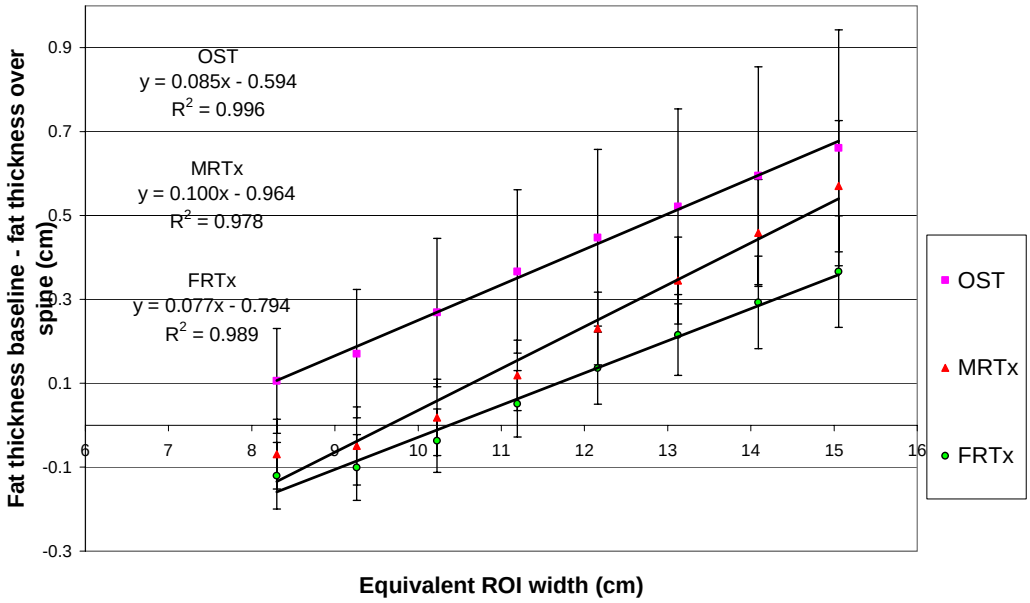

Figure 7.14 Comparison of the relationship between the fat thickness in baseline of the ROI used to measure BMD relative to that over spine for L3+L4 level for the OST, MRTx and FRTx groups. SEE: OST=0.013 cm, MRTx=0.038 cm FRTx=0.021 cm. The gradient of regression line was significantly different to 0 in all cases with $p<0.001$.Standard errors in gradients: OST=0.002 cm per cm, MRTx=0.006 cm per cm, FRTx=0.003 cm per cm. Error bars are 95% CI of each data point.

7.5.2 Discussion

As with the IBD group, the average fat thickness within the soft tissue baseline increased with ROI width for the other subject groups. There was a large variability in fat thickness measurements between subjects within groups as reflected by the relatively high standard deviation (SD).

The results are presented in more detail in appendix B to D. At this stage in the work all results are for the average of each study population.

The findings provide further evidence to corroborate those with the IBD group that there is a greater fat thickness in the baseline of lumbar spine ROI than over the spine for ROI widths generally used in clinical practice. This difference was statistically significant for the IBD, OST and MRTx groups ($p<0.05$) but not for the FRTx group ($p=0.092$). For a 11.5 cm ROI, the maximum difference in fat thickness was 0.4 cm which equates to a BME of 0.02 g/cm^2 and a T-score of 0.2. Errors in T-score of this magnitude are unlikely to cause a major problem for clinical diagnosis of osteoporosis.

For the OST group, the fat thickness within the baseline was greater than that over the vertebrae for all ROI widths (Fig. 7.13). This would be expected from inspection of the fat thickness profiles as there are no minima in fat thickness adjacent to the spine (Fig. 7.8). For the other groups, the narrowest ROI contains a smaller fat thickness in baseline relative to that over the spine. This is plausible due to the initial decrease in fat thickness seen when moving laterally from the spine on the corresponding fat thickness distribution profile (Fig's 5.3, 7.9, 7.10).

As mentioned previously, the difference in fat thickness between the baseline of a 12.5 cm ROI and over the spine was found by Tothill *et al*. (1992; 1994a) to be 6.7 to 17 mm. The corresponding differences in fat thickness for the current data were 3.0 mm, 5.1 mm, 2.5 mm and 1.6 mm for the IBD, OST, MRTx and FRTx groups respectively.

Assuming that the accuracy of BMD measurement depends only on fat distribution, the ideal ROI would contain an equal average fat thickness in baseline to that in soft tissue over the spine. For all the study populations, ROI widths smaller than those generally used in clinical practice give an equal fat in the baseline and over spine with values ranging from 7.0 to 10.4 cm. There was no significant difference in these widths between the study populations. The implication of narrowing the lumbar spine ROI is

discussed in chapter 6. In reality, it is the attenuation of the combined fat and lean within the soft tissue baseline and over the vertebrae that is important.

There was no significant interaction in the regression gradients for difference in baseline and CB fat thickness between study populations indicating that the ROI width had a similar effect on baseline fat thickness in all populations.

7.6 Relationship between Lumbar Spine BMD Measured from Lumbar Spine Images and Fat Thickness within Soft Tissue Baseline Extracted from DXA Whole Body Images

7.6.1 Results

It is evident from figure 7.15 that for all populations there was a significant positive correlation between the fat thickness within the baseline of the lumbar spine ROI and the corrected L3+L4 BMD measured for an equivalent width ROI. Widening the ROI effectively increases the fat thickness in the baseline whilst the fat thickness over the vertebrae remains constant. The effect of this was an apparent increase in BMD of 0.070± 0.003 g/cm^2 per cm fat, 0.062± 0.004 g/cm^2 per cm fat and 0.056± 0.004 g/cm^2 per cm of fat for the OST, MRTx and FRTx groups respectively (Table 7.8, Fig. 7.15). This value can therefore be classed as the BEF of fat. Even though these values vary considerably, an ANOVA test indicated there was no significant difference in the mean BEF between study groups (p=0.288). Repeated measurement analysis on data in figures 7.15 and 6.7 showed that the interaction between the gradients for the four study populations was not significant, indicating that the gradients were not significantly different (p=0.236).

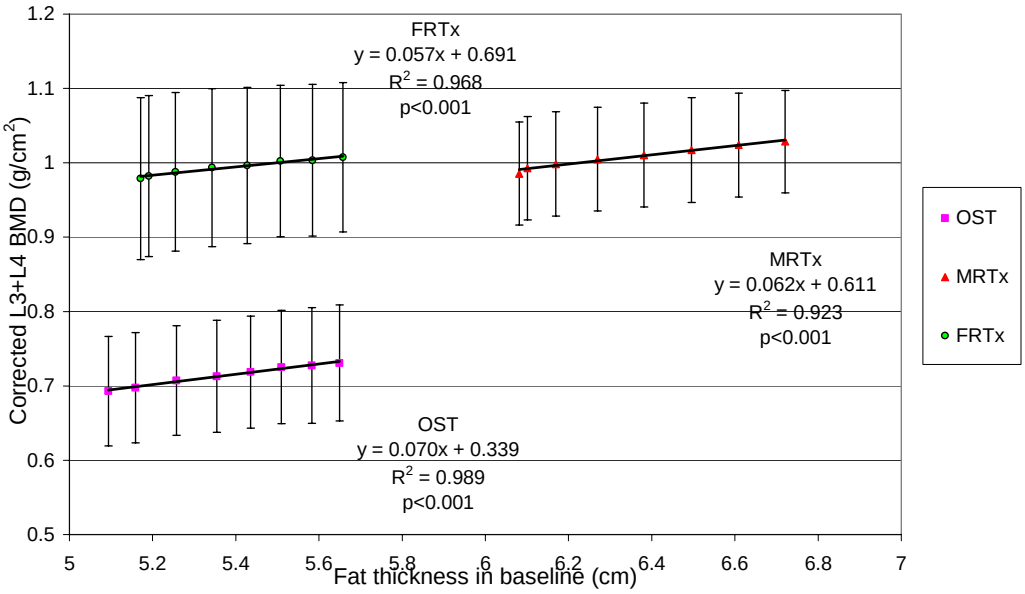

Figure 7.15 Relationship between the fat thickness within the soft tissue baseline extracted from DXA WB scans and the phantom corrected BMD for an equivalent ROI width. Each data point represents a different width of ROI. Data are for the L3+L4 level and averaged over OST, MRTx and FRTx groups. Standard error in gradient: OST=0.003 g/cm^2 per cm, MRTx=0.004 g/cm^2 per cm, FRTx=0.004 g/cm^2 per cm. SEE: OST=0.002 g/cm^2, MRTx=0.003 g/cm^2, FRTx=0.002 g/cm^2. Error bars represent 95% CI.

	BEF (g/cm^2 per cm fat) ± standard error in gradient	"True" BMD (g/cm^2)	Difference between the BMD for a particular ROI width and the true BMD for a 0.5 cm difference in fat thickness between the baseline and over the spine ± SEE (%)	Difference between BMD expected for a ROI width with an equal fat in the baseline to over the spine and that for a 11.5 cm ROI and "true" BMD (%)
IBD	0.051±0.001	0.970	2.6±0.1	1.1
OST	0.070±0.003	0.687	5.0±0.0	3.9
MRTx	0.062±0.004	0.995	3.1±0.4	1.2
FRTx	0.056±0.004	0.988	2.8±0.2	1.7

Table 7.8 Comparison of BEF, "true" BMD, and expected BMD errors with each ROI when assuming the "true" BMD is accurate and also when comparing to the BMD expected with a 11.5 cm ROI.

As expected, the mean “true BMD” for the OST group was significantly lower than that of the other groups ($p<0.001$) with no significant difference between the other groups ($p = 1.000$).

In all cases, a linear regression model suggested that the “true BMD”, or that expected when the fat thickness in baseline is equal to that over the vertebrae, is lower than the BMD measured with a standard ROI of 11.5 cm (Table 7.8, Appendix B, C, D). An ANOVA test indicated that the magnitude of this difference in BMD was significantly different between the groups ($p<0.001$). A Bonferroni post hoc test confirmed this was due to a significantly higher difference between “true BMD” and that measured with a 11.5 cm ROI for the OST population compared to the other three ($p<0.001$). There was no significant difference between the other groups.

If this BMD is the “true” BMD, the data in figure 7.16 and table 7.8 suggests that potentially errors up to 5% in L3+L4 BMD could occur for a 0.5 cm difference in fat thickness between the baseline compared to that over the spine for the OST group. There was a significant interaction between the data for each group in figure 7.16 indicating that the regression gradients were significantly different ($p<0.05$). This difference was between the OST group and other groups with no significant interaction between the regression lines for the MRTx, FRTx and IBD groups.

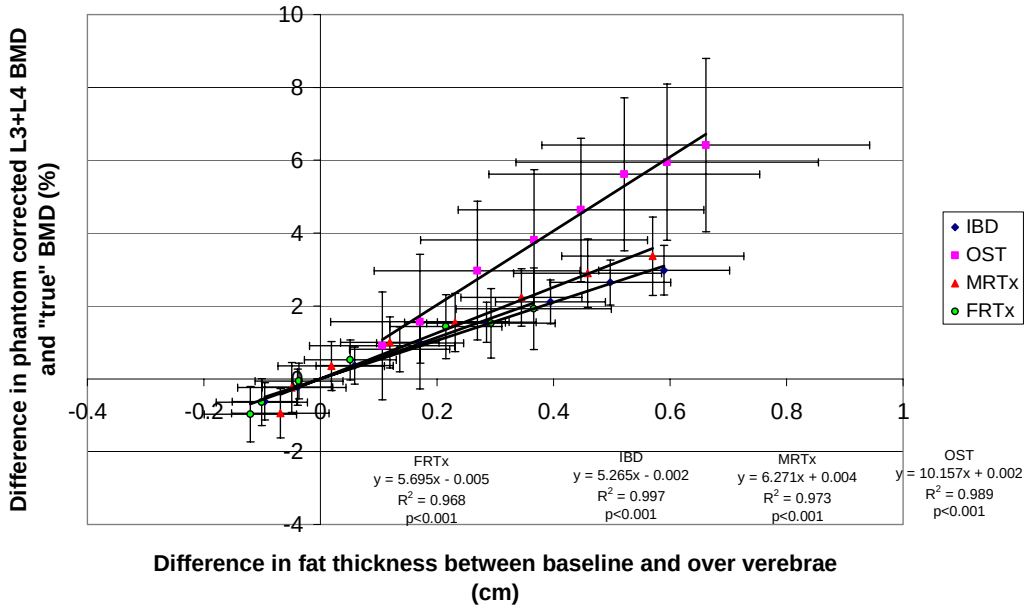

Figure 7.16 Relationship between the deviation in fat thickness in baseline with respect to that over the vertebrae and the difference in BMD reported with equivalent width ROI compared to the "true" BMD. This is assuming the "true" BMD occurs when the fat in baseline is equivalent to that over the vertebrae. ROI. Data are for the L3+L4 level and averaged over the groups of IBD, OST, MRTx and FRTx patients. Standard error in gradients: IBD = 0.13 % per cm, OST= 0.45 % per cm, MRTx=0.43 % per cm, FRTx=0.42% per cm. SEE: IBD=0.09% OST=0.24%, MRTx=0.27%, FRTx=0.21%. Error bars represent 95% CI.

The difference between fat thickness in the baseline of the largest and smallest ROI used in this work ranged from 0.5 cm (FRTx) to 0.6 cm (MRTx) (Table 7.9). These fat thickness differences translated to BME values in the range 0.024 to 0.030 g/cm^2. The difference in baseline fat thickness between the largest and smallest ROI was not significantly different as confirmed with an ANOVA test (p=0.194). Also, there was no significant difference between the four groups for the L3+L4 BMD measured with the largest and smallest ROI (p=0.108). It appears that the BME of fat measured from WB scans predicts the observed change in BMD measured directly from lumbar spine scans with a residual error of 0.01 g/cm^2. The difference in BMD measured with two widths of ROI varied by a maximum of 30% from the BME of the difference in the fat

thickness within the baseline of the equivalent ROI (Table 7.9). An ANOVA test showed that the mean difference between the observed change in L3+L4 BMD and the BME of change in baseline fat thickness was not statistically significant between the four groups (p=0.298).

	Difference in fat thickness between baseline of largest and smallest ROI (cm)	BME (g/cm^2)	Observed change in BMD from lumbar spine scans between largest and smallest ROI (g/cm^2)	Difference between observed change in BMD and BME of fat thickness in baseline (%)
IBD	0.69	0.034	0.035	-3
OST	0.56	0.028 (0.03)	0.039 (0.04)	-28
MRTx	0.64	0.030 (0.03)	0.043 (0.04)	-30
FRTx	0.49	0.024 (0.02)	0.029 (0.03)	-17

Table 7.9 Differences in fat thickness between the largest and smallest ROI used for lumbar spine analysis and the BME compared to the change in BMD observed with the equivalent width ROI. Results show that on average the observed change in BMD is 0.01 g/cm^2 higher than that predicted from fat thickness measurements.

Table 7.10 and figures 7.17 to 7.19 show that for all study populations, there was a significant positive correlation as the ROI width increased between the observed changes in phantom corrected L3+L4 BMD and the BME of fat within equivalent width ROI. An ANOVA test showed that there was no significant difference in the y-intercept between the groups. Repeated measurement analysis confirmed there was a significant interaction between the regression gradients in figures 7.17 to 7.19 and 6.10 (p=0.003) with the difference in gradients occurring between the IBD and FRTx data (p=0.001).

	Gradient (g/cm^2 per g/cm^2)	Y-intercept (g/cm^2)	R^2
IBD	1.002±0.024	-0.002±0.001	0.9972
OST	0.728±0.031	-0.001±0.001	0.9847
MRTx	0.867±0.029	-0.006±0.001	0.9945
FRTx	0.931±0.068	-0.004±0.001	0.9741

Table 7.10 Results of linear regression analysis for the relationship between the observed changes in phantom corrected L3+L4 BMD and those predicted by the BME of fat thickness within baseline of the ROI from WB scans.

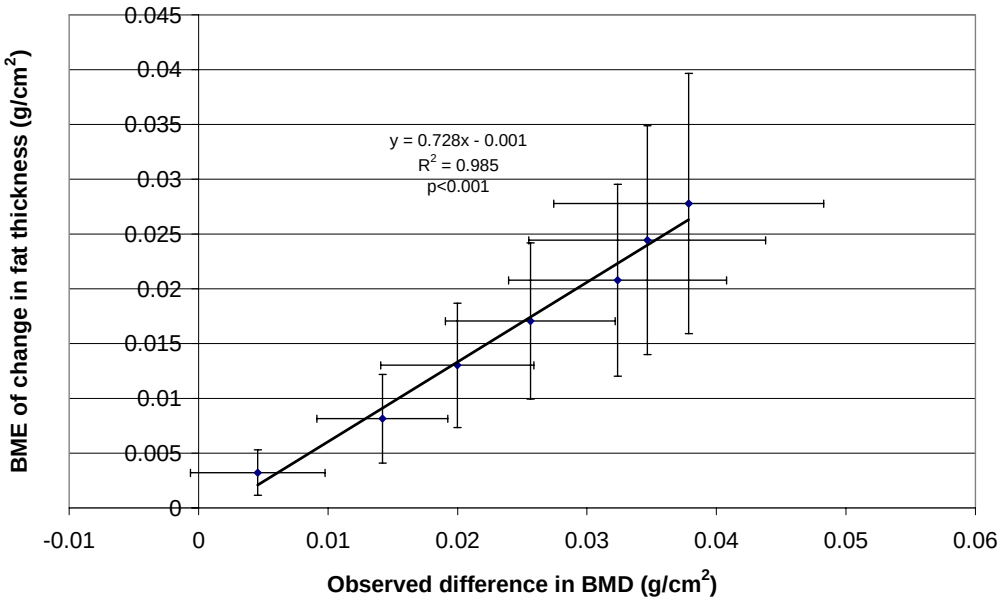

Figure 7.17 Relationship between the observed difference in phantom corrected L3+L4 BMD as the width of the ROI increased and the BME of the difference in fat thickness within the baseline of equivalent width ROI. Data are average for 10 patients with confirmed osteoporosis (OST). Standard error in gradient is 0.031 g/cm^2 per g/cm^2 and SEE is 0.001 g/cm^2. Error bars represent ±95% CI.

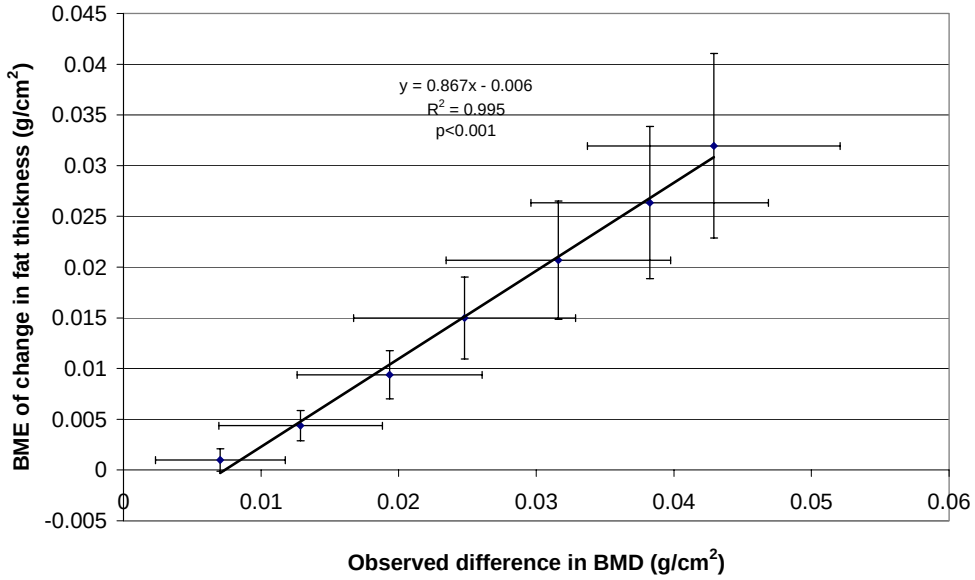

Figure 7.18 Relationship between the observed difference in phantom corrected L3+L4 BMD as the width of the ROI increased and the BME of the difference in fat thickness within the baseline of equivalent width ROI. Data are average for 20 MRTx patients 3 months post renal Tx. Standard error in gradient is 0.029 g/cm^2 per g/cm^2 and SEE = 0.001 g/cm^2. Error bars represent ±95% CI.

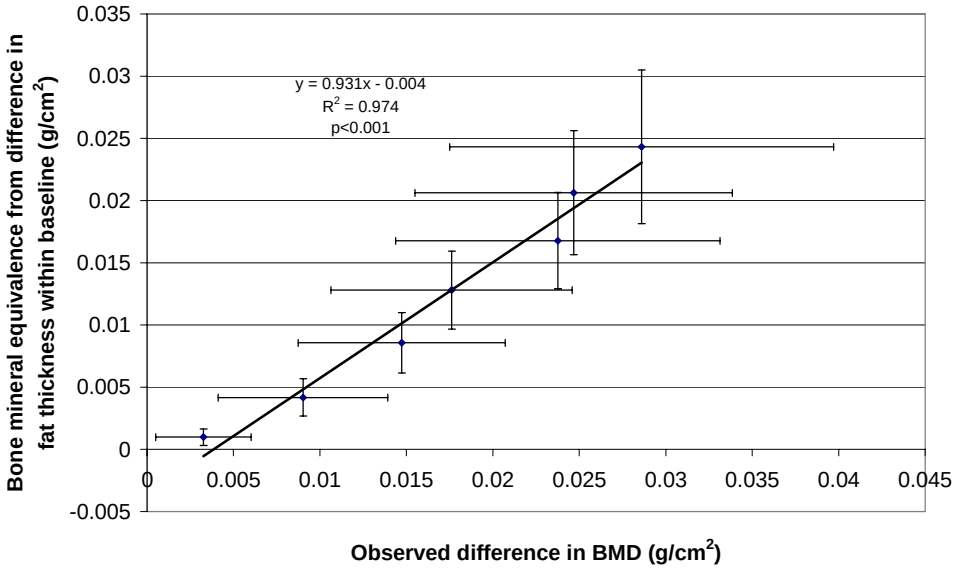

Figure 7.19 Relationship between the observed difference in phantom corrected L3+L4 BMD as the width of the ROI increased and the BME of the difference in fat thickness within the baseline of equivalent width ROI. Data are average for 20 FRTx patients approximately 3 months post renal Tx. Standard error in gradient = 0.068 g/cm^2 per g/cm^2 and SEE=0.002 g/cm^2. Error bars represent ±95% CI.

7.6.2 Discussion

The observations from the OST, MRTx and FRTx groups were generally in agreement with published results and those from the IBD group. There was a significant association between fat thickness within the baseline of the ROI and the phantom corrected L3+L4 BMD measured for an equivalent width ROI. This again supports the theory that the measurement of L3+L4 BMD is influenced by the fat thickness within the baseline of the ROI. The dependence of L3+L4 BMD on baseline fat thickness, or BEF, is similar to that measured by others and that calculated for IBD subjects in chapter 6 (0.051 ± 0.001 g/cm^2) (Table 7.8). The average BEF over all groups would be 0.060 ± 0.008 g/cm^2 of bone mineral per cm fat which is 36% higher than that measured by Hangartner and Johnston (1990) for the QDR-1000 and approximately 20% higher than measured by Tothill and Pye (1992) for the Hologic QDR-1000. This difference is likely to be due to the method used to obtain the data. The BEF derived by these investigators is based on phantom measurements whereas the value derived in this work is based on human fat. An ANOVA test proved that the difference in BEF between groups was not statistically significant ($p=0.288$). The large variation in BEF within each group is likely to be the reason for this. The bone mineral equivalence of abdominal fat should not vary between diagnostic groups and therefore it is suspected that the measurements presented in table 7.8 were influenced by lean tissue which has a higher physical density than fat. Some lean tissues may be falsely interpreted by DXA as being fatty. Even though the difference between the mean BEF for the groups was not significant, the value for the OST study group deviated most from published data and from the BEF for the IBD group. Due to the relatively large sample number, the BEF for the IBD group is statistically the most reliable and represents data from a group of subjects with a large variation in age. The OST group were significantly older and therefore likely to have a greater thickness of fat next to the spine as muscle turns to fat with increasing age. Also, as age increases and in osteoporosis the amount of fatty YM increases thereby elevating the

amount of fat in the bone region making lumbar spine BMD measurements less accurate. As the plot of BMD against baseline fat thickness was used to calculate BEF in this work, YM may influence the measurement.

The maximum difference in fat thickness between the largest and smallest ROI equated to a BME of 0.028, 0.030 and 0.024 g/cm^2 for the OST, MRTx and FRTx groups respectively, which are close to that found for the IBD group (0.034±0018 g/cm^2). Using equation 6.6, the BME convert to a decrease in T-score of 0.34, 0.28, 0.34 and 0.24 for IBD, OST, MRTx and FRTx groups respectively. Errors in T-score of this magnitude are unlikely to cause a misdiagnosis unless the patient's BMD is on the threshold between osteopaenia and osteoporosis. The data presented in this chapter is averaged over each study population and therefore caution should be taken when applying to an individual. In some patients, the non-uniform distribution of fat may cause relatively large differences in the average fat thickness in baseline of a standard width ROI and over vertebrae with the potential for significant errors in T-score.

It appears that for all the subject populations, changes in BMD measured from lumbar spine scans can be predicted from the fat thickness within the baseline of the equivalent ROI measured from WB scans with a systematic error of 0.01 g/cm^2. This systematic error is likely to be inherent in the method used to derive the data and therefore can be accounted for when using this method for other groups.

The maximum mean difference between observed and predicted BMD measurements for any one group was -30%. Although this seems high, it equates to only 0.013 g/cm^2 of bone mineral. Such a small amount will only change the T-score by 0.13. It can therefore be assumed that using the method outlined in chapters 6 and 7 to predict changes in BMD from changes in fat within the baseline measured from DXA WB scans is associated with an error of ±0.01g/cm^2 or ±0.1 T-score units. The difference in baseline fat thickness between the largest and smallest ROI was not significantly different between the four study populations. As

shown in table 7.9, the observed change in BMD was predicted most successfully from the change in fat thickness within the baseline for the IBD group and least successfully for the MRTx group. As the difference in baseline fat thickness is not significantly different for these two groups, the success of predicting a BMD change is unlikely to be related to the degree of fat inhomogeneity within lumbar spine ROI. The mean discrepancy between the observed change in BMD and the BME of change in fat thickness ranged from -3% to -30%. The large variation in this parameter for the subjects composing each group explains why the group means are not significantly different. It is therefore likely that the success of predicting the change in BMD from changes in fat thickness is better for the IBD group due to the wider variation in subjects within that group i.e. 50 compared to 10 and 20 in the other groups. Hence, it appears that it is not the diagnostic group which determines the success of the method on a group basis but the number and variability of subjects within the group. To confirm this statistically, additional subjects are required in the OST group as it appears the model works least successfully for older patients and those with a low BMD. This was not possible during the current study due to the lack of osteoporotic patients who had a WB scan as well as the routine spine and hip scans.

The success of the model for predicting changes in observed BMD using the BME from WB scan data were quantified using the regression model fitted to the data as shown in figures 7.17 to 7.19. A perfect model gives a regression gradient of 1 and y-intercept of 0. The y-intercept was close to 0 in all cases and not significantly different between groups (Table 7.10). A Bonferroni post hoc test only showed a significant difference between the mean gradient for the IBD group and the FRTx group ($p<0.001$). This result was unexpected based on the mean values for the gradients but is possibly due to the large variation in the gradients within the FRTx group. Repeated measurement analysis did not show a significant interaction between the gradients for the OST group and the other three study populations which adds strength to the argument that the success of the method is not related to diagnostic group.

If the error associated with predicting changes in BMD from BME is taken to be the standard error in the gradient for the regression line, the errors in predicted BMD would be ±0.024 g/cm^2, ±0.031 g/cm^2, ±0.029 g/cm^2 and ±0.068 g/cm^2 for the IBD, OST, MRTx and FRTx groups respectively. Accounting for the errors, the observed and predicted BMD values are close for all groups. Factors that may influence the success of method include the magnitude of BMD changes observed from lumbar spine measurements as ROI width increases and the relative differences between fat in baseline and over spine. Both these factors were investigated and there did not appear to be an association in either case.

As discussed previously, when the fat thickness in the baseline is greater than that over the spine, DXA BMD measurements are likely to be over estimated and vice versa. To test this theory, the BMD in each ROI was compared to the BMD expected when the fat is uniformly distributed across the ROI which is assumed to be the "true" BMD. For the OST group, the BMD was always overestimated compared to the "true" value which is plausible as the fat in baseline was always greater than over spine. With the MRTx and FRTx groups, the smallest ROI underestimated the BMD as expected when the fat thickness in the baseline was less than over the spine. For the other ROI the fat thickness was greater in the baseline and the BMD was overestimated in relation to the "true" value.

When attempting to estimate errors in lumbar spine BMD it is important that the research is carried out on study populations that are representative of the general population attending for BMD assessment. The MRTx and FRTx patients used in this work were in the recovery stage post Tx and therefore are unlikely to be reflective of the majority of DXA patients. The OST group has a significantly lower mean BMD and a higher average age and therefore would represent a large proportion of the patients seen in a bone densitometry centre. The IBD group is the largest group and hence likely to be most representative of the general population as subjects cover a large age range and, for the majority of

subjects, the BMD measured at the time of their scan was within the normal range. The mean BMD of the IBD groups was not significantly different to that for the MRTx and FRTx groups. The limitation with this group is that the subjects are all female but a large proportion of DXA patients are female. The four groups chosen are quite diverse and therefore the subjects that compose them should cover the BMD and body composition spectrum seen in the general population.

The IBD group contained a relatively large number of subjects but it is acknowledged that the other groups were composed of small numbers due to the lack of data from subjects who had undergone a WB scan as well as the standard spine scan. The majority of published work investigating accuracy errors in BMD due to fat thickness also have a small study population e.g. Svendsen *et al*. (1995) used 14 cadavers and Tothill and Pye (1992) used 20 subjects to investigate the impact of soft tissue on accuracy errors.

Whilst this work has highlighted the magnitude of potential errors in BMD due to the non-uniform distribution of fat, the ultimate aim is to use the data presented in this thesis in clinical practice. The limitations of the proposed method to predict changes in BMD from the fat thickness in the baseline are discussed in chapter 6. Up to this point all the data are averaged over numerous subjects and therefore the model will be tested on an individual basis in chapter 8.

7.7 Conclusions

When repeating the data analysis performed on IBD subjects in chapters 4,5, and 6, the same conclusions can be reached. In summary, the increase in BMD as ROI width increases appears to be the result of an increase in the fat thickness in baseline relative to that over the vertebrae. Despite the large variation in the BEF for abdominal fat between the groups, the difference was not statistically significant. Applying the model developed on IBD subjects to three other subject populations has shown

it is possible to predict changes in L3+L4 lumbar spine BMD from DXA WB fat thickness measurements to within 0.01 g/cm^2. Even though it appears the method is not so successful in the OST group, statistically the method works equally well in the other three subject populations. It appears that the success of the method on a group level is due to the number and variability of subjects within that group and not the medical condition of the diagnostic group. Data for additional subjects needs be gathered for the OST group to investigate this further.

Chapter 8

Quantification of the Fat Thickness within the DXA Lumbar Spine ROI from DXA WB images and the Relationship to the Measured Lumbar Spine BMD for Individual Subjects

8.1 Introduction

It was suggested in previous chapters that changes in lumbar spine BMD can be predicted by measuring the fat thickness within the region corresponding to the lumbar spine baseline from DXA whole body (WB) scans. The results presented in chapter 7 show that the proposed method works with varying success in four subject groups when the data is averaged over the study population. To use this method in clinical practice, the errors in BMD must be predicted for individual patients.

The aims of this chapter are to investigate for each individual:

- The dependence of L3+L4 BMD and baseline fat thickness on ROI width.
- The bone mineral equivalence of abdominal fat (BEF).
- Accuracy of predicting changes in L3+L4 BMD from changes in fat thickness within the soft tissue baseline of lumbar spine ROI using WB images.
- Factors that determine the success of the model to predict lumbar spine BMD from baseline fat thickness.

8.2 Methods

Lumbar spine and WB images for each subject within the IBD, OST, MRTx, and FRTx groups were analysed with the methods outlined in chapters 4 to 6 and summarised in figure 7.1. In total there were 100 subjects.

In summary, for each subject:

- The phantom corrected L3+L4 BMD from lumbar spine scans was plotted against ROI width.
- The fat thickness within the baseline corresponding to L3+L4 BMD measurements estimated from WB scans was plotted against ROI width.
- The corrected L3+L4 BMD was plotted against the fat thickness within the corresponding baseline from WB scans. From these graphs the BEF was calculated for each individual.

Each data set mentioned above was fitted to a linear regression model using SPSS and the strength of the association between parameters tested using the Pearson's correlation coefficient. A p-value <0.05 defined statistical significance. The linear regression gradients reflected the dependence of BMD or fat thickness on the ROI width and also the dependence of BMD on fat thickness within the baseline.

The difference between the phantom corrected L3+L4 BMD measured with each ROI width and the smallest ROI was compared with the BME of the difference in fat thickness within the baseline for the corresponding width ROI. Linear regression analysis was performed on this data to examine how accurately changes in BMD can be predicted from changes in fat thickness within the baseline. A p-value <0.05 indicated a statistically significant association. The model was considered most successful when the gradient was close to 1 and the y-intercept 0. For each subject, the gradient of the regression model linking observed changes in BMD as the ROI increased and the BME of changes in fat

thickness was plotted against (1) gradient of BMD vs width, (2) gradient of fat thickness in baseline vs width and (3) the BEF derived from observed changes in BMD and fat thickness measured from WB scans.

The fat thickness profiles were plotted for five subjects where the observed change in BMD was successfully predicted by the BME of the fat thickness within the baseline with a gradient between 0.8 and 1.2. Also plotted were fat thickness profiles for five subjects where the model was less successful with a gradient greater than 2 or less than 0.2. Data were only shown for a selection of subjects but similar trends were seen across the 100 subjects.

8.3 Results

In general there was an increase in L3+L4 BMD as the ROI width increased. However, as shown in figure 8.1, there was a wide range of gradients ranging from -0.007 g/cm^2 to 0.015 g/cm^2 per cm. The gradient of the regression line was significantly different to 0 ($p<0.05$) in 91 out of 100 cases. The correlation between BMD and ROI width was significant in 91 out of 100 cases ($p<0.05$).

As can be seen from figure 8.2, in all but 2 cases the fat thickness in regions equivalent to the lumbar spine soft tissue baseline increased as the ROI width increased. The gradient of the regression model varied considerably from -0.04 to 0.25 cm fat per cm. The regression line was significantly different to ($p<0.01$) in 96 out of 100 cases and there was a significant correlation ($p<0.01$) between the fat thickness in baseline and ROI width for 96 out of 100 subjects.

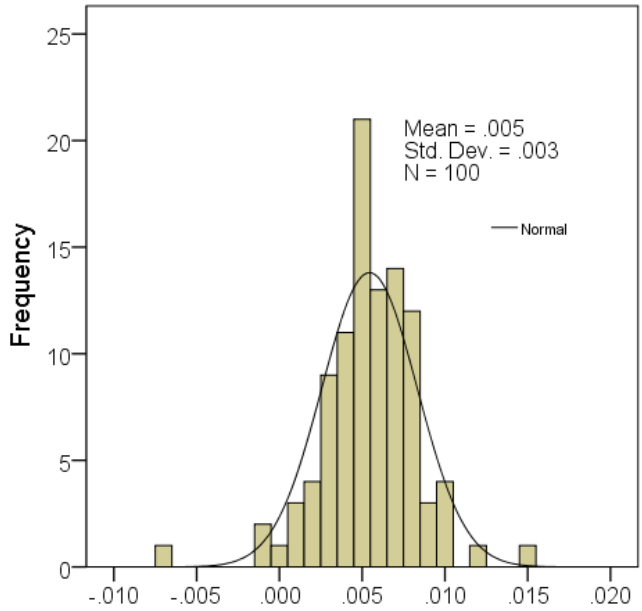

Gradient of linear regression line for BMD changes with ROI width (g/cm^2 cm^{-1})

Figure 8.1 Range of linear regression gradients for changes in corrected L3+L4 BMD with lumbar spine ROI width for 100 subjects from the IBD, OST, MRTx, and FRTx groups.

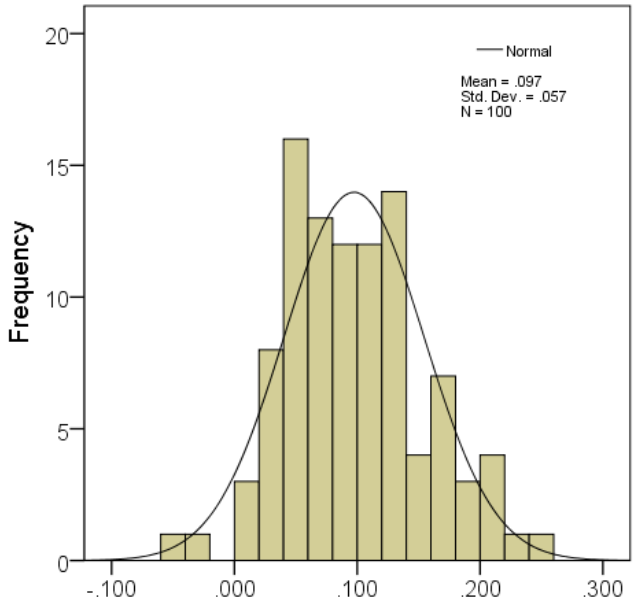

Gradient of changes in fat thickness in baseline with ROI width (cm/cm)

Figure 8.2 Range of linear regression gradients for changes in fat thickness within baseline of lumbar spine ROI with ROI width for 100 subjects from the IBD, OST, MRTx, and FRTx groups. Results show the gradient ± standard error in gradient.

Figure 8.3 shows there was a large variation in the difference between the average fat thickness in a baseline of 11.5 cm ROI width and that assumed to be over the spine. In 22% of individuals was the fat thickness in the baseline equal to that estimated to be over the spine and in 68% of cases there was a greater thickness of fat adjacent to the spine than over the spine.

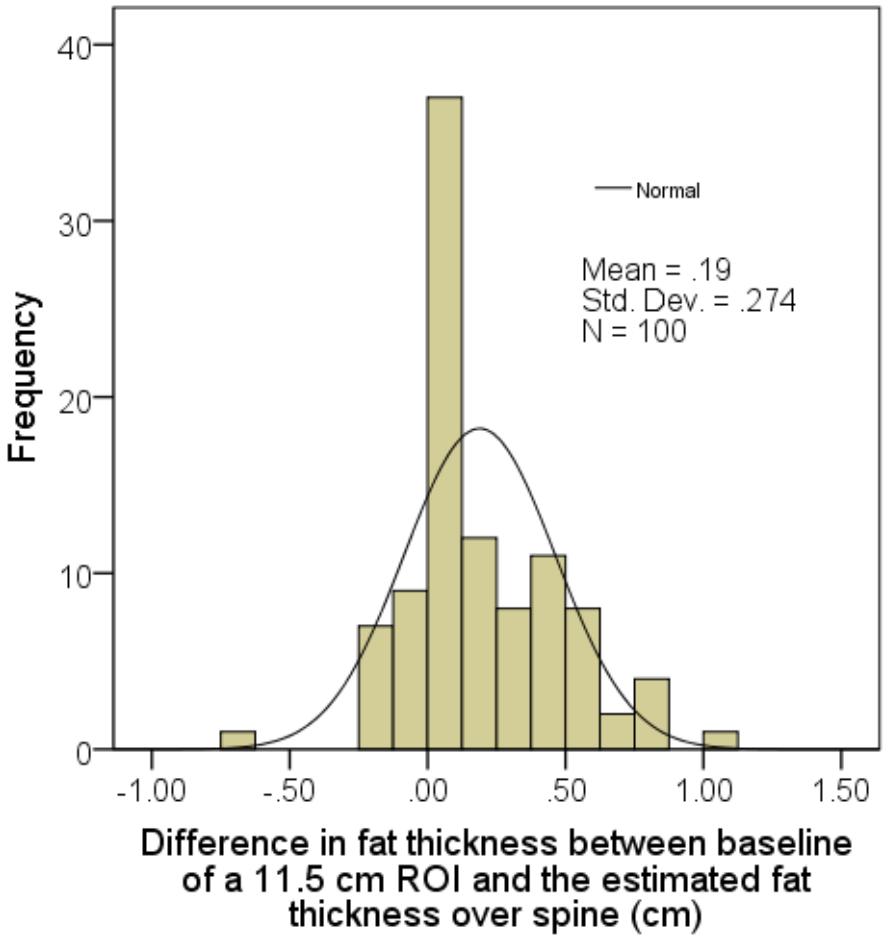

Figure 8.3 Range of difference between fat thickness in baseline of a 11.5 cm ROI and that assumed to be over the spine for 100 individual subjects.

There was a significant linear relationship ($p<0.05$) between L3+L4 BMD and fat thickness in the baseline in 84 out of 100 cases. The relationship between the magnitude of change in corrected L3+L4 BMD and the fat

thickness within the baseline was significant ($p<0.001$). Hence, the greater the change in fat thickness as the ROI width increases, the larger is the change in measured BMD. There was no significant relationship between the difference in BMD between the largest and smallest ROI and the BME of the difference in fat thickness between the largest and smallest ROI.

The gradient of the regression model linking the phantom corrected L3+L4 BMD and fat thickness within the baseline showed that the BEF of abdominal fat varied considerably from -0.059 g/cm^2 per cm fat to 0.395 g/cm^2 per cm fat as shown in figure 8.4. The average (±SD) BEF was 0.068 ± 0.051 g/cm^2 per cm fat.

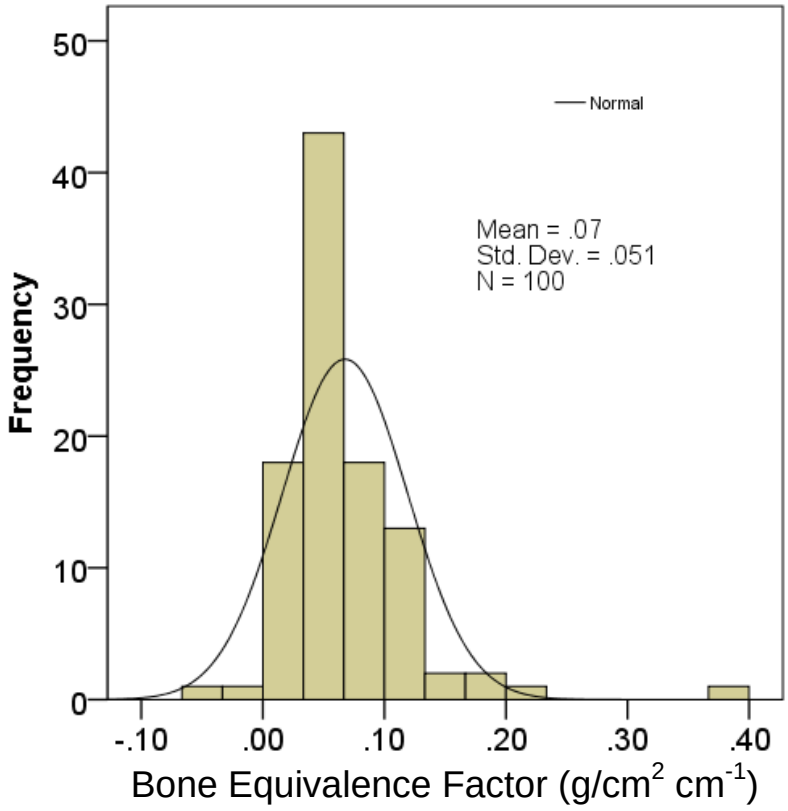

Figure 8.4 Gradient of regression model for changes in corrected L3+L4 BMD measured from lumbar spine DXA scans and the fat thickness in an equivalent baseline measured from DXA WB scans for IBD, MRTx, FRTx and OST subjects. The gradient represents the bone equivalence factor of abdominal fat.

For the largest (15.0 cm) and smallest (8.3 cm) ROI used in this work, the BME of the difference in fat thickness within the baseline predicted the difference in phantom corrected BMD measured with the equivalent width ROI with an accuracy ranging from -0.080 to 0.063 g/cm^2 with an average of 0.017±0.023 g/cm^2. The degree of variability between subjects is shown in figure 8.5.

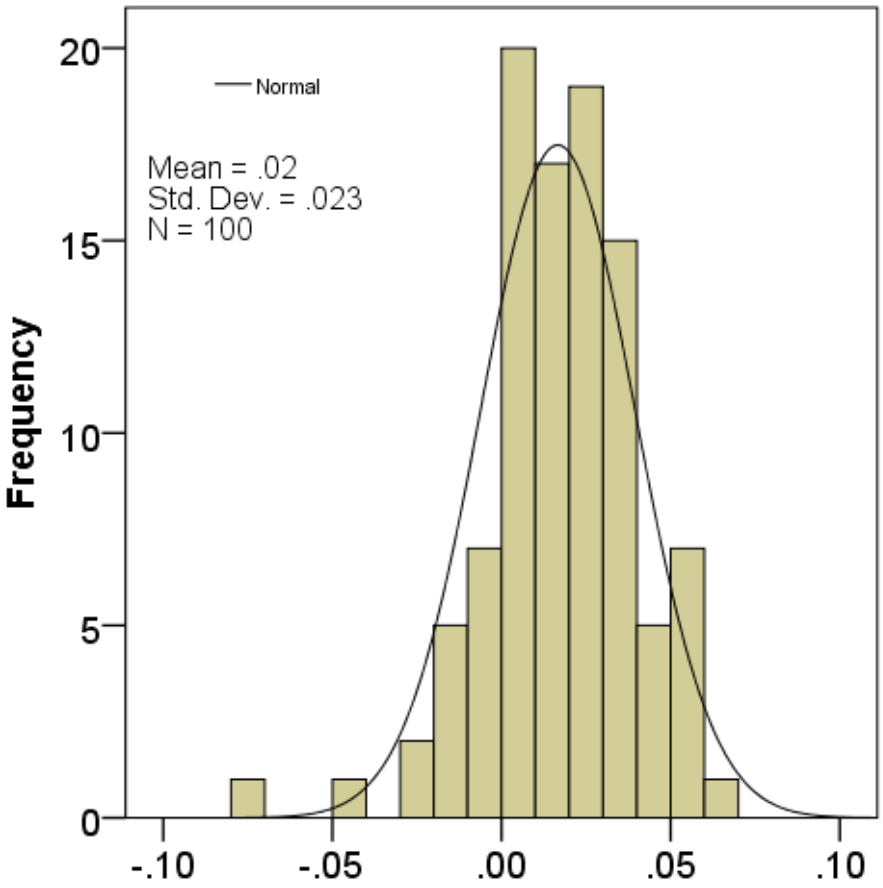

Figure 8.5 Range of values for difference between the measured phantom corrected L3+L4 BMD for largest and smallest ROI and the BME of the difference in fat thickness within the baseline of the largest and smallest ROI for 100 subjects.

The model used to predict changes in phantom corrected L3+L4 BMD from the fat thickness within the baseline was classed as successful when the gradient of the regression line linking the observed BMD and BME was 1 and y-intercept 0. For the 100 subjects, the gradient varied from -0.777 to 2.589 as shown in figure 8.6. The gradient was significantly different to 0 and the correlation significant in 89 of 100 instances ($p<0.05$).

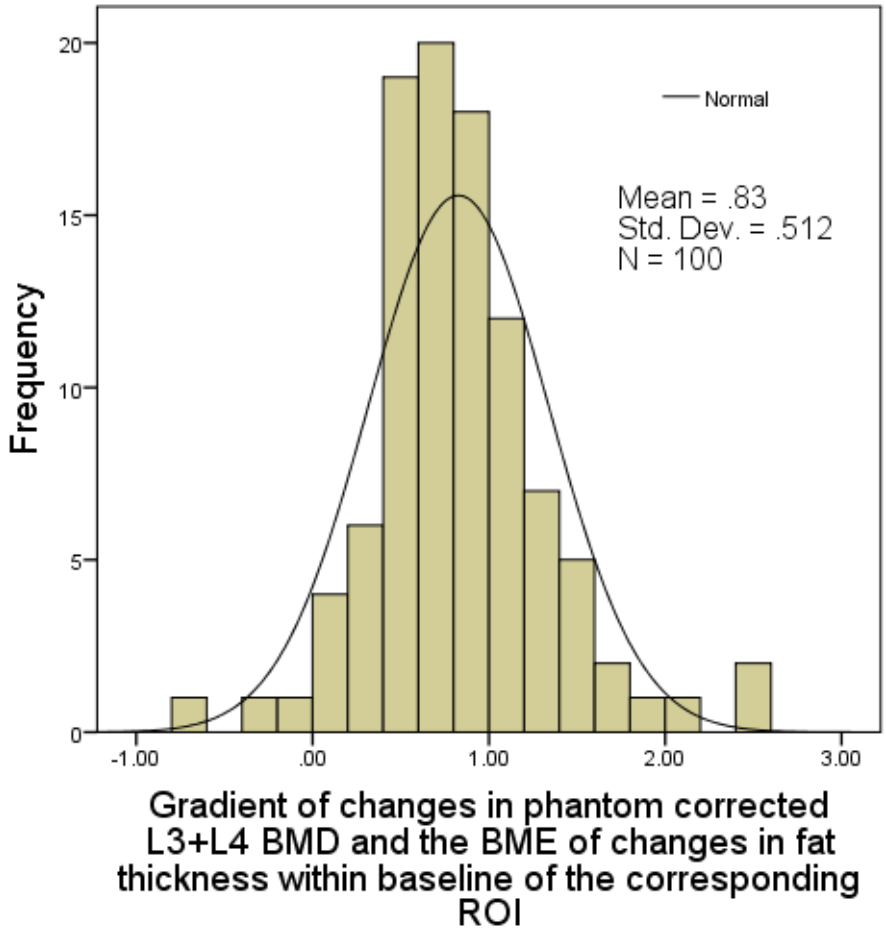

Figure 8.6 Range of regression line gradients for difference in measured phantom corrected L3+L4 BMD and the BME of fat thickness within baseline.

The y-intercept was within ±0.01 g/cm^2 of 0 for 85 out of 100 subjects. The gradient of the regression model to predict changes in BMD from changes in fat thickness did not appear to be linked to the magnitude of change in corrected L3+L4 BMD as ROI increased or the actual BMD measured with a 11.5 cm ROI.

Figure 8.7a implies that in the majority of cases where there was a strong positive correlation between observed changes in BMD and those predicted by the BME of fat thickness within the baseline, there was a stronger correlation between the corrected L3+L4 BMD and the baseline fat thickness. The outliers appear to occur when the relationship between BMD and fat thickness within the baseline is not significant. Also a negative relationship between BMD and fat thickness gave a negative relationship between the observed BMD changes and BME. On removing the outliers in figure 8.7a, the regression equation became y=1.0797x-0.0759 (R^2=0.8463). The data without outliers is shown in figure 8.7b together with the regression line and its 95% CI. The relationship between BMD and fat thickness was confirmed when scrutinising individual plots and examples for two individuals are given in figure 8.8 to 8.10.

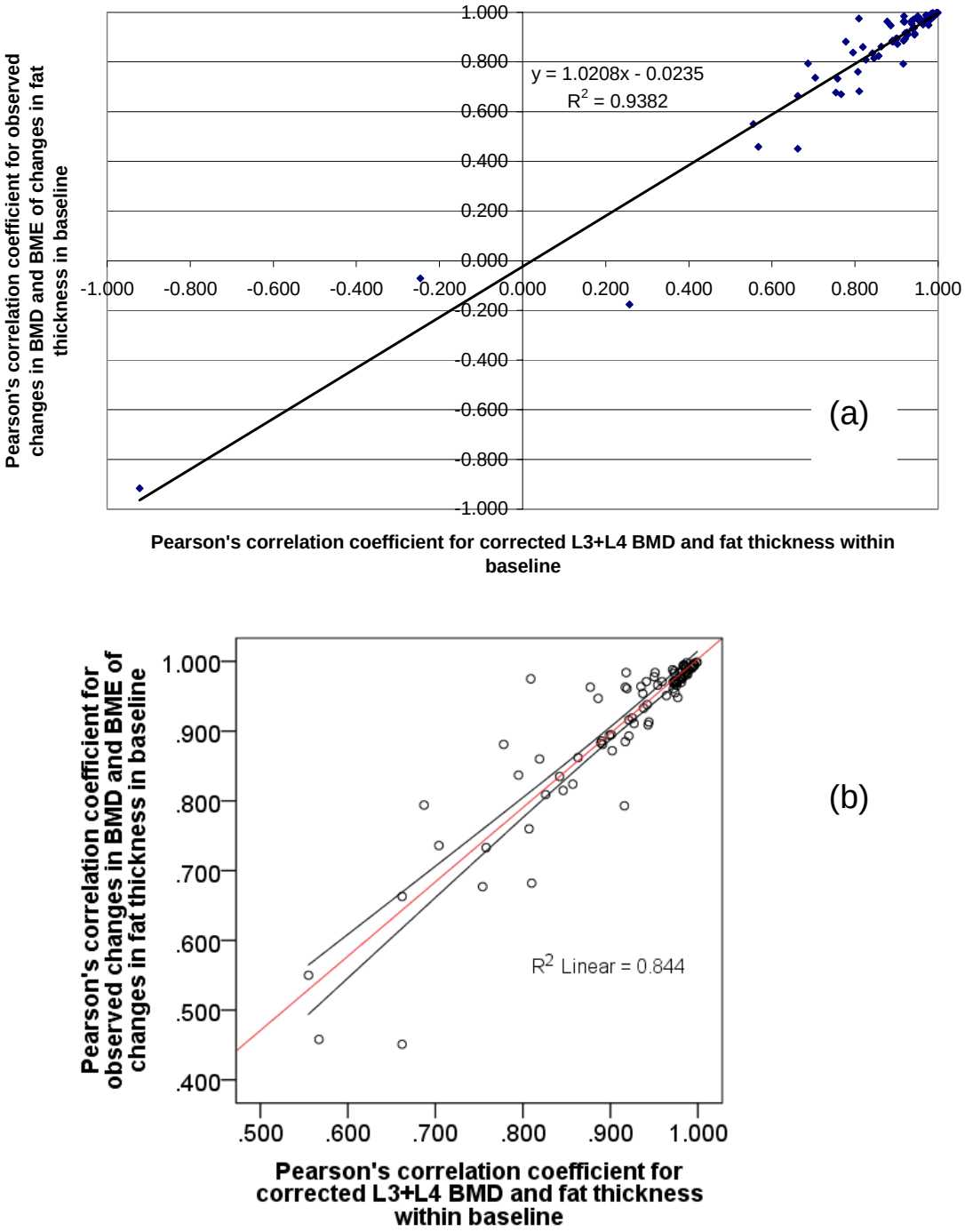

Figure 8.7 Relationship between Pearson's correlation coefficient for changes in corrected L3+L4 BMD and fat thickness in baseline and the Pearson's correlation coefficient for observed changes in BMD and BME of changes in fat thickness in baseline as ROI width increases. Data indicates that a stronger correlation between reported BMD and fat thickness results in a more linear relationship from which BMD can be predicted from fat in baseline. Data in (a) were re-plotted in (b) removing the outliers and showing the 95% CI of the line.

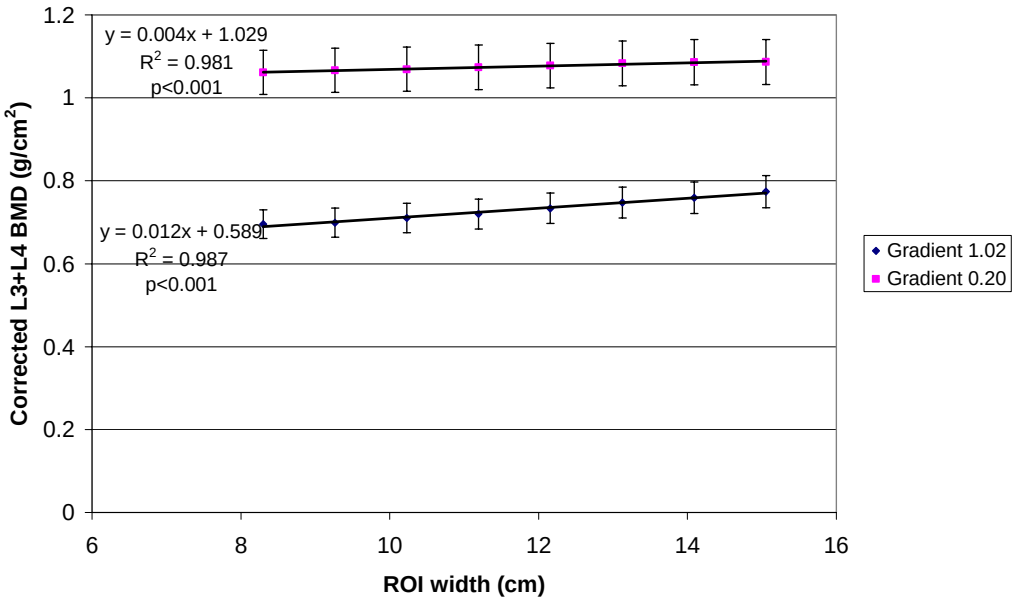

Figure 8.8 Relationship between the corrected L3+L4 BMD and the ROI width for a case where the model to predict changes in BMD from fat thickness in baseline is successful (gradient 1.02) and for a case where the model was less successful (gradient 0.2). Error bars are 95% CI.

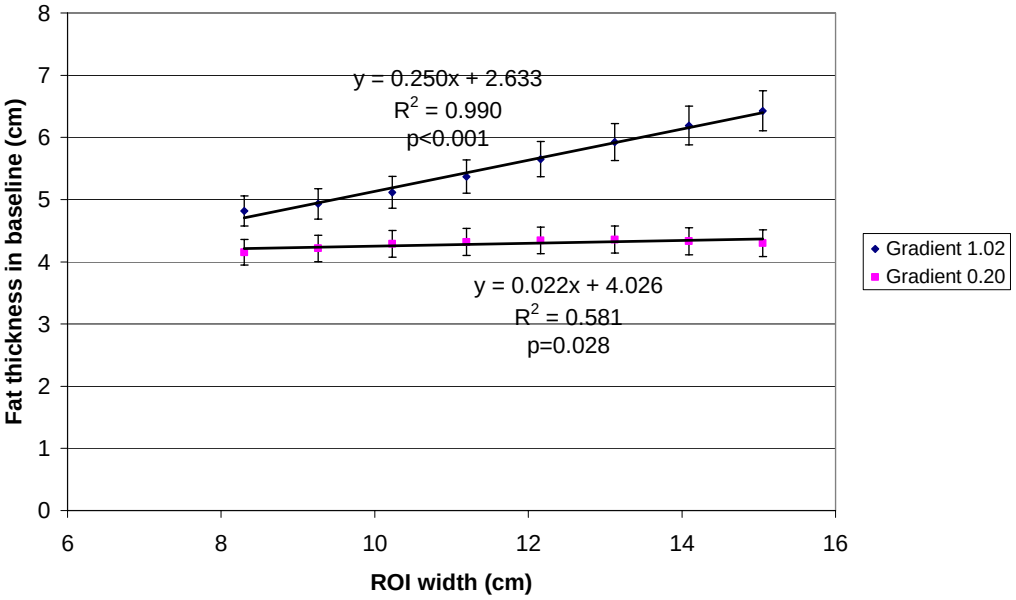

Figure 8.9 Relationship between the fat thickness within the baseline and the ROI width for a case where the model to predict changes in BMD from fat thickness in baseline is successful (gradient 1.02) and for a case where the model was less successful (gradient 0.2). Error bars are the 95% CI.

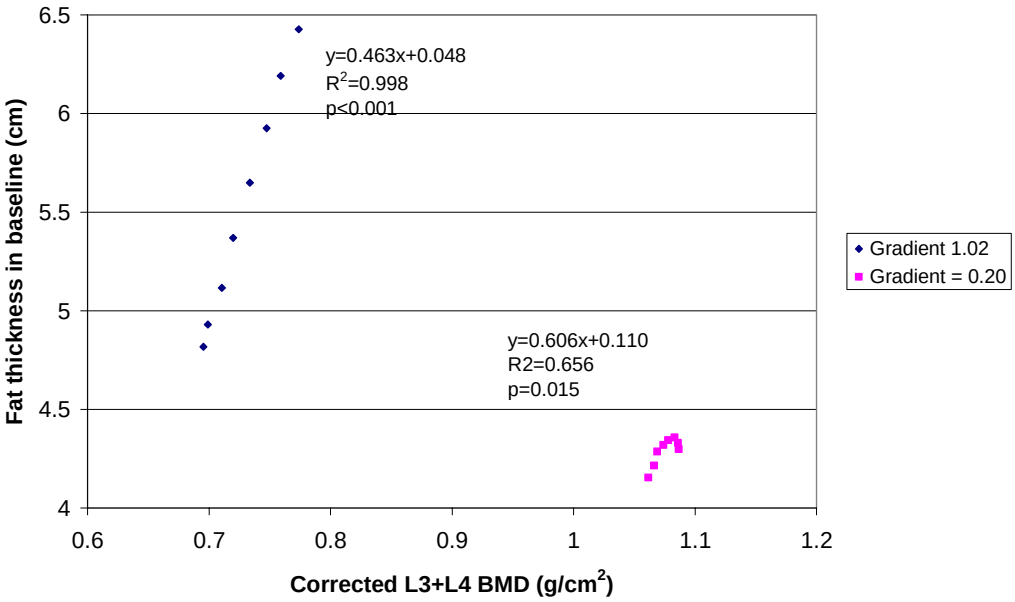

Figure 8.10 Relationship between the corrected L3+L4 measured BMD and the fat thickness within the baseline for a case where the model to predict changes in BMD from fat thickness in baseline is successful (gradient 1.2) and for a case where the model was less successful (gradient 0.2). Error bars were not displayed to enable expansion of the y-axis to demonstrate the differences in trend of the graphs.

Figure 8.11 suggests that the success of the method to predict changes in BMD from the BME of changes in fat thickness within the baseline appears to be linked with the BEF of abdominal fat. On removing the outliers from figure 8.11a and fitting an exponential model to the data (fig. 8.11b), the regression gradient linking observed changes in BMD and the BME of fat thickness was 1 when the BEF was 0.05 g/cm^2 per cm fat. This was close to the value used to convert the fat thickness into BME.

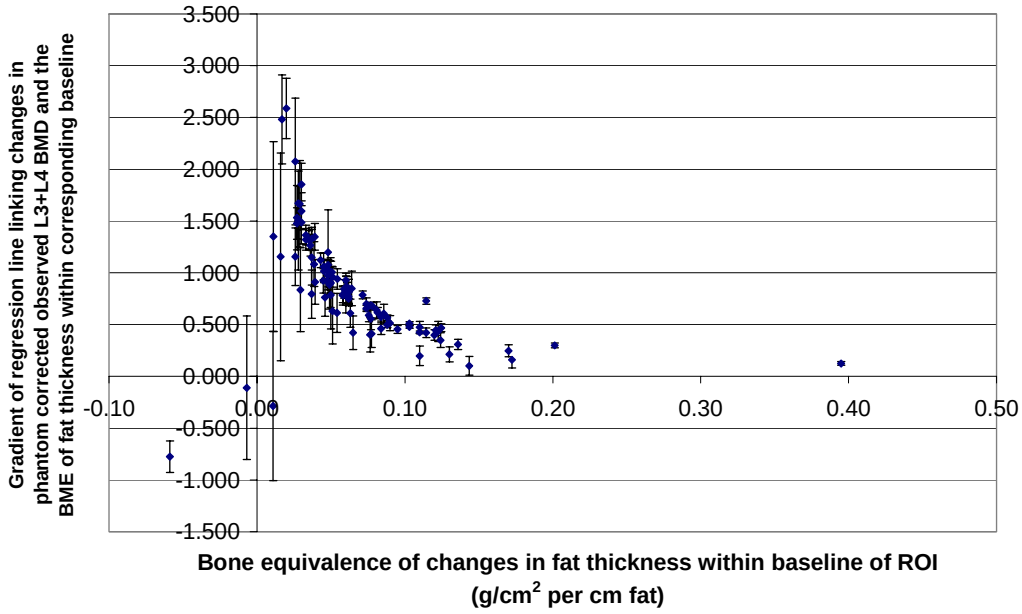

(a)

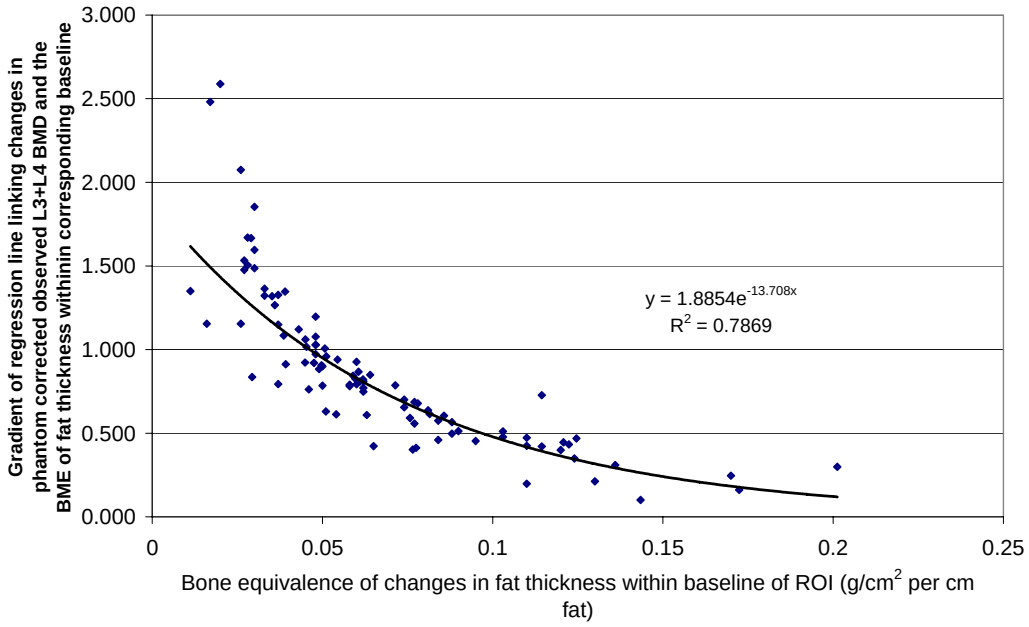

(b)

Figure 8.11 Relationship between bone equivalence of fat measured from DXA whole body scans and the gradient of the regression model linking the observed change in corrected L3+L4 BMD and the BME of changes in fat thickness within baseline. For perfect model where gradient is 1 then BEF would be approximately 0.05 g/cm^2 per cm fat.

The fat profiles from 5 subjects where the BME of the fat within the baseline appeared to predict the observed change in measured BMD well with a regression line gradient within 0.1 of 1 are shown in figure 8.12.

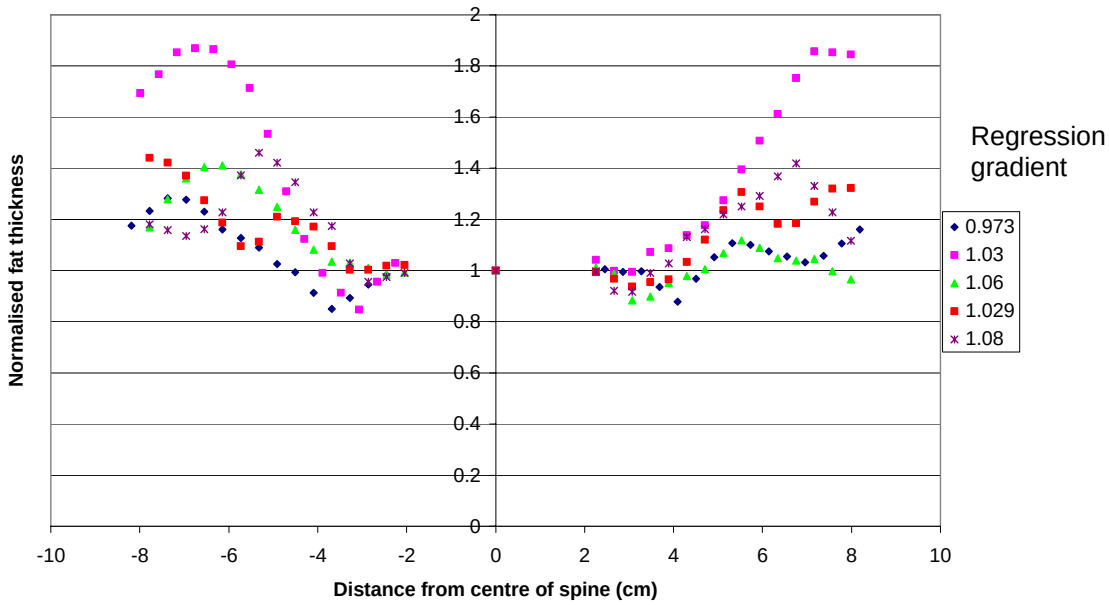

Figure 8.12 Abdominal fat profiles derived from WB data where the gradient of the regression line linking the observed change in lumbar spine BMD and that predicted from the fat in the baseline was between 0.9 and 1.1. Data normalised to CB fat thickness.

Figure 8.13a shows profiles from subjects where the model was less successful and the linear regression gradient less than 0.2 whereas figure 8.13b shows fat profiles for three subjects where the gradient was greater than two. These results suggest the greater the inhomogeneity in the fat thickness and the more symmetrical the profiles changes in BMD can be predicted more accurately from fat in baseline.

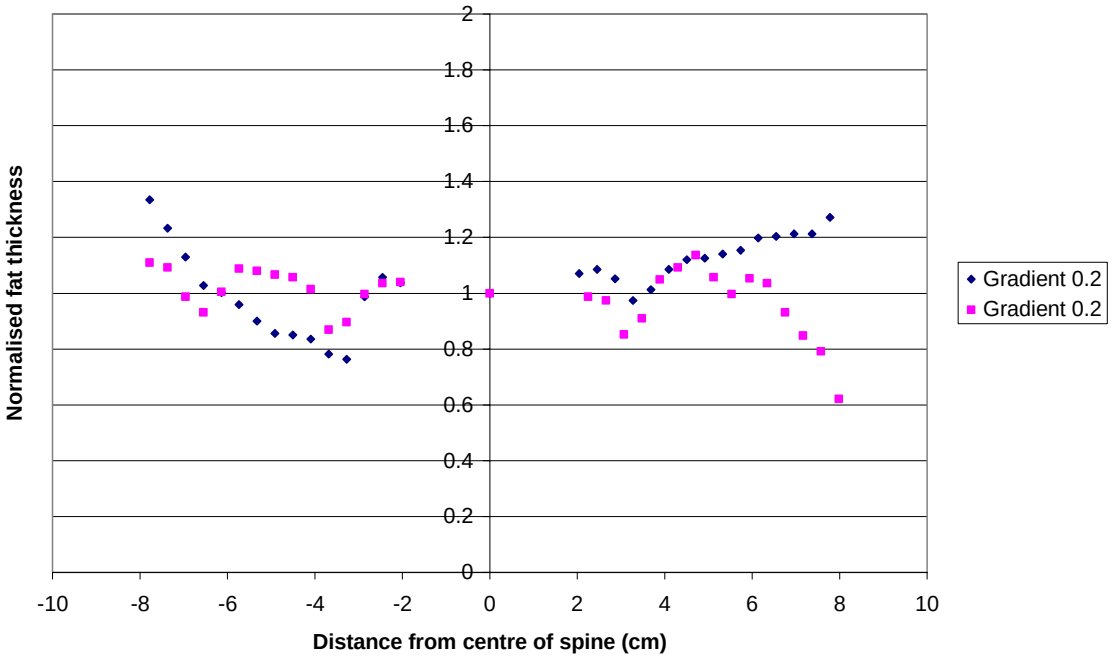

Figure 8.13a Abdominal fat profiles derived from WB data where the gradient of the regression line linking the observed change in lumbar spine BMD and that predicted from the fat in the baseline was less than 0.2.

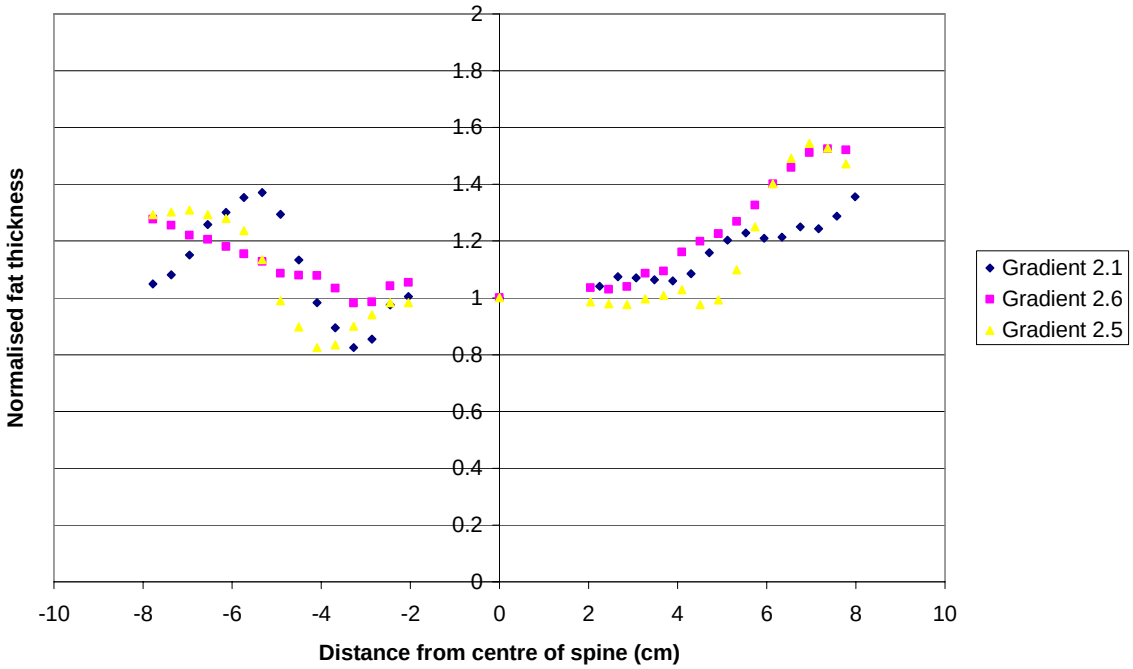

Figure 8.13b Abdominal fat profiles derived from WB data where the gradient of the regression line linking the observed change in lumbar spine BMD and that predicted from the fat in the baseline was greater than 2.

8.4 Discussion

Performing the lumbar spine and WB analysis described in previous chapters on individuals has highlighted the large variability in abdominal fat thickness and distribution within the general population. In general, the results are in accord with those seen when averaging BMD and fat thickness over the four study populations with an apparent increase in L3+L4 BMD and fat thickness within the baseline as the width of the lumbar spine ROI increases (Figs 8.1 and 8.2). In 91% of subjects the gradient of the regression line linking L3+L4 BMD and ROI width was significantly different to 0 and for baseline fat thickness and ROI width this was 96%. The magnitude of this dependence of BMD and fat thickness on ROI width varied considerably between the subjects. The results presented here provide further evidence to support the theory that the increase in corrected L3+L4 BMD is due to an increase in fat thickness within the baseline relative to that over the lumbar spine (Fig. 8.4).

Throughout this work, 11.5 cm was chosen as the standard ROI width as this is within the range generally used in clinical practice. Of concern in the current work is the difference between the fat thickness in the baseline of the ROI and that in soft tissue over the vertebrae. Whilst the absolute values vary considerably, there was a greater fat thickness in the baseline soft tissue in 68% subjects for a 11.5 cm ROI. As has been discussed previously, a greater thickness of fat within the baseline compared to over the spine can cause the BMD to be overestimated. A large deviation in abdominal fat thickness measurements within study populations has also been shown by others, as reflected in large standard deviations in measurements. One example is the difference in fat thickness in baseline compared to that over the vertebrae in men for the L2 to L4 level quoted by Tothill and Pye (1992) i.e. 6.7±8.1 mm. It has been suggested by others that interpreting changes in BMD due to changes in body composition on an individual basis is difficult due to the large variability within a group of subjects (Yu *et al.* 2012).

To investigate the implication of the inhomogeneity in fat distribution throughout the lumbar spine scan ROI, the largest difference between the fat thickness in baseline of a 11.5 cm ROI and over the spine was 1.1 cm. Using the Tothill and Pye (1992) BEF this equates to a BME of 0.055 g/cm^2 and a T-score difference of -0.6. In contrast, the smallest difference was 0 cm. For 91% of subjects the difference is within ± 0.5 cm translating into a T-score of ±0.3. For 51% of subjects the difference is less than ±0.1 cm giving a potential error in T-score of ±0.1. These observations imply that, in many patients, the inhomogeneity in fat over and adjacent to spine within a ROI of 11.5 cm is unlikely to have a major impact on T-score and therefore on the clinical diagnosis of osteoporosis based on the WHO criteria.

It should be stressed that the measurement of fat thickness over the vertebrae used in this work is an estimate based on the attenuation of soft tissue immediately adjacent to the vertebrae and therefore may not be accurate. The actual attenuation of the dual-energy X-ray beams in the region of the vertebrae will be affected by yellow, or fatty, bone marrow. Hence, for an equal fat thickness within the soft tissue over bone and in a region adjacent to bone, there will potentially be a greater total fat thickness attenuating the X-ray beams in the bone region than reflected in CB measurement used in this work. The consequence of this will be an error in the value used to represent the difference between baseline fat thickness and the fat thickness over the vertebrae.

The bone equivalence of the abdominal fat, the BEF, calculated for individuals from the linear regression model linking measured BMD and baseline fat thickness, varied from the average value of 0.068±0.051 g/cm^2 per cm by -13% to 484% showing that one value would not apply to all patients. In forming reference ranges related to clinical measurements, an average over a population is usually taken. If this was the case for the BEF, the current findings indicate that potentially large errors could be introduced due to the variability amongst individuals. The BEF for the grouped data was in agreement with the average for the individuals with

0.051±0.001 g/cm^2 per cm, 0.070±0.003 g/cm^2 per cm, 0.062±0.004 g/cm^2 per cm and 0.056±0.004 g/cm^2 per cm for the IBD, MRTx, FRTx, and OST groups respectively. The average over all groups was 0.060±0.008 g/cm^2 (Fig. 8.14). It was shown in chapter 7 that the difference between mean BEF for each group (p=0.288) and between any combination of two groups was not statistically significant. When looking at 100 sets of data for individuals, there was no significant difference between the average BEF and that for the average of each group due to the large variability in BEF between subjects (p=1.000). It is suspected that the measurements of fat thickness are influenced by lean tissue which has a higher physical density than fat. Due to the relatively large sample number, the BEF for the IBD group is statistically the most reliable and represents data from subjects with a relatively large variation in age. As shown in figures 5.6 and 5.8, there are a variety of structures within the abdomen in the region of L3 and L4, for example muscle and the intestines. The tissue density and composition of each of these structures differ from these of abdominal fat and may vary slightly between individuals. It is probable that there are a variety of tissues other than pure fat in the small STB placed next to the spine. Some lean tissues may be interpreted by DXA as being fatty. As it is the DXA FM data within the STB that are used to derive the BEF, there may be an inaccuracy in this value. The position of organs within the abdomen may vary slightly relative to the spine between individuals and therefore the variation in tissues included in the STB may vary thereby affecting the BEF.

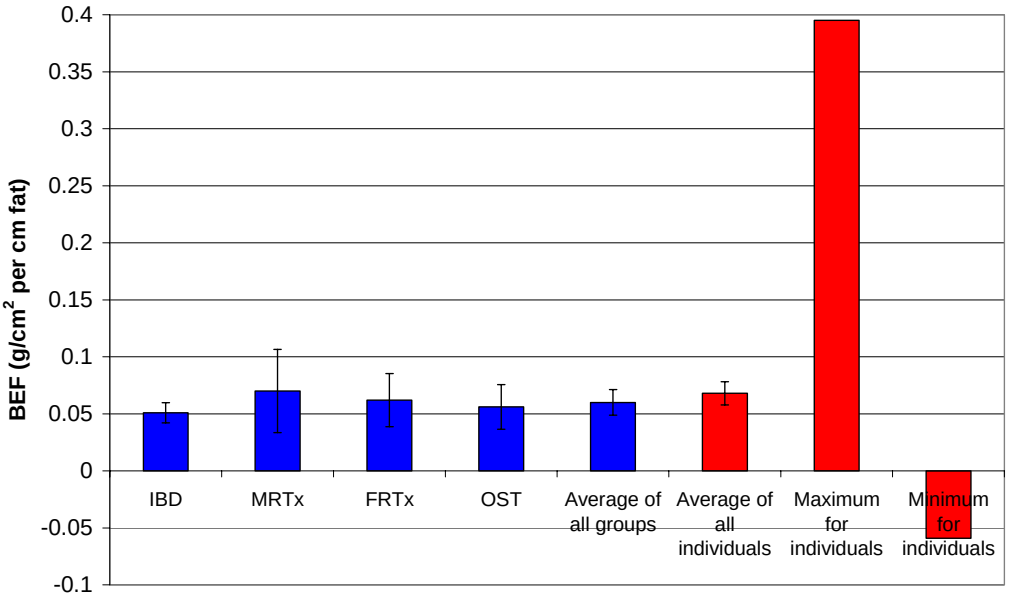

Figure 8.14 Comparison of the bone equivalence factors of abdominal fat derived from different study populations and that found when averaging over all individuals within these groups.

The success of predicting changes in L3+L4 BMD from changes in fat thickness within the baseline was investigated by comparing the lumbar spine BMD measured with the largest and smallest ROI with the BME of the difference in fat thickness between the corresponding baseline regions from WB images. For the 100 subjects, the BME of changes in fat thickness agreed with the observed change in BMD to within the range -0.080 g/cm^2 to 0.063 g/cm^2 with an average of 0.017 ± 0.023 g/cm^2. Such discrepancies would cause an average T-score accuracy error of 0.2. When averaging the data for all subjects within the IBD, OST, MRTx and FRTx subject populations in chapter 7, the observed difference in corrected L3+L4 BMD measured with a ROI of 8.3 cm and 15.1 cm was also predicted from the change in fat thickness in the baseline to within 0.013 g/cm$^{2.}$ Considering the subjects individually, this was achieved to within 0.01 g/cm^2 in 38% of cases. A measurement error of 0.01 g/cm^2, or 0.1 in T-score, is unlikely to introduce errors that would affect the clinical diagnosis of osteoporosis.

The validity of extracting fat thickness from DXA WB scans and converting to a BME was tested by systematically increasing the ROI width to include more fat in the baseline whilst the fat thickness over the spine remained constant. For a perfect model, the BME of fat differences between two baseline regions would be equal to the difference in lumbar spine BMD measured with the equivalent width ROI. When plotting these two quantities against each other for various ROI widths, the ideal model to predict changes in BMD from the fat thickness in baseline would have a gradient of 1 and a y-intercept of 0. The model appeared to be successful when averaging the data from the subjects within the IBD, MRTx and FRTx groups and to lesser extent the OST group. However, current observations highlight how the success of the model can vary considerably on an individual level. The difficulty in assessing the success of the method is defining a benchmark to categorise success as the human body varies between individuals and a single model is unlikely to be perfect for every individual. Data from all individuals was examined in depth to look for factors which determine the success of the model in terms of the gradient being close to 1. There did not appear to be any association with the absolute BMD, changes in BMD as ROI increased or the absolute fat thickness. However, the magnitude of change in fat thickness as ROI width increased, and hence the shape of the fat profile appeared to be a factor. It can be assumed that a larger gradient for changes in baseline fat thickness with ROI width reflects a greater inhomogeneity in fat thickness within the scan ROI. The model also appeared to be more successful when the relationship between the corrected L3+L4 BMD and the baseline fat thickness was strongest as indicated by a Pearson's correlation coefficient close to 1 (Fig. 8.7).

Examining individual fat profiles revealed that the gradient for the linear regression model used predict changes in BMD from fat thickness changes was closer to 1 when the profiles were more symmetrical and had a more defined shape (Figs 8.12, 8.13). This was especially noticeable for the cases where the gradient was less than 0.2 as the profile was considerably asymmetrical. Referring back to the groups of

subjects, the average fat thickness profile for the group with the lowest gradient linking BME and changes in BMD (OST) was also less symmetric than for the other groups. Even though for some individuals the fat thickness profiles showed considerable variation, they were not symmetrical. In these cases, when averaging the fat in an area each side of the spine changes in fat thickness often cancelled out resulting in a smaller overall change in fat thickness as ROI width increased.

The relationship between the success of the model to predict changes in BMD and the BEF is shown in figure 8.11. It can be seen that removing the negative points results in an approximately exponential curve with a cluster of measurements at 0.05 g/cm^2 per cm fat when the gradient of the measured BMD verses BME is 1. The BEF for each subject was derived from lumbar spine BMD and DXA WB measurements independent of any published BEF whereas the gradient of the model linking the measured BMD and BME used a BME calculated with a BEF of 0.05 g/cm^2 per cm fat taken from work by Tothill and Pye (1992). The BEF has units of g/cm^2 per cm of fat and the gradient of the measured BMD and BME model is measured BMD divided by the measured fat thickness multiplied by 0.05. Therefore the gradient of regression model linking the two sets of data is given by equation 8.1 and, as can be seen, the gradient should ideally be 0.05. In light of these results, it can be assumed that the method works when BEF measured from lumbar spine and WB data for the subject is equal to the BEF used to convert fat thickness into a BME.

$$Gradient = \frac{(Fatthickness \times 0.05)}{(BMD)} \times \frac{(BMD)}{(Fatthickness)} \quad (8.1)$$

An interesting observation from figure 8.7 was that a negative BEF resulted in a negative relationship between BME of baseline fat and the observed BMD. This strengthens the argument that the BEF is linked with the success of a model to predict BMD from baseline fat thickness. As the BEF represented the relationship between changes in measured BMD and baseline fat thickness, this confirms that it is the correlation between

these parameters that determines how well the model to predict changes in BMD works.

Another measure of success of the model to predict BMD changes from BME of fat is the y-intercept of the regression line. As this was within ±0.01 g/cm^2 in 85% cases then this was not used to grade the success of the model.

The aim of this thesis was to predict accuracy errors in BMD measurements caused by a non-uniform distribution of fat within the scan ROI for individual patients. The considerable variation in the measured BEF and the success of a model to convert fat thickness to a BME suggests any correction needs to be made on an individual basis. It appears that, in many cases, fat thickness measurements can predict BMD changes to within 0.01 g/cm^2. The cases where the model appears to work best are those for which there appears to be a greater inhomogeneity in fat distribution. Conveniently these are the cases where the BME of baseline fat compared to that over the vertebrae could become important. To quantify the influence of baseline fat thickness on the measured BMD, the difference in fat thickness between the baseline of the largest and smallest ROI was related to the L3+L4 BMD reported with corresponding ROI. It is likely that for small differences in fat thickness between the largest and smallest ROI reflected by flatter and less symmetrical fat thickness profile, the difference in BMD between these ROI is not as well predicted from the BME of baseline fat as measurement errors have a greater influence and the changes in both fat thickness and BMD are likely to be so small that they are not significant. Also the error introduced by neglecting yellow marrow fat may be more prominent.

To put into context the impact of the potential accuracy error in BMD due to the BME of the difference in fat in the baseline of a 11.5 cm ROI compared to that over the spine, the BME of the difference in fat was expressed as a percentage of the actual BMD measured with a 11.5 cm ROI. The smallest difference in fat thickness was 0 cm thus no error

introduced. The largest fat difference was 1.1 cm translating to a BME of 0.055 g/cm^2 which was approximately 6% of the BMD measured with a 11.5 cm ROI. As the characteristics of the subjects that compose the groups of individuals used in this work are varied, this population is likely to reflect quite well the general patient population attending for BMD assessment by DXA. Hence it could be assumed that the 6% error may be expected in the general population. This error is not dissimilar to that found for DPA measurements of spine BMD which have been quoted as 3 to 10%. For DXA AP spine BMD measurements, it has been reported that a non-uniform soft tissue distribution causes accuracy errors of 5.3% (Svendsen *et al.* 1995) and 3 and 6% for a group of males and females respectively (Tothill and Pye 1992). Caution must be taken when comparing these published values to the 6% value found in the current work as they were calculated from different measurements. However, it is encouraging that they are in good agreement.

The current work could be applied to clinical practice if the patient had a WB scan and the difference in fat thickness between a region corresponding to the baseline used for lumbar spine measurements and over the vertebrae is converted to a BME using a BEF. It is likely that only in cases where the fat thickness profile is considerably inhomogeneous would further analysis be necessary. Due to the large variation in BEF measured in-vivo in this work, it is recommended that either a published value such as that from Tothill and Pye (1992) is used or it is measured for the individual by plotting the change in measured BMD as ROI increases against the difference in fat thickness within the baseline. It is accepted that due to time constraints this may not be practical for every patient.

Performing a WB scan to calculate the BME in difference in fat over and adjacent to the spine is unlikely to be necessary for every patient. However, it is unclear from this work how to filter out those patients in which a WB scan would be useful. When there is an unreliable BMD result or an unexpected and significant change in longitudinal BMD

measurements a WB scan may be useful. There does not appear to be a link between the inhomogeneity of abdominal fat and BMI or trunk width, as shown in chapter 6. A longitudinal study comparing fat profiles and corresponding lumbar spine BMD measurements over time in individuals would provide more information to aid in filtering out those patients requiring a WB scan in order to improve the accuracy and precision of DXA BMD measurements.

8.5 Conclusions

In the majority of individuals, there was an increase in lumbar spine BMD as the ROI width increased and this appeared to be due to the increase in fat thickness within the baseline region of the lumbar spine ROI. The bone mineral equivalence of abdominal fat varies considerably between individuals and caution must be taken when using the average value of 0.068 ± 0.051 g/cm^2 due to the wide range of values observed in this work.

It appears that the method to predict BMD changes from the BME of fat measured from WB scans works best when (1) there is a stronger correlation between the measured L3+L4 BMD and fat thickness within the baseline; (2) the increase in fat thickness within the baseline as the ROI width increases is larger and (3) the fat thickness profiles are more symmetrical and exhibit a greater variation.

The L3+L4 BMD measured with a 11.5 cm ROI appears to be overestimated by a maximum of 6% due to the non-uniform distribution of fat within the lumbar spine ROI when using this width ROI.

It appears that in many cases it is possible to predict a change in L3+L4 lumbar spine BMD due to the BME of fat within the baseline measured from WB scans to within 0.017 g/cm^2.

The current observations suggest that errors in BMD due to the inhomogenous distribution of abdominal fat are likely to be of little

significance to the diagnosis of osteoporosis for many patients. However, it appears that it is possible to use DXA WB scans to estimate the inaccuracy in BMD due to the fat thickness in baseline relative to that over the spine in cases where the non-uniformity of fat within the ROI is greatest.

Chapter 9
Discussion and Future Developments

9.1 Discussion

9.1.1 General

Osteoporosis is characterized by a low bone mineral density (BMD) and decreased bone strength resulting in an increased fracture risk. Osteoporosis is a major cause of morbidity with consequently a great financial burden on the NHS. An important goal in osteoporosis management is to predict fracture risk and a low BMD is one of the most important risk factors. To diagnose osteoporosis and assess disease progression or response to therapy, an accurate and precise method of measuring BMD is of importance.

Dual-energy X-ray absorptiometry (DXA) is currently regarded as the gold-standard for measuring BMD with high precision (Cullum *et al*. 1989; Laskey *et al.* 1991; Haddaway *et al.* 1992; Blake and Fogelman 2008). However, the accuracy is compromised by two assumptions: (1) the body is composed of only soft tissue and bone mineral and (2) the composition of tissue overlying bone is the same as that adjacent to bone.

The hypothesis for this thesis was that the accuracy of lumbar spine BMD measurements with DXA is compromised due to the non-uniform distribution of abdominal fat and that it is possible to correct for this effect by measuring fat from DXA whole body (WB) images.

Questions that needed answering during this work were:

(1) Can the distribution of abdominal fat at the level of the lumbar vertebrae be quantified from DXA WB scans?

(2) Using the data from WB images, is the distribution of fat non-uniform within a typical lumbar spine analysis ROI?

(3) What is the impact of this non-uniform distribution on lumbar spine BMD?

Initially in-vivo data analysis were performed on a group of female IBD patients with the data from all subjects combined. As the results were encouraging, the work was extended to a group of females with confirmed osteoporosis, a group of male renal transplant patients and a group of female renal transplant patients. Due to the considerable variation in the results between individuals within any one group, the analysis was repeated for individual patients.

9.1.2 Validation

The measurement of lumbar spine BMD by DXA is dependent on the region of soft tissue used to compensate for soft tissue over the vertebrae as discussed in chapter 2. It has been reported that the width of this region influences the BMD result (Hansen *et al.* 1990; Tothill and Pye 1992). As a starting point for this work, this was confirmed for the QDR-1000W in a phantom study reported in chapter 3. A dependence of BMD, BMC and BA on lumbar spine ROI width was observed which is considered to be an artefact associated with the area of soft tissue within the baseline region.

The Hologic WB sub-regional analysis software was validated for measurement of abdominal fat and lean tissue in small analysis regions (STB) as shown in figure 5.1. Aspects investigated were the (1) accuracy of dimensions of the analysis regions; (2) accuracy of the line spacing

and point resolution factors supplied by Hologic; (3) linearity and accuracy of WB FM and LM measurements; and (4) validity of combining data from DXA WB and lumbar spine scans.

9.1.3 Dependence of DXA Lumbar Spine BMD Measurement on Width of Analysis Region

Chapter 4 reports the findings of an in-vivo investigation into the influence of ROI width on lumbar spine BMD using combined data for a group of 50 female patients with IBD. The variation in L1+L2 BMD, BMC and BA as ROI width increased was less than that for L3+L4. There was an interaction between the regression lines for L1+L2 and L3+L4 BMD indicating that the ROI width influenced the BMD differently for these pairs of vertebrae. The change in BMD as the ROI increased was not significantly different for L3 and L4. This was confirmed by the fact that there was no interaction between the regression lines, which justified combining the data for these vertebrae ($p<0.001$).

Changes in BA were strongly correlated with changes in BMC. This supports the view of others that changes in BMD may be false depending on changes in BA (Tothill and Avenell 1998). Compensating the in-vivo BMD measurements for the BMD changes observed in the phantom as ROI increased as reported in chapter 3, decreased the dependence of BMD on ROI width. However, there remained a residual increase in combined L3+L4 BMD as the ROI increased.

The results in chapter 4 highlighted how the ROI width must be carefully selected and standardised for all measurements to avoid accuracy and precision errors. With Hologic scanners, the software presents a default ROI width but the user can change this manually. One manufacturer GE Lunar uses an automatic width fitting algorithm within software which varies the ROI width depending on the attenuation of the soft tissue within the scan ROI. Whilst this may improve accuracy the precision may be affected.

9.1.4 Quantification Abdominal fat Distribution from DXA Whole Body Images

A review of relevant literature indicated that accuracy errors in lumbar spine BMD due to the non-uniform distribution of abdominal fat can be considerable, but that the absolute magnitude of these errors and their impact on clinical diagnosis is still under debate (Svendsen *et al.* 1995; Bolotin *et al.* 2001a; Bolotin and Sievanen 2001b; Bolotin *et al.* 2003; Bolotin 2007; Tothill and Hannan 2007). It has been documented that a greater thickness of fat within the soft tissue adjacent to the lumbar spine than in the soft tissue overlying it will cause the BMD to be overcorrected by the software. This would cause the BMD to be falsely high and vice versa (Cullum *et al*. 1989; Hangartner and Johnston 1990; Hansen *et al.* 1990). To improve the accuracy of DXA measurements a method to correct for the presence of fat is required.

Is has been shown by others using CT measurements that there is a greater thickness of fat adjacent to the spine than overlying the spine as discussed in chapter 2 (Tothill and Pye 1992; Tothill and Avenell 1994a; Formica *et al.* 1995; Svendsen *et al.* 1995; Svendsen *et al.* 2002). However, no reports were found of the Hologic QDR-1000W sub-regional analysis software being used to quantify abdominal fat distribution as has been done in this work. The results in chapters 5 and 7 showed that DXA WB images can be used to form abdominal fat thickness profiles with sufficient detail to quantify inhomogeneity in the distribution of fat within regions corresponding to those used for lumbar spine BMD measurement. The variation in fat thickness across the abdomen within regions corresponding to those used for BMD assessment was greater at the L3+L4 level and therefore more likely to influence the accuracy of L3 and L4 BMD measurements. The shape of the fat thickness profiles were consistent with the abdominal anatomy seen on CT images of a comparable location, and thus provided confidence in the measurements. An interesting observation in chapter 5 was that a non-uniform distribution

of fat may be more of a problem in lean subjects, due to a larger difference between fat thickness in the baseline and over the spine.

9.1.5 Quantification of Fat Thickness within the DXA Lumbar Spine ROI from DXA WB images and the Relationship to the Measured Lumbar Spine BMD

Changes in L1+L2 BMD with ROI width in chapter 4 were smaller, probably due to less variation in fat thickness within the scan ROI observed in chapter 5 for the IBD group. It was therefore decided to concentrate on L3+L4 throughout the remainder of this work. For all study populations, there was no significant interaction between the L3 and L4 regression gradients for variation in BMD, BMC and BA with ROI width indicating the regression lines were not significantly different. This finding strengthens the argument for combining data for L3+L4 in this work.

Increasing the ROI width to include more soft tissue within the baseline effectively caused an increase in baseline fat thickness relative to that over the vertebrae. The ROI width had a significant effect on baseline fat thickness in all study populations. There was not a significant interaction between the regression gradients indicating the effect of ROI width on baseline fat thickness was not significantly different between the study populations. Using the information within the fat thickness profiles, it was confirmed for all study populations that the increase in L3+L4 BMD as the ROI width increased was strongly correlated with an increase in the average fat thickness within the baseline region. This association was derived using the L3+L4 BMD that had been compensated for observations in a phantom with a uniform baseline region.

Consistently for all study populations, based on results in chapter 5 to 7 it was concluded that there is a significantly greater thickness of fat in the baseline soft tissue region than that assumed to be over the vertebrae for ROI widths generally used in clinical practice. This has also been reported by other workers. For the groups of subjects, the difference in fat

thickness between the baseline of a 11.5 cm ROI and that estimated to be over the vertebrae for L3-L4 region ranged from 1 mm (3%) to 4 mm (7.4%). For a 12.5 cm ROI this range was 1.6 mm to 5.1 mm which is smaller than that found in two studies by the Tothill group (1992; 1994a) who measured 6.7 to 17 mm for the region L2-L4. The maximum difference in fat thickness measured in this work (4 mm) converts to a BME of 0.02 g/cm^2 and a T-score of 0.2 unit which will only cause a misdiagnosis of osteoporosis if the result is borderline. The difference between fat thickness in the baseline and that in the CB was significantly influenced by ROI width. There was no significant interaction between the regression gradients for each group ($p=0.249$) confirming that the fat thickness changed to the same extent in all study populations. Over all ROI widths, the difference between the baseline and CB fat thickness did not vary significantly between groups ($p=0.994$).

The gradient of the linear regression model for the relationship between L3+L4 BMD and fat thickness within the baseline represents the bone equivalence of fat. This value is based on the assumption that changes in BMD are only dependent on baseline fat thickness. The BME of 1 cm of abdominal fat, the BEF, was shown to be 0.051±0.001 g/cm^2, 0.070± 0.003 g/cm^2, 0.062± 0.004 g/cm^2 and 0.056± 0.004 g/cm^2 for the IBD, OST, MRTx and FRTx groups respectively with the average over the 4 groups being 0.060± 0.008 g/cm^2. There was no significant difference in the mean BEF between the four study populations probably because of the large variation in BEF within each group. The bone mineral equivalence of abdominal fat should not vary between diagnostic groups and therefore it is suspected that the measurements of fat thickness are influenced by lean tissue which has a higher physical density than fat. The BEF for the IBD group is statistically the most reliable due to the sample size, and also this group is composed of a group of subjects with a relatively large variation in age. Another factor to consider is the variety of structures within the abdomen in the region of L3 and L4, e.g. muscles and intestines. The physical density of the tissues composing these structures will be different to abdominal fat and may vary slightly between

individuals. It is therefore probable that there are a variety of tissues, other than pure fat, in the small STB placed next to the spine. DXA may interpret the attenuation of the dual-energy X-rays by these tissues as being due to fat and therefore the mass of these tissues will contribute to the FM. Any variation in the physical density of the tissues included in the STB may cause a variation in the BEF. The BEF published by others for the Hologic QDR-1000 and 1000W were 0.044 g/cm^2 per cm by Hangartner and Johnston (1990) and 0.049 g/cm^2 for lard and 0.050 g/cm^2 for stearic acid by Tothill and Pye (1992). Differences are expected as the values were derived using completely different methods, the main one being the fact that BEF in the current work was derived from DXA WB and lumbar spine in-vivo measurements whereas the published values are from phantom studies. It is suggested that a value based on human fat is more accurate but until further studies are done, fat thickness was converted into a BME using the BEF published by Tothill and Pye (1992) for stearic acid.

A limitation with the work in this thesis is that measurement of FM over the spine is estimated from the attenuation of soft tissue in a bone free region adjacent to bone. This was confirmed in chapters 5 and 7 from the consistent agreement between the FM in the STB next to the vertebrae and that in the CB. In reality, the total fat thickness in a region of bone plus soft tissue would be the combined soft tissue fat thickness and the thickness of the fat within YM contained in bone. The error due to neglecting YM fat is likely to be of more importance in the elderly and in osteoporotic individuals.

A problem faced during this work was the lack of a true in-vivo BMD measurement with which to compare BMD results and therefore it was not possible to define the ideal ROI width to give an accurate BMD. A true measure of BMD can only be achieved in cadaver studies such as those published by Svendsen *et al.* (1995). In order to estimate the potential inaccuracy in L3+L4 BMD from DXA measurements in chapters 6, 7 and 8, it was assumed that the “true” value of BMD occurs when the fat

thickness within the baseline equals that estimated to be over the bone using CB measurements. For all groups, reducing the ROI width to approximately 7 to 10 cm appeared to minimise the accuracy errors due to soft tissue distribution. This is not recommended for routine clinical measurements as potentially the precision would be compromised. Despite the variation in these “ideal ROI” widths, the difference between the study populations was not statistically significant One notable finding from the results is a small systematic error in the BMD expected using the ROI width recommended by Hologic (11.5 cm) when assuming the “true” BMD occurs when fat is uniformly distributed throughout the scan ROI. To estimate the potential error in the BMD measurement, the BME of the difference between the fat thickness in a baseline of a 11.5 cm ROI and that assumed to be over the vertebrae was expressed as a percentage of the BMD measured with a ROI width of 11.5 cm. It was shown that, in theory, 1%, 2.8%, 0.5% and 1.5% of the measured L3+L4 BMD is potentially an error due to the non-uniform distribution of fat within the scan ROI for the IBD, OST, MRTx and FRTx groups respectively. Expressed as T-score units the difference in fat thickness would result in an error of 0.1, 0.2, 0.1, and 0.2 for the four groups. Such an error is unlikely affect the clinical diagnosis of osteoporosis based on WHO criteria.

The strong relationship between the observed change in phantom corrected L3+L4 BMD as the ROI increases and the BME of fat within the baseline of the corresponding ROI suggests that errors in BMD can be predicted from the FM extracted from WB images. The success of prediction was determined from the gradient of the linear regression model linking measured changes in BMD and those predicted from changes in fat thickness. The model was deemed successful when the gradient was close to 1. The results were encouraging for the IBD, MRTx and FTx groups with gradients of 1.002±0.024, 0.867±0.029 and 0.931 ±0.068 respectively. However the gradient was only 0.728±0.031 for the OST group which may be due to the relatively small number of subjects (10) compared to the IBD group with 50 subjects. It was shown that by

converting the difference in baseline fat thickness between the largest and smallest ROI into a BME, it is possible to predict changes in L3+L4 lumbar spine BMD from DXA WB fat thickness measurements to within 0.001 g/cm^2, 0.011 g/cm^2, 0.013 g/cm^2, 0.005 g/cm^2 for the four groups. This error equates to 0.1 T-score unit and therefore is unlikely to be of concern. It should be noted that this figure was found from averaging the data for each study population.

It appears that the model works least successfully for the OST group. However, statistical analysis showed that the regression gradient for the BME of change in baseline fat thickness against the observed change in BMD was not significantly different to that for the other study populations. The difference between the baseline fat thickness in the largest and smallest ROI was not significantly different between the four groups (p= 0.194) suggesting the uniformity of fat within the ROI is not significantly different. Also, the difference in the BMD measured with the largest and smallest ROI was not significantly different between the groups (p=0.108). The only statistical differences between the OST group and the other three groups, other than the number of subjects, are:

(1) The BMD is significantly lower for the OST group. DXA BMD measurements are known to be less accurate and precise when the actual BMD is low. This may introduce errors into the data used to construct the model.

and

(2) The average age of the OST group is greater than that of the other groups. Hence, these subjects are likely to have a greater fat thickness next the spine which probably explains why the fat thickness in the baseline is always greater than that in the CB even at smallest ROI widths.

When increasing the ROI width, the variation in BMD, average baseline fat thickness and the difference between baseline and CB fat was not significantly different between study populations. To investigate if the

difference in the number of subjects is influencing the success of the model on a group basis, each group should be composed of equal numbers which unfortunately was not possible.

9.1.6 Quantification of Fat Thickness within DXA Lumbar Spine ROI from DXA WB images and the Relationship to the Measured Lumbar Spine BMD for Individual Subjects

Due to the large variability in fat thickness between subjects in each group, it was decided to repeat the analysis on an individual basis. The general trend in results was in agreement with the observations made on group data. In the majority of individuals there was an increase in lumbar spine L3+L4 BMD as the ROI width increased. This appeared to be due to the increase in fat thickness within the baseline region of the lumbar spine ROI. The BEF for abdominal fat was seen to vary considerably between subjects from -0.050 ± 0.051 g/cm^2 per cm fat to 0.395 ± 0.051 g/cm^2 per cm fat. These findings highlight that caution must be taken when using the average value for the 100 subjects (0.068 ± 0.051 g/cm^2 per cm fat) as there is individual variation of up to 484%. It was reassuring that the average BEF found from individual analysis was close to that for the average of the groups which was 0.060 ± 0.008 g/cm^2. As mentioned in section 9.1.5, the BEF of abdominal fat should not vary between individuals, and therefore it is suspected that relatively lean tissues are contributing to the fat mass.

The large variation between the fat thickness in the baseline and that over the vertebrae for the 100 individuals implies that any correction for fat distribution should be made on an individual patient basis. This difference in fat thickness for a 11.5 cm ROI ranged from 0 cm to 1.1 cm over the 100 subjects with an average of 0.2 ± 0.3 cm (mean ±SD). Such deviations are also seen in results published by others (Tothill and Pye 1992; Tothill and Avenell 1994a).

As regards the data from 100 individuals, the L3+L4 BMD measured with a 11.5 cm ROI appears to be overestimated by a maximum of 6% due to the non-uniform distribution of fat within the lumbar spine ROI. This value was deduced by converting the fat thickness measured from WB images into a BMD using the Tothill and Pye (1992) BEF and is within the range quoted by others. Tothill and Pye (1992) measured an average of 3 to 6% for males and females respectively and up to 10% looking at individuals. In probably the most extensive study on soft tissue accuracy errors using cadavers, Svendsen *et al.* (1995) measured a random accuracy error of 3-4% for AP spine measurements. The similarity was encouraging as different methods were used to obtain these figures.

Within individuals, the success of the model to predict changes in BMD from the BME of changes in fat thickness varied considerably with gradients varying from -0.777 to 2.589. Benchmarking the success against a gradient of 1, it appears that the method worked best when (1) there was a stronger correlation between the measured L3+L4 BMD and fat thickness within the baseline; (2) the increase in fat thickness within the baseline as the ROI width increased was larger and (3) the fat thickness profiles were more symmetrical with a larger difference between the minimum and maximum fat thickness.

It appears that in many individuals it is possible to predict a change in L3+L4 lumbar spine BMD from DXA WB fat thickness measurements to within 0.017 g/cm^2 or a T-score of 0.2. This is slightly higher than 0.013 g/cm^2 found with groups of subjects as expected.

The observations made when assessing the impact of differences in fat thickness within the ROI for individuals suggest that errors in BMD due to the inhomogenous distribution of abdominal fat are likely to be of little significance to the diagnosis of osteoporosis for many patients. However, it was shown that in some individuals the difference between the fat thickness within the baseline of a 11.5 cm ROI and over the vertebrae may be as large as 1.1 cm resulting in a BME of 0.055 g/cm^2 which

translates into an error of 0.6 in T-score. Such an error has the potential to cause a misdiagnosis of osteoporosis based on WHO criteria.

Data from individuals were examined in an attempt to filter out those patients in whom the inhomogeneity in fat thickness within the ROI is great enough to cause a considerable error in BMD. The trunk width, the width of the subcutaneous fat layer and BMI were investigated. From the data available, it is not possible to identify patients in which a correction for a non-uniform fat distribution is necessary based on body size.

9.1.7 Quantification of Inaccuracy in Lumbar Spine BMD from the Ratio of Abdominal Fat and Lean Tissue Thickness Measured from DXA Whole Body Images

The hypothesis in this work was concerned only with the difference between fat thickness in the soft tissue baseline of the lumbar spine ROI and that over the vertebrae as a cause of the inaccuracy in lumbar spine BMD. This reflected the approach of many other workers. However, for accurate BMD measurement the important factor is that the attenuation of soft tissue along all photon paths through bone is identical to that through paths adjacent to bone. In the DXA calculation of BMD, it is neither the thickness nor difference in the thicknesses of fat or lean tissues between the bone and non-bone regions that is important but the relative amounts of fat and lean tissue, as stressed by Bolotin *et al.* (2003). The composition of soft tissue can be represented by the ratio of fat to lean area densities or thickness. Theory suggests that it is likely that the fat to lean ratio is the most appropriate parameter for mimicking the R-value used in BMD calculation.

A separate study, not reported in this thesis, used WB scans to quantify the lean tissue distribution at the level of L3+L4 using the method developed for extraction of FM in chapter 5. The profile of the distribution of F:L within abdominal soft tissue at the level of the lumbar vertebrae was similar to the fat thickness profiles for the subject groups.

Subsequently, the ratio of fat to lean tissue area density (F:L) within abdominal soft tissue at the level of L3+L4 was quantified. The difference between F:L of soft tissue over L3+L4 and that in the soft tissue baseline was correlated to the L3+L4 BMD reported with an equivalent width ROI.

As the lumbar spine ROI width increases, DXA WB measurements indicate that the amount of lean decreases whilst the F:L increases. Consequently, the difference between the F:L of baseline tissue relative to that over the spine also increased. For a 11.5 cm ROI, the F:L for the subject groups was between 3% and 9% higher in baseline than over the spine. A significant ($p<0.05$) positive relationship between the measured L3+L4 BMD and the F:L of baseline soft tissue suggested that the increase in L3+L4 BMD was due to an increase in the F:L within soft tissue baseline region of the ROI. In agreement with the results in chapters 6 and 7, reducing the ROI width below 11.5 cm is likely to minimise the error due to a non-uniform fat distribution. When converting the difference in F:L between baseline tissue within a 11.5 cm ROI and that over the spine into a BME, there are potentially BMD errors of 0.8±0.1% for the IBD, MRTx and FRTx groups and 3.2% for the OST group. When considering fat only, this was 2.8% for the OST group. In agreement with the work on fat thickness, the error was highest for the OST group. Due to time constraints, only group analysis was done on fat and lean data.

Further work is required to determine if quantifying the inhomogeneity in F:L within the lumbar spine ROI is a more viable method of predicting errors in lumbar spine BMD.

9.1.8 Summary

This study has gone some may towards enhancing the understanding of the influence of fat on lumbar spine measurements. Whilst it is acknowledged that presence of lean is important, it is likely that fat will have the largest influence on accuracy errors and therefore the approach

used in chapter 6, 7, and 8 and that in similar work by others is valid. The findings of this thesis agree with others that the distribution of fat is non-uniform within the region used for lumbar spine BMD analysis at the L3+L4 level. However, it is believed that the approach in this work combining measurements from DXA WB and lumbar spine scans is original.

Using measurements from DXA WB scans to estimate the accuracy error in BMD due to the non-uniform distribution of fat within the scan ROI has many advantages over using CT scans. The biggest advantage is that scans are performed with a single scanner during a single visit by the patient. The patient will be in approximately the same position for both scans and, with the current fan beam scanners, the WB scan only adds 3 minutes to total visit. It is acknowledged that data analysis could be time consuming but the process could be simplified using only 3 regions of analysis – one over the spine and 1 each side of spine to coincide with the width of the ROI used to calculate lumbar spine BMD. The difference in the fat thickness between the baseline and CB could then be converted to a BME. If a fat thickness profile was constructed and data analysis performed as outlined in section 6.2.2, the ideal ROI width could be found to ensure the fat thickness within baseline soft tissue matches that in soft tissue over the vertebrae. This would potentially improve accuracy. The limitation with this method is that CB value is not an accurate measure of fat over vertebrae. Another disadvantage is that there is an additional radiation dose associated with the WB scan. Despite being very small this should be weighed up against the potential improvement in accuracy of the BMD result and consequences on patient management. It is believed that the largest source of uncertainty in the measurements presented comes from matching the lumbar spine ROI with soft tissue regions on the WB scans.

The results presented in this thesis show that in many individuals, the difference in fat between baseline and over vertebrae is unlikely to cause problems and therefore a WB scan is unnecessary. Where problems are

suspected, the extra time and effort to quantify the fat distribution would be cost-effective is it would avoid a mis-diagnosis. Based on the findings of the current work, there does not appear to be a simple way to filter out patients in which an adjustment for BMD accuracy is necessary. It is suggested that WB scans are used to quantify abdominal fat distribution when there is an unreliable lumbar spine BMD result or a significant and unexpected increase or decrease in BMD between longitudinal scans.

The effect of a non-uniform distribution of fat within the lumbar spine scan ROI could be assessed more accurately if the fat thickness was measured from the information contained within a lumbar spine scan. This would remove the problem of two different scans with different scan positions and scan modes and would also improve the accuracy of aligning soft tissue regions. This data are potentially available within spine scans but not revealed by the manufacturer. This has however been achieved by GE/Lunar (Suh *et al.* 2002; Leslie *et al.* 2010).

It was stated by Tothill and Pye (1992) that whilst “it is important to appreciate the possibility of errors resulting from fat non-uniformity, there is probably no practical way of making correction”. It is believed that the method used within this thesis to estimate likely errors in BMD from the difference in fat thickness within the scan ROI could potentially be used on an individual to estimate the error due to the difference in fat over and adjacent to spine. It is acknowledged that there are limitations with the DXA WB method and it may not give a 100% accurate correction resulting in a 100% accurate BMD. However, the method would allow an appreciation of the potential errors in BMD which should be considered by the clinician when reviewing the DXA results to make a clinical diagnosis and decide upon patient management. Also the DXA WB method is likely to be of importance if the patient changes weight drastically between scans. Any correction method for BMD measurements must be thoroughly validated. It is possible that an improvement in accuracy using a correction method might lead to worse

precision. A full validation of the methods proposed in this work is required using more patient data.

9.2 Future Developments

Pencil beam DXA scanners have been superseded by fan beam scanners and so it is not possible to repeat or add to any measurements presented in this thesis. However, should this be possible the additional work that would add to the integrity of this work are listed below.

(1) Measure the BEF in-vitro.

The BEF for fat was taken from work by Tothill and Pye (1992) who measured it for the Hologic QDR-1000. Ideally this should be measured for the scanner on which the in-vivo measurements were performed.

(2) Perform a longitudinal study.

It would be interesting to perform a longitudinal study following a series of patients over time to investigate if the abdominal fat thickness profiles change and if this is reflected in changes in BMD. The patients comprising the renal Tx group had a DXA spine and WB scan approximately every 3 months post Tx and therefore would be a good group to look at. As there is a 3 month interval between the scans in the renal Tx study, a real change in bone mineral would not be expected and therefore any changes are likely to be false. A retrospective prediction of actual changes in BMD could be performed by looking at relative changes in fat thickness between the baseline and over the spine and converting this to a BME and comparing this to the observed change in BMD.

(3) Investigate how the difference in patient position between lumbar spine and WB scans affects the abdominal fat distribution.

In order to do this ethical approval would be needed to perform a WB scan on a subject in the lumbar spine scan position. The abdominal fat thickness profile would then be compared to that seen when the same subject is lying flat in the position for a WB scan.

(4) Perform a more detailed in-vitro validation of method.

The validation studies in chapter 3 were very basic. As part of this work it was planned to construct a phantom that simulated the fat distribution within the abdomen. The phantom would be such as to enable the fat thickness over the spine and adjacent to the spine to be changed simultaneously and independently. Despite designing such a phantom, it was not possible to construct it before the QDR-1000W was removed from Cardiff.

(5) Compare the fat thickness measured from CT images with fat thickness measured from DXA WB images for the same subject.

It was shown in chapters 6,7, and 8 that the features of the fat thickness profiles compare well with structures seen on published CT images. However, it would be interesting to compare fat thickness measurements made from DXA WB images with those measured from a CT image at the level of the lumbar vertebrae for the same subject. No CT images were available for the patients scanned as part of the IBD, OST or renal Tx groups and therefore it was not possible make this comparison. However, during course of this study preliminary work was done comparing fat profiles at the L3+L4 level derived from Hologic Discovery A WB images and CT images corresponding to the L4-L5 region. Due to time constraints, this work was placed on hold. It is intended to repeat the work outlined in this thesis on a group of subjects scanned with the Hologic discovery A and therefore CT images will be used at this time to enhance the work.

(6) Investigate the possibility of obtaining soft tissue attenuation data from Hologic lumbar spine scans in order to measure fat thickness.

In a preliminary study using the Lunar DPXL scanner, Suh *et al.* (2002) used the R-value (%fat) in the AP DXA scan mode to measure abdominal fat. A similar approach could be used using Hologic scanners.

(7) Repeat work on fan-beam DXA scanner.

Whilst work presented in this thesis confirms that the distribution of abdominal fat within the region of the lumbar spine is non-uniform and

suggests the potential magnitude of consequential BMD errors, the work needs to be repeated on a fan-beam scanner to make the results applicable to current clinical practice. Any measurements made on a pencil beam cannot be transferred to a fan beam system as a significant difference in measurements between these systems has been well documented (Bouyoucef *et al.* 1996; Barthe *et al.* 1997; Ellis and Shypailo 1998).

Preliminary investigations with the Hologic Discovery A fan beam scanner confirmed the dependence of BMD on ROI width was similar to that for the Hologic QDR-1000W pencil beam scanner. It appears that the edge detection algorithm has been improved since that used in QDR-1000W software as a complete bone map is achievable with a narrower ROI. Due to improvements in the software, it is possible to produce more detailed soft tissue profiles with smaller regions of interest (STB).

9.3 Conclusions

This study provides further evidence that in-vivo and in-vitro BMD lumbar spine measurements are dependent on the ROI width and therefore highlight the importance of standardising the width to minimise accuracy and precision errors. Abdominal fat thickness profiles derived from DXA WB images can be used to quantify abdominal fat distribution. There was a strong positive correlation between in-vivo changes in L3+L4 BMD and fat thickness within the baseline. It is likely that the changes in L1 and L2 BMD are less significant due to the relatively flat fat thickness profile at that level. The bone equivalence of abdominal fat was found to vary greatly and therefore an average value may not be sufficient for all subjects.

When converting the difference between the baseline fat thickness for two different ROI widths into a BME, it appears possible to predict the difference in the actual BMD measured to within 0.013 g/cm^2 for groups and 0.017 g/cm^2 for individuals.

Due to a non-uniform distribution of fat within a standard ROI of 11.5 cm, errors up to 6% were observed for individuals and up to 3% for the groups. Throughout this work errors were largest for the osteoporotic subjects. The maximum difference in fat thickness between the baseline of a 11.5 cm ROI and the CB seen with 100 subjects corresponded to an equivalent in T-score of 0.6 which could potentially cause a misdiagnosis of osteoporosis. However when averaging the data for each group, this gave a T-score of 0.2. It can therefore be concluded that, in the majority of patients, errors introduced by a non-uniform distribution of fat are unlikely to cause a mis-diagnosis but the results highlight the potential for this to happen in some patients.

The hypothesis for this thesis was that the accuracy of lumbar spine BMD measurements with DXA is compromised due to the non-uniform distribution of abdominal fat and that it is possible to correct for this effect by measuring fat from DXA WB images. It is believed that the aims of this thesis were achieved. It has been proved using DXA WB images that the distribution of abdominal fat at the level of the lumbar vertebrae is non-uniform. The potential for abdominal fat to compromise the accuracy of lumbar spine BMD measurements in certain individuals was demonstrated. Where there is a considerable difference between the fat thickness in the soft tissue baseline and that over the spine, measurements from DXA WB images can be used to correct lumbar spine BMD. A method to filter out patients in whom an adjustment for lumbar spine BMD measurement accuracy is necessary has not been found during this work. However, it is recommended that DXA WB scans are used to quantify abdominal fat distribution when there is a significant and unexpected increase or decrease in lumbar spine BMD between scans. The clinical application of the proposed method to correct lumbar spine BMD requires further investigation.

Bibliography

Allen, R. D. M. and Chapman, J. R. (1994). A manual of renal transplantation, Edward Arnold.

Arden, N. K. and Cooper, C. (2002). Osteoporosis in patients with inflammatory bowel disease. Gut **50**: 9-10.

Arngrimsson, S. A., Evans, E. M., Saunders, M. J., *et al.* (2000). Validation of body composition estimates in male and female distance runners using estimates from a four-component model. Am J Hum Biol **12**: 301-314.

Barnett, E. and Nordin, B. E. C. (1960). The radiological diagnosis of osteoporosis: A new approach. Clin Radiol **11**: 166-174.

Barthe, N., Braillon, P., Ducassou, D., *et al.* (1997). Comparison of two Hologic DXA systems (QDR 1000 and QDR 4500/A. Br J Radiol **70**: 728-739.

Behnke, A. R. (1942). Physiologic studies pertaining to deep sea diving and aviation, especially in relation to the fat content and composition of the body. Harvey Lect **37**: 198-265.

Bernstein, C. N., Blanchard, J. F., Leslie, W., *et al.* (2000). The incidence of fracture among patients with inflammatory bowel disease. Ann Intern Med **133**: 795-799.

Bertin, E., Marcus, C., Ruiz, J. C., *et al.* (2000). Measurement of visceral adipose tissue by DXA combined with anthropometry in obese humans. Int J Obes **24**: 263-270.

Binkley, N., Krueger, D. and Vallarta-Ast, N. (2003). An overlying fat panniculus affects femur bone mass measurement. J Clin Densitom **6**(3): 199-204.

Black, D. M., Arden, N. K., Palermo, L., *et al.* (1999). Prevalent vertebral deformities predict hip fractures and new vertebral deformities but not wrist fractures. J Bone Miner Res **14**(5): 821-828.

Black, D. M., Delmas, P. D., Eastell, R., *et al.* (2007). Once-yearly zoledronic acid for treatment of postmenopausal osteoporosis. N Engl J Med **356**: 1809-1822.

Blake, G. M. (2001). Bone densitometry update: Which measurement is best? RAD magazine **27**(308): 35-36.

Blake, G. M. and Fogelman, I. (1997b). Technical principles of dual energy X-ray absorptiometry. Semin Nucl Med **XXVII** (3): 210-228.

Blake, G. M. and Fogelman, I. (2008). How important are BMD accuracy errors for the clinical interpretation of DXA scans? J Bone Miner Res **23**(4): 457-462.

Blake, G. M., Griffith, J. F., Yeung, D. K. W., *et al.* (2009). Effect of increasing vertebral marrow fat content on BMD measurement, T-score status and fracture risk prediction by DXA. Bone **44**: 495-501.

Blake, G. M., McKeeney, D. B., Chhaya, S. C., *et al.* (1992). Dual-energy X-ray absorptiometry: The effects of beam hardening on bone density measurements. Med. Phys. **19**(2): 459-465.

Blake, G. M., Naeem, M. and Boutros, M. (2006). Comparision of effective dose to children and adults from dual X-ray absorptiometry examinations. Bone **38**: 935-942.

Blake, G. M., Rea, J. A. and Fogelman, I. (1997). Vertebral morphometry studies using dual-energy X-ray absorptiometry. Semin Nucl Med **XXVII**(3): 276-290.

Blake, G. M., Wahner, H. W. and Fogelman, I. (1999). The evaluation of osteoporosis: Dual energy X-ray absorptiometry and ultrasound in clinical practice (Second edition), Martin Dunitz Ltd.

Bolotin, H. H. (1998). Analytic and quantitative exposition of patient-specific systematic inaccuracies inherent in planar DXA-derived in vivo BMD measurements. Med. Phys. **25**(2): 139-150.

Bolotin, H. H. (2007). DXA in vivo BMD methodology: An erroneous and misleading research and clinical gauge of bone mineral status, bone fragility, and bone remodelling. Bone **41**: 138-154.

Bolotin, H. H. and Sievanen, H. (2001b). Inaccuracies inherent in dual-energy X-ray absorptiometry in vivo bone mineral density can seriously mislead diagnostic/prognostic interpretations of patient-specific bone fragility. J Bone Miner Res **16**(5): 799-805.

Bolotin, H. H., Sievanen, H. and Grashuis, J. L. (2003). Patient-specific DXA bone mineral density inaccuracies: Quantitative effects of nonuniform extraosseous fat distributions. J Bone Miner Res **18**(6): 1020-1027.

Bolotin, H. H., Sievanen, H., Grashuis, J. L., *et al.* (2001a). Inaccuracies inherent in patient-specific dual-energy X-ray absorptiometry bone

mineral density measurements: comprehensive phantom-based evaluation. J Bone Miner Res **16**(2): 417-426.

Bouyoucef, S. E., Cullum, I. D. and Ell, P. J. (1996). Cross-calibration of a fan-beam X-ray densitometer with a pencil-beam system. Br J Radiol **69**: 522-531.

Braillon, P., Lapillonne, A., Giraud, S., *et al.* (1998). Precision of body composition measurements by dual energy X-ray absorptiometry. Appl Radiat Isot **49**(5/6): 501-502.

Burge, R. T. (2001). The cost of osteoporotic fractures in th UK: Projections for 2000-2020. Journal of Medical Economics **4**: 51-62.

Busscher, I., Ploegmakers, J. J. W., Verkerke, G. J., *et al.* (2010). Comparative anatomical dimensions of the complete human and porcine spine. Eur Spine J **19**: 1104-1114.

Cameron, J. R., Mazess, R. B. and Sorenson, J. A. (1968). Precision and accuracy of bone mineral determination by direct photon absorptiometry. Invest Radiol **3**: 141-150.

Cann, C. E. (1988). Quantitative CT for determination of bone mineral density: a review. Radiology **166**: 509-522.

Compston, J. E., Laskey, M. A., Croucher, P. I., *et al.* (1992). Effect of diet-induced weight loss on total body bone mass. Clin Sci **82**: 429-432.

Compston, J. E. and Rosen, C. J. (2009). Fast facts: Osteoporosis (sixth edition), Heath Press.

Cooper, C. (1997). The crippling consequences of fractures and their impact on quality of life. Am J Med **103**(2A): 12S-19S.

Crawley, E. O., Evans, W. D. and Owen, G. M. (1988). A theoretical analysis of the accuracy of single-energy CT bone-mineral measurements. Phys Med Biol **33**(10): 1113-1127.

Cristy, M. (1981). Active bone marrow distribution as a function of age in humans. Phys. Med. Biol. **26**(3): 389-400.

Cullum, I. D., Ell, P. J. and Ryder, J. P. (1989). X-ray dual-photon absorptiometry; a new method for the measurement of bone density. Br J Radiol **62**(739): 587-592.

Delmas, P. D., Ensrud, K. E., Harris, S., *et al.* (1999). Raloxifene therapy for 3 years reduces the risk of incident vertebral fractures in postmenopausal women. Calcif Tissue Int **64**: S43.

Diessel, E., Fuerst, T., Njeh, C. F., *et al.* (2000). Evaluation of a new body composition phantom for quality control and cross-calibration of DXA devices. J Appl Physiol **89**: 599-605.

Dinca, M., Fries, W., Luisetto, G., *et al.* (1999). Evolution of osteopaenia in inflammatory bowel disease. Am J Gastroenterol **94**(5): 1292-1297.

Drake, R. L., Vogl, A. W., Mitchell, A. W. M., *et al.* (2008). Grays' Atlas of Anatomy, Churchill Livingstone.

Dunnill, M. S., Anderson, J. A. and Whitehead, R. (1967). Quantitative histological studies on age changes in bone. J Pathol Bacteriol **94**: 275-291.

Ellis, K. J. and Shypailo, R. J. (1998). Bone mineral and body composition measurements: Cross-calibration of pencil-beam and fan-beam dual-energy absorptiometers. J Bone Miner Res **13**(10): 1613-1618.

Ensrud, K. E., Nevitt, M. C., Palermo, L., *et al.* (1999). What proportion of incident morphometric vertebral fractures are clinically diagnosed and vice versa? J Bone Min Res **14**: S138.

Ettinger, B., Black, D. M., Mitlak, B. H., *et al.* (1999). Reduction of vertebral fracture risk in postmenopausal women with osteoporosis treated with raloxifene. JAMA **282**(7): 637-645.

Farrell, T. J. and Webber, C. E. (1989). The error due to fat inhomogeneity in lumbar spine bone mineral measurements. Clin Phys Physiol Meas **10**(1): 57-64.

Farrell, T. J. and Webber, C. E. (1990). Triple photon absorptiometry cannot correct for fat inhomogeneities in lumbar spine bone mineral measurements. Clin Phys Physiol Meas **11**(1): 77-84.

Fogelman, I. and Blake, G. M. (2000). Different approaches to bone densitometry. J Nucl Med **41**: 2015-2025.

Formica, C., Loro, M., Gilsanz, V., *et al.* (1995). Inhomogeneity in body fat distribution may result in inaccuracy in the measurement of vertebral bone mass. J Bone Miner Res **10**(10): 1504-1511.

Forsen, L., Sogaard, A. J., Meyer, H. E., *et al.* (1999). Survival after hip fracture: short- and long-term excess mortality according to age and gender. Osteoporos Int **10**: 73-78.

Friedl, K. E., DeLuca, J. P., Marchitelli, L. J., *et al.* (1992). Reliability of body-fat estimations from a four-component model by using density, body water, and bone mineral measurements. Am J Clin Nutr **55**: 764-770.

Genant, H. K. and Boyd, D. (1977). Quantitative bone mineral analysis using dual energy computed tomography. Invest Radiol **12**: 545-551.

Genant, H. K., Li, J., Wu, C. Y., *et al.* (2000). Vertebral fractures in osteoporosis: A new method for clinical assessment. J Clin Dens **3**(3): 281-290.

Glickman, S. G., Marn, C. S., Supiano, M. A., *et al.* (2004). Validity and reliability of dual-energy X-ray absorptiometry for the assessment of abdominal adiposity. J Appl Physiol **97**(2): 509-514.

Gluer, C. and Genant, H. K. (1989). Impact of marrow fat on accuracy of quantitative CT. J Comput Assist Tomogr **13**(6): 1023-1035.

Gokhale, R., Favus, M. J., Karrison, T., *et al.* (1998). Bone mineral density assessment in children with inflammatory bowel disease. Gastroenterology **114**: 902-911.

Gotfredsen, A., Podenphant, J., Norgaard, H., *et al.* (1988). Accuracy of lumbar spine bone mineral content by dual photon absorptiometry. J Nucl Med **29**: 248-254.

Griffiths, M. R., Noakes, K. A. and Pocock, N. A. (1997). Correcting the magnification error of fan beam densitometers. J Bone Miner Res **12**(1): 119-123.

Gundry, C. R., Miller, C. W., Ramos, E., *et al.* (1990). Dual-energy radiographic absorptiometry of the lumbar spine: clinical experience with two different systems. Radiology **174**: 539-541.

Haddaway, M. J., Davie, M. W. J. and McCall, I. W. (1992). Bone mineral density in healthy normal women and reproducibility of measurements in spine and hip using dual-energy X-ray absorptiometry Br J Radiol **65**(771): 213-217.

Hangartner, T. N. and Johnston, C. C. (1990). Influence of fat on bone measurements with dual-energy absorptiometry. Bone and Mineral **9**: 71-81.

Hansen, M. A., Hassager, C., Overgaard, K., *et al.* (1990). Dual-energy X-ray absorptiometry: A precise method of measuring bone mineral density in the lumbar spine. J Nucl Med **31**(7): 1156-1162.

Harris, S. T., Watts, N. B., Genant, H. K., *et al.* (1999). Effects of risedronate treatment on vertebral and nonvertebral fractures in women with postmenopausal osteoporosis. JAMA **282**(14): 1344-1352.

Hartsock, R. J., Smith, E. B. and Petty, C. S. (1965). Normal variations with aging of the amount of hematopoietic tissue in bone marrow from the anterior iliac crest. Am J Clin Pathol **43**: 326-331.

Herd, R. J. M., Blake, G. M., Parker, J. C., *et al.* (1993). Total body studies in normal British women using dual energy X-ray absorptiometry. Br J Radiol **66**(784): 303-308.

Heymsfield, S. B., Lichtman, S., Baumgartner, R. N., *et al.* (1990). Body composition of humans: comparison of two improved four-compartment models that differ in expense, technical complexity, and radiation exposure. Am J Clin Nutr **52**: 52-58.

Hipgrave, B. (2010). Painting in bone on DXA scans. Personal communication.

Ho, C. P., Kim, R. W., Schaffler, M. B., *et al.* (1990). Accuracy of dual-energy radiographic absorptiometry of the lumbar spine: cadaver study. Radiology **176**: 171-173.

Hofer, M. (2007). CT teaching manual, Thieme.

ICRU (2009). International Commission on Radiation Units and Measurements. Report 81. Quantitative Aspects of Bone Densitometry (2009).

Javaid, K. (2011). Denosumab: a new therapy for osteoporosis. Osteoporosis Review **19**(1): 1-6.

Jebb, S. A., Goldberg, G. R., Jennings, G., *et al.* (1995). Dual-energy X-ray absorptiometry measurements of body composition: effects of depth and tissue thickness, including comparisons with direct analysis. Clin Sci **88**: 319-324.

Justesen, J., Stenderup, K., Ebbesen, E. N., *et al.* (2001). Adipocyte tissue volume in bone marrow is increased with aging and in patients with osteoporosis. Biogerontology **2**: 165-171.

Kamel, E. G., McNeill, G. and Van Wijk, M. C. W. (2000). Usefulness of anthropometry and DXA in predicting intra-abdominal fat in obese men and women. Obes Res **8**(1): 36-42.

Kanis, J. A., Johnell, O., Oden, A., *et al.* (2002). Ten-year risk of osteoporotic fracture and the effect of risk facture on screening strategies. Bone **30**: 251-258.

Keene, G. S., Parker, M. J. and Pryor, G. A. (1993). Mortality and morbidity after hip fractures. Br Med J **307**: 1248-1250.

Kelly, T. L. (2006). Auto low density spine and hip: An improved bone map for low density DXA exams. Hologic Report.

Kelly, T. L. (2010). Painting in bone on DXA scans. Personal communication.

Kelly, T. L., Berger, N. and Richardson, T. L. (1998). DXA body composition: theory and practice. Appl Radiat Isot **49**(5/6): 511-513.

Kiebzak, G. M., Faulkner, K. G., Wacker, W., *et al.* (2007). Effect of precision error on T-scores and the diagnostic classification of bone status. J Clin Dens **10**(3): 239-243.

Kohort, W. M. (1998). Preliminary evidence that DEXA provides an accurate assessment of body composition. J Appl Physiol **84**(1): 372-377.

Kotzki, P. O., Mariano-Goulart, D. and Rossi, M. (1991). Theoretical and experimental limits of triple photon energy absorptiometry in the measurement of bone mineral. Phys Med Biol **36**(4): 429-437.

Kuiper, J. W., van Kuijk, C., Grashuis, J. L., *et al.* (1996). Accuracy and the influence of marrow fat on quantitative CT and dual-energy X-ray absorptiometry measurements of the femoral neck in vitro. Osteoporosis Int **6**: 25-30.

Lane, N. E. and Sambrook, P. N. (2006). Osteoporosis and the osteoporosis of rheumatic diseases Mosby Elsevier.

Laskey, M. A. (1996). Dual-energy X-ray absorptiometry and body composition. Nutrition **12**(1): 45-51.

Laskey, M. A., Flaxman, M. E., Barber, R. W., *et al.* (1991). Comparative performance in vitro and in vivo of Lunar DPX and Hologic QDR-1000 dual energy X-ray absorptiometers. Br J Radiol **64**(767): 1023-1029.

Leslie, W. D., Ludwig, S. M. and Morin, S. (2010). Abdominal fat from spine dual-energy X-ray absorptiometry and risk for subsequent diabetes. J Clin Endocrinol Metab **95**(7): 3272-3276.

Lewis, M. K., Blake, G. M. and Fogelman, I. (1994). Patient dose in dual X-ray absorptiometry. Osteoporos Int **4**: 11-15.

Mack, P. B., O'Brien, A. T., Smith, J. M., *et al.* (1939). A method for estimating the degree of mineralization of bones from tracings of roentgenograms. Science **89**: 467.

Marie, P. J., Ammann, P., Boivin, G., *et al.* (2001). Mechanisms of action and therapeutic potential of strontium in bone. Calcif Tissue Int **69**: 121-129.

Marshall, D., Johnell, O. and Wedel, H. (1996). Meta-analysis of how well measures of bone mineral density predict occurrence of osteoporotic fractures. BMJ **312**(7041): 1254-1259.

Martin, P., Verhas, M., Als, C., *et al.* (1993). Influence of patient's weight on dual-photon absorptiometry and dual-energy X-ray absorptiometry measurements of bone mineral density. Osteoporosis Int **3**: 198-203.

Mazess, R. B., Bisek, J. and Trempe, J. (1991a). Effects of tissue thickness on fat content and bone using DEXA. Bone and Tooth Society Meeting September 1991s: 280.

Mazess, R. B., Trempe, J. A., Bisek, J. P., *et al.* (1991b). Calibration of dual-energy X-ray absorptiometry for bone density. J Bone Miner Res **6**(8): 799-806.

Meunier, P. J., Roux, C., Seeman, E., *et al.* (2004). The effects of strontium ranelate on the risk of vertebral fracture in women with postmenopausal osteoporosis. N Engl J Med **350**(5): 459-468.

Michael, G. J. and Henderson, C. J. (1998). Monte Carlo modelling of an extended DXA technique. Phys Med Biol **43**: 2583-2596.

Milliken, L. A., Going, S. B. and Lohman, T. G. (1996). Effects of variations in regional composition on soft tissue measurements by dual-energy X-ray absorptiometry. Int J Obes **20**(7): 677-682.

Mosekilde, L. and Mosekilde, L. (1990). Sex differences in age-related changes in vertebral body size, density and biomechanical competence in normal individuals. Bone **11**: 67-73.

National Osteoporosis Society (2006). Drug Treatments for Osteoporosis. Patient information booklet.: 3.

National Osteoporosis Society (2011). Hormone replacement therapy for the treatment and prevention of osteoporosis. Osteoporosis Review **19**(1): 8-12.

Nielsen, S. P., Barenholdt, O., Diessel, E., *et al.* (1998). Linearity and accuracy errors in bone densitometry. Br J Radiol **71**: 1062-1068.

Nord, R. H. (1998). DXA body composition properties: inherent in the physics or specific to scanner type? Appl Radiat Isot **49**(5/6): 517-518.

Nord, R. H. and Payne, R. K. (1990). Standards for body composition calibration in DEXA. Current Research in Osteoporosis and bone Mineral Measurement. E. F. J. Ring. London, British Institute of Radiology**:** 27-28.

Osnes, E. K., Lofthus, C. M., Meyer, H. E., *et al.* (2004). Consequences of hip fracture on activities of daily life and residential needs. Osteoporosis Int **15**: 567-574.

Park, Y. W., Heymsfield, S. B. and Gallagher, D. (2002). Are dual-energy X-ray absorptiometry regional estimates associated with visceral adipose tissue mass? Int J Obes **26**: 978-983.

Peel, N. F. A. and Eastell, R. (1995). Comparison of rates of bone loss from the spine measured using two manufacturers' densitometers. J Bone Miner Res **10**(11): 1796-1801.

Pettit, R. J., Jones, E. A. and Evans, W. D. (2005). The effect of varying the width of the analysis box on the results obtained from paediatric lumbar spine DXA. Third International Conference on Children's Bone Health. Sorrento. **36 (Suppl 1):** S67.

Prior, B. M., Cureton, K. J., Modlesky, C. M., *et al.* (1997). In vivo validation of whole body composition estimates from dual-energy X-ray absorptiometry. J Appl Physiol **83**(2): 623-630.

Pritchard, J. E., Nowson, C. A., Strauss, B. J., *et al.* (1993). Evaluation of dual energy X-ray absorptiometry as a method of measurement of body fat. Eur J Clin Nutr **47**(3): 216-228.

Ramsdale, S. J. and Bassey, E. J. (1994). Changes in bone mineral density associated with dietry-induced loss of body mass in young women. Clin Sci **87**(3): 343-348.

RCP (1999). Royal College of Physicians. Osteoporosis: clinical guidelines for prevention and treatment. London, England. .

Reed, G. W. (1966). The assessment of bone mineralization from the relative transmission of ^{241}Am and ^{137}Cs radiations. Phys. Med. Biol. **11**: 174.

Reginster, J. Y., Seeman, E., De Vernojoul, M. C., *et al.* (2005). Strontium ranelate reduces the risk of nonvertebral fractures in postmenopausal women with osteoporosis: Treatment of peripheral osteoporosis (TROPOS) study. J Clin Endocrinol Metab **90**(5): 2816-2822.

Roos, B. O., Hansson, T. H. and Skoldborn, H. (1980). Dual photon absorptiometry in lumbar vertebrae: Evaluation of the baseline error. Acta Radiologica Oncology **19**: 111-114.

Rosholm, A., Hyldstrup, L., Baeksgaard, L., *et al.* (2001). Estimation of bone mineral density by digital X-ray radiogrammetry: theoretical background and clincal testing. Osteoporosis Int **12**: 961-969.

Roubenhoff, R., Kehayias, J. J., Dawson-Hughes, B., *et al.* (1993). Use of dual-energy X-ray absorptiometry in body-composition studies: not yet a "gold-standard". Am J Clin Nutr **58**: 589-591.

Seeley, R. R., Stephens, T. D. and Tate, P. (1988). Anatomy and physiology (Second edition), Mosby Year Book.

Sheng, H. and Huggins, R. A. (1979). A review of body composition studies with emphasis on total body water and fat. Am J Clin Nutr **32**: 630-647.

Shypailo, R. J., Posada, J. K. J. and Ellis, K. J. (1998). Whole-body phantoms with anthropomorphic-shaped skeletons for evaluation of dual-energy X-ray absorptiometry measurements. Appl Radiat Isot **49**(5/6): 503-505.

Siris, E. and Delmas, P. D. (2008). Assessment of 10-year absolute fracture risk: a new paradigm with worldwide application. Osteoporosis Int **19**: 383-384.

Snead, D. B., Birge, S. J. and Kohort, W. M. (1993). Age-related differences in body composition by hydrodensitometry and dual-energy X-ray absorptiometry. J Appl Physiol **74**(2): 770-775.

Sobnack, R., Lees, B., Stevenson, J. C., *et al.* (1990). Inconsistent bone mineral density results of lumbar spine specimens using dual energy X-

ray (bone) absorptiometers from three manufacturers. Nucl Med Comm: 193.

Sorenson, J. A., Duke, P. R. and Smith, S. W. (1989). Simulation studies of dual-energy X-ray absorptiometry. Med. Phys. **16**(1): 75-80.

Stein, I. (1937). The evaluation of bone density in the roentgenogram by the use of ivory wedges. Am J Roentgenol Rad Ther **37**: 678-682.

Stein, J. A. (1990). Bone densitometer. United States Patent, Hologic, Inc., Waltham, Mass.

Suh, Y., Kim, D. and Lee, I. (2002). Usefulness of lumbar AP spine DXA for measuring the percentage of perilumbar regional fat and predicting visceral fat in obese postmenopausal women. Nutrition **18**: 84-85.

Svendsen, O. L., Haarbo, J., Hassager, C., *et al.* (1993a). Accuracy of measurements of body composition by dual-energy X-ray absorptiometry in vivo. Am J Clin Nutr **57**: 605-608.

Svendsen, O. L., Hassager, C., Bergmann, I., *et al.* (1993b). Measurement of abdominal and intra-abdominal fat in postmenopausal women by dual energy X-ray absorptiometry and anthropometry: comparision with computerized tomography. Int J Obes **17**: 45-51.

Svendsen, O. L., Hassager, C. and Christiansen, C. (1993c). Effect of an energy-restrictive diet, with or without exercise, on lean tissue mass, resting metabolic rate, cardiovascular risk factors, and bone in overweight postmenopausal women. Am J Med **95**: 131-140.

Svendsen, O. L., Hassager, C., Skodt, V., *et al.* (1995). Impact of soft tissue on in vivo accuracy of bone mineral measurements in the spine, hip, and forearm: a human cadaver study. J Bone Miner Res **10**(6): 868-873.

Svendsen, O. L., Hendel, H. W., Gotfredsen, A., *et al.* (2002). Are soft tissue composition of bone and non-bone pixels in spinal bone mineral measurements by DXA similar? Impact of weight loss. Clin Physiol & Func Im **22**: 72-77.

Swanpalmer, J., Kullenberg, R. and Hannson, T. (1998). Measurement of bone mineral using multiple-energy X-ray absorptiometry. Phys Med Biol **43**: 379-387.

Tanaka, Y. and Inoue, T. (1976). Fatty marrow in the vertebrae. A parameter for hematopoietic activity in the aged. J Gerontol **31**(5): 527-532.

Tothill, P. (2005). Dual-energy X-ray absorptiometry measurements of total-body bone mineral during weight change. J Clin Dens **8**(1): 31-38.

Tothill, P. and Avenell, A. (1994a). Errors in dual-energy X-ray absorptiometry of the lumbar spine owing to fat distribution and soft tissue thickness during weight change. Br J Radiol **67**(793): 71-75.

Tothill, P. and Avenell, A. (1998). Anomalies in the measurement of changes in bone mineral density of the spine by dual-energy X-ray absorptiometry. Calcif Tissue Int **63**: 126-133.

Tothill, P., Avenell, A., Love, J., *et al.* (1994b). Comparisons between Hologic, Lunar and Norland dual-energy X-ray absorptiometers and other techniques used for whole-body soft tissue measurements. Eur J Clin Nutr **48**(11): 781-794.

Tothill, P., Avenell, A. and Reid, D. M. (1994c). Precision and accuracy of measurments of whole-body bone mineral: comparisons between Hologic, Lunar and Norland dual-energy X-ray absorptiometers. Br J Radiol **67**(804): 1210-1217.

Tothill, P., Fenner, J. A. K. and Reid, D. M. (1995). Comparisons between three dual-energy X-ray absorptiometers used for measuring spine and femur. Br J Radiol **68**(810): 621-629.

Tothill, P. and Hannan, W. J. (2007). Precision and accuracy of measuring changes in bone mineral density by dual-energy X-ray absorptiometry. Osteoporosis Int **18**: 1515-1523.

Tothill, P., Hannan, W. J., Cowen, S., *et al*. (1997). Anomalies in the measurement of changes in total-body bone mineral by dual-energy X-ray absorptiometry during weight change. J Bone Miner Res **12**(11): 1908-1921.

Tothill, P., Hannan, W. J. and Wilkinson, S. (2001). Comparisons between a pencil beam and two fan beam dual energy X-ray absorptiometers used for measuring total body bone and soft tissue. Br J Radiol **74**: 166-176.

Tothill, P., Laskey, M. A., Orphanidou, C. I., *et al.* (1999). Anomalies in dual energy X-ray absorptiometry measurements of total-body bone mineral during weight change using Lunar, Hologic and Norland instruments. Br J Radiol **72**: 661-669.

Tothill, P. and Pye, D. W. (1992). Errors due to non-uniform distribution of fat in dual X-ray absorptiometry of the lumbar spine. Br J Radiol **65**(777): 807-813.

Valkema, R., Verheij, L. F., Blokland, A. K., *et al.* (1990). Limited precision of lumbar spine dual-photon absorptiometry by variations in the soft-tissue background. J Nucl Med **31**(11): 1774-1781.

van Staa, T. P., Dennison, E. M., Leufkens, H. G. M., *et al.* (2001). Epidemiology of fractures in England and Wales. Bone **29**(6): 517-522.

Vestergaard, P., Borglum, J., Heickendorff, K., *et al.* (2000). Artifact in bone mineral measurements during a very low calorie diet. J Clin Dens **3**(1): 63-71.

Wahner, H. W., Dunn, W. L., Mazess, R. B., *et al.* (1985). Dual-photon Gd-153 absorptiometry of bone. Radiology **156**: 203-206.

Wahner, H. W. and Fogelman, I. (1994). The evaluation of osteoporosis: Dual energy X-ray absorptiometry in clinical practice.

Webber, C. (1987). The effect of fat on bone mineral measurements in normal subjects with recommended values of bone, muscle, and fat attenuation coefficients. Clin Phys Physiol Meas **8**: 143-158.

World Health Organisation. Assessment of fracture risk and its application to screening for postmenopausal osteoporosis. WHO technical report. Series 843. WHO, Geneva, Switzerland. 1994.

Yang, S., Fuerst, T., Lu, Y., *et al.* (1997). Changes in spine bone mineral density correlate with changes in spine area: an artifact of edge detection methods? J Bone Min Res **12**(Supplement 1): S176.

Yu, E. W., Thomas, B. J., Brown, J. K., *et al.* (2012). Simulated increases in body fat and errors in bone mineral density measurements by DXA and QCT. J Bone Miner Res **27**(1): 119-124.

Appendix A

Quality Control Plots for the Hologic Spine Phantom Covering the Period of the Current Study

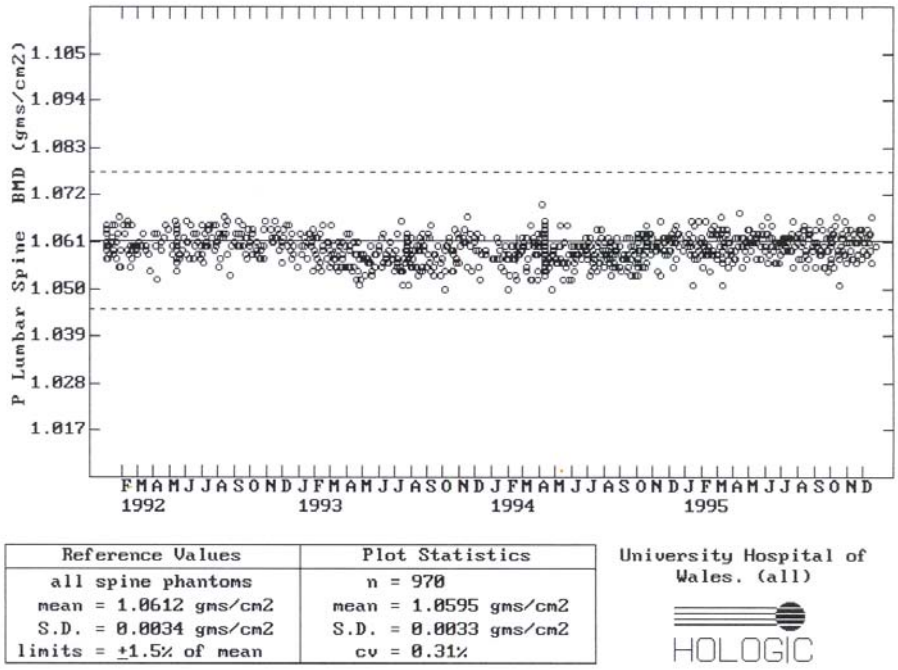

Figure A1 Quality control plot for L1 to L4 BMD of the Hologic spine phantom between 1992 and 1995.

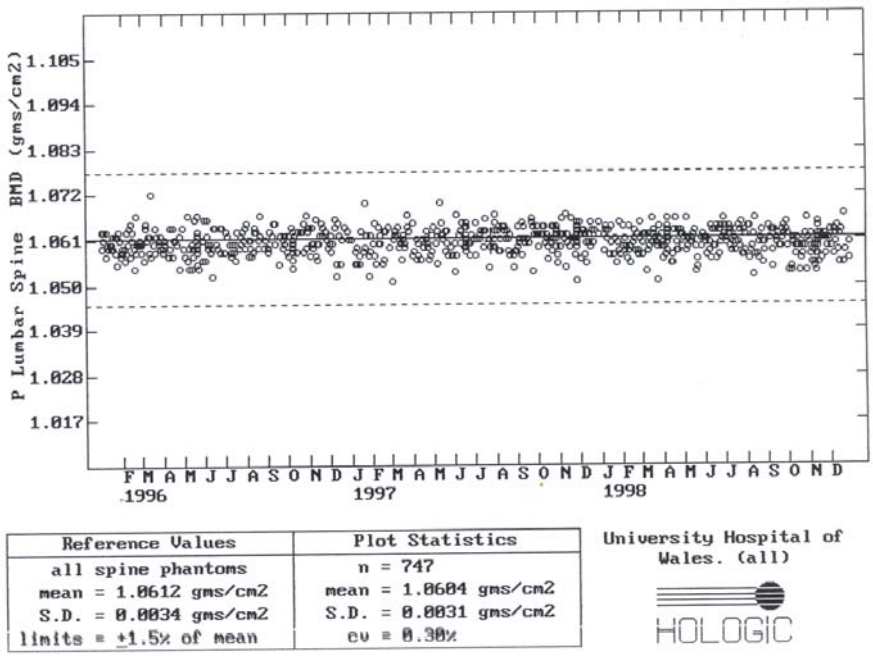

Figure A2 Quality control plot for L1 to L4 BMD of the Hologic spine phantom between 1996 and 1998.

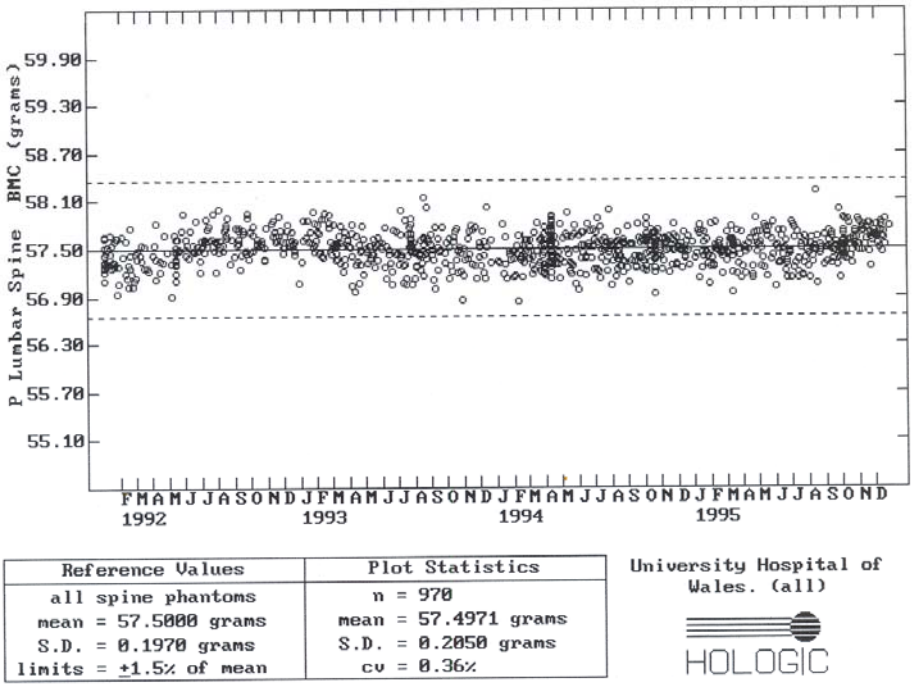

Figure A3 Quality control plot for L1 to L4 BMC of the Hologic spine phantom between 1992 and 1995.

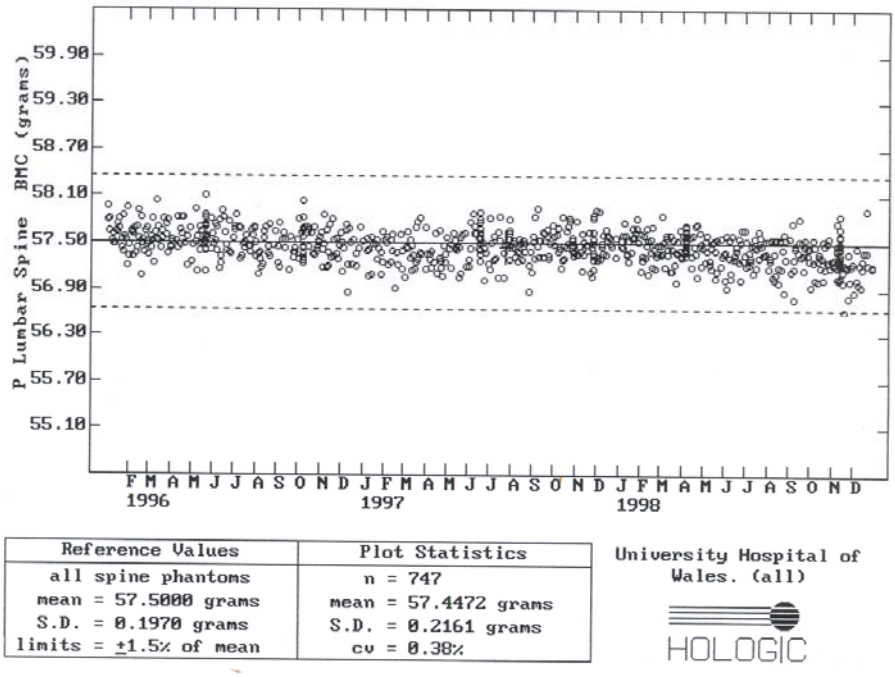

Figure A4 Quality control plot for L1 to L4 BMC of the Hologic spine phantom between 1996 and 1998.

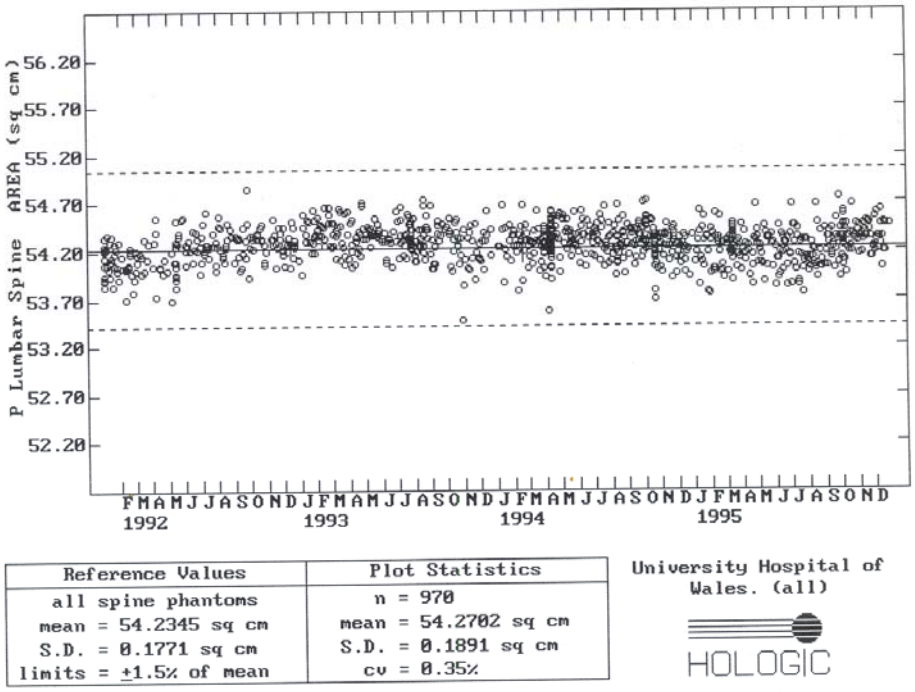

Figure A5 Quality control plot for L1 to L4 BA of the Hologic spine phantom between 1992 and 1995.

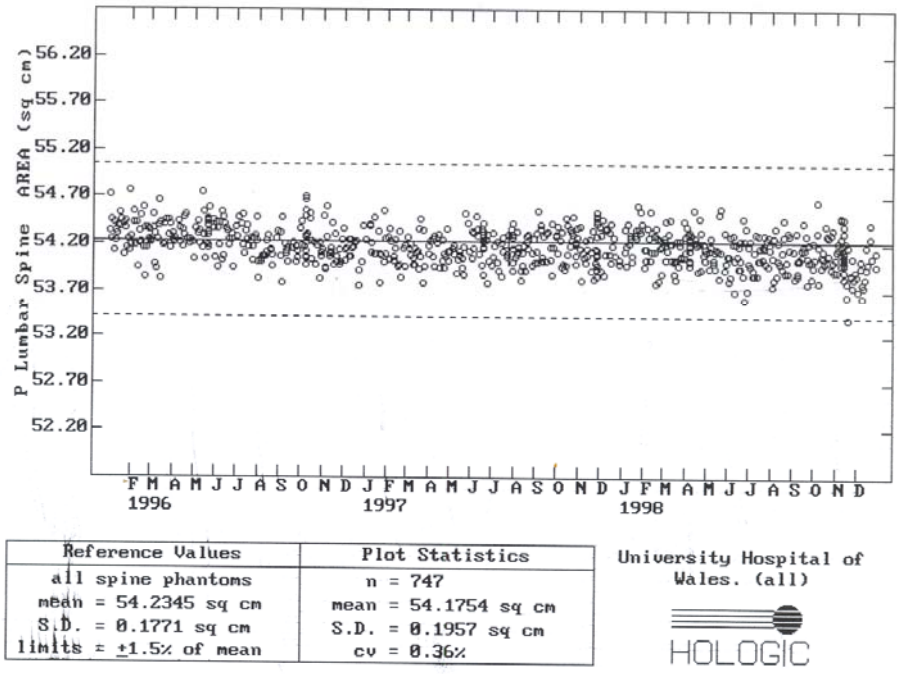

Figure A6 Quality control plot for L1 to L4 BA of the Hologic spine phantom between 1996 and 1998.

Appendix B

Prediction of Inaccuracy in Lumbar Spine BMD for a group of Patients with Confirmed Osteopenia or Osteoporosis

The results presented in this appendix were obtained when performing data analysis on lumbar spine and whole body images as discussed in chapter 7 for a group of subjects with a low BMD.

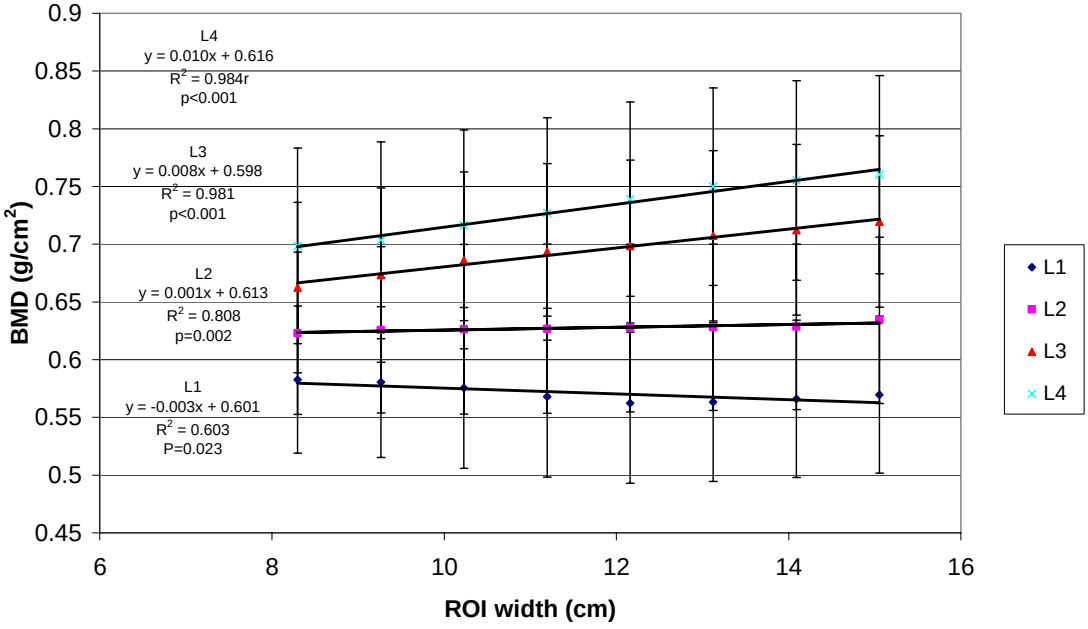

Figure B1 Relationship between measured lumbar spine BMD and the width of the lumbar spine ROI. Data are the average (± 95% CI) for 10 subjects in OST group. SEE: L1 = 0.005 g/cm^2, L2 = 0.002 g/cm^2, L3 = 0.003 g/cm^2, L4 = 0.003 g/cm^2. Errors in slope were L1±0.001 g/cm^2 per cm, L2±<0.001 g/cm^2 per cm, L3±<0.001 g/cm^2 per cm, L4±0.001 g/cm^{2}per cm.

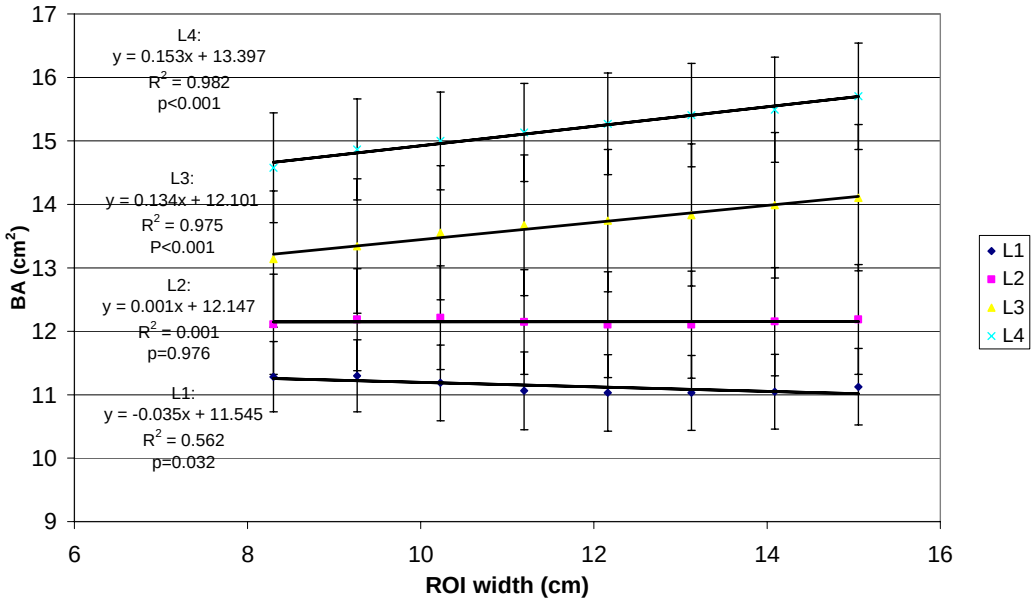

Figure B2 Relationship between measured lumbar spine BA and the width of the lumbar spine ROI. Data are the average (± 95% CI) for 10 subjects in OST group. SEE: L1 = 0.08 cm^2, L2 = 0.05 cm^2, L3 = 0.05 cm^2, L4 = 0.05 cm^2. Errors in slope were L1±0.01 cm^2 per cm, L2±0.01 cm^2 per cm, L3±0.01 cm^2 per cm, L4 ±0.01 cm^2 per cm.

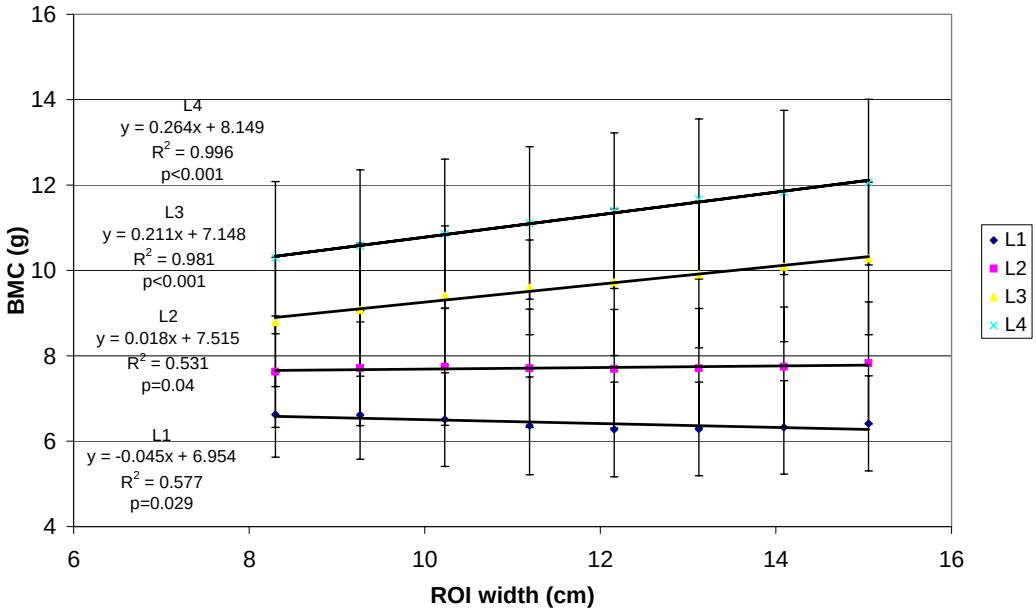

Figure B3 Relationship between measured lumbar spine BMC and the width of the lumbar spine ROI. Data are the average (± 95% CI) for 10 subjects in OST group. SEE: L1 = 0.1g, L2 = 0.04 g, L3 = 0.08 g, L4 = 0.04 g. Errors in slope were L1±0.02 g/cm, L2±0.01 g/cm, L3±0.01 g/cm. L4±0.01 g/cm.

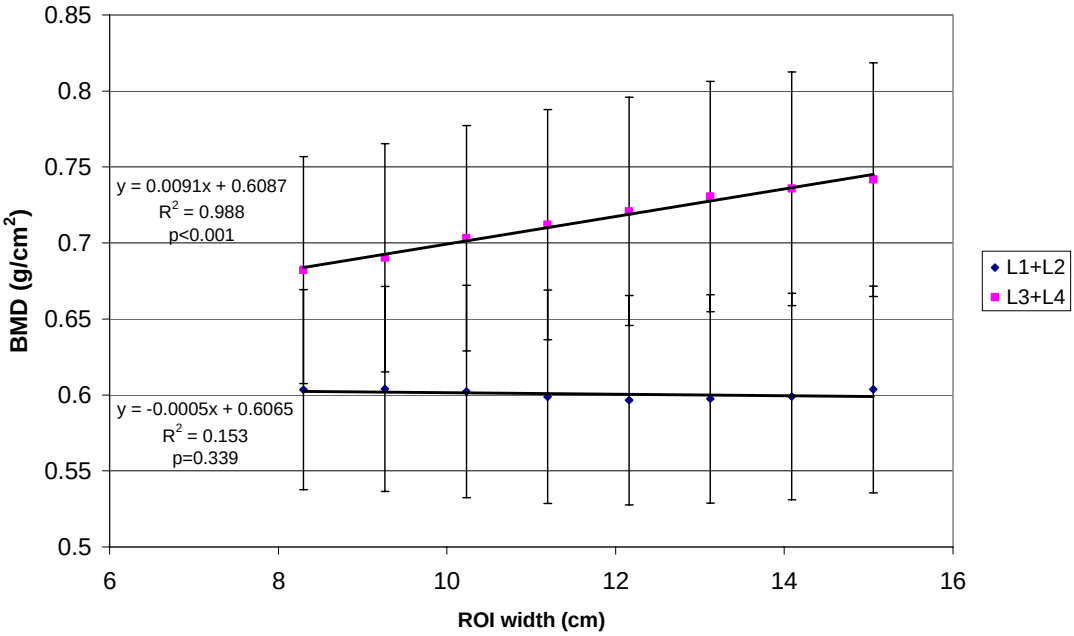

Figure B4 Relationship between measured combined L1+L2 and L3+L4 BMD and the width of the lumbar spine ROI. Data are the average (± 95% CI) for 10 subjects within the OST group. SEE: L1+L2 = 0.003 g/cm^2; L3+L4 = 0.003 g/cm^2. Errors in slope are L1+L2 ±<0.001 g/cm^2 per cm and L3+L4 ±<0.001 g/cm^2 per cm.

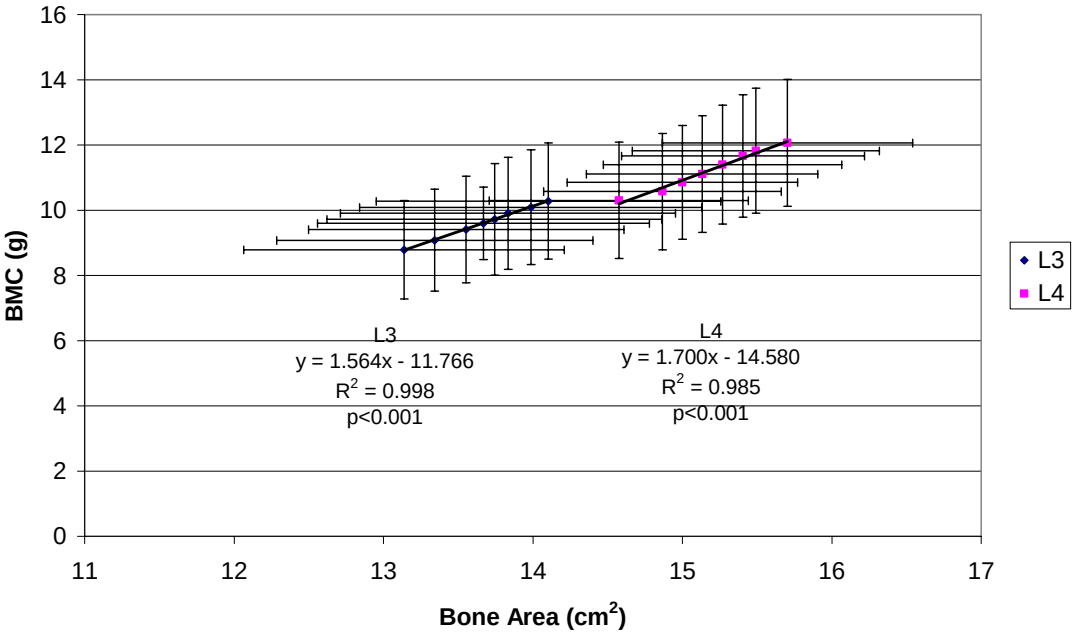

Figure B5 Relationship between BMC and BA and the width of the lumbar spine ROI for L3 and L4. Data are the average for 10 subjects within the OST group (±95% CI). Errors for slope of regression lines are ±0.026 g/cm^2 for L3 and ±0.087g/cm^2 for L4. Pearson's correlation coefficient was L3 = 0.999 (p<0.001) and L4=0.992 (p<0.001).

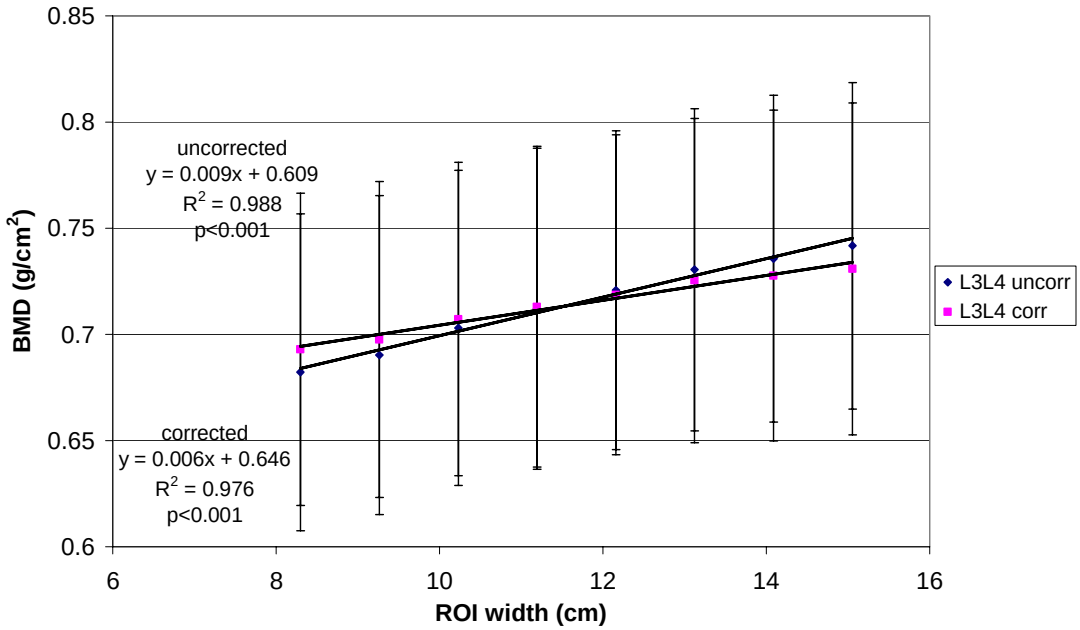

Figure B6 Relationship between the corrected and uncorrected L3+L4 BMD and the width of the lumbar spine ROI. Data are the average for 10 subjects (±95% CI) within the OST group. SEE: uncorrected = 0.003 g/cm^2 and corrected BMD = 0.002 g/cm^2. Standard error of slope is ±<0.001 g/cm^2 per cm for both uncorrected and corrected L3+L4 BMD.

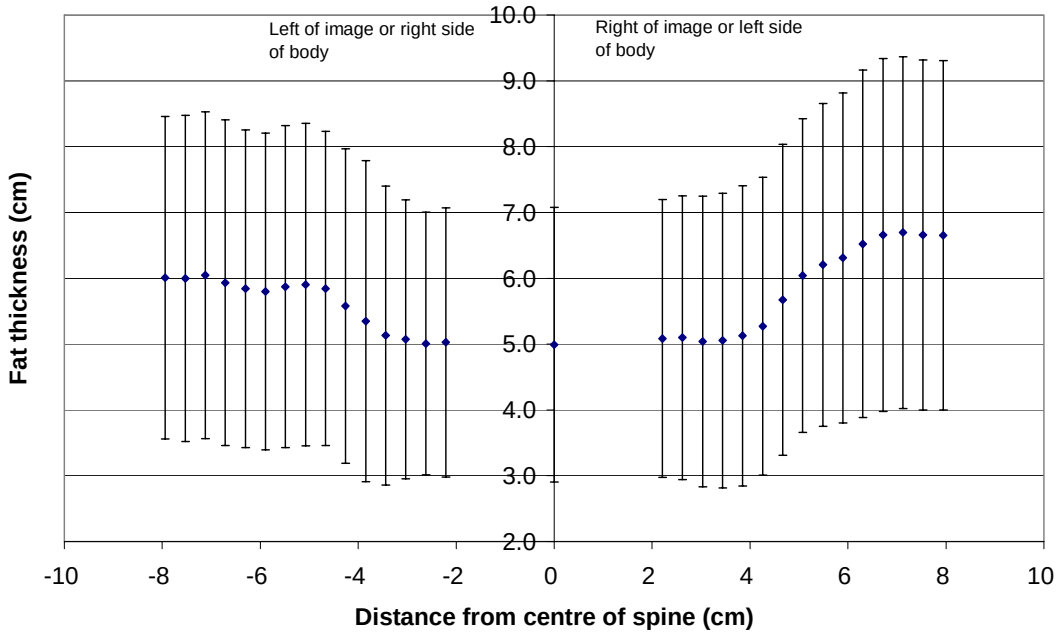

Figure B7 Variation in abdominal fat thickness at the level of L3+L4 with distance from the centre of lumbar spine. Data are average for 10 subjects in OST group (± 95% CI).

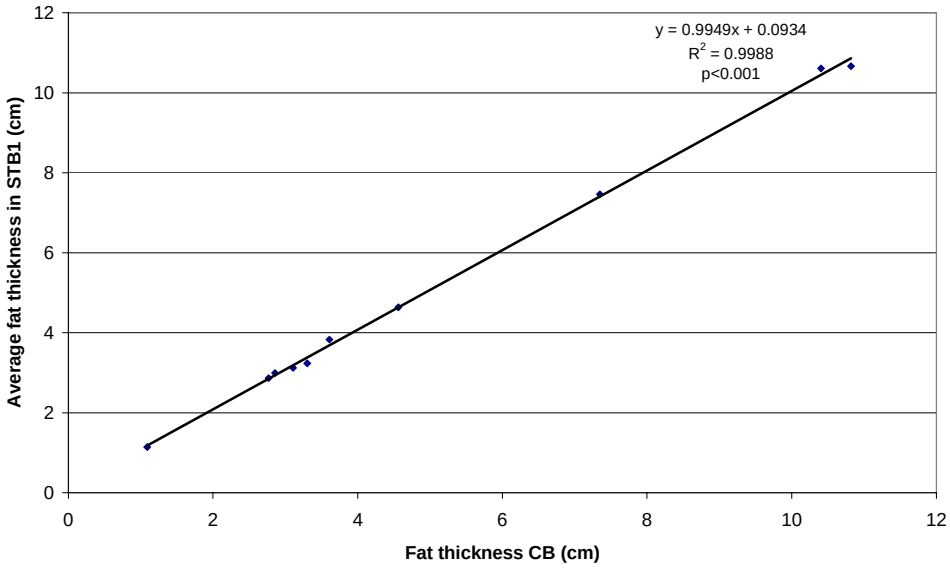

Figure B8 Relationship between fat thickness in the CB over the vertebrae and the first STB adjacent to the vertebrae. Standard error of gradient is 0.012 cm per cm and SEE = 0.12 cm.

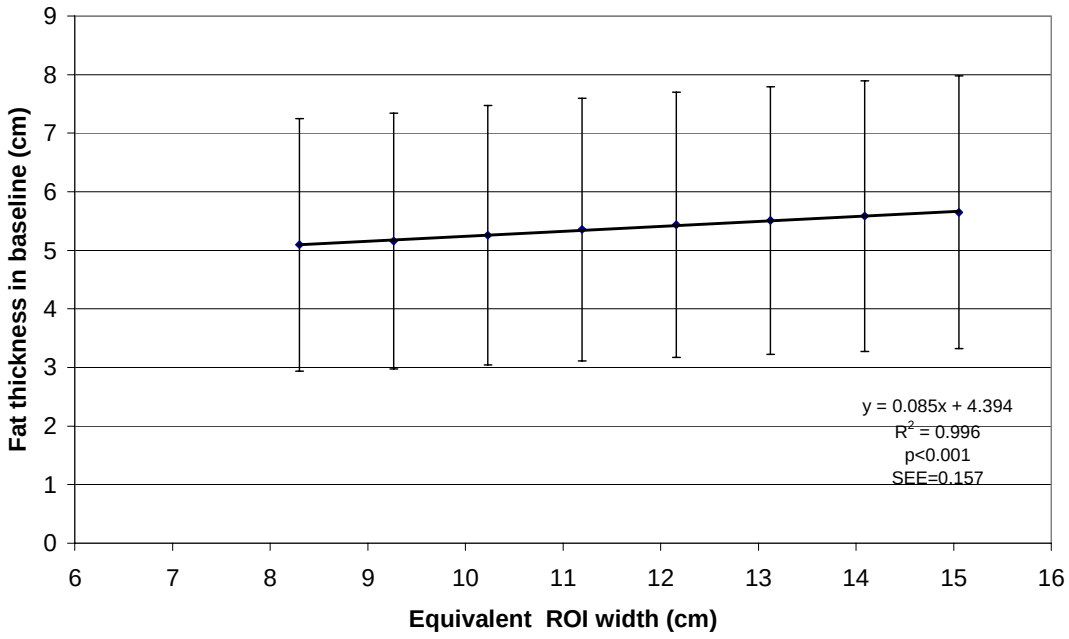

Figure B9 Average fat thickness in soft tissue regions adjacent to L3+L4 that are equivalent to those used as a baseline region for lumbar spine BMD analysis. The data are averaged over 10 subjects in OST group (±95% CI). SEE = 0.01 cm and standard error in gradient is ± 0.002 cm fat per cm.

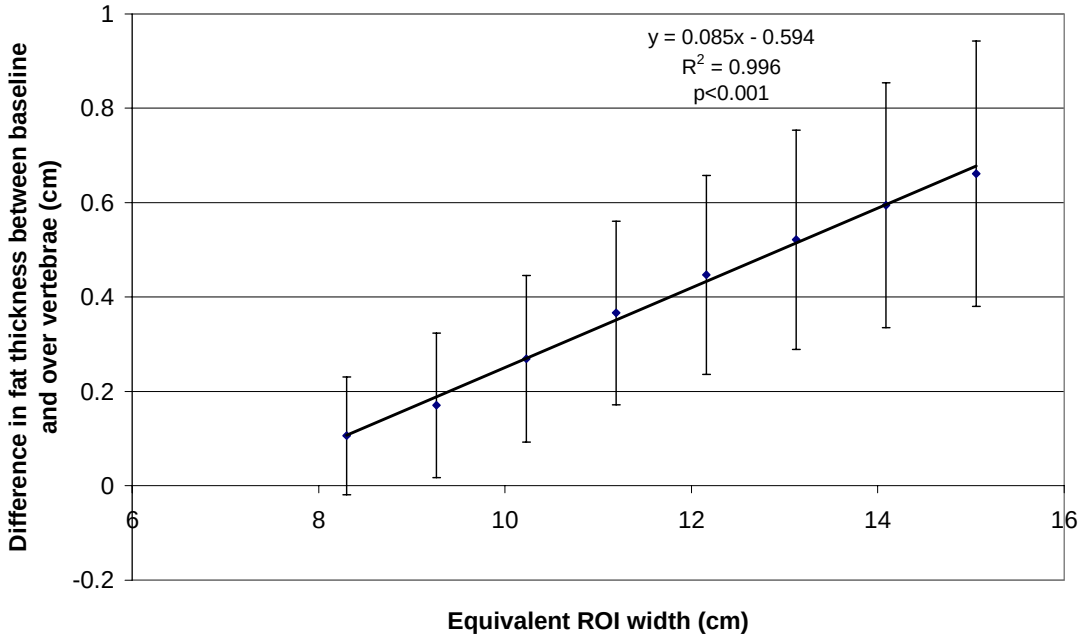

Figure B10 Fat thickness in the baseline soft tissue relative to that over vertebrae measured from WB images for ROI widths equivalent to those used in the measurement of L3+L4 BMD. Linear regression analysis shows that a ROI width of 7 cm would give an equal fat thickness in the soft tissue baseline and over vertebrae. Data are averaged over 10 subjects within OST group (±95% CI). SEE = 0.01 cm and standard error of gradient is ±0.002 cm fat per cm.

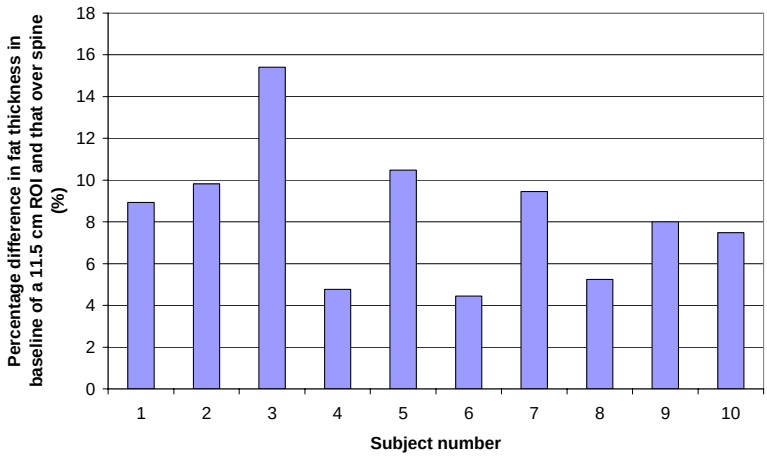

Figure B11 Comparison of the fat thickness over the spine with the average in the baseline of a 11.5 cm ROI at the level of L3+L4. Expressed as a percentage difference the average difference was 8.4 ± 3.3 % i.e. the fat thickness in the baseline was approximately 8% greater than over the vertebrae (range = 4.4% to 15.4%).

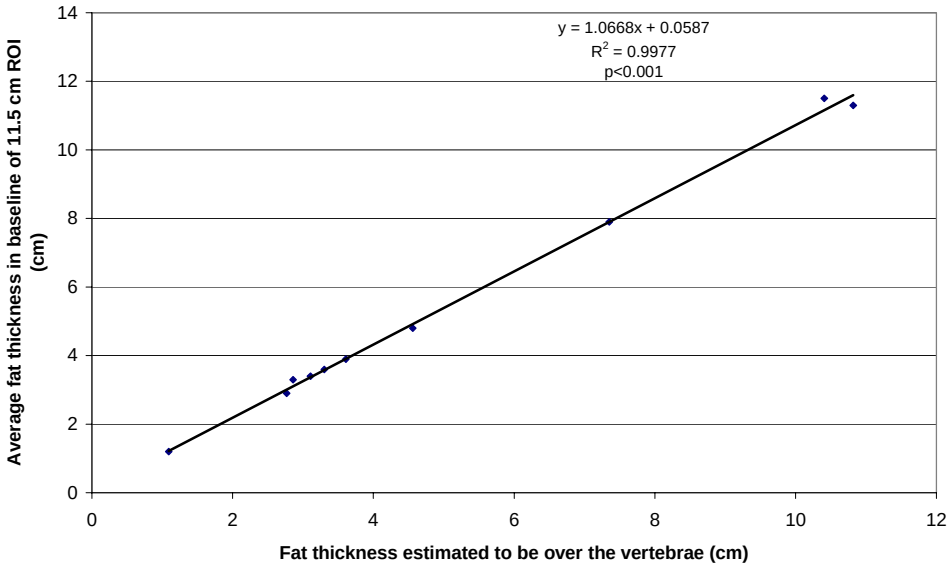

Figure B12 Relationship between the fat thickness in the baseline of the Hologic recommended ROI width and that in that over the vertebrae at the level of L3+L4 for 10 subjects in OST group. SEE = 0.184 cm, standard error of gradient = 0.018 cm per cm.

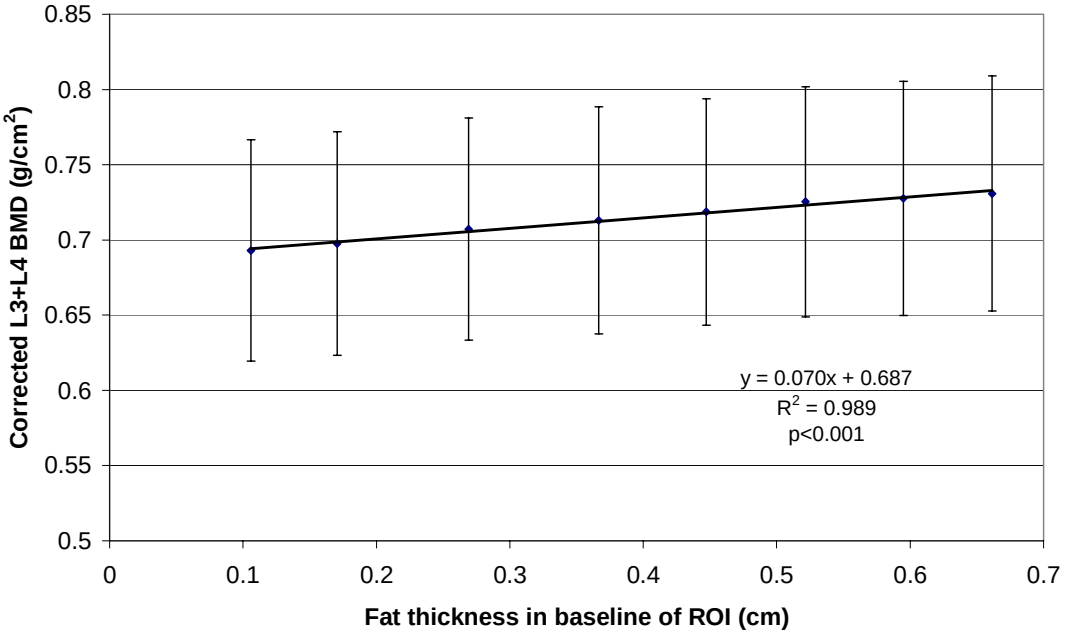

Figure B13 Relationship between the fat thickness within the soft tissue baseline extracted from DXA WB scans and the phantom corrected L3+L4 BMD for equivalent ROI width. Each data point represents a different width of ROI from 8.3 cm to 15.1 cm. Data are for the L3+L4 level and averaged over 10 subjects. BMD is mean ± 95% CI. SEE = 0.002 g/cm^2 and error in gradient is ±0.003 g/cm^2 per cm fat.

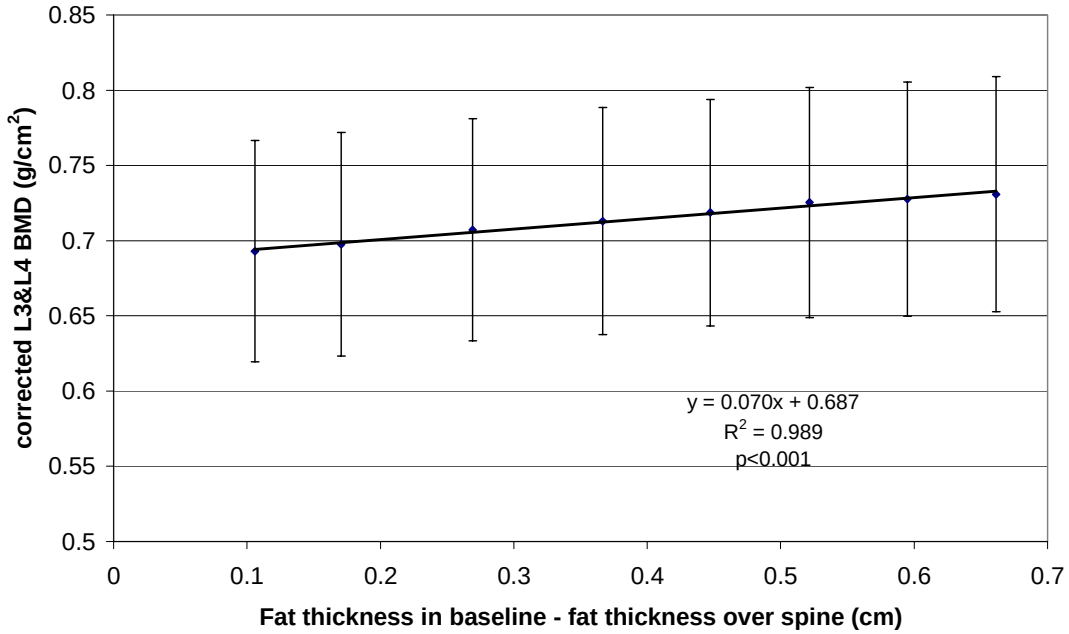

Figure B14 Relationship between the fat thickness in baseline relative to that to in the CB over spine and the reported L3+L4 BMD for average of 10 subjects in OST group (±95% CI). SEE = 0.002 g/cm^2, error on slope = 0.003 g/cm^2 per cm.

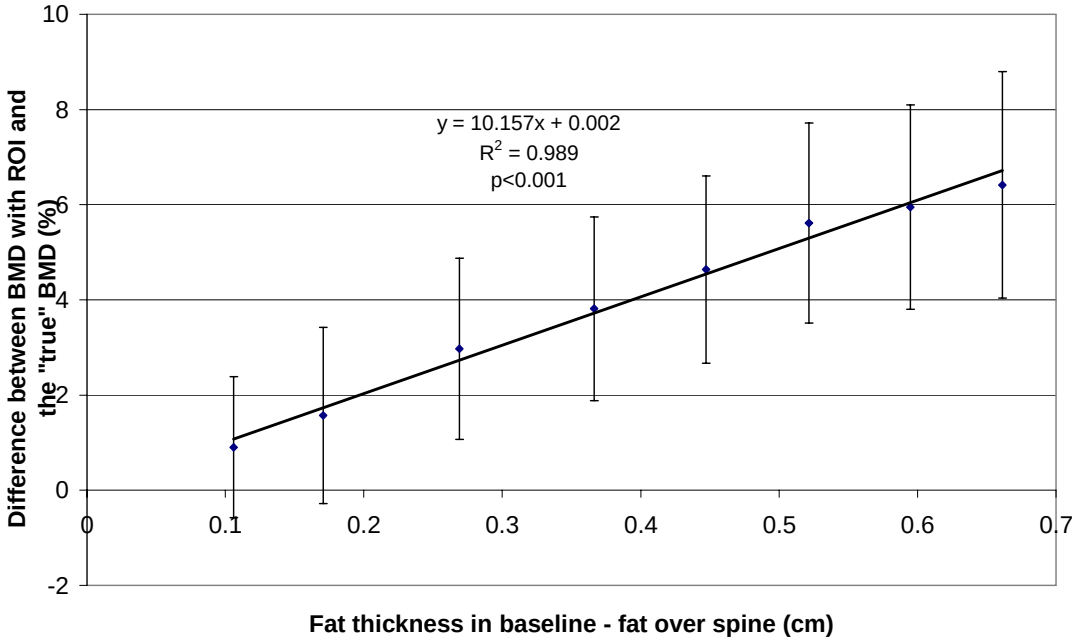

Figure B15 Relationship between the fat thickness in the baseline relative to that over the vertebrae and the potential errors in L3+L4 due to a non-uniform fat distribution. Errors in BMD estimated by assuming true BMD is 0.687 g/cm^2. Data are for L3+L4 level and averaged over 10 subjects in OST group (± 95% CI). SEE: 0.2% and error of gradient is 0.5 % per cm.

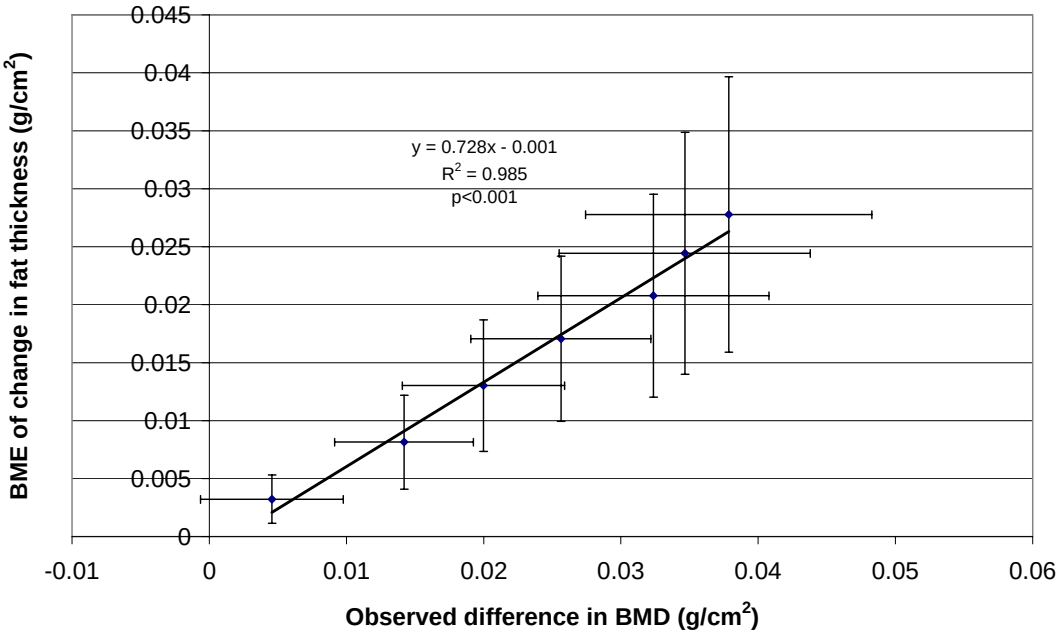

Figure B16 Relationship between the observed difference in phantom corrected L3+L4 BMD and the bone mineral equivalence (BME) of the difference in fat thickness within the baseline of equivalent width ROI. The data are average over 10 subjects within OST group. SEE = 0.001 g/cm^2, error of gradient ±0.031 g/cm^2 per g/cm^2. Error bars are ±95% CI.

Appendix C

Prediction of Inaccuracy in Lumbar Spine BMD for a group of Male Patients Three months Post Renal Transplant

The results presented in this appendix were obtained when performing data analysis on DXA lumbar spine and whole body images, as discussed in chapter 7, for a group of 20 male subjects 3 months post renal transplant (MRTx).

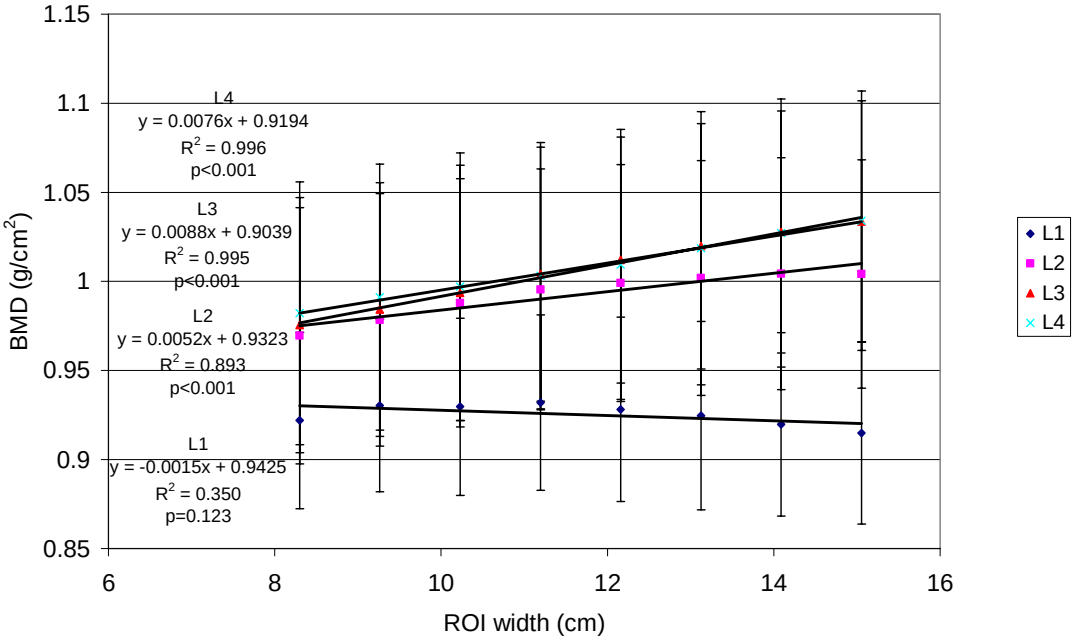

Figure C1 Relationship between measured lumbar spine BMD and the width of the lumbar spine ROI. Data are the average (± 95% CI) for 20 subjects in MRTx group. SEE: L1 = 0.005 g/cm^2, L2 = 0.005 g/cm^2, L3 = 0.002 g/cm^2, L4 = 0.001 g/cm^2. Errors in slope were L1±0.001 g/cm^2 per cm, L2±0.001 g/cm^2 per cm, L3±<0.001 g/cm^2 per cm, L4±<0.001 g/cm^{2}per cm.

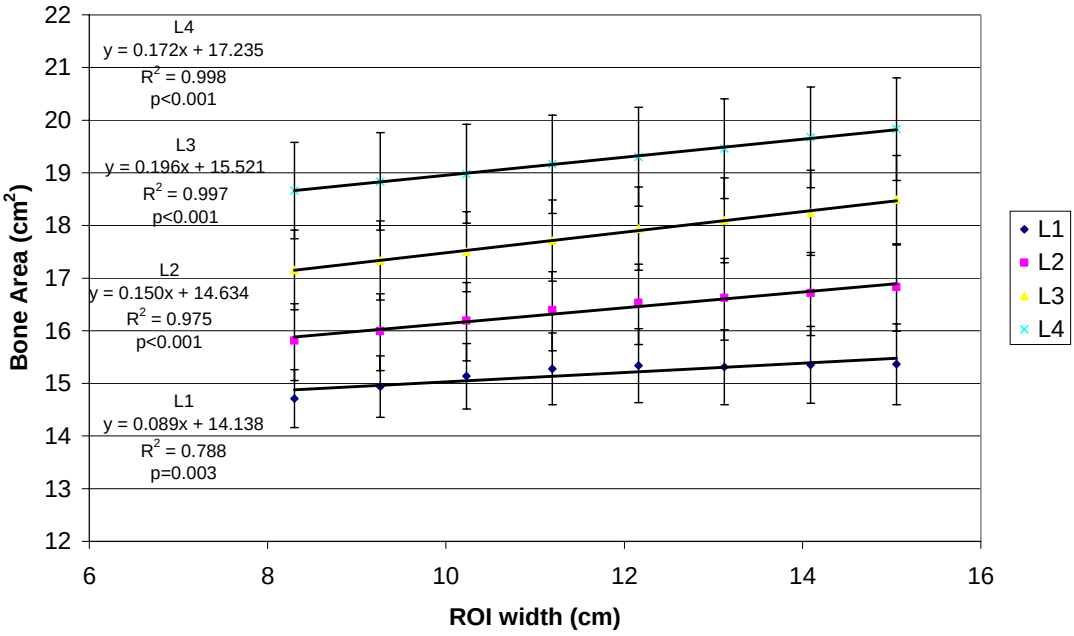

Figure C2 Relationship between measured lumbar spine BA and the width of the lumbar spine ROI. Data are the average (± 95% CI) for 20 subjects in MRTx group. SEE: L1 = 0.12 cm^2, L2 = 0.06 cm^2, L3 = 0.03 cm^2, L4 = 0.02 cm^2. Errors in slope were L1±0.02 cm^2 per cm, L2±0.01 cm^2 per cm, L3±<0.01 cm^2 per cm, L4 ±0.03 cm^2 per cm.

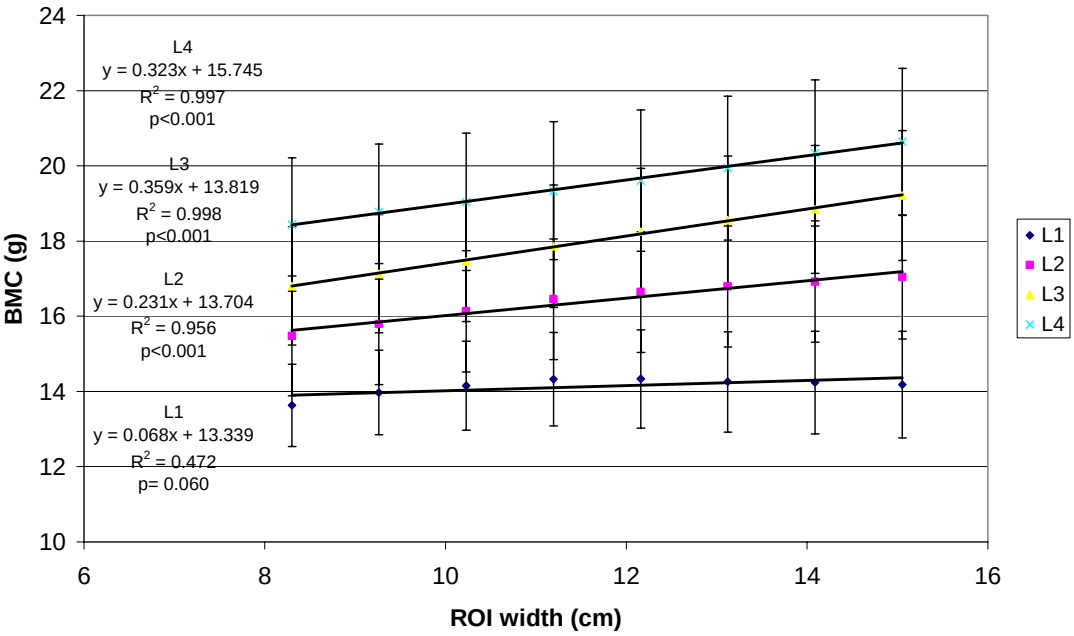

Figure C3 Relationship between measured lumbar spine BMC and the width of the lumbar spine ROI. Data are the average (± 95% CI) for 20 subjects in MRTx group. SEE: L1 = 0.18 g, L2 = 0.13 g, L3 = 0.04 g, L4 = 0.04 g. Errors in slope were L1±0.03 g/cm, L2±0.02 g/cm, L3±0.01 g/cm. L4±0.01 g/cm.

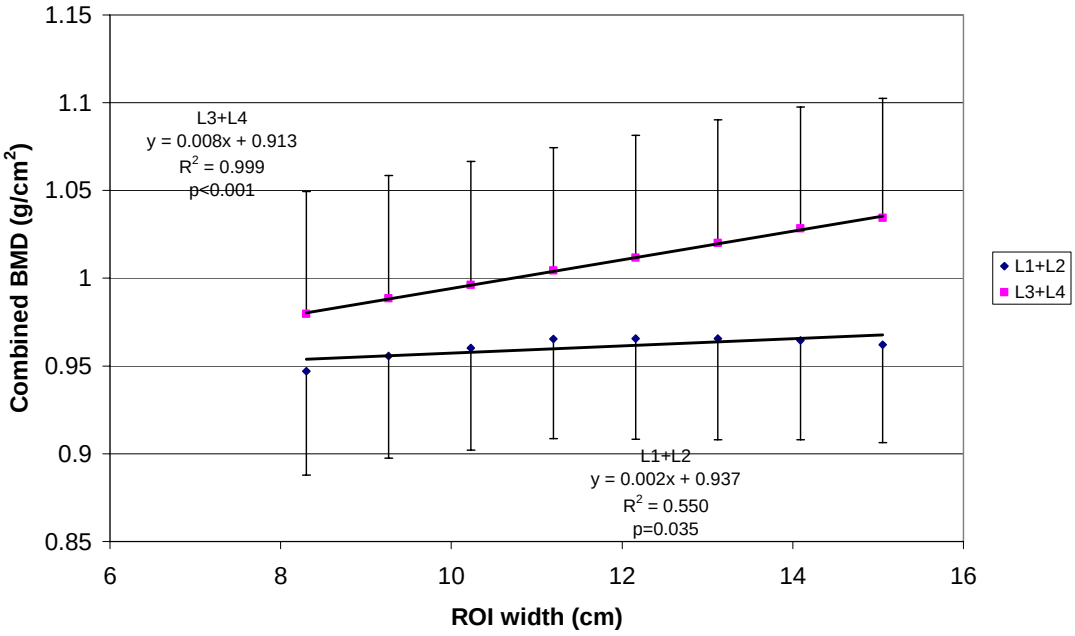

Figure C4 Relationship between measured combined L1+L2 and L3+L4 BMD and the width of the lumbar spine ROI. Data are the average (± 95%) for 20 subjects within the MRTx group. SEE: L1+L2 = 0.005 g/cm^2; L3+L4 = 0.001 g/cm^2. Errors in slope are L1+L2± 0.001 g/cm^2 per cm and L3+L4 ±<0.001 g/cm^2 per cm.

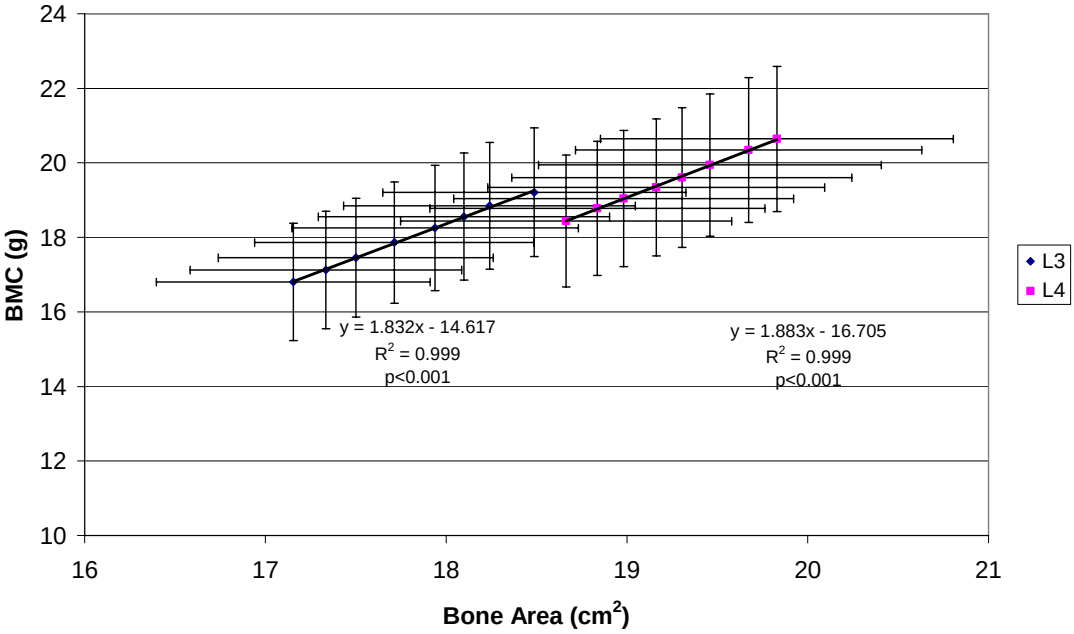

Figure C5 Relationship between BMC and BA and the width of the lumbar spine ROI for L3 and L4. Data are the average for 20 subjects within the MRTx group (±95% CI). Errors for slope of regression lines are ±0.023 g/cm^2 for L3 and ±0.021 g/cm^2 for L4. Pearson's correlation coefficient was L3 = 1.000 (p<0.001) and L4= 1.000 (p<0.001).

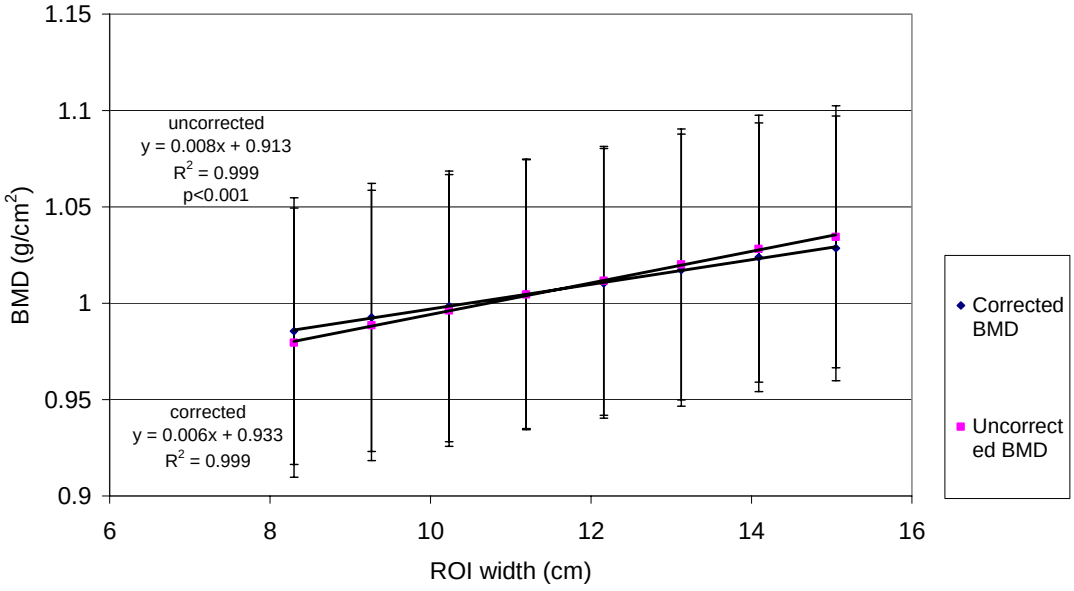

Figure C6 Relationship between the corrected and uncorrected L3+L4 BMD and the width of the lumbar spine ROI. Data are the average for 20 subjects within the MRTx group (±95% CI). SEE: uncorrected = 0.001 g/cm^2 and corrected BMD = 0.001 g/cm^2. Standard error of slope is ±<0.001 g/cm^2 per cm for both uncorrected and corrected L3+L4 BMD.

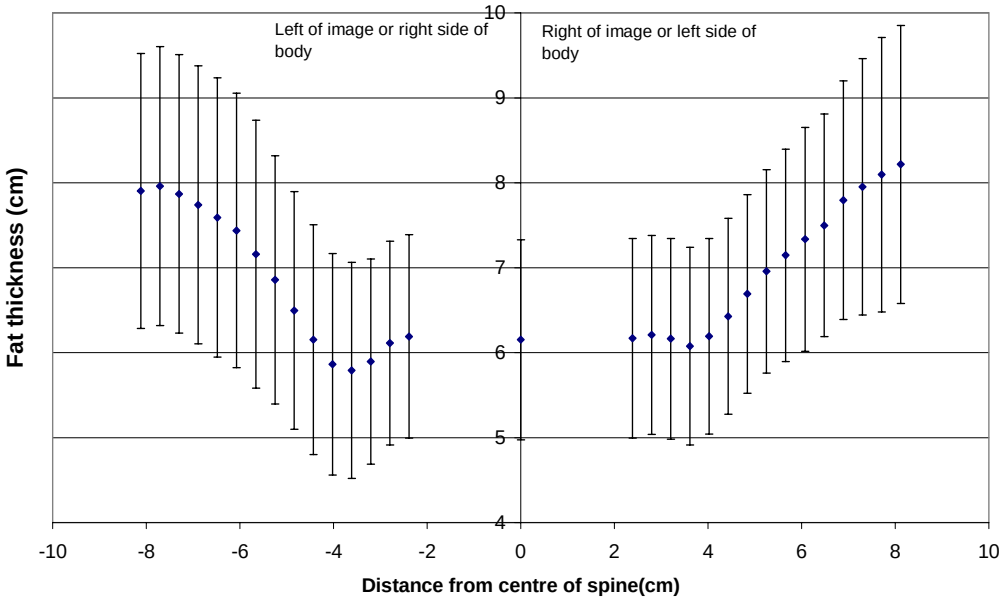

Figure C7 Variation in abdominal fat thickness at the level of L3+L4 with distance from the centre of lumbar spine. Data are average for 20 subjects in MRTx group (± 95% CI).

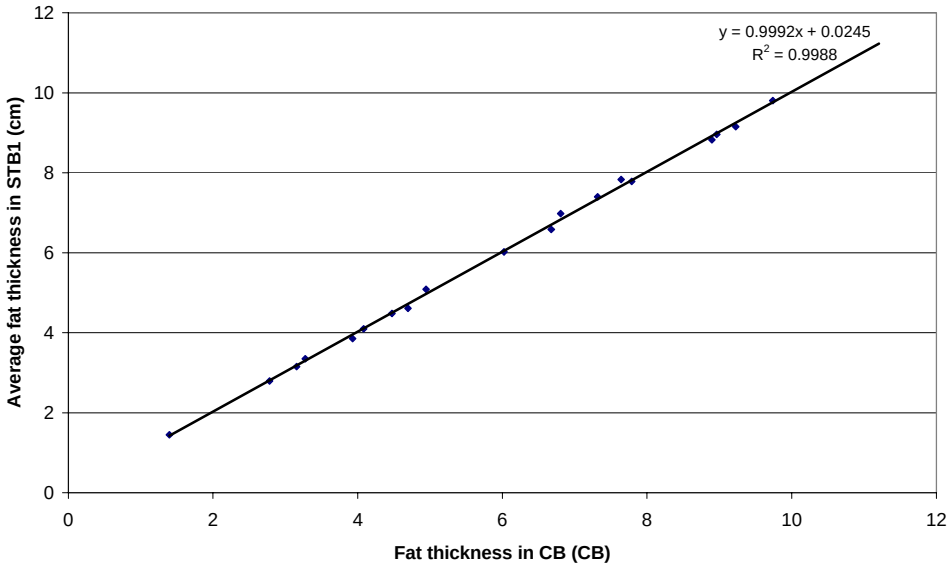

Figure C8 Relationship between the fat thickness measured for the CB over the vertebrae and the first STB adjacent to the vertebrae. Standard error of gradient is 0.01 cm per cm and SEE = 0.1 cm.

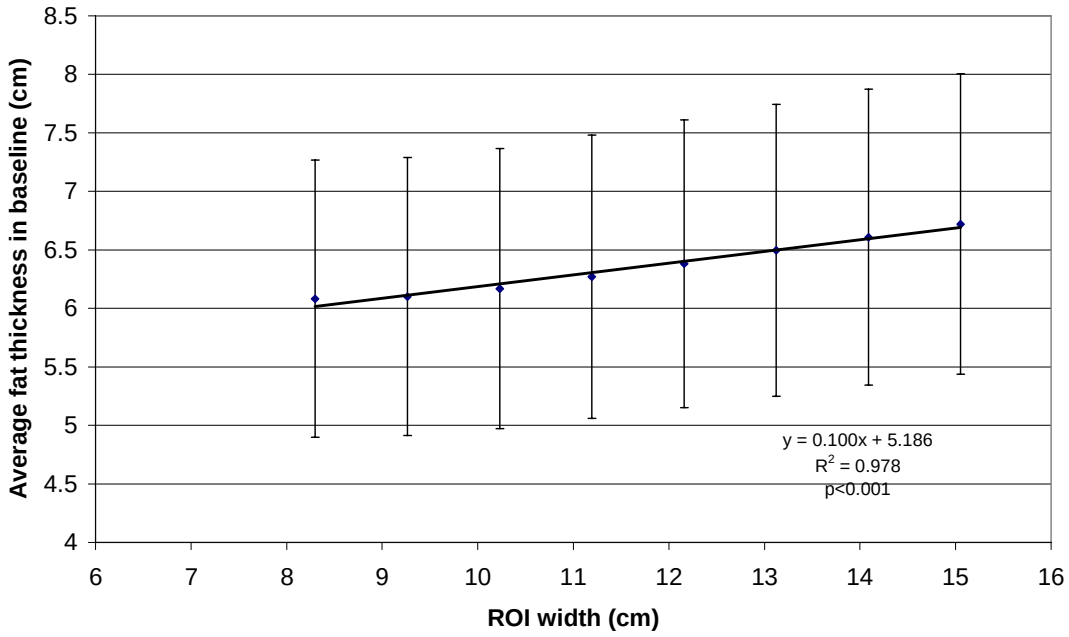

Figure C9 Average fat thickness in soft tissue regions adjacent to L3+L4 that are equivalent to those used as a baseline region for lumbar spine BMD analysis in chapter 4. The data are averaged over 20 subjects in MRTx group (±95% CI). SEE = 0.04 cm and standard error in gradient is ±0.01 cm fat per cm.

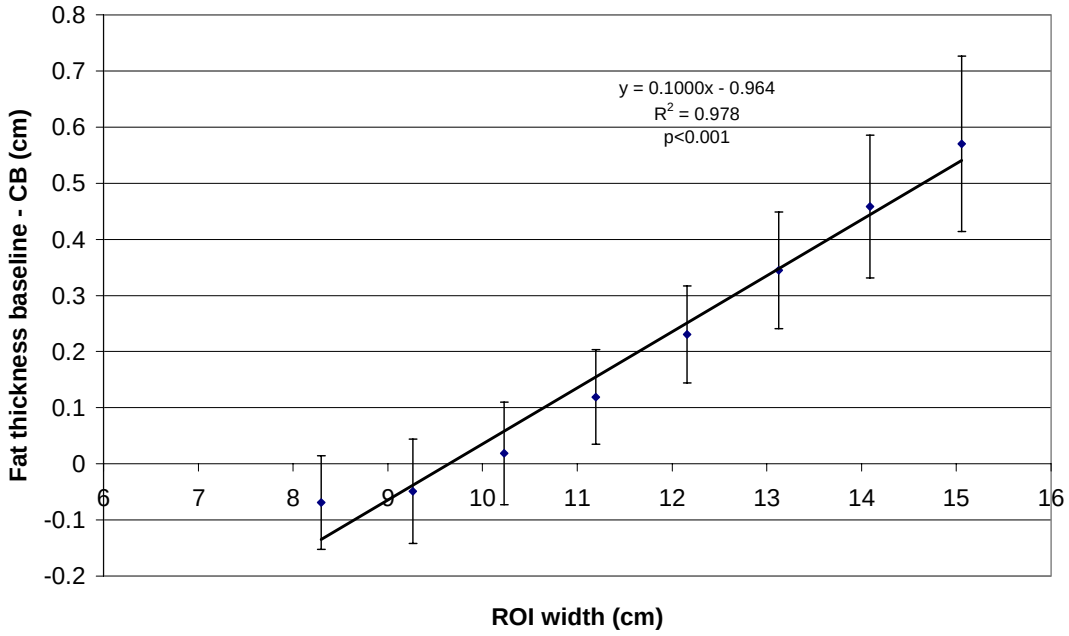

Figure C10 Fat thickness in the baseline soft tissue relative to that over vertebrae measured from WB images for ROI widths equivalent to those used in the measurement of L3+L4 BMD. Linear regression analysis shows that a ROI width of 9.7 cm would give an equal fat thickness in the soft tissue baseline and over vertebrae. Data are averaged over 20 subjects within MRTx group (±95% CI). SEE =0.04 cm and standard error of gradient is ±0.01 cm fat per cm.

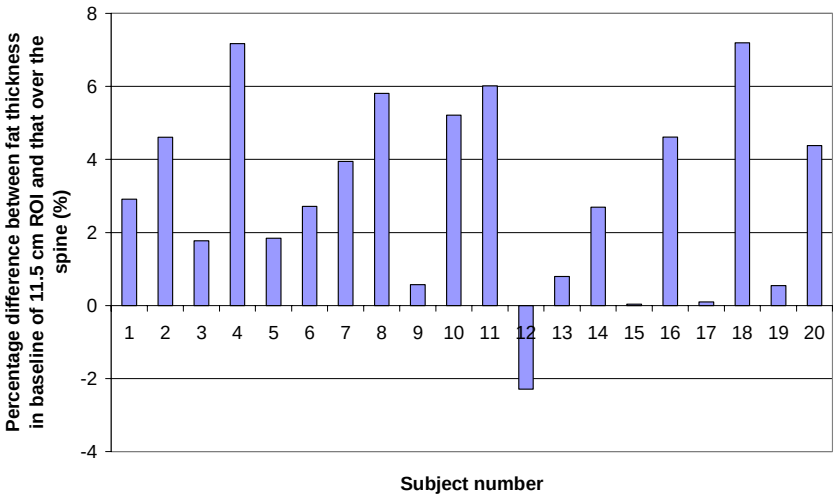

Figure C11 Comparison of the fat thickness over the spine with the average in the baseline of a 11.5 cm ROI at the level of L3+L4. Expressed as a percentage difference the average difference was 3.0 ± 2.6 % i.e. the fat thickness in the baseline was approximately 3 % greater than over the vertebrae (range = -2.3 % to 7.2 %).

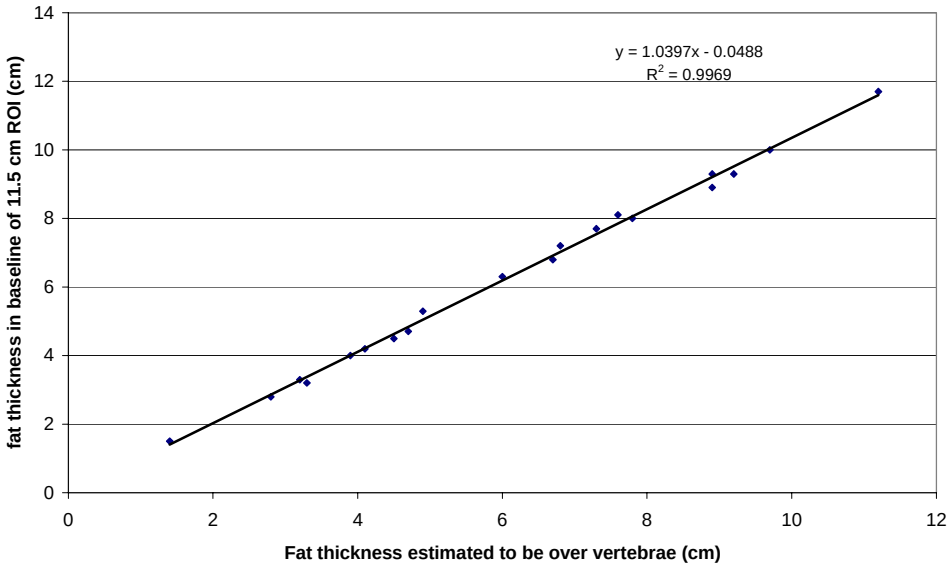

Figure C12 Relationship between the fat thickness in the baseline of the Hologic recommended ROI width and that in that over the vertebrae at the level of L3+L4 for 20 subjects in MRTx group. SEE = 0.15 cm, standard error of gradient ± 0.01 cm per cm.

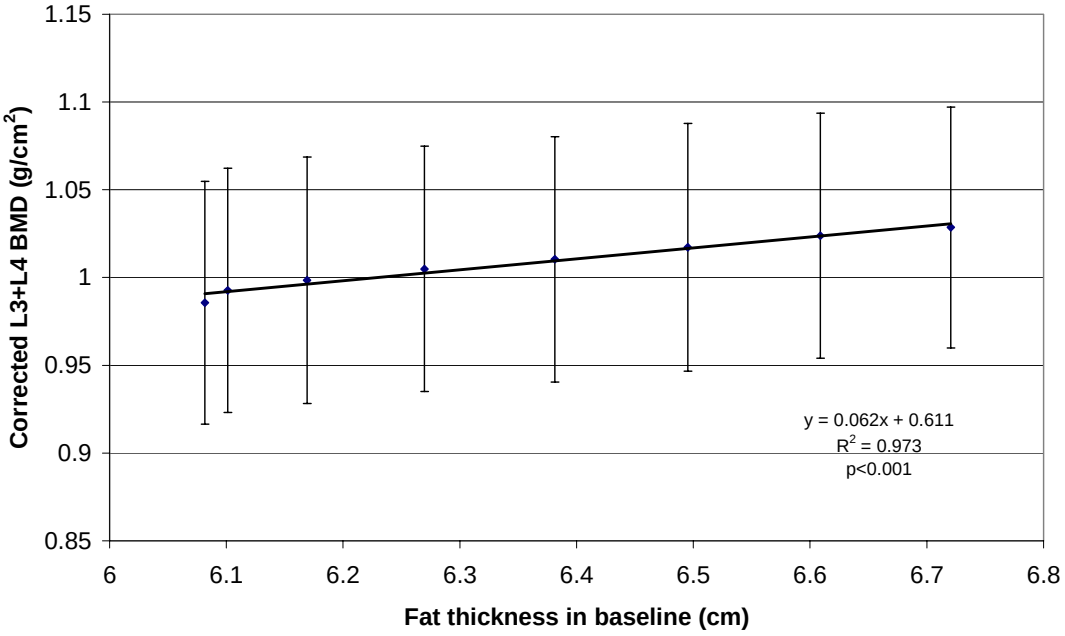

Figure C13 Relationship between the fat thickness within the soft tissue baseline extracted from DXA WB scans and the phantom corrected L3+L4 BMD for equivalent ROI width. Each data point represents a different width of ROI from 8.3 cm to 15.1 cm. Data are for the L3+L4 level and averaged over 20 subjects. BMD is mean ± 95% CI. SEE = 0.003 g/cm^2 and error in gradient is ±0.004 g/cm^2 per cm fat.

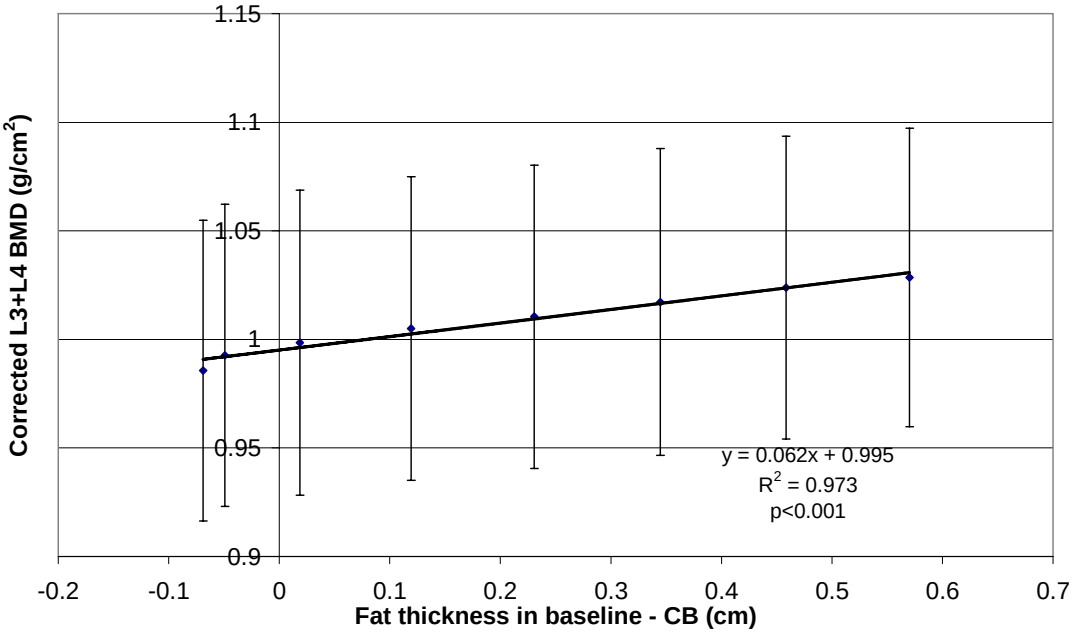

Figure C14 Relationship between the fat thickness in baseline relative to that to in the CB over spine and the reported L3+L4 BMD for average of 20 subjects in MRTx group (±95% CI). SEE = 0.003 g/cm^2, error on slope = 0.004 g/cm^2 per cm.

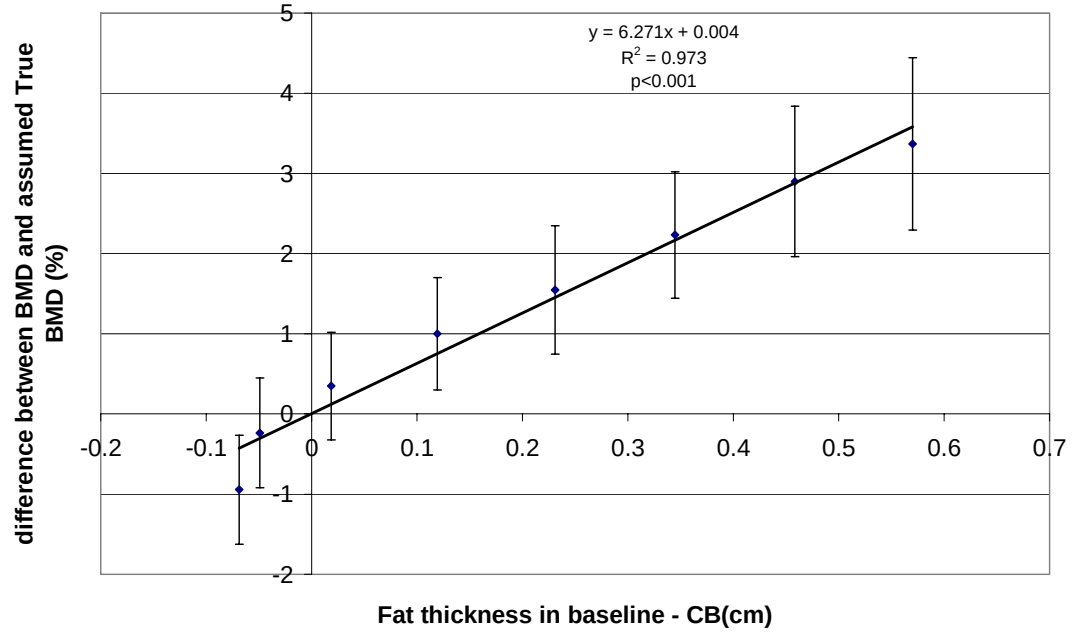

Figure C15 Relationship between the fat thickness in the baseline relative to that over the vertebrae and the potential errors in L3+L4 due to a non-uniform fat distribution. Errors in BMD estimated by assuming true BMD is 0.995 g/cm^2. Data are for L3+L4 level and averaged over 20 subjects in MRTx group (± 95 CI). SEE: 0.3% and error of gradient is 0.4 % per cm.

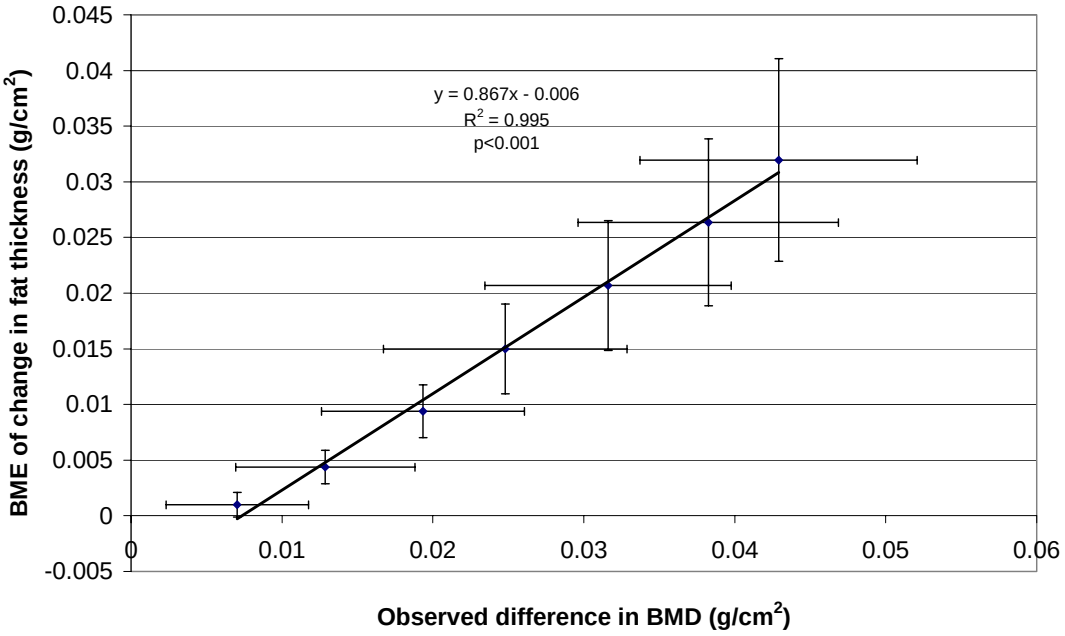

Figure C16 Relationship between the observed difference in phantom corrected L3+L4 BMD and the bone mineral equivalence (BME) of the difference in fat thickness within the baseline of equivalent width ROI. The data are average over 20 subjects within MRTx group. SEE = 0.001 g/cm^2, error of gradient ±0.029 g/cm^2 per g/cm^2. Error bars are ±95% CI.

Appendix D

Prediction of Inaccuracy in Lumbar Spine BMD for a Group of Female Patients Three Months Post Renal Transplant

These results were obtained when performing data analysis on lumbar spine and whole body images as discussed in chapter 7 for a group of 20 female subjects 3 months post renal transplant (FRTx).

The results match the full set that was presented for the IBD group in chapters 4,5, and 6.

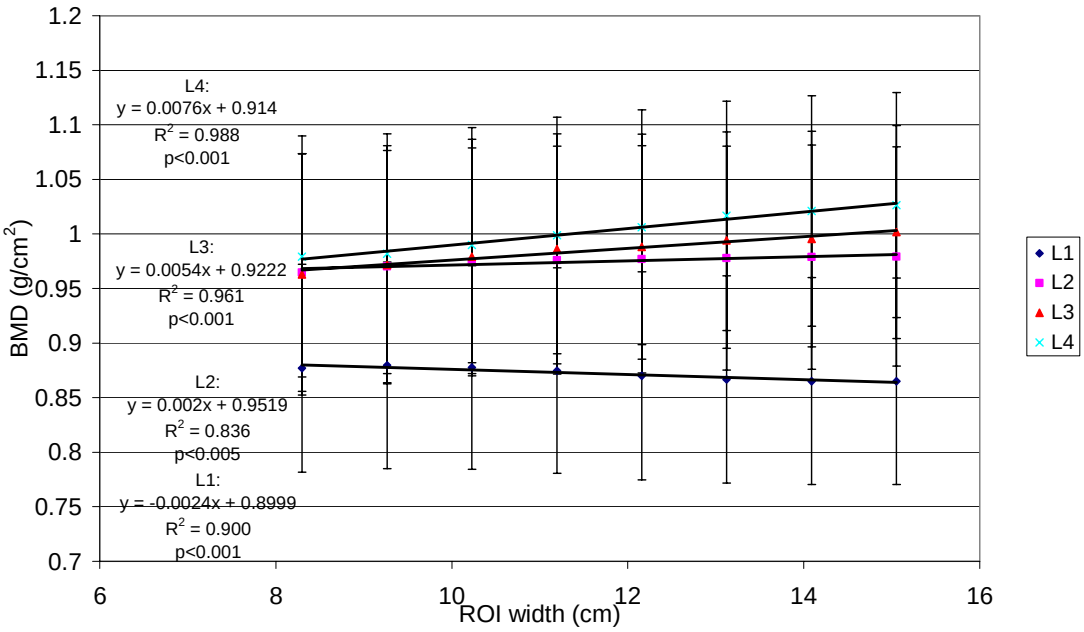

Figure D1 Relationship between measured lumbar spine BMD and the width of the lumbar spine ROI. Data are the average (± 95% CI) for 20 subjects in FRTx group. SEE: L1 = 0.002 g/cm^2, L2 = 0.002 g/cm^2, L3 = 0.003 g/cm^2, L4 = 0.002 g/cm^2. Errors in slope were L1±<0.001 g/cm^2 per cm, L2±<0.001 g/cm^2 per cm, L3±<0.001 g/cm^2 per cm, L4±<0.001 g/cm^{2}per cm.

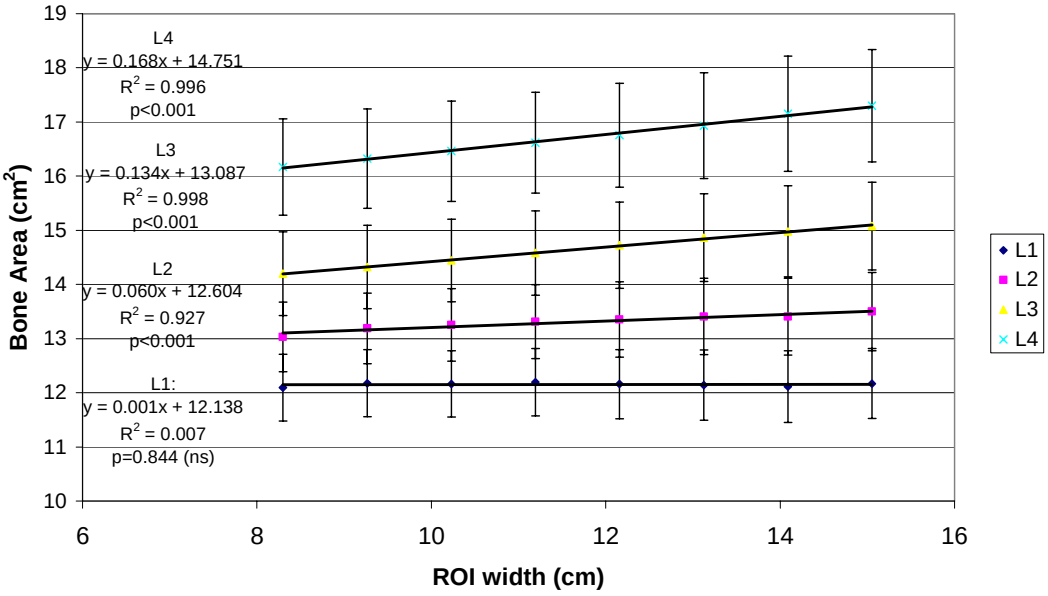

Figure D2 Relationship between measured lumbar spine BA and the width of the lumbar spine ROI. Data are the average (±95% CI) for 20 subjects in FRTx group. SEE: L1 = 0.04 cm^2, L2 = 0.04 cm^2, L3 = 0.01 cm^2, L4 = 0.03 cm^2. Errors in slope were L1±0.01 cm^2 per cm, L2±0.01 cm^2 per cm, L3±<0.01 cm^2 per cm, L4 ±0.01 cm^2 per cm.

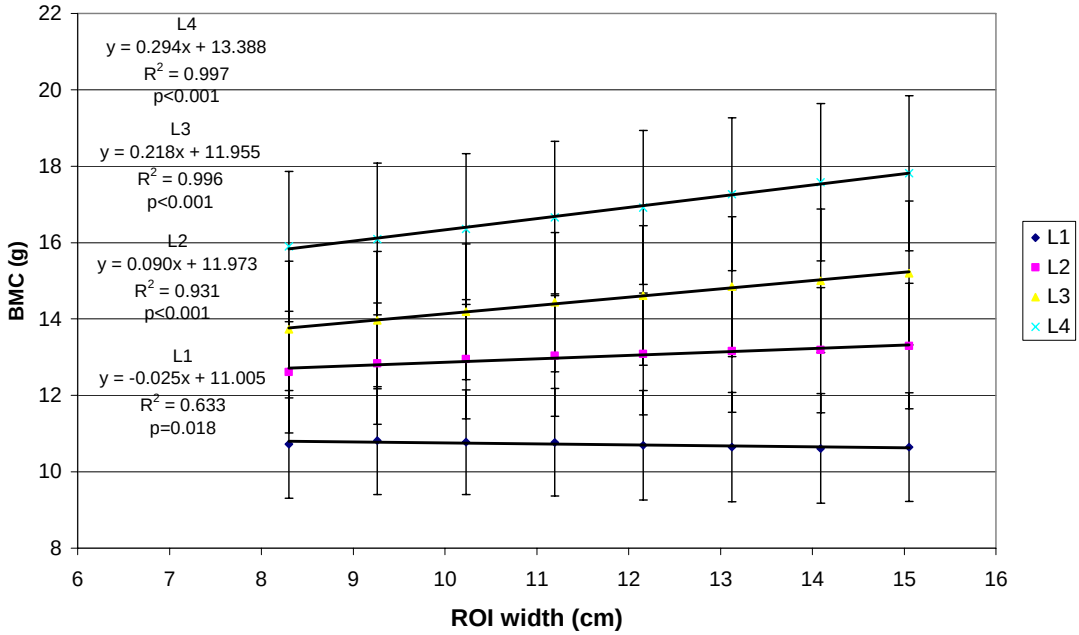

Figure D3 Relationship between measured lumbar spine BMC and the width of the lumbar spine ROI. Data are the average (± 95% CI) for 20 subjects in FRTx group. SEE: L1 = 0.05 g, L2 = 0.06 g, L3 = 0.03 g, L4 = 0.04 g. Errors in slope were L1± 0.01 g/cm, L2±0.01 g/cm, L3±0.01 g/cm. L4±0.01 g/cm.

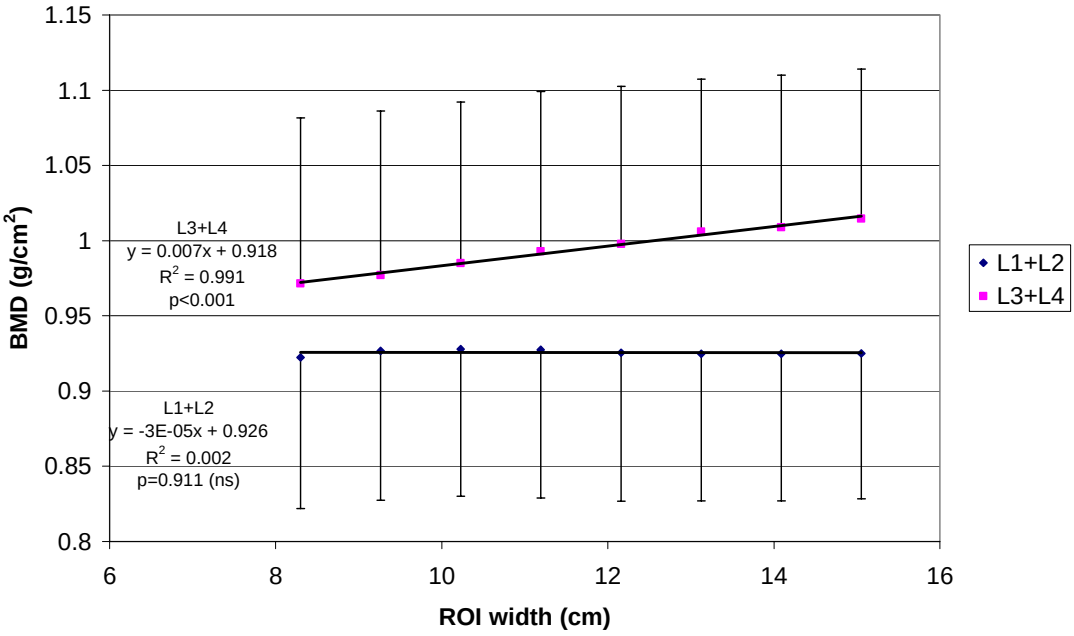

Figure D4 Relationship between measured combined L1+L2 and L3+L4 BMD and the width of the lumbar spine ROI. Data are the average (± 95% CI) for 20 subjects within the FRTx group. SEE: L1+L2 = 0.002 g/cm^2; L3+L4 = 0.002 g/cm^2. Errors in slope are L1+L2 ± <0.001 g/cm^2 per cm and L3+L4 ±<0.001 g/cm^2 per cm.

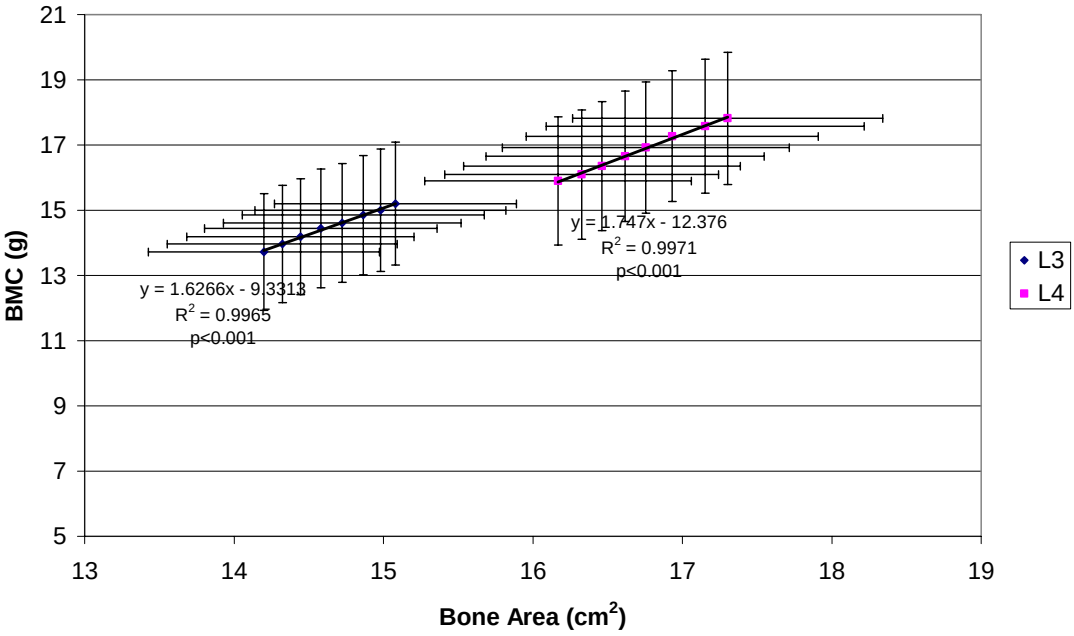

Figure D5 Relationship between BMC and BA and the width of the lumbar spine ROI for L3 and L4. Data are the average (±95% CI) for 20 subjects within the MRTx group. Errors for slope of regression lines are ±0.04 g/cm^2 for L3 and ± 0.04 g/cm^2 for L4. Pearson's correlation coefficient was L3 = 0.998 (p<0.001) and L4=0.999 (p<0.001).

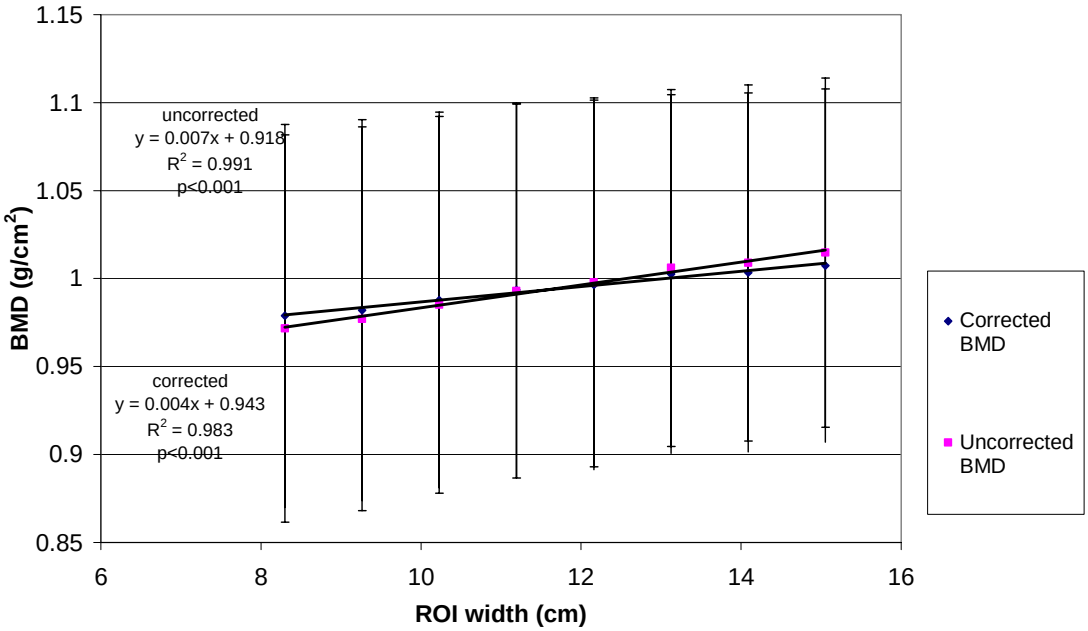

Figure D6 Relationship between the corrected and uncorrected L3+L4 BMD and the width of the lumbar spine ROI. Data are the average for 20 subjects within the FRTx group (±95% CI). SEE: uncorrected = 0.002 g/cm^2 and corrected BMD = 0.001 g/cm^2. Standard error of slope is ±<0.001 g/cm^2 per cm for both uncorrected and corrected L3+L4 BMD.

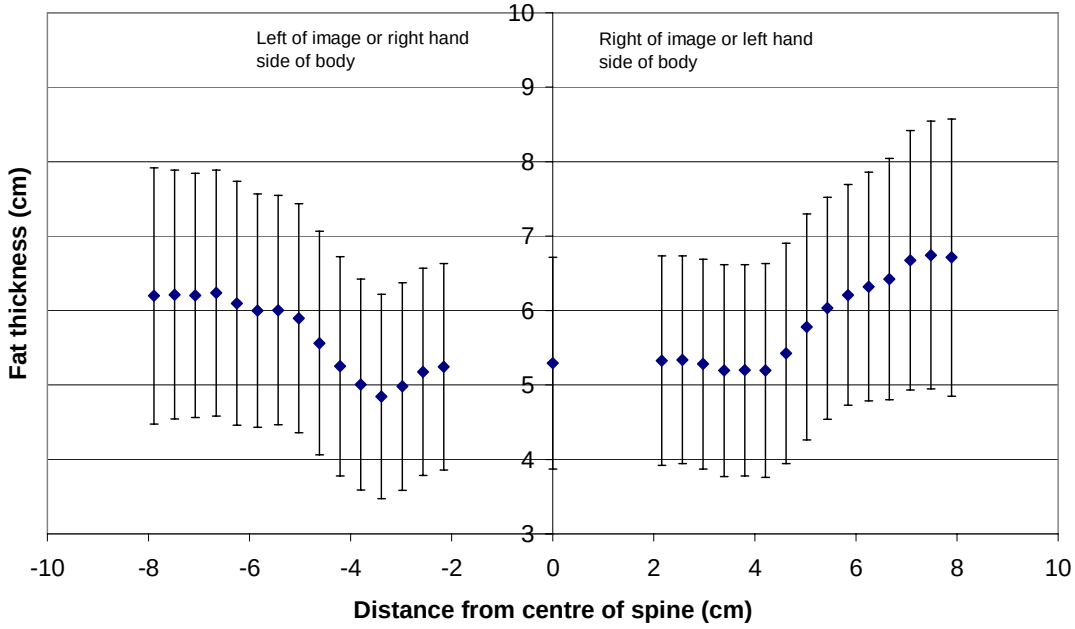

Figure D7 Variation in abdominal fat thickness at the level of L3+L4 with distance from the centre of lumbar spine. Data are average for 20 subjects in FRTx group (± 95% CI).

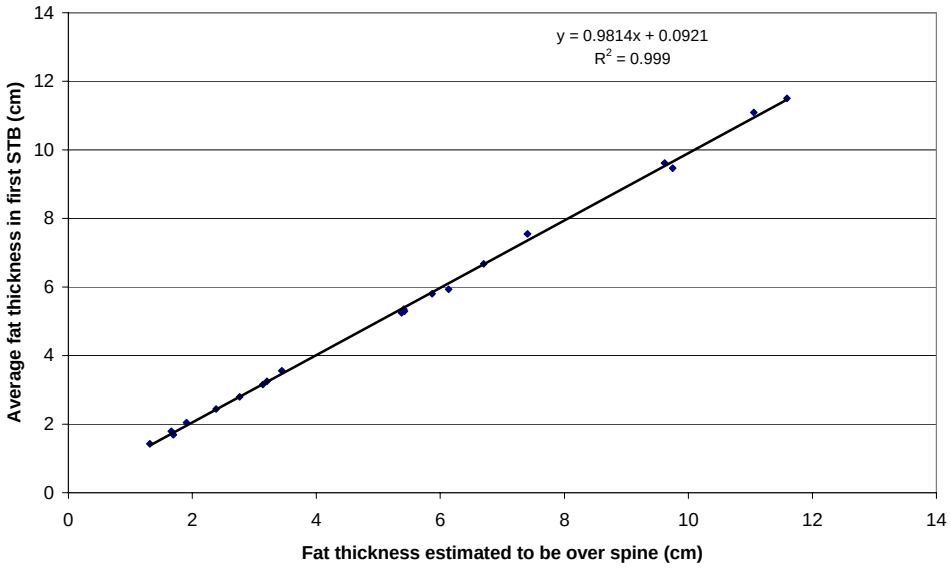

Figure D8 Relationship between fat thickness measured for the CB over the vertebrae and the first STB adjacent to the vertebrae. Standard error of gradient is ± 0.01 cm per cm and SEE = 0.10 cm.

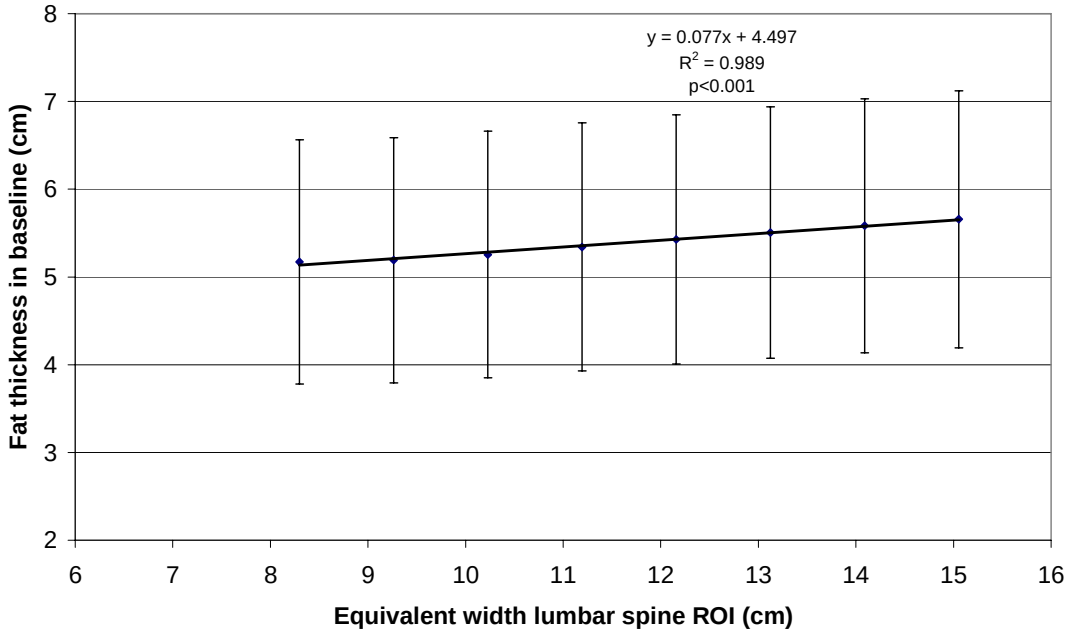

Figure D9 Average fat thickness in soft tissue regions adjacent to L3+L4 that are equivalent to those used as a baseline region for lumbar spine BMD analysis in chapter 4. The data are averaged over 20 subjects in FRTx group (± 95% CI). SEE = 0.02 cm and standard error in gradient is ± 0.003 cm fat per cm.

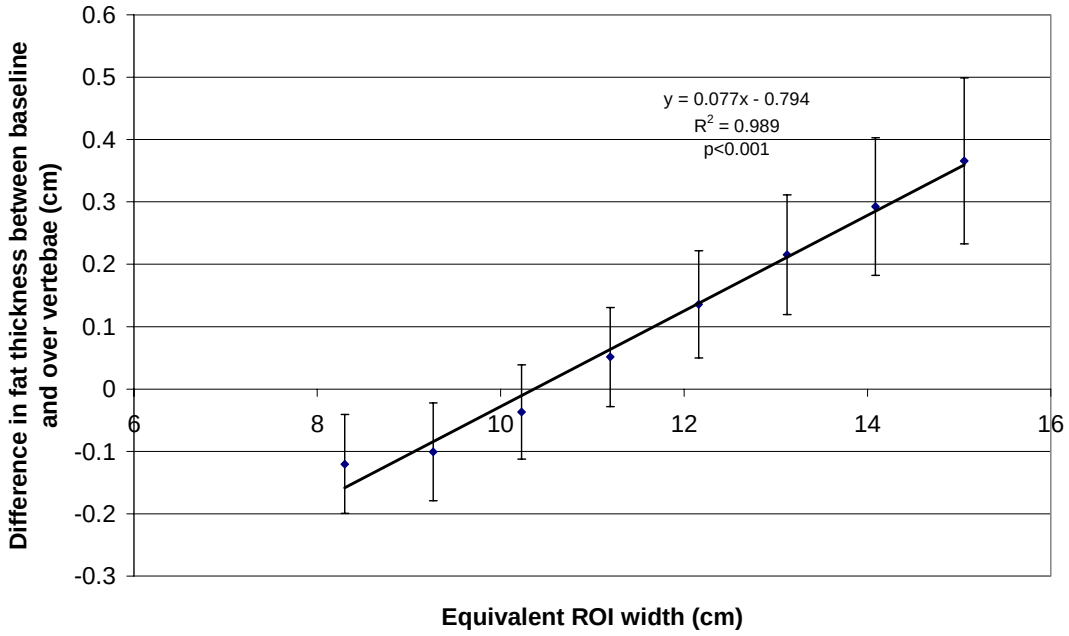

Figure D10 Fat thickness in the baseline soft tissue relative to that over vertebrae measured from WB images for ROI widths equivalent to those used in the measurement of L3+L4 BMD. Linear regression analysis shows that a ROI width of 10.4 cm would give an equal fat thickness in the soft tissue baseline and over vertebrae. Data are averaged (±95% CI) over 20 subjects within FRTx group. SEE = 0.02 cm and standard error of gradient is ±0.003 cm fat per cm.

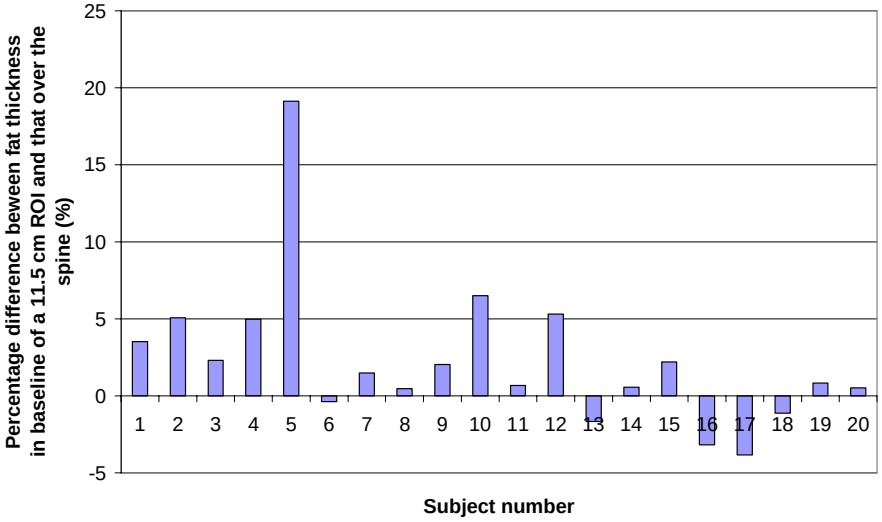

Figure D11 Comparison of the fat thickness over the spine with the average in the baseline of a 11.5 cm ROI at the level of L3+L4. Expressed as a percentage difference the average difference was 2.3 ± 4.8 % i.e. the fat thickness in the baseline was approximately 2 % greater than over the vertebrae (range = -1.7 % to 19.1 %).

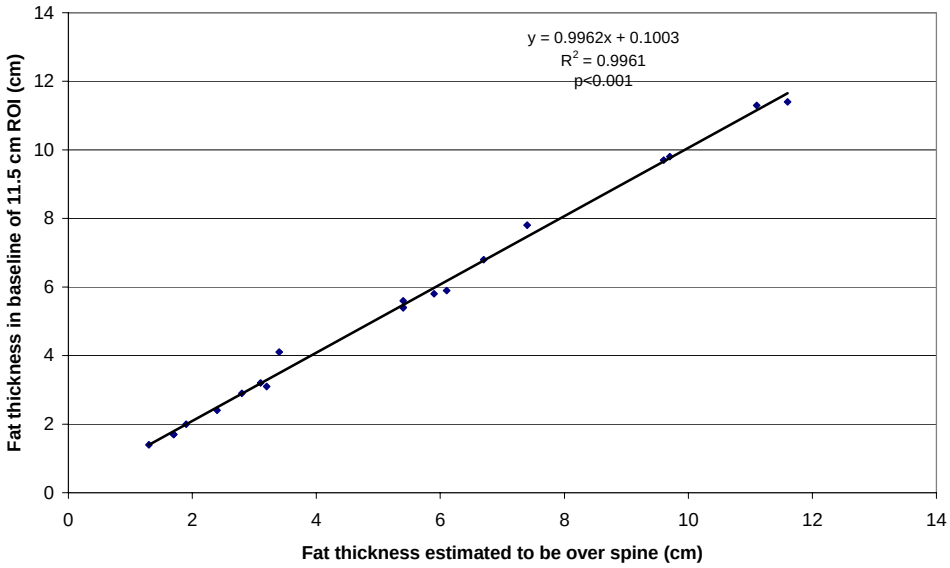

Figure D12 Relationship between the fat thickness in the baseline of the Hologic recommended ROI width and that in that over the vertebrae at the level of L3+L4 for 20 subjects in FRTx group. SEE = 0.2 cm, standard error of gradient = 0.01 cm per cm.

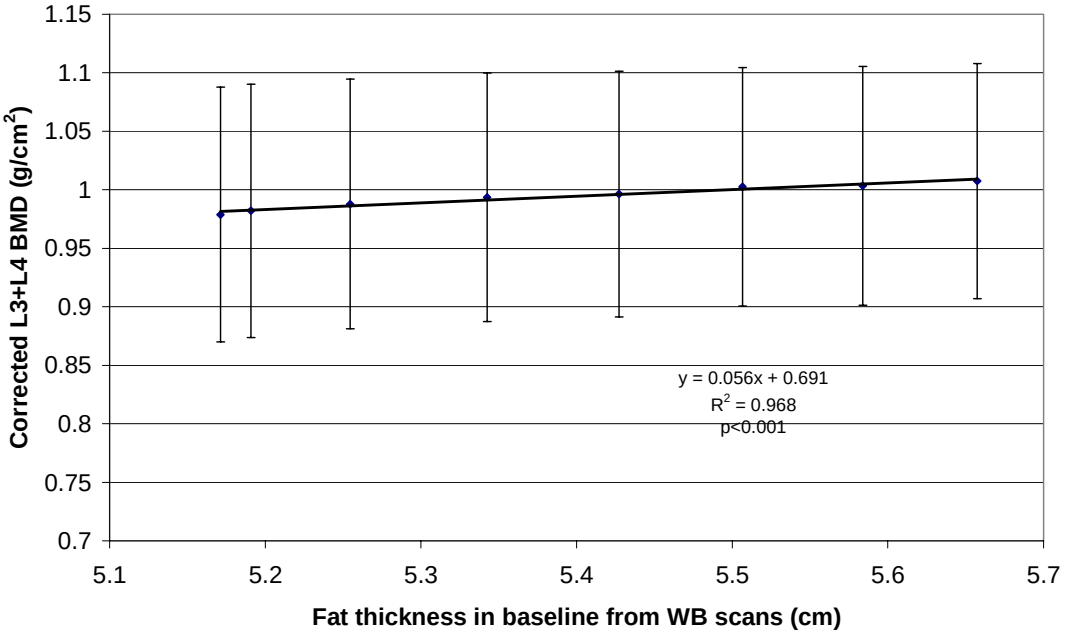

Figure D13 Relationship between the fat thickness within the soft tissue baseline extracted from DXA WB scans and the phantom corrected L3+L4 BMD for equivalent ROI width. Each data point represents a different width of ROI from 8.3 cm to 15.1 cm. Data are for the L3+L4 level and averaged over 20 subjects. BMD is mean ± 95% CI. SEE = 0.002 g/cm^2 and error in gradient is ± 0.004 g/cm^2 per cm fat.

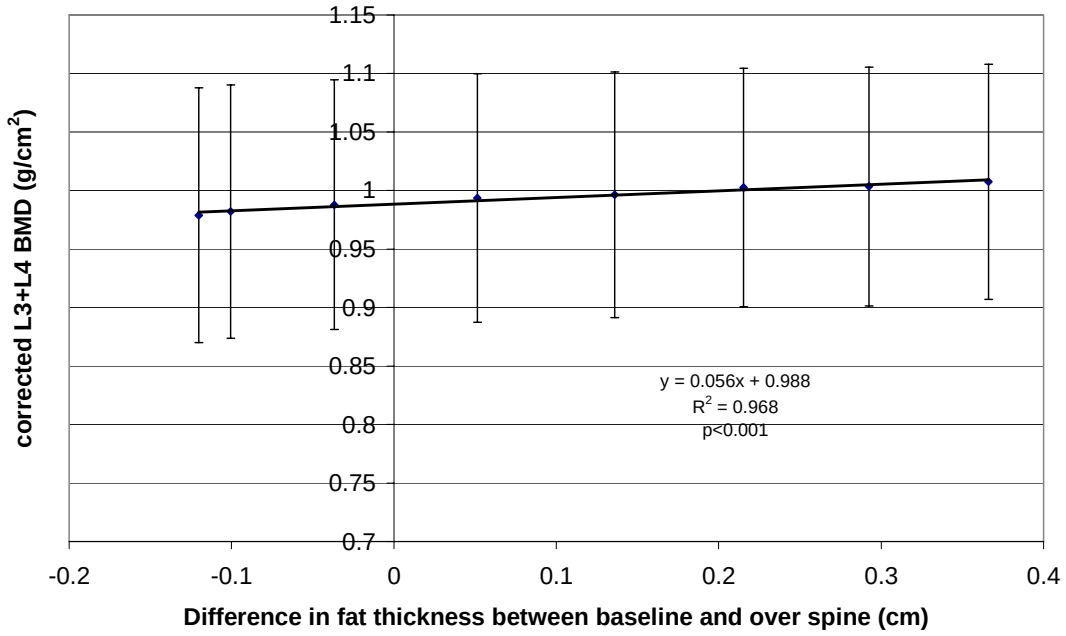

Figure D14 Relationship between the fat thickness in baseline relative to that to in the CB over spine and the reported L3+L4 BMD for average (±95% CI) of 20 subjects in FRTx group. SEE = 0.002 g/cm^2, error on slope = 0.004 g/cm^2 per cm.

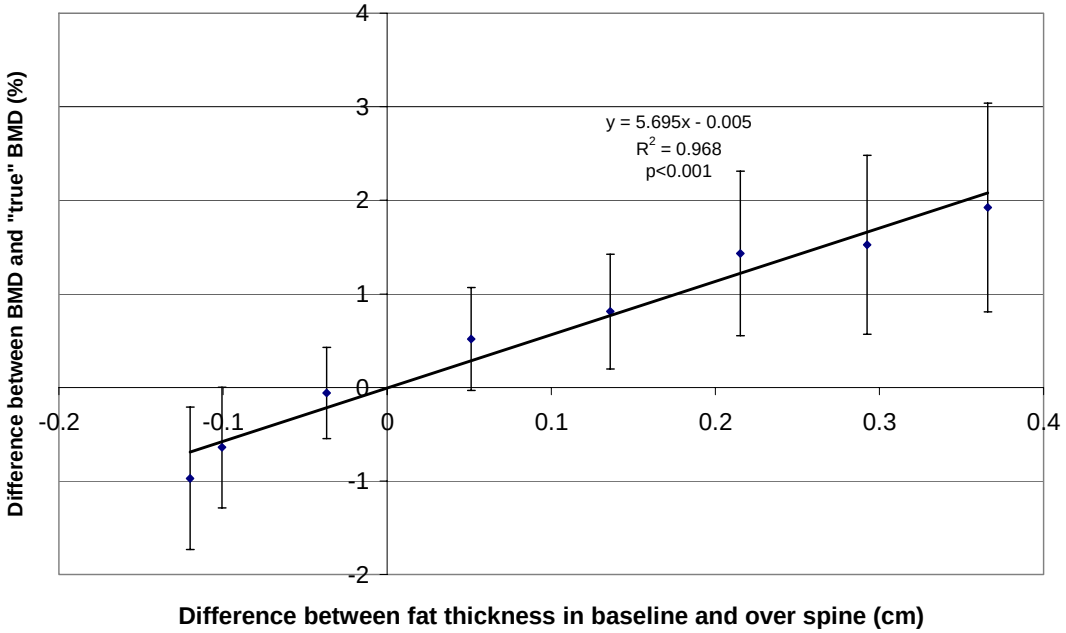

Figure D15 Relationship between the fat thickness in the baseline relative to that over the vertebrae and the potential errors in L3+L4 due to a non-uniform fat distribution. Errors in BMD estimated by assuming true BMD is 0.988 g/cm^2. Data are for L3+L4 level and averaged (±95% CI) over 20 subjects in FRTx group. SEE: 0.2% and error of gradient is 0.4 % per cm.

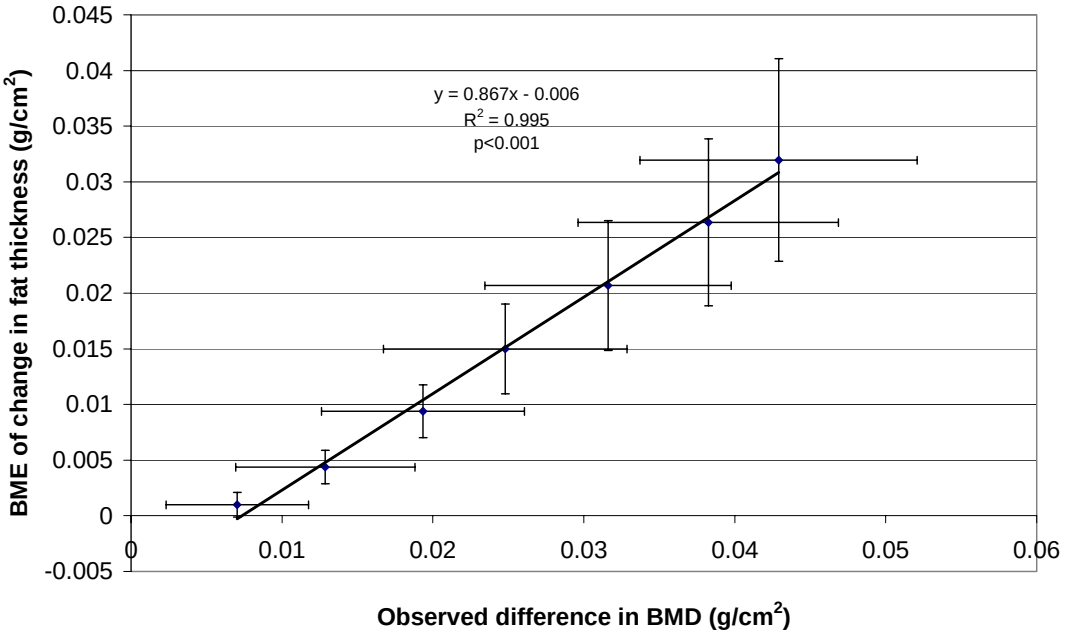

Figure D16 Relationship between the observed difference in phantom corrected L3+L4 BMD and the bone mineral equivalence (BME) of the difference in fat thickness within the baseline of equivalent width ROI. The data are average over 20 subjects within FRTx group. SEE = 0.002 g/cm^2, error of gradient ±0.068 g/cm^2 per g/cm^2. Error bars are 95% CI.